

TECHNISCHE UNIVERSITÄT MÜNCHEN

Fakultät Wissenschaftszentrum Weihenstephan für Ernährung, Landnutzung und Umwelt
Lehrstuhl für Chemie Biogener Rohstoffe

Development of enzymatic cascade reactions toward the synthesis of 1,4-butanediol

Barbara Beer

Vollständiger Abdruck der von der Fakultät Wissenschaftszentrum Weihenstephan für Ernährung, Landnutzung und Umwelt der Technischen Universität München zur Erlangung des akademischen Grades eines

Doktors der Naturwissenschaften (Dr. rer. nat.)

genehmigten Dissertation.

Vorsitzender:

Prof. Dr. Wolfgang Liebl

Prüfer der Dissertation:

1. Prof. Dr. Volker Sieber

2. Prof. Dr. Reinhard Sterner

Die Dissertation wurde am 30.07.2018 bei der Technischen Universität München eingereicht und durch die Fakultät Wissenschaftszentrum Weihenstephan für Ernährung, Landnutzung und Umwelt am 28.01.2019 angenommen.

Table of contents

Summary	i
1 Introduction	1
1.1 1,4-Butanediol	1
1.1.1 Applications and market size	1
1.1.2 Production – state of the art	2
1.2 <i>In vivo</i> versus <i>in vitro</i> enzymatic cascade reactions	6
1.2.1 Definition of the term enzymatic cascade reaction	6
1.2.2 Comparison of <i>in vivo</i> and <i>in vitro</i> enzymatic cascade reactions	6
1.3 Development of <i>in vitro</i> enzymatic cascade reactions	8
1.3.1 Pathway design and the role of enzyme promiscuity	8
1.3.2 Characterization of enzymes	9
1.3.3 Enzyme engineering	10
1.4 An <i>in vitro</i> enzymatic cascade reaction from D-glucose to BDO	12
1.5 Aim of this work	14
1.5.1 Identification of enzymes for the oxidation of D-glucose to D-glucarate	14
1.5.2 Enzyme characterization and engineering	14
1.5.3 Setup of <i>in vitro</i> enzymatic cascade reactions	14
2 Materials	15
2.1 Chemicals	15
2.2 Enzymes	15
2.3 Kits	15
2.4 Devices	16
2.5 Software and databases	18
2.6 Cultivation media and antibiotics	19
2.6.1 Culture media	19
2.6.2 Antibiotics	20
2.7 Bacterial strains	20
2.8 Plasmids and Strings DNA fragments	20
2.9 Oligodeoxyribonucleotides	22
3 Methods	23
3.1 Microbiological methods	23
3.1.1 Cultivation and storage of <i>E. coli</i> strains	23
3.1.2 Determination of the optical density of <i>E. coli</i> cell suspensions	23
3.1.3 Preparation of competent <i>E. coli</i> cells for chemical transformation	23
3.1.4 Transformation of chemically competent <i>E. coli</i> cells	24
3.1.5 Expression of recombinant genes in <i>E. coli</i>	24
3.2 Molecular biological methods	25
3.2.1 Determination of DNA concentrations	25

3.2.2	Agarose gel electrophoresis.....	25
3.2.3	Amplification of DNA using PCR.....	26
3.2.4	Isolation and purification of plasmid DNA from <i>E. coli</i>	27
3.2.5	Isolation of DNA fragments.....	27
3.2.6	Enzymatic manipulation of DNA fragments.....	27
3.2.7	Simple Cloning.....	28
3.2.8	Sequencing of DNA fragments.....	29
3.3	Protein analytics.....	30
3.3.1	Determination of protein concentrations by UV spectroscopy.....	30
3.3.2	Determination of protein concentrations with the Bradford assay.....	31
3.3.3	Determination of the FAD content of NADH oxidase.....	31
3.3.4	SDS polyacrylamide gel electrophoresis.....	31
3.3.5	Protein purification.....	32
3.3.6	Storage of protein preparations.....	33
3.3.7	Determination of enzymatic activity.....	33
3.3.8	Determination of enzyme stability.....	35
3.4	Single enzyme reactions.....	36
3.4.1	Analytical single enzyme reactions.....	36
3.4.2	Preparative single enzyme reactions.....	37
3.5	<i>In vitro</i> enzymatic cascade reactions.....	37
3.5.1	Synthesis of 5-hydroxy-2-oxovalerate.....	37
3.5.2	Synthesis of α -ketoglutarate.....	38
3.6	Instrumental analytics.....	38
3.6.1	High performance liquid chromatography.....	38
3.6.2	Mass spectroscopy.....	40
3.6.3	Nuclear magnetic resonance spectroscopy.....	40
4	Results.....	41
4.1	Identification of enzymes for the oxidation of D-glucose to D-glucarate.....	41
4.1.1	UDP-glucose-6-dehydrogenases.....	41
4.1.2	Alcohol dehydrogenases from <i>Agrobacterium tumefaciens</i>	43
4.1.3	Alcohol dehydrogenases from <i>Sphingomonas</i> species A1.....	43
4.2	Enzyme characterization and engineering.....	60
4.2.1	A water-forming NADH oxidase from <i>Lactobacillus pentosus</i> suitable for the regeneration of synthetic biomimetic cofactors.....	61
4.2.2	Thermostabilization of the uronate dehydrogenase from <i>Agrobacterium tumefaciens</i> by semi-rational design.....	71
4.3	Evaluation of <i>in vitro</i> enzymatic cascade reactions toward BDO.....	81
4.3.1	<i>In vitro</i> enzymatic cascade reaction to 5-hydroxy-2-oxovalerate.....	81
4.3.2	<i>In vitro</i> metabolic engineering for the production of α -ketoglutarate.....	85
4.3.3	Identification of a side product formed from Kgsa.....	95
5	Discussion and Outlook.....	96
5.1	From D-glucose to D-glucarate with two enzymes.....	96
5.2	Synthesis of 5-hydroxy-2-oxovalerate.....	99
5.3	Enzymatic cascade reaction for the production of α-ketoglutarate.....	100
5.4	Implications for BDO production.....	101

5.5	More enzymatic cascade reactions.....	104
6	Appendix	106
6.1	Gene sequences	106
6.2	Analysis of reaction products of SpsADH	108
6.3	Analysis of 4-APEBA derivatives by HPLC/MS.....	112
6.4	Half-life of UDH under various conditions	113
6.5	Supplemental Information: Substrate scope of a dehydrogenase from <i>Sphingomonas</i> species A1 and its potential application in the synthesis of rare sugars and sugar derivatives	114
6.6	Supplemental Information: A water-forming NADH oxidase from <i>Lactobacillus pentosus</i> suitable for synthetic biomimetic cofactors	116
6.7	Supplemental Information: <i>In vitro</i> metabolic engineering for the production of α -ketoglutarate	118
7	Abbreviations	121
8	List of figures	124
9	List of tables	125
10	References.....	126
11	Acknowledgments.....	132
12	Curriculum Vitae.....	133

Summary

1,4-butanediol is a platform chemical for a number of plastics and synthetic materials that are omnipresent in our everyday life. It is produced from petroleum with an annual amount of about three million tons in 2017. More sustainable, biotechnological processes have been developed lately that use engineered microorganisms for the fermentation of D-glucose to 1,4-butanediol. Common problems encountered in cell-based approaches, such as low titers, productivity and laborious downstream processes, can possibly be overcome by a cell-free *in vitro* process using purified enzymes in an artificial enzymatic cascade reaction. In the proposed pathway, D-glucose is converted to 1,4-butanediol in eight steps and the reaction can be divided into three modules: an oxidative module, where D-glucose is converted to D-glucarate, a dehydration module including one decarboxylation yielding ketoglutaric semialdehyde, and a reductive module with another decarboxylation leading to the final product 1,4-butanediol. Only one cofactor, NAD⁺, is necessary, which is recycled within the cascade reaction. In order to keep the cofactor balanced, one oxidation reaction has to be catalyzed using molecular oxygen as the oxidative agent. For the dehydration module suitable enzymes have already been identified in another work, for which catalytic amounts of Mg²⁺ need to be supplied. Lastly, thiamine pyrophosphate has to be added for activity of the decarboxylase of the reductive module.

In the oxidative module, not all enzymes needed for the three oxidation steps do naturally exist. Therefore, in the first part of this thesis, enzymes converting similar substrates were investigated for their ability to recognize D-glucose or D-gluconate. Among the enzymes tested, a short-chain alcohol dehydrogenase/reductase from *Sphingomonas* species A1 (SpsADH) was discovered, which exhibits a broad substrate scope toward various aldonates and polyols. Besides other substrates, it is able to oxidize D-gluconate to L-gulonate. Furthermore, a promiscuous activity of the same enzyme toward uronic acids leads to the formation of D-glucarate. This should now allow the direct oxidation of D-glucose to D-glucarate with only two enzymes instead of nine enzymes in mammals or five enzymes in an engineered *Escherichia coli* (*E. coli*). Namely D-glucose oxidase, a natural enzyme with commercial uses, and SpsADH.

In the second part of the thesis, two enzymes were studied in detail: NADH oxidase from *Lactobacillus pentosus* and uronate dehydrogenase from *Agrobacterium tumefaciens*. NADH oxidase is a cofactor recycling enzyme, and although it is not part of the cascade reaction to 1,4-butanediol, it allows the investigation of separate modules. We could show that it is a water-forming oxidase and that it can be activated with FAD *in vitro*. As most enzymes, it is most active in a pH range of 6 to 8 with an optimum temperature of 37 °C. Furthermore, it also utilizes cheap, non-natural cofactors, which are under development to make cofactor-dependent enzyme reactions more economic in the future.

Uronate dehydrogenase was applied in the cascade reactions developed in this thesis. Since it was shown previously that it exhibits only a low half-life, it was engineered for higher stability. Using a semi-rational approach, it was possible to identify a triple variant including two neutral drift mutations with greater thermodynamic as well as kinetic stability than the wildtype enzyme.

Finally, two *in vitro* enzymatic cascade reactions were investigated. One for the synthesis of 2-keto-5-hydroxyvalerate and one for the synthesis of α -ketoglutarate. The first three steps are the same in both pathways and are derived from the reaction route from D-glucose to 1,4-butanediol: D-gluconate is oxidized by uronate dehydrogenase to D-glucarate. The sequential action of glucarate dehydratase and

5-keto-4-deoxyglucarate dehydratase then lead to ketoglutaric semialdehyde. In the first route, this intermediate is reduced by an alcohol dehydrogenase to 2-keto-5-hydroxyvalerate, the substrate of the decarboxylase of the reductive module. Here, an internal recycling of NAD^+/NADH is achieved by the first and the last enzyme. However, it was found that the enzyme for the reduction was not active or stable enough, leading to low conversion of D-glucuronate due to insufficient cofactor supply, or to the accumulation of ketoglutaric semialdehyde, depending on the reaction setup. This explanation was not found before a new analytical method was developed, originally designed for the second investigated *in vitro* enzymatic cascade reaction for the synthesis of α -ketoglutarate.

Here ketoglutaric semialdehyde dehydrogenase was used in the last step for the oxidation of ketoglutaric semialdehyde, while NAD^+ recycling was achieved with NADH oxidase. By optimizing the initial cofactor and NADH oxidase concentrations, the conversion of D-glucuronate rose from 20% to 100% and a yield of >90% was reached. However, the reaction took 150 h due to the diffusion limit of oxygen from air into solution. When the reaction was performed in a bubble reactor, only 5 h were necessary, resulting in a space-time-yield of $2.8 \text{ g L}^{-1} \text{ h}^{-1}$. Furthermore, we found that wildtype uronate dehydrogenase was stabilized in the presence of other proteins and its inactivation is not a bottleneck.

1 Introduction

1.1 1,4-Butanediol

1.1.1 Applications and market size

1,4-Butanediol (BDO) is a non-natural, color- and odorless, non-corrosive liquid at room temperature. It has a high boiling point of 230 °C and is miscible with water, most alcohols, esters, ketones, glycol ethers, and acetates ("International Chemical Safety Cards (ICSC) 1104," 1999). BDO is an important platform chemical in the chemical industry with a worldwide production capacity of 3.2 million tons (Plotkin, 2016). Half of the total BDO production is dehydrated to tetrahydrofuran (THF), which is used to make fibers such as spandex and other performance polymers or as a solvent. BDO is also utilized to synthesize polybutylene terephthalate, an engineering thermoplastic, γ -butyrolactone, the starting material for N-methyl-2-pyrrolidone and 2-pyrrolidone, and polyurethanes (Ostgard, 2015) (Figure 1). These intermediates are further processed, for instance to medicines, cosmetics, artificial leather, pesticides, plasticizers, hardener, solvents, and rust remover, etc.

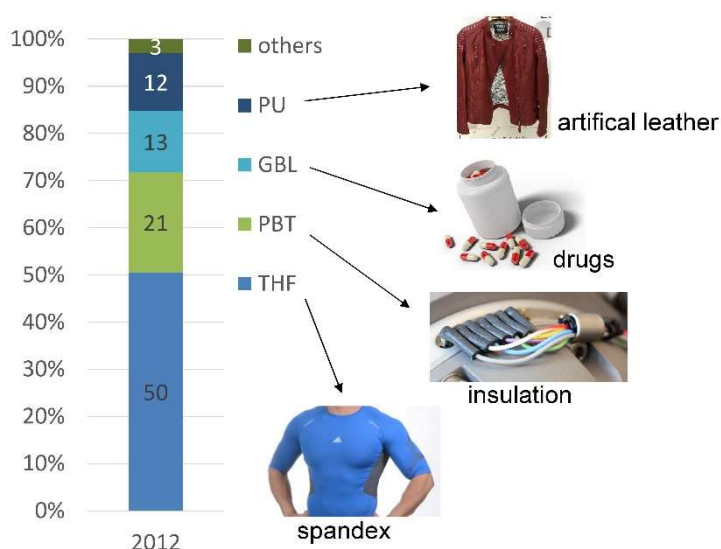


Figure 1: Products made from BDO
The main applications of BDO are the production of tetrahydrofuran (THF, 50%), polybutylene terephthalate (PBT, 21%), γ -butyrolactone (GBL, 13%), and polyurethanes (PU, 12%). In 2012 a total of 1,560 kt BDO were produced. The figure is adapted from Ostgard (2015); the photographs are available without copyright.

The market size for BDO, in terms of value, is projected to reach \$8.96 billion by 2019, registering a compound annual growth rate of 8.23% between 2014 and 2019 ("1,4-Butanediol Market by Technology", 2015). Most BDO and THF is produced and consumed in Asia, especially in China and Japan (Figure 2). The key participants in the global 1,4-butanediol market include BASF SE (Germany), Dairen Chemicals (Taiwan), LyondellBasell Chemicals (The Netherlands), Shanxi Sanwei Group (China), International Specialty Products (USA), Invista (USA), and Mitsubishi Chemicals (Japan).

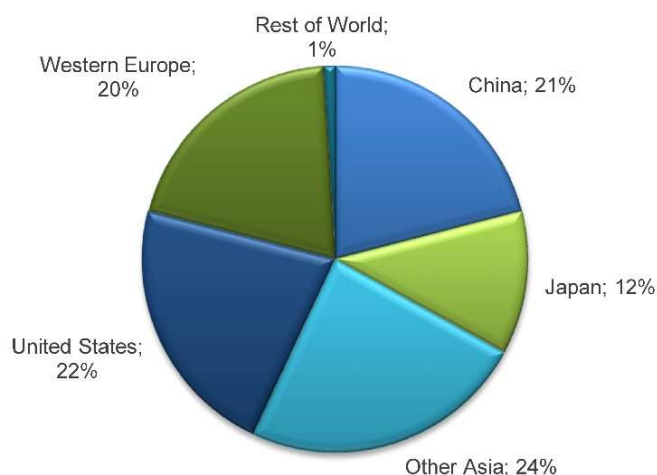


Figure 2: Global consumption of BDO by region (2010)

In 2010 most BDO was consumed in Asia with China making up for 21%, Japan 12%, and the rest of Asia for 24%. In the United States and Western Europe 22% and 20% of the total BDO were used, respectively (Vaswani, 2012)

1.1.2 Production – state of the art

Various production routes to BDO exist, which use either the petroleum-derived substrates acetylene, maleic anhydride, propylene and butadiene, or the renewable resource D-glucose (Figure 3). The first commercial process to BDO, invented in 1930, is the Reppe process, named after the German chemist Walter Reppe (Lang, 2008). Here, one mole of acetylene reacts with two moles of formaldehyde at 90 °C and 1 bar to 1,4-butynediol employing a modified CuBi catalyst. A possible side product can be partially reacted propargyl alcohol, which is recycled together with formaldehyde. In a second step, 1,4-butynediol is hydrogenated to BDO at 60-150 °C and 25-250 bar using a Nickel catalyst. The selectivity to 1,4-butanediol reaches about 95% based on 1,4-butynediol (Weissermel and Arpe, 2008). Despite acetylene being an explosive under pressure (2 bar), this is still the major route for BDO production worldwide and increases further due to the high production volume of Chinese companies (Ostgard, 2015) (Figure 4).

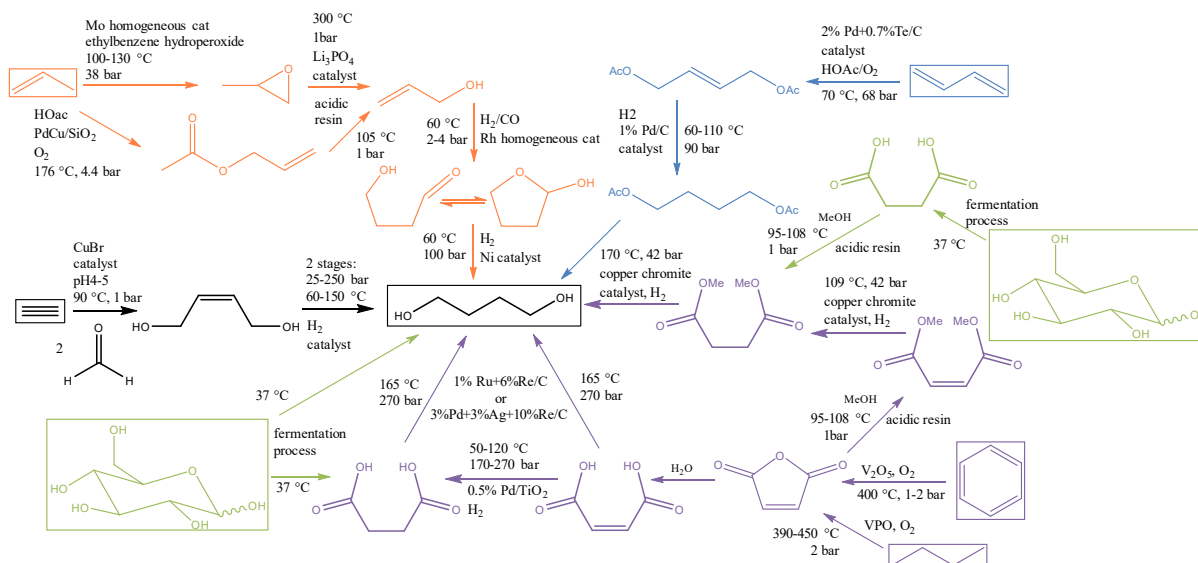


Figure 3: Commercial BDO production processes

Black: acetylene-based (Reppe) process; orange: propylene-based processes; blue: butadiene-based process; purple: maleic anhydride processes; green: sugar-based processes. Figure adapted from Ostgard (2015).

The other routes were developed since the 1970`s: The Mitsubishi route, which is based on the oxidative acetoxylation of butadiene with acetic acid followed by hydrogenation and hydrolysis to BDO ("Mitsubishi Chemical: 1,4-Butandiol & tetrahydrofuran technology," 2017). In 1990, Arco Chemical developed a route to BDO from propylene oxide. The Arco process starts with the isomerization of propylene oxide to allyl alcohol, which then undergoes hydroformylation with synthesis gas ($H_2 + CO$) to give 4-hydroxybutyraldehyde. In the last step, it is hydrogenated to BDO (Vaswani, 2012). Dairen Chemical in Taiwan operates a similar process that starts with allyl alcohol made from allyl acetate instead of propylene oxide ("Dairen Chemical Corp.,"). In the mid-1990s, two companies developed technologies for converting maleic anhydride to BDO. Johnson Matthey Davy Technologies, a British licensing company, developed a route to BDO that involves the initial conversion of maleic anhydride to its methyl or ethyl diester. The diester is then hydrogenated to BDO and the reconstituted methanol or ethanol is recycled ("The DAVY™ butanediol process," 2017). At about the same time, BP Chemical developed a version of this technology, in which maleic anhydride is directly hydrogenated to BDO and THF (Plotkin, 2016). Improvements to the conventional routes to BDO are still under research: UOP (Des Plaines, Illinois, USA) issued a patent for improving the acetylene-based route to BDO (US Patent 9,205,398, Dec. 8, 2015); and China Petroleum & Chemical (Beijing, China), in collaboration with the Fushun Research Institute of Petroleum and Petrochemicals (China), has been awarded a patent on improvements to the maleic acid based route to BDO (US Patent 9,168,509, Oct. 27, 2015).

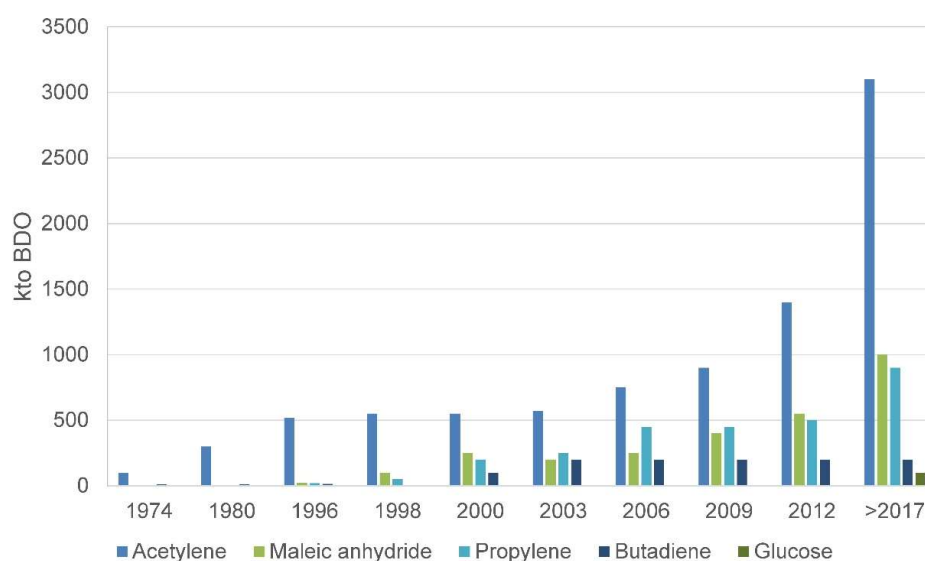


Figure 4: BDO production history and forecast

The production of BDO is dominated by the acetylene process. Especially in the last years, high amounts were manufactured by Chinese companies. (Ostgard 2015). The fabrication based on maleic anhydride and propylene rose in similar fashion, however, Ostgard proposes that maleic anhydride processes will not prevail due to low yields and high costs of mitigating maleic acid corrosion. The fermentation of D-glucose still plays a minor role in BDO manufacturing and it remains to be seen, whether it will come out ahead.

However, the finite nature of crude oil as well as the climate change urges the chemical industry to replace energy-intensive petrochemical processes in order to assure the supply of base and special chemicals in the future. Already, bio-based approaches for producing BDO begin to challenge the conventional routes as they promise: (1) independence from price volatility of petroleum derived

chemicals, (2) reduced carbon footprint, and (3) improved process economics compared to the conventional routes.

The first biotechnological route, described and applied by Genomatica Inc. (USA) in an Italy-based plant, is the direct fermentation of D-glucose to bio-BDO via the tricarboxylic acid (TCA) cycle by an engineered *Escherichia coli* (*E. coli*) strain (Burgard et al., 2016). Since BDO is a non-natural chemical, a new biosynthetic pathway had to be constructed with enzymes that function on non-native substrates. Starting from the TCA cycle intermediate succinyl-CoA, five heterologous steps were required. The enzymes for these reactions were identified by bioinformatic analysis of known enzymes acting on similar substrates or performing analogous transformations (Figure 5, blue arrows). In total, 19 enzymes are involved in the conversion of D-glucose to BDO, which reaches titers of $>125 \text{ g L}^{-1}$, rates of $>3.5 \text{ g L}^{-1} \text{ h}^{-1}$, and a yield of 0.40 g g^{-1} (80% of theoretical yield). Remaining side-products are acetate, ethanol, glutamate, and 4-aminobutyrate.

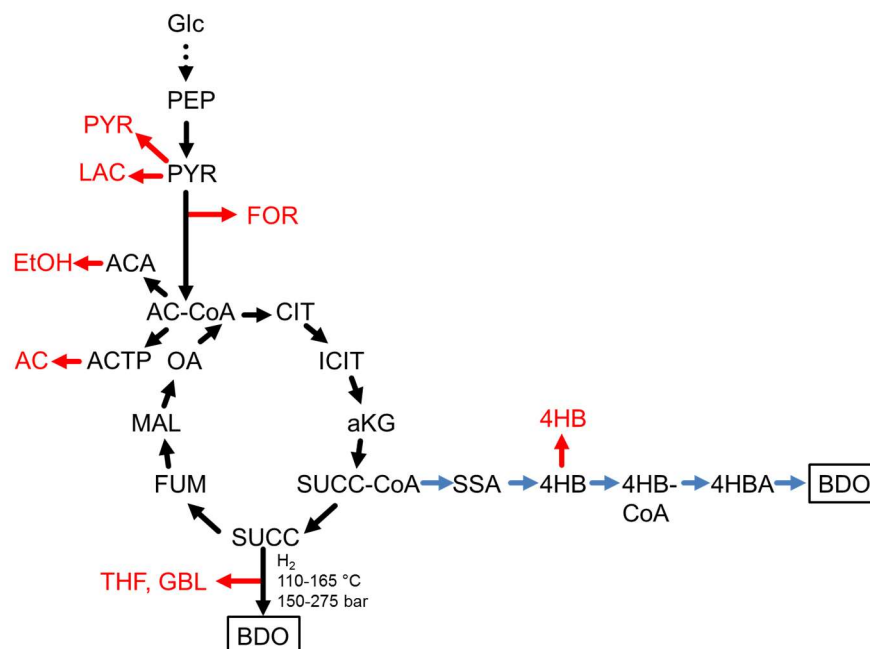


Figure 5: Fermentation processes for bio-BDO starting from D-glucose via the TCA cycle

Glc: D-glucose, PEP: phosphoenolpyruvate, PYR: pyruvate, LAC: lactate, FOR: formate, Ac-CoA: acetyl-CoA, ACA: acetaldehyde, EtOH: ethanol, ACTP: acetylphosphate, AC: acetate, CIT: citrate, ICIT: isocitrate, aKG: α -ketoglutarate, SUCC-CoA: succinyl-CoA, SUCC: succinate, FUM: fumarate, MAL: malate, OA: oxaloacetate, SSA: succinate semialdehyde, 4HB: 4-hydroxybutyrate, 4HB-CoA: 4-hydroxybutyryl-CoA, 4HBA: 4-hydroxybutanal, BDO: 1,4-butanediol, THF: tetrahydrofuran, GBL: γ -butyrolactone.

Black arrows: natural metabolic pathway (solid: one enzyme, dotted: nine enzymes), blue arrows: artificial pathway, red arrows: side products. The figure is adapted from Vaswani (2012).

To obtain such high titers, productivity and yield, great efforts were necessary: Overall, 16 sequences (14 encoding enzymes) were deleted from the host genome, 5 genes (encoding enzymes) were overexpressed, and nine enzymes were engineered for better performance properties (Burgard et al., 2016). These optimizations were identified and performed by a set of methods: metabolic modeling, dynamic modeling, ^{13}C flux analysis, transcriptomics, proteome profiling, directed evolution, targeted overexpression and gene deletions, modifications of the host genome to increase phage resistance and genome stability, and fermentation process optimization. The pure product (over 99.5%) is obtained by a rather energy-intensive process, which is due to the high boiling point of BDO. First, the broth is

sterilized, and cells are removed by centrifugation. The cell-free solution is then ultrafiltrated to remove large biomolecules and passed over an ion exchange column to remove salts. Finally, water is evaporated and the crude product is purified further by distillation. A life cycle analysis of this process, compared to the traditional petrochemical Reppe process, revealed up to 83% lower total CO₂-equivalent emissions per kg BDO and 67% lower fossil energy usage (Burgard et al., 2016).

A similar route was developed by BioAmber Inc. (USA), who collaborated with Evonik Industries (Germany), Dupont (USA), and Johnson Matthey Davy Technologies (Great Britain) for the production of bio-BDO and THF. Here, bio-BDO is obtained by the chemical hydrogenation of bio-succinic acid, which is produced by fermentation of D-glucose using an engineered *Escherichia coli* strain (Vaswani, 2012). The metabolic pathway is very similar to the one for direct BDO production, since an intermediate of the TCA cycle is produced. Therefore, the same side-products as above can be formed with exception of 4-hydroxybutyrate. The following chemical hydrogenation is performed at 110-165 °C and 150-275 bar. The catalyst used is 0.4% Fe, 1.9% Na, 2.66% Ag, 2.66% Pd, 10% Re on 1.8 mm carbon support. With this catalyst 99.7% succinic acid are converted to BDO with over 90% selectivity and minimal side reactions of THF and γ -butyrolactone (Bhattacharyya and Manila, 2011).

The major drawback that is still encountered in fermentation of microorganisms in general, is the different objective of the operator and the host cell: While the cell attempts to live, grow and replicate, the operator requires the desired product in high titers, productivity, and yield. Using enzymatic cascade reactions *in vitro* is a promising way to separate these different needs from another.

1.2 *In vivo* versus *in vitro* enzymatic cascade reactions

1.2.1 Definition of the term enzymatic cascade reaction

A cascade reaction or cascade catalysis is, in a broad definition, the combination of various chemical steps in one pot without isolation of the intermediates. (Kroutil and Rueping, 2014). The advantages of cascade reactions are therefore the possibility to avoid instable reaction intermediates, drive thermodynamically unfavorable reactions towards completion, and lower costs due to the absence of multiple purification steps.

Enzymatic cascade reactions are comprised of biocatalysts (enzymes). In contrast, cascade reactions can also be constituted of chemical catalysts or a mixture of both, termed chemo-enzymatic cascade reactions.

The fermentation of microorganisms is an *in vivo* enzymatic cascade reaction. Here, the complex reaction cascades of a cell are used to produce a chemical of interest. *In vitro* enzymatic cascade reactions, newly termed Systems Biocatalysis, is an emerging concept of organizing enzymes *in vitro* to construct complex reaction cascades for an efficient, sustainable synthesis of valuable, chemical products (Fessner, 2015). These reaction pathways can be derived from natural metabolic pathways or they can be artificial. Other terms, which relate to similar concepts, are: *in vitro* metabolic engineering (G. S. Chen et al., 2017; Guo et al., 2017; Myung et al., 2014; Ninh et al., 2014), Synthetic Pathway Biotransformations (SyPaB) (Y.-H. P. Zhang et al., 2010), the Synthetic Biochemistry System (Korman et al., 2014), Synthetic Metabolic Engineering (Ye et al., 2012), and Cell-Free Metabolic Engineering (CFME) (Dudley et al., 2014; Guterl et al., 2012). Depending on the platform, purified/semi-purified enzymes or crude cell lysates are used.

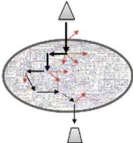
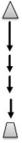
1.2.2 Comparison of *in vivo* and *in vitro* enzymatic cascade reactions

While both concepts share the advantage of utilizing cheap and renewable substrates, e.g., abundant sugars, other considerations concerning the reaction design vary greatly. Fermentation relies on the metabolism of the cell, which is still not understood to such an extent that consequences of changes to the metabolic network can easily be predicted (Petzold et al., 2015). The regulatory mechanisms for cell growth and gene expression and the need to transport substrates and products across the cell membrane further increase the complexity. Adjustments to the metabolic network by genetic engineering to redirect the flux of the substrate into the desired product, although possible, are hard to predict and cannot be transferred from one organism to another. Furthermore, these adjustments are limited to physiological conditions in order to maintain cell viability. In addition, only a very limited number of microorganisms can to date be genetically engineered at all. With no such needs, *in vitro* enzymatic cascade reactions and artificial pathways can be constructed without interference of enzymes competing for the same substrates and even toxic compounds can be obtained with that approach. Furthermore, enzyme promiscuity can be used as an advantage, as non-native side activities can become the main activity by choosing the reaction conditions accordingly. It is also possible to construct modules that can first be analyzed and optimized alone, before operated together (Taniguchi et al., 2017). Changes of the system, like adjustment of enzyme concentrations, pH, temperature, or the solvent, are easy to perform and predictable. The major drawbacks of *in vitro* enzymatic cascade reactions are the high costs for enzyme

production and purification, and the need to supply cofactors and energy equivalents, all of which is naturally available in the cell. In addition, enzymes can be less stable *in vitro* than *in vivo*, further increasing expenses. However, with prizes for enzyme purification decreasing (Y.-H. P. Zhang et al., 2016) and advances in stabilizing enzymes *in vitro* (Silva et al., 2017), Systems Biocatalysis may be on the road to industrial application. Also, because downstream processing is usually easier than with fermentation broths, as less components have to be removed to obtain a pure product. In fermentations, often a number of side products are formed and yields are diminished if the substrate is used up by the cell for growth.

The advantages and disadvantages of *in vivo* and *in vitro* enzymatic cascade reactions are summarized in Table 1.

Table 1: Comparison of *in vivo* and *in vitro* enzymatic cascade reactions

Type of enzymatic cascade reaction	<i>In vivo</i> 	<i>In vitro</i> 
Reaction design	<ul style="list-style-type: none"> + Cheap, renewable substrates can be used + Optimization by metabolic engineering, directed evolution or selection possible - Cell viability has to be maintained - Not transferrable from one organism to another 	<ul style="list-style-type: none"> + Cheap, renewable substrates can be used + Freedom in pathway design + Artificial pathways possible, especially with promiscuous enzymes + Toxic compounds or intermediates can be produced
Controllability	<ul style="list-style-type: none"> - Transportation across cell boundaries necessary - Fermentation conditions are predefined by the host organism - Modifications are hard to predict due to complex regulatory mechanisms for cell growth and gene expression 	<ul style="list-style-type: none"> + No barriers + Enzyme concentrations can be adjusted easily + Reaction conditions can be chosen by the operator + Changes are predictable + Modular setup possible, which allows analysis and optimization with less complexity
Costs	<ul style="list-style-type: none"> + The cell's production, regeneration and recycling pathways can be used for enzymes and cofactors - Downstream-processing can be laborious and costly 	<ul style="list-style-type: none"> + Separation and purification of products is less complex + Various cofactor regeneration systems are available - Purified enzymes and cofactors need to be supplied - Enzymes can be less stable <i>in vitro</i>
Product titer and yield	<ul style="list-style-type: none"> + High titers can be achieved with sufficient substrate - Substrate is partially used up by the cell for growth - Side products can be formed 	<ul style="list-style-type: none"> + High titers and yields are possible + No or less formation of side products
Application	Various examples	At research stage

1.3 Development of *in vitro* enzymatic cascade reactions

1.3.1 Pathway design and the role of enzyme promiscuity

One of the main advantages of *in vitro* enzymatic cascade reactions is the freedom in pathway design. Enzymes can be assembled in any constellation according to the desired reactions. Even though this is in theory also true for *in vivo* pathway design with heterologous expression systems at hand, one still needs to take into account the cell's energetics and metabolism. As this is a highly complex system, advantageous changes cannot be predicted easily. Computational tools have been developed to assist in finding the pathway best suited for the desired product and to identify genes for deletion to ensure substrate flux into the product (Carbonell et al., 2016; Medema et al., 2012). However, the optimization by such "design-build-test" (DBT) cycles are time-consuming as they depend on cell growth. In contrast, *in vitro* DBT cycles are fast and do not require special equipment like fermenters.

In general, complexity is a main obstacle in enzymatic cascade reactions. Natural enzymes have evolved various control mechanisms for the cell to maintain a balanced metabolism and survive under various environmental conditions. Therefore, enzymes are subject to nonlinear kinetics, such as Michaelis–Menten-type kinetics, which is often complicated by feedback, cooperative or allosteric elements. With this in mind, *in vitro* enzymatic cascade reactions should only involve a minimum of enzymes and cofactors to obtain the target compound. Furthermore, cofactor balance to avoid the stoichiometric use of such expensive substrates is a pre-requisite for an economical process and can be achieved either within the cascade reaction or by including regeneration modules. One of the main advantages of *in vitro* enzymatic cascade reactions is the design of artificial pathways that can be constructed to obtain non-natural compounds, to shorten natural metabolic pathways or to bypass cofactor usage (Bogorad et al., 2013; Guterl et al., 2012; Ye et al., 2012). This can be accomplished, for example, by combining various pathways that occur naturally in different organisms or by using promiscuous enzymes.

Enzyme promiscuity, that is, relaxed specificity, is more and more appreciated in white biotechnology (Arora et al., 2014). It can be divided into catalytic promiscuity, where different chemical reactions are catalyzed by the same enzyme, substrate promiscuity, where different substrates are converted by the same type of chemistry, and condition promiscuity, where the reaction can be guided by medium engineering (Arora et al., 2014; Hult and Berglund, 2007). Furthermore, enzyme promiscuity can be present in native enzymes, called natural promiscuity, or the enzyme can be engineered to perform a promiscuous activity, called induced promiscuity. Substrate promiscuity (also referred to as substrate ambiguity) has already been reported in 1898 for maltase by Hill. However, the definition of substrate promiscuity is still not coherent in literature. Therefore, Gupta (2016) states that this term should only be used when substrates other than the physiologically relevant substrate/s are accepted. It is generally accepted that natural substrate and catalytic promiscuity hold an evolutionary potential. New functions can evolve without negative trade-offs in the native activity, leading to a generalist enzyme. Later on, the generalist can become a specialist for a new catalytic function (Copley, 2014, 2015; Khersonsky and Tawfik, 2010). The mechanisms leading to promiscuity are so far not fully understood. One hypothesis is active site plasticity, which is achieved, for instance, by flexible loops in proximity to a highly ordered core structure (Nobeli et al., 2009; Pandya et al., 2014). Others are substrate ambiguity by different

modes of interactions within the same active site (Sevrioukova and Poulos, 2013), and cofactor ambiguity caused by different metal-cofactors bound in the active site (Baier et al., 2015).

Promiscuous enzymes can be identified *in vitro* by screening against a set of substrates to generate a substrate specificity profile. Here, the reaction conditions can be different from the physiological conditions. Thereby, the enzymes can be “forced” to handle substrates usually not encountered *in vivo*. Computational tools have also been developed to assist in finding promiscuous activities, like MINEs, SABER, or ECBLAST (Jeffryes et al., 2015; Nosrati and Houk, 2012; Rahman et al., 2014). However, they are limited to enzymes with known crystal structures.

Even though promiscuous enzymes can also be applied in *in vivo* enzymatic cascade reaction, the main activity needs to be cancelled or else the enzyme would mainly perform its natural reaction instead of the desired promiscuous reaction. *In vitro*, this problem is circumvented by supplying only the substrate of interest in the reaction mixture. Therefore, less effort has to be taken to abolish the activity toward the native substrate.

1.3.2 Characterization of enzymes

In order to orchestrate enzymes in an *in vitro* enzymatic cascade reaction, experimental information on the enzymes involved needs to be collected. This includes, but is not limited to, kinetic parameters (V_{\max} and K_m), activity profiles in regard of substrates, pH values, buffers, metal ions, and temperatures. More specific information for a certain cascade reaction is the effect of high concentrations of a cascade’s initial substrate and end product, as these are present in high amounts during the reaction, and can therefore cause inhibition. But also intermediates that are only present in low quantities can inhibit enzymes and should be taken into account, if they can be isolated. Enzyme stability is also a measure, which should be assessed, as it plays a critical role in *in vitro* enzymatic cascade reactions. Different types of criteria can be used to define and measure enzyme stability: (1) thermodynamic stability, (2) thermal stability, (3) kinetic stability, and (4) process stability (Bommarius and Paye, 2013).

Thermodynamic stability

The thermodynamic stability of an enzyme is given by the Gibbs free energy of unfolding ΔG at a given temperature with

$$\Delta G = -RT \ln(K) \quad (1)$$

ΔG : Change in Gibbs free energy, R: universal gas constant, T: temperature, K: equilibrium constant

Assuming a two-state model native [N] \leftrightarrow unfolded [U], the equilibrium constant, $K = [N]/[U]$, can be derived by measuring the native and unfolded fractions of the protein at a given temperature, usually 25 °C.

Thermal stability

The thermal stability is described by the melting temperature (T_m). At this temperature half of the protein is present in the unfolded state with $K = 1$ and thus $\Delta G = 0$ (see equation 1). Whereas the thermodynamic

stability of mesophilic and thermophilic proteins can be the same at temperatures below T_m , thermophilic proteins are characterized by a higher thermal stability.

Kinetic stability

The kinetic stability refers to the unfolding kinetics of a protein and can be assessed by the half-life $t_{1/2}$ at defined conditions. Thereby, first-order deactivation kinetics are assumed, which allows the determination of the apparent deactivation constant ($k_{d, app}$) by time-dependent activity measurements. $[N]$ refers to the protein in the active native state:

$$[N](t) = [N]_0 e^{-(k_{d, app})t} \quad (2)$$

The half-life is then defined by the time, after which 50% activity (=enzyme in the native state) is left.

$$t_{1/2} = \frac{-\ln(0,5)}{k_{d, app}} \quad (3)$$

Process stability

Process stability compares the kinetic stability of an enzyme to its activity and is a measure of its productivity. Usually it is given by the *total turnover number* TTN. The TTN is a dimensionless number calculated from the apparent catalytic turnover ($k_{cat, app}$) divided by the apparent deactivation constant ($k_{d, app}$):

$$TTN = \frac{k_{cat, app}}{k_{d, app}} \quad (4)$$

Together, the data from activity profiles, inhibitory effects, and stability, can guide medium engineering to enhance both activity and stability of the enzymes within the cascade reaction to ensure complete conversion of the substrate to the desired product (Bommarius and Paye, 2013; Castillo et al., 2016). In addition, it can be used to model an enzymatic cascade reaction *in silico* to obtain information on possible bottlenecks and how enzyme concentrations can be adjusted to one another (Hold et al., 2016; Ringborg and Woodley, 2016).

1.3.3 Enzyme engineering

Natural enzymes often do not display (all) the characteristics needed for their application in an *in vitro* enzymatic cascade reaction. These are: high activity toward the substrate of interest, no inhibition, and high stability at the desired reaction conditions. As already described in the section above, medium engineering can be a way to reach these goals. However, usually a compromise between all enzymes of the cascade reaction has to be found, which comes at the cost of efficiency.

Enzyme engineering is the method of choice to alter enzyme properties by modifying the sequence of the protein, and hence its structure. It is a rather young technique that became possible with the development of the polymerase chain reaction by Kary Mullis in 1983 and the establishment of oligonucleotide-based, site-directed mutagenesis by Michael Smith in 1982. For this, they were awarded the Nobel Prize in Chemistry 1993. Since the 1990s, enzyme engineering has been applied extensively to elucidate enzyme function and mechanisms, and also to alter the properties of enzymes. For the latter, the pioneering work of Francis Arnold and Willem Stemmer in using directed evolution (by error-prone

PCR and DNA shuffling, respectively) for the creation of mutant libraries in combination with high-throughput screening, was a breakthrough (W.-p. Chen and Kuo, 1993; Stemmer, 1994). This approach recreates the natural evolutionary process of variation and screening/selection without the need of in-depth knowledge of the sequence or mechanism of the enzyme. Contrary, rational design based on computational techniques is the second approach that emerged for engineering desired protein properties. Bringing both concepts together, combinatorial/semi-rational methods were developed, which shortlist sequence libraries of evolutionary approaches or assist directed evolution methodologies. By semi-rational design, smaller, higher quality libraries are generated, which reduces the screening effort tremendously. For comparison, the sequence space of a small protein of 400 amino acids is 20^{400} or, if for example only one amino acid is exchanged for any of the other 19 amino acids in this protein, there are already 7,600 different variants. For two amino acids, the number rises to 144,400, for three the total is about 2.7×10^6 and for four substitutions it is 5.2×10^7 . Using information on protein sequence, structure, function and predictive algorithms, researchers preselect target sites – so-called hot spots – and can limit amino acid diversity. Thereby a focused library with reduced size and proposedly higher functional content is built. To highlight this methodology, some examples of sequence- and structure-based enzyme redesigns are given:

The enantioselectivity of an esterase was enhanced using the 3DM database (Nobili et al., 2013). This database (<https://3dm.bio-product.nl>) integrates protein sequence and structural information from GenBank and the Protein Databank (PDB) to construct comprehensive alignments of protein superfamilies (Kuipers et al., 2010). It includes self-updating information on the functional role of individual amino acid residues and details on their mutability from literature.

The HotSpot Wizard 2.0 server (<https://loschmidt.chemi.muni.cz/hotspotwizard>) assists researchers in finding the most beneficial amino acid substitution by combining information from sequence and structure database searches with functional data to create a mutability map for a target protein (Bendl et al., 2016; Pavelka et al., 2009). One of many examples from “the bench” is the engineering of a xylanase for enhanced activity and pH stability (Wang et al., 2016).

Different studies have shown that protein stability at high temperatures and in organic solvents can be increased by introducing ancestral or consensus residues (Dror et al., 2014; Lehmann et al., 2000). It is assumed that conserved amino acids contribute to enzyme stability, since they have survived the evolutionary process. The conserved residues are identified by multiple sequence alignments of related proteins.

Since the methods for mutagenesis, computational tools and their combinations are so numerous, they cannot be covered in this brief introduction of enzyme engineering. Reviews on the subject were written, for instance, by Turner (2009), Lutz (2010), Davids (2013), Packer and Liu (2015), and Khushboo and Krishna (2016).

Often the engineering of new properties comes at the cost of stability (Tokuriki and Tawfik, 2009). Approaches to tackle this problem are: (1) developing algorithms from datasets that correlate function and stability (Carlin et al., 2017), (2) engineering enzymes from thermophiles, which are usually more stable than enzymes from mesophiles (Besenmatter et al., 2007), (3) screening for both, activity and stability, by creating neutral drift libraries, where only stable variants are selected for further rounds of directed evolution (Bommarius and Paye, 2013).

1.4 An *in vitro* enzymatic cascade reaction from D-glucose to BDO

Due to the disadvantages faced in fermentation processes in general and in the production of BDO in particular, an artificial *in vitro* enzymatic cascade reaction from D-glucose to BDO was proposed by Sieber et al. (2012) (Figure 6). It can be divided into three modules: (1) An oxidative module, where D-glucose is converted to D-glucarate, (2) a dehydration module, where two water molecules as well as one carbon dioxide is released to form ketoglutaric semialdehyde, and (3) a reductive module including a second decarboxylation, which yields the final product BDO.

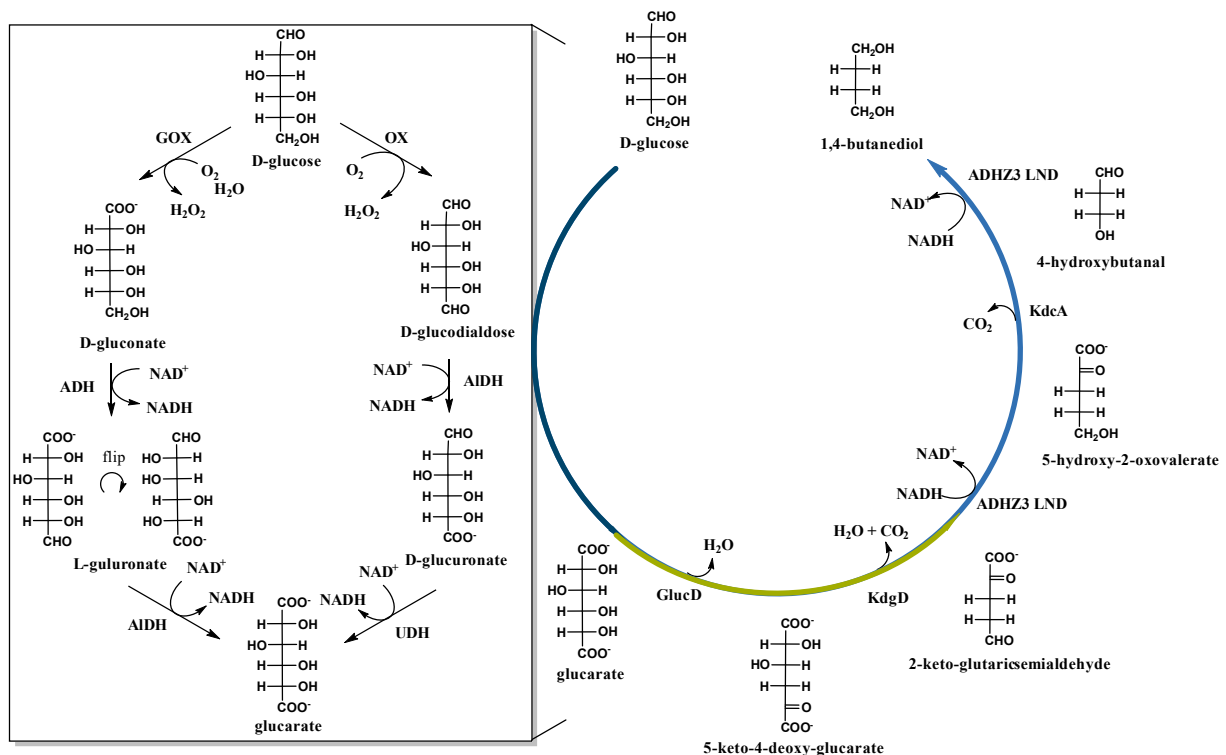


Figure 6: Proposed *in vitro* enzymatic cascade reaction from D-glucose to BDO

Dark blue: oxidative module: D-glucose is converted to D-glucarate. Here, two routes are possible (box). The first one starts with the oxidation of D-glucose at C1 by glucose oxidase (GOX), followed by two oxidations of the terminal C-atom by an alcohol dehydrogenase (ADH) and aldehyde dehydrogenase (AIDH). In the second route D-glucose is oxidized by an oxidase (OX) at C6, followed by oxidation of C6 by an AIDH and oxidation at C1 by uronate dehydrogenase (UDH).

Green: dehydration module: two water molecules as well as one carbon dioxide is released to form ketoglutaric semialdehyde by the action of glucarate dehydratase (GlucD) and 5-keto-4-deoxy-glucarate dehydratase (KdgD).

Light blue: reductive module including a second decarboxylation, which yields the final product BDO. Here, the triple variant of ADHZ3 from *E. coli* with the amino acid substitutions S199L/S200N/N201D (ADHZ3 LND) and the branched-chain ketoacid decarboxylase (KdcA) are involved.

The first module, the oxidation of D-glucose to D-glucarate, is crucial for this short route to BDO as natural pathways involve up to nine different enzymes. Two pathways are theoretically possible (Figure 6, box): one starts with the oxidation of C1 to D-gluconate by glucose oxidase (GOX). For the subsequent non-natural oxidations of C6 to L-gulonate and further to D-glucarate, NAD^+ -dependent alcohol and aldehyde dehydrogenases (ADH and AIDH) need to be identified. The second possible pathway starts with the non-natural oxidation of D-glucose at C6 by an oxidase (OX) yielding D-glucodialdose. This intermediate probably forms a ring (Parikka and Tenkanen, 2009), therefore, an AIDH must oxidize C1 instantly to give D-glucuronate, which can be converted to D-glucarate by uronate dehydrogenase (UDH)

from *Agrobacterium tumefaciens* (Boer et al., 2010; Pick et al., 2015). Again, the last two steps generate two moles of NADH.

The second part of the cascade reaction is constituted of two dehydratases, which can be found in the natural degradation pathway of D-glucarate in various species. Glucarate dehydratase (GlucD) from *Actinobacillus succinogenes* and 5-keto-4-deoxyglucarate dehydratase (KdgD) from *Acinetobacter baylyi* (Pick et al. 2017) were selected in a previous work (Pick, in progress). KdgD also catalyzes a decarboxylation, yielding ketoglutaric semialdehyde. Both dehydratases are Mg²⁺-dependent.

In the reductive module, the alcohol dehydrogenase Z3 (ADHZ3) from *E. coli* reduces the semialdehyde. This enzyme has been engineered for cofactor ambiguity and the triple variant S199L/S200N/N201D (ADHZ3 LND) accepts both, NADH as well as its native cofactor NADPH (Pick et al., 2014). After decarboxylation by the branched-chain ketoacid decarboxylase (KdcA) from *Lactobacillus lactis*, ADHZ3 LND also catalyzes the second reduction to BDO.

The only cofactor necessary in this cascade reaction is NAD⁺ and it is recycled within the cascade. Additionally, Mg²⁺ and thiamine pyrophosphate have to be added in catalytic amounts for the activity of the dehydratases and KdcA, respectively. Along with D-glucose, oxygen has to be supplied as a substrate for the oxidase.

1.5 Aim of this work

1.5.1 Identification of enzymes for the oxidation of D-glucose to D-glucarate

In either pathway leading from D-glucose to D-glucarate, one enzyme can be found in nature, GOX and UDH, respectively. However, for the remaining reactions, enzymes need to be identified. That is, either an ADH and AIDH or an OX and an AIDH. From natural pathways using similar substrates and from literature research, enzyme candidates for the first oxidation steps should be identified and tested for their activity toward the two commercially available substrates D-glucose or D-gluconate, respectively.

1.5.2 Enzyme characterization and engineering

For the evaluation of separate modules of the cascade reaction, NAD(H) recycling will be necessary. For NADH recycling the commercially available formate dehydrogenase from *Candida boidinii* can be used; whereas for NAD⁺ recycling, a water-forming NADH oxidase (NOX) should be characterized in this work.

Enzymes exhibiting poor properties for the application within the proposed cascade reaction should be engineered. The focus was on UDH from *Agrobacterium tumefaciens* for enhanced stability. Furthermore, KdcA from *Lactobacillus lactis* was engineered for enhanced activity toward the unnatural substrate 5-hydroxy-2-oxovalerate (Hov) in the Master thesis of Johannes Weigl (2014).

1.5.3 Setup of *in vitro* enzymatic cascade reactions

For the screening of KdcA variants with increased activity toward Hov, the substrate is not commercially available. Therefore, it should be synthesized from D-glucuronate using the enzymes UDH, GlucD, KdgD, and ADHZ3 LND in a cascade reaction.

Another interesting target compound that can be synthesized from D-glucuronate is α -ketoglutarate. For this, only ADHZ3 LND needs to be replaced with 2-keto-glutaric semialdehyde dehydrogenase (KgsalDH) from *Pseudomonas putida* in the last step. In this cascade reaction, two NAD⁺ molecules are consumed and regeneration of the cofactor can be accomplished with NOX (see 1.5.2). This cascade reaction should be examined to evaluate the best conditions for these enzymes to work in one pot, the influence of different initial cofactor concentrations as well as the initial concentration of the cofactor recycling enzyme NOX, and inhibitory effects of the substrate, intermediates, and the product on the enzymes. Furthermore, since NOX is oxygen-dependent, the effect of two reactor designs, with and without oxygen supplementation, will be tested. These results will also be of interest for the cascade reaction from D-glucose to BDO, since the oxidation of D-glucose should be performed with an oxygen-dependent oxidase.

2 Materials

2.1 Chemicals

All chemicals were of analytical or biochemical purity and were purchased from the following companies:

AppliChem GmbH	Darmstadt
Bio-Rad Laboratories GmbH	Munich
Biozym Scientific GmbH	Hess. Oldendorf
Bode Chemie GmbH	Hamburg
Carl Roth GmbH & Co. KG	Karlsruhe
GE Healthcare Europe GmbH	Freiburg
Gerbu Biotechnik GmbH	Gailberg
Life Technologies GmbH	Darmstadt
Merck KGaA	Darmstadt
Serva Electrophoresis GmbH	Heidelberg
Sigma-Aldrich	Deisenhofen
VWR International GmbH	Darmstadt

2.2 Enzymes

Restriction enzymes were purchased from New England Biolabs GmbH, Frankfurt (Main). The polymerases used in this work were from the following companies:

OptiTherm DNA-Polymerase	Rapidozym GmbH, Berlin
Taq DNA Polymerase with ThermoPol® Buffer	New England Biolabs GmbH, Frankfurt (Main)
Phusion High-Fidelity DNA-Polymerase	New England Biolabs GmbH, Frankfurt (Main)

Bovine UDP-glucose-6-dehydrogenase (U7251) and formate dehydrogenase (FDH) from *Candida boidinii* (F8649-50UN) were from Sigma Aldrich, Deisenhofen.

2.3 Kits

GeneJET™ Plasmid Miniprep Kit	Thermo Fischer Scientific, Fermentas, St.Leon-Rot
NucleoSpin® Gel and PCR Clean-up Kit	Macherey-Nagel GmbH & Co. KG, Düren
CloneJET PCR Cloning Kit	Thermo Fischer Scientific, Fermentas, St.Leon-Rot
Roti®-Nanoquant Kit	Carl Roth GmbH & Co. KG, Karlsruhe

2.4 Devices

Given in alphabetical order.

Autoclave: Varioklav 135S

Thermo Fischer Scientific

Centrifuges:

Sorvall RC 6+

Thermo Fischer Scientific

Rotor F10-6x500y

Piramoon Technologies Inc, Santa Clara, USA

Rotor F9-4x1000y

Piramoon Technologies Inc, Santa Clara, USA

Rotor SH-3000

Thermo Fischer Scientific

Rotor SS-34

Thermo Fischer Scientific

Fresco 21 Centrifuge

Thermo Fischer Scientific

Concentrator Savant SpeedVac Plus SC210A

Thermo Fischer Scientific

with Savant Refrigerated Vapor Trap RVT100

Freezer -20 °C

Liebherr-Hausgeräte, Ochsenhausen

Freezer -80 °C Forma 906 -86°C ULT

Thermo Fischer Scientific

Freeze-dryer Alpha 2-4 LD plus

Martin Christ Gefriertrocknungsanlagen GmbH

with vacuum pump RC 6

VACUUBRAND GmbH + Co. KG

Gel documentation: Gel iX Imager

Intas Science Imaging Instruments GmbH,
Göttingen

Gel electrophoresis:

Agarose electrophoresis apparatus

Bio-Rad Laboratories GmbH Munich

Mini-sub cell GT system

SDS electrophoresis chambers

Bio-Rad Laboratories GmbH Munich

Mini-PROTEAN®-Tetra Cell

Bio-Rad Laboratories GmbH Munich

Mini-Protean®3Multi-Casting Chamber

Bio-Rad Laboratories GmbH Munich

Power supply PowerPac™ Basic

Bio-Rad Laboratories GmbH Munich

Heating oven Function Line T12

Thermo Fischer Scientific, Heraeus

High-pressure homogenizer

Cell Disruption System Basic Z

Constant Systems, Daventry, Great Britain

Homogenizer Ultra Turrax T18 basic

IKA-Werke GmbH & C. KG, Staufen

Incubation cabinets:

Climate chamber KBF 240 E5.1/C

BINDER GmbH, Tuttlingen

Incubator Function Line B12

Thermo Fischer Scientific, Heraeus

Incubation shakers:

HAT Minitron

Infors AG, Bottmingen/Basel, Switzerland

MaxQ 2000

Thermo Fischer Scientific

TiMix 5 control

Edmund Bühler GmbH, Hechingen

Liquid chromatography:

ÄKTA™ purifier equipped with

GE Healthcare Europe GmbH, Freiburg

Pump P-900

GE Healthcare Europe GmbH, Freiburg

Sample pump UP-960

GE Healthcare Europe GmbH, Freiburg

Control unit UPC-900	GE Healthcare Europe GmbH, Freiburg
Columns:	
HisTrap FastFlow 5 mL	GE Healthcare Europe GmbH, Freiburg
HiTrap Desalting HiPrep 26/10 Desalting	GE Healthcare Europe GmbH, Freiburg
UltiMate 3000 RS LC System equipped with	Thermo Fischer Scientific, Dionex, Idstein
Degasser SRD 3400	Thermo Fischer Scientific, Dionex, Idstein
Pump module 3400RS	Thermo Fischer Scientific, Dionex, Idstein
Auto sampler WPS 3000TRS	Thermo Fischer Scientific, Dionex, Idstein
Column compartment TCC3000RS	Thermo Fischer Scientific, Dionex, Idstein
Diode array detector 3000RS	Thermo Fischer Scientific, Dionex, Idstein
Columns:	
Metrosep A Supp 10-250/4.0	
250 mm, particle size 4,6 µm	Deutsche Metrohm GmbH, Filderstadt
Gravity C18	
100 mm, 2 mm i.d.; particle size 1.8 µm	Macherey-Nagel
Magnetic stirrer:	
MR 3001 K	Heidolph Instruments GmbH & Co.KG, Schwabach
VMS-C7	VWR International GmbH
Variomag Telesystem	Thermo Fischer Scientific
Microliter pipets, electric:	
Transferpette® S -8 electronic 10-200 µL	BRAND GmbH & Co. KG, Wertheim
Research pro 8x 1200 µL	Eppendorf AG, Hamburg
Research pro 12x 300 µL	Eppendorf AG, Hamburg
Microwave MH 25 ED	ECG, Prague, Czech Republic
Microliter pipets, manual:	
Transferpette® S : 0,1-10.000 µL	BRAND GmbH & Co. KG, Wertheim
Microliter syringe, 25 µL	Hamilton AG, Bonaduz, Switzerland
PCR equipment:	
MJ Mini™ Personal Thermo Cycler	Bio-Rad Laboratories GmbH
MyCycler™ Thermal Cycler	Bio-Rad Laboratories GmbH
CFX96 Touch	Bio-Rad Laboratories GmbH
Ultrapure water system PURELAB Classic	ELGA LabWater, Celle
Ultrasonic Cleaner	VWR International GmbH
Ultrasonic homogeniser UIS250v	Hielscher Ultrasonics GmbH, Teltow
Sonotrode VialTweeter	
Sonotrode LS24d10	
pH meter and electrodes:	
FiveGo™	Mettler-Toledo GmbH, Gießen
FiveEasy™	Mettler-Toledo GmbH, Gießen
InLab® Expert Pro pH 0-14 ; 0-100 °C	Mettler-Toledo GmbH, Gießen
InLab® Micro Pro pH 0-14 ; 0-100 °C	Mettler-Toledo GmbH, Gießen

Rocking platform	VWR International GmbH, Darmstadt
Scales:	
Microscales Pioneer™ TE6101	Ohaus Europe GmbH, Nänikon, Switzerland
TE1502S	Sartorius AG, Göttingen
Thermoblock Tmix	Sartorius AG, Göttingen
Titrators:	
Titroline 7750	
Titroline 7000	Thermo Fischer Scientific
UV-Vis spectrophotometer:	
Multiskan Spectrum	Thermo Fischer Scientific
Varioskan	Thermo Fischer Scientific
Infinite 200 pro	Tecan Group Ltd., Männedorf, Switzerland
Nanophotometer P-class	Implen, Westlake Village, USA
Vacuum pump PC 2004 VARIO	VACUUBRAND GmbH & Co. KG, Wertheim
Vortex Genie 2	Scientific Industries Inc, Bohemia, USA
Waterbath ED-33	JULABO Labortechnik GmbH, Seelbach

2.5 Software and databases

Literature research:

SciFinder	Chemical Abstract Service (CAS); https://scifinder.cas.org/scifinder
NCBI	National Center for Biotechnology Information, http://www.ncbi.nlm.nih.gov/
Braunschweig Enzyme Database (BRENDA)	Technische Universität Braunschweig, Institut für Biochemie und Biotechnologie, http://www.brenda-enzymes.info/

In silico manipulation of DNA sequences:

Clone Manager 6	Scientific & Educational Software, USA
GATC™Viewer	GATC Biotech AG, Konstanz, http://www.gatcbiotech.com/en/textbausteine/downloadsundntzlicheLinks.html
Double Digest Finder	New England Biolabs GmbH, Frankfurt (Main) https://www.neb.com/tools-and-resources/interactive-tools/double-digest-finder

Sequence homology

Basic Local Alignment Search Tool	National Center for Biotechnology Information, http://blast.ncbi.nlm.nih.gov/
-----------------------------------	---

Protein characteristics

ProtParam tool	ETH Zürich, Swiss Institute of Bioinformatics http://web.expasy.org/protparam/
----------------	--

Other software

ChemDraw Ultra 12.0	Perkin Elmer Informatics, USA
Chem3D Pro 12.0	Perkin Elmer Informatics, USA
SigmaPlot 11.0	Systat Software GmbH, Erkrath
PyMOL v1.3r1 edu	DeLano Scientific LLC, USA
Yet Another Scientific Artificial Reality Application (YASARA)	YASARA Biosciences GmbH, Austria

2.6 Cultivation media and antibiotics

Heat-stable cultivation media, buffers, and solutions were autoclaved for 20 min at 121 °C and 2 bar. Heat-unstable solutions were filtered through a sterile syringe filter holder (0.2 µm, VWR International GmbH). For cultivation media consisting of various solutions, all solutions were sterilized before mixing. Fixed media were obtained by adding 1.5 % (w/v) agar-agar before autoclaving. All media used are listed in 2.6.1. For selective medium, sterilized antibiotics (2.6.2) were added after the medium was cooled down. Purified water, ddH₂O, (PURELAB Classic) was used for all media, buffers, and solutions. They were stored at room temperature, if not otherwise specified.

2.6.1 Culture media**LB medium (Bertani, 1951)**

0.5% (w/v) yeast extract, 1.0% (w/v) NaCl, 1.0% (w/v) tryptone

TB medium

1.2% (w/v) peptone, 2.4% (w/v) yeast extract, 1.25% (w/v) K₂HPO₄, 0.25% (w/v) KH₂PO₄

TBSB medium

TB medium containing sorbitol and betaine.

1.2% (w/v) peptone, 2.4% (w/v) yeast extract, 1.25% (w/v) K₂HPO₄, 0.25% (w/v) KH₂PO₄, 18.2% (w/v) sorbitol

After autoclaving 5 mM betaine (from a sterile 5 M stock solution) were added.

Autoinduction medium (Studier, 2005)**ZY-medium:**

0.5% (w/v) yeast extract, 1.0% (w/v) tryptone

50x 5052-solution:

25% (w/v) glycerin, 2.5% (w/v) D-glucose monohydrate, 10% (w/v) lactose monohydrate

20x NPS-solution:

6.6% (w/v) (NH₄)₂SO₄, 13.6% (w/v) KH₂PO₄, 14.2% (w/v) Na₂HPO₄

After sterilization the medium was prepared as follows:

	Volume (mL)	Final concentration
ZY-medium	928	
1 M MgSO ₄	1	1 mM
50x 5052	20	1x
20x NPS	50	1x
antibiotic 100 mg/mL	1	100 µg/mL
total volume	1000	

2.6.2 Antibiotics

Stock solutions of antibiotics were filtered (syringe filter holder 0.2 μm , VWR International GmbH) and stored in aliquots of 1 mL at -20 °C.

Ampicillin stock solution (1000x):

100 mg/mL ampicillin sodium salt

Kanamycin stock solution (1000x):

30 mg/mL kanamycin sulfate or 100 mg/mL kanamycin sulfate

2.7 Bacterial strains

For cloning, the strains *E. coli* XL1-Blue, DH5 α , JM109, and DH10B were used. For gene expression, *E. coli* BL21(DE3) was used. Table 2 gives details about the genotype and the reference of each strain.

Table 2: Bacterial strains

Strain	Genotype	Reference
<i>E. coli</i> XL1-Blue	<i>recA1 endA1 gyrA96 thi-1 hsdR17 supE44 relA1 lac</i> [F' <i>proAB lacIq</i> Δ M15 Tn10 (Tet ^R)]	Stratagene (Heidelberg)
<i>E. coli</i> DH5 α	F- <i>endA1 glnV44 thi-1 recA1 relA1 gyrA96 deoR nupG Φ80dlacZ</i> Δ M15 Δ (<i>lacZYA-argF</i>)U169, <i>hsdR17</i> (rK- mK+), λ -	Life Technologies (Darmstadt)
<i>E. coli</i> JM109	F' <i>traD36 proA⁺B⁺ lacI^q Δ(lacZ)M15/ Δ(lac-proAB) glnV44 e14⁻ gyrA96 recA1 relA1 endA1 thi hsdR17</i>	New England Biolabs GmbH, (Frankfurt (Main))
<i>E. coli</i> DH10B	F- <i>mcrA Δ(mrr-hsdRMS-mcrBC) ϕ80lacZ</i> Δ M15 Δ <i>lacX74 recA1 endA1 araD139 Δ(ara, leu)7697 galU galK λ-rpsL nupG</i> /pMON14272 / pMON7124	Life Technologies (Darmstadt)
<i>E. coli</i> BL21(DE3)	F- <i>ompT gal dcm hsdS_B(r_B⁻ m_B⁻) λ(DE3)</i>	Novagen (Merck, Darmstadt)

2.8 Plasmids and Strings DNA fragments

In Table 3 all plasmids and Geneart Strings DNA fragments (GeneArt, Regensburg) used or generated in this work are listed.

Table 3: Plasmids

Plasmid	Size (base pairs)	Description	Reference
pET28a	5369	Kan ^R ColE1 P _{lac} lacZ' <i>lacI</i> , gene expression vector with T7-expression system under the control of a lac-operator.	Novagen (Merck, Darmstadt)
pJET1.2	2974	Amp ^R , rep (pMB1), <i>eco47IR</i> , P _{lacUV5} , T7 promotor Cloning vector with blunt ends, which encodes a lethal gene when religated.	Thermo Fischer Scientific, (St.Leon-Rot)

Plasmid	Size (base pairs)	Description	Reference
pMA-T-ugdh-S.p.	3592	Amp ^R , contains <i>ugdh</i> from <i>Streptococcus pyogenes</i> ; codon-optimized for <i>E. coli</i>	GeneArt (Regensburg)
pET28a-NHis-ugdh-S.p.	6502	Kan ^R , contains <i>ugdh</i> from <i>Streptococcus pyogenes</i> ; codon-optimized for <i>E. coli</i> , cloned via restriction sites <i>NdeI</i> and <i>XhoI</i>	This work
pET28a-NHis-ugdh-E.c.	6460	Kan ^R , <i>ugdh</i> from <i>E. coli</i> , cloned via restriction sites <i>NdeI</i> and <i>XhoI</i>	This work
pJET-spsadh-NADP	3770	Amp ^R , contains GeneArt Strings DNA fragments of <i>spsadh-P</i> from <i>Sphingomonas</i> species A1, codon-optimized for <i>E. coli</i> . Cloned into pJET1.2 by blunt end ligation.	This work Strings DNA fragment: GeneArt (Regensburg)
pET28a-NHis-spsadh-NADP	6070	Kan ^R , <i>spsadh-P</i> from <i>Sphingomonas</i> species A1, codon-optimized for <i>E. coli</i> ., cloned via restriction sites <i>NdeI</i> and <i>XhoI</i>	This work
pJET- spsadh-NAD	3800	Amp ^R , contains GeneArt Strings DNA fragments of <i>spsadh</i> from <i>Sphingomonas</i> species A1, codon-optimized for <i>E. coli</i> . Cloned into pJET1.2 by blunt end ligation.	This work Strings DNA fragment: GeneArt (Regensburg)
pET28a-NHis-spsadh-NAD	6100	Kan ^R , contains GeneArt Strings DNA fragments of <i>spsadh</i> from <i>Sphingomonas</i> species A1, codon-optimized for <i>E. coli</i> ., cloned via restriction sites <i>NdeI</i> and <i>XhoI</i>	This work
pCBR-NHis-udh-A.t.	6138	Kan ^R , <i>udh</i> from <i>Agrobacterium tumefaciens</i> , cloned via <i>BsaI</i>	Pick et al. 2015
pCBR-NHis-glucD-A.s.	6669	Kan ^R , <i>glucD</i> from <i>Actinobacillus succinogenes</i> , cloned via <i>BsaI</i>	Generated by André Pick
pCBR-NHis-kdgD-A.b.	6252	Kan ^R , <i>kdgD</i> from <i>Acinetobacter baylyi</i> , cloned via <i>BsaI</i>	Pick et al. 2017
pET28a-NHis-adhZ3(LND)-E.c.	6313	Kan ^R , <i>adhZ3 LND</i> from <i>E. coli</i> , via quikchange	Pick et al. 2014
pET28a-NHis-kgsaldh-P.p.	6874	Kan ^R , <i>kgsaldh</i> form <i>Pseudomonas putida</i> , cloned via restriction sites <i>NdeI</i> and <i>XhoI</i>	This work
pET28a-NHis-nox-L.p.	6655	Kan ^R , <i>nox</i> from <i>Lactobacillus pentosus</i> , cloned via restriction sites <i>NdeI</i> and <i>XhoI</i>	Generated by Wolfgang Ott

2.9 Oligodeoxyribonucleotides

Oligodeoxyribonucleotide (primers) used for polymerase chain reactions were synthesized by biomers.net GmbH and are listed in Table 4.

Table 4: Oligodeoxyribonucleotides

Restriction sites are underlined, start and stop codons are bold.

Name	Length [-mer]	Application	Sequence (5'→3')
T7 Promotor	20	Forward primer for colony PCR	TAATACGACTCACTATAGG G
T7 Terminator	19	Reverse primer for colony PCR	CTAGTTATTGCTCAGCGG T
F-e.c.ugdh-NdeI	32	Forward primer for <i>ugdh</i> from <i>E. coli</i>	ATCGC <u>CATATG</u> AAAATCAC CATTCCGGTACTG
R-e.c.ugdh-XhoI	30	Reverse primer for <i>ugdh</i> from <i>E. coli</i>	ATCGCTCGAG TTAG TCGC TGCCAAAGAGAT
VF-s.p.ugdh	51	Simple cloning primer for <i>ugdh</i> from <i>Streptococcus pyogenes</i>	CGTGATATCTTTGGTCCG GAT TA ACTCGAGCACCAC CACCACCACCACTGA
VR-s.p.ugdh	45	Simple cloning primer for <i>ugdh</i> from <i>Streptococcus pyogenes</i>	TACCGGCAACTGCAATTT <u>CATATG</u> GCTGCCGCGCG GCACCAGGC
IF-s.p.ugdh	46	Simple cloning primer for <i>ugdh</i> from <i>Streptococcus pyogenes</i>	GGCCTGGTGCCGCGCGG CAGC <u>CATATG</u> AAAATTGC AGTTGCCGGTA
IR-s.p.ugdh	50	Simple cloning primer for <i>ugdh</i> from <i>Streptococcus pyogenes</i>	CAGTGGTGGTGGTGGT GTG <u>CTCGAG</u> TTA ATCGCG ACCAAAGATATCAG
F-kgsaldh-NdeI	36	Forward primer for <i>kgsaldh</i> from <i>Pseudomonas putida</i>	CGACAGC <u>CATATG</u> CCTGAG ATCCTCGGCCATAACTTC
R-kgsaldh-XhoI	39	Reverse primer for <i>kgsaldh</i> from <i>Pseudomonas putida</i>	GACGATCTCGAG TCAG AT CGCCCCGTCACTCCACTG ACC

3 Methods

Part of the method descriptions are derived or directly taken from the standard operating procedures of the Chair of Chemistry of Biogenic Resources, Technical University of Munich.

3.1 Microbiological methods

3.1.1 Cultivation and storage of *E. coli* strains

The following solutions were used:

99.5% p.a. glycerol

Liquid nitrogen

Preparation of liquid and solid media see 2.6

E. coli strains were cultivated at 37 °C in shaking flasks on a rotary shaker at 250 rpm (Thermo Fischer Scientific, MaxQ 2000). Strains with selection markers were cultivated in media containing the corresponding antibiotic. The cell growth was measured by the optical density (OD) of *E. coli* liquid cultures (3.1.2).

For the cultivation of single colonies, cell suspensions were spread on agar plates containing antibiotics, if appropriate, and were incubated at 37 °C.

For long-term storage, cell suspension were mixed with glycerol (50 % (v/v) final concentration), shock-frozen in liquid nitrogen and kept at –80 °C.

3.1.2 Determination of the optical density of *E. coli* cell suspensions

The OD of *E. coli* liquid cultures was measured at 600 nm in plastic cuvettes (Thermo Fischer Scientific, Multiskan Spectrum) in a total volume of 1 mL. An OD₆₀₀ of 1 corresponds to approximately 3.2x10⁸ cells/mL.

3.1.3 Preparation of competent *E. coli* cells for chemical transformation

The following solution were used:

• **50 mM CaCl₂ (sterile)**

• **85% (v/v) CaCl₂ (50 mM) with 15% (v/v) glycerol (sterile)**

Starting from a single colony, a preculture was prepared and 2 mL were used to inoculate 100 mL main culture. The cells were incubated at 37 °C on a rotary shaker (250 rpm) until an OD of 0.5-0.6 was reached. Next, the cells were harvested (Sorvall RC 6+ Centrifuge with SH-3000 rotor, 3.500g, 15 min, 4 °C) and cautiously washed with 10 mL ice-cold CaCl₂ solution. The volume was then increased to 50 mL and the cells were incubated for 1 h on ice. After harvesting, the cells were resuspended in 85% (v/v) CaCl₂ solution with 15% (v/v) glycerol to reach an OD of 50. Aliquots of 100 µL were shock-frozen in 1.5 mL reaction vessels and stored at –80 °C.

For the determination of the transformation efficiency, an aliquot of competent cells was transformed with 1 ng plasmid DNA (detailed procedure see 3.1.4). After a regeneration phase of 45-60 min, 100 μ L each of a dilution series were spread on agar plates and incubated at 37 °C overnight. The transformation efficiency was then calculated using the following formula:

$$T_E = \frac{n_{colonies} \times f}{m_{DNA}} \quad (5)$$

T_E	Transformation efficiency (colonies per μ g DNA)
$N_{colonies}$	Number of colonies on an agar plate
f	Dilution factor
m_{DNA}	DNA used for transformation in μ g

3.1.4 Transformation of chemically competent *E. coli* cells

Chemically competent cells were thawed on ice for about 10 min. 1 to 10 μ L (10 to 100 ng) plasmid DNA was added and the cells were incubated on ice for 30 min. After a heat shock at 42 °C for 60 s, the cells were cooled again for 5 min on ice and then resuspended in 900 μ L in pre-warmed LB medium. After a regeneration phase of 1 h at 37 °C on a rotary shaker (250 rpm), 100 μ L of the diluted cell suspension as well as 100 μ L of the resuspended cell pellet were spread on agar plates and incubated at 37 °C overnight.

3.1.5 Expression of recombinant genes in *E. coli*

For the expression of recombinant genes, *E. coli* BL21(DE3) was transformed with the corresponding plasmids from Table 3.

3.1.5.1 Gene expression for analytics

For the analysis of gene expression into soluble proteins, small-scale expression tests were performed in a volume of 20 mL of various selective media (2.6) in a 100 mL shaking flask. From a single colony, a preculture (5 mL) was prepared, which was used for inoculation of the main cultures. After 3 h at 37 °C and 150 rpm, cultures were induced with 1 mM isopropyl- β -D-thiogalactopyranoside (IPTG), if necessary, and were incubated either at 16 °C or at 37 °C overnight.

Cells were then harvested (2 to 4 mL), resuspended in 1 mL of buffer, and disrupted by sonication (sonotrode *VialTweeter*, 100 % amplitude, 0.6 ms, 3x 45 sec pulse/45 sec cooling on ice). The soluble fraction was obtained by centrifugation (14.000 g, 30 min, 4 °C) and both the soluble and insoluble fraction were analyzed by SDS-PAGE (3.3.4).

3.1.5.2 Gene expression for protein preparation

For the preparation of recombinant proteins, the corresponding genes were expressed in a volume of 200 to 1000 mL of selective medium (2.6) in a 1000 to 5000 mL shaking flask. The choice of medium depended on the outcome of gene expression tests (3.1.5.1). From a single colony, a preculture (50 mL) was prepared, which was used for inoculation of the main cultures to reach an OD of 0.1. The cells were incubated 3 h at 37 °C and 150 rpm until an OD of 0.5-0.6 was reached. Then cultures were induced with 1 mM IPTG, if necessary, and were incubated overnight either at 16 °C or at 37 °C, depending on

the outcome of the gene expression tests. The cells were harvested by centrifugation (Sorvall, RC 6+ Centrifuge with SH-3000 rotor, 4.000g, 15 min, 20 °C) and either directly used for protein purification (3.3.5) or stored at -20 °C.

3.2 Molecular biological methods

3.2.1 Determination of DNA concentrations

The concentration of DNA solutions was measured photometrically at 260 nm (Thermo Fischer Scientific, Multiskan or Implen, Nanophotometer P-class). According to the law of Lambert-Beer, at 260 nm and a layer thickness of 1 cm, an extinction of 1.0 corresponds to 50 µg/mL of double stranded DNA or 33 µg/mL of single stranded DNA. Pure DNA solutions do not show extinction above 300 nm and the ratio of the extinction at 260 nm over 280 nm (A_{260}/A_{280}) is at least 1.8 (Mülhardt, 2009).

3.2.2 Agarose gel electrophoresis

The following solutions were used:

1 % (w/v) agarose solution:

5 g agarose were heated in 500 mL 1x TAE buffer and stored at 60 °C.

50x TAE buffer:

2 M Tris(hydroxymethyl)-aminomethane (TRIS); 0.05 M ethylenediaminetetraacetic acid (EDTA) and 57.1 mL pure acetic acid were dissolved in ddH₂O in a total volume of 1000 mL ddH₂O.

10 mg/mL ethidium bromide (1000x)

For gel staining, 500 mL 1x TAE buffer containing 0.01 mg/mL ethidium bromide was used.

Destaining solution

500 mL 1x TAE buffer.

6x loading dye

10 mM TRIS pH 7.6; 60 mM EDTA; 60 % glycerol (v/v); 0.03 % (w/v) bromophenol blue; 0.03 % (w/v) xylene cyanol

DNA fragments were separated by electrophoresis according to their length using 1 % (w/v) agarose gels. Gels were prepared using gel chambers with an appropriate sample comb. DNA solutions were mixed with loading dye to a final concentration of 1x and pipetted into the sample pockets. The electrophoresis was run at 110 Volt for 25 min. The DNA in the gel was stained with ethidium bromide (15 min) and background stains were reduced by destaining for another 15 min. Documentation was performed under UV light (Sharp et al., 1973) using the INTAS, Gel iX Imager. For reference, a DNA standard from New England Biolabs GmbH (*2-Log DNA Ladder*) was used.

3.2.3 Amplification of DNA using PCR

The polymerase chain reaction (PCR) allows the enzymatic amplification of DNA fragments *in vitro* (Mullis and Faloona, 1987; Saiki et al., 1988).

The annealing temperature (T_A) corresponded to the lower melting temperature of the two primers minus 3 °C, whereas the melting temperatures of the primers was given by the manufacturer.

3.2.3.1 Standard PCR

For the amplification of genes for cloning, *PhusionTM High Fidelity* DNA polymerase (Thermo Fischer Scientific) was applied. The reactions were carried out in a volume of 50 μ L each in a thermocycler (Bio-Rad Laboratories GmbH, MJ MiniTM Personal Thermo Cycler or MyCyclerTM Thermal Cycler), whereby 50-100 ng template DNA, 0.5 mM of each primer, 0.2 mM of each dNTP, 1 unit (U) DNA polymerase, and 1x *PhusionTM HF* buffer (containing 1.5 mM $MgCl_2$) was used. The reaction conditions are summarized in Table 5.

Table 5: Standard PCR protocol

Stage	Temperature	Time	Number of cycles
Initial denaturation	98 °C	30 s	1x
Denaturation	98 °C	10 s	
Annealing	T_A °C	30 s	25x-30x
Extension	72 °C	30 s/kB	
Final extension	72 °C	10 min	1x
Storage	16 °C	∞	

This procedure was also applied for the amplification of genes from genomic DNA. Here, instead of template DNA, cells of the organism of interest were added from an agar plate or the cells were resuspended in 100 μ L ddH₂O and 1 μ L of the suspension was used as the template. The initial denaturation step was prolonged to 5 min to disrupt the cells.

3.2.3.2 Colony PCR

In order to verify the correct insertion of DNA fragments into plasmids, the *E. coli* cells that were transformed (3.1.4) with ligation reactions (3.2.6.2 and 3.2.6.3), were analyzed by colony PCR. For this, cells of single colonies from agar plates were resuspended in 100 μ L LB medium and 1 μ L of this suspension was used as a template in the PCR reaction. The cells were disrupted by a prolonged initial denaturation step. Primers in proximity of the inserted DNA sequence were used (Table 4) together with either the OptiTherm DNA polymerase (Rapidozym GmbH) or the Taq DNA polymerase (New England Biolabs GmbH). In a total volume of 20 μ L 0.5 mM of each primer, 0.2 mM of each dNTP, the OptiTherm DNA polymerase buffer BD with $MgCl_2$ or ThermoPol[®] buffer, respectively, and 1 U polymerase were mixed. The reaction conditions are summarized in Table 6.

Table 6: Colony PCR protocol

Stage	Temperature	Time	Number of cycles
Initial denaturation	95 °C	5 min	1x
Denaturation	95 °C	40 s	
Annealing	53 °C	30 s	25x-30x
Extension	72 °C	1 min/kB	
Final extension	72 °C	10 min	1x
Storage	16 °C	∞	

3.2.4 Isolation and purification of plasmid DNA from *E. coli*

Plasmid DNA was produced with *E. coli* DH5 α or XL1-blue. Isolation and purification were performed using the *GeneJET™ Plasmid Miniprep Kit* (Thermo Fischer Scientific, Fermentas). The instructions of the manufacturer were followed, whereby 4 mL of cell culture was used and plasmid DNA was eluted from the column with 30 to 50 μ L of ddH₂O. The plasmids were stored at -20 °C.

3.2.5 Isolation of DNA fragments

DNA fragments were cut from agarose gels under UV light using a scalpel and extracted using the *NucleoSpin® Gel and PCR Clean-up Kits* (Macherey-Nagel) following the instructions of the manufacturer. The DNA was eluted with 30 to 50 μ L ddH₂O and stored at -20 °C.

3.2.6 Enzymatic manipulation of DNA fragments

3.2.6.1 Cleavage of double stranded DNA with restriction endonucleases

For the specific cleavage of double stranded DNA type IIP restriction endonucleases were used. These restriction enzymes recognize specific palindromic sequences and either create single stranded overhangs, so called sticky ends, or blunt ends upon cleavage within these sequences. For small-scale tests, 200 ng DNA were incubated with 10 to 20 U of enzyme for 2 to 3 h at the temperature specified by the manufacturer.

For preparations used for ligation, 2-5 μ g DNA were digested, whereby the amount of enzyme used was calculated with equation 6.

$$U_{Verdau} = \frac{BP_{assay\ DNA}}{RS_{assay\ DNA}} \times \frac{RS_{target\ DNA}}{BP_{target\ DNA}} \times m_{DNA} \times f \div t \quad (6)$$

$BP_{assay\ DNA}$ Number of base pairs of the assay DNA used by the manufacturer

$S_{assay\ DNA}$ Number of restriction site of the restriction enzyme to be used in the assay DNA.

$BP_{target\ DNA}$ Number of base pairs of the target DNA

$S_{target\ DNA}$ Number of restriction sites of the restriction enzyme to be used in the target DNA

m_{DNA} Amount of target DNA to be used in μ g

f Scaling factor for f -fold excess of restriction enzyme

t Incubation time of the restriction reaction

A maximum of 10% of the total volume was comprised of glycerol-containing restriction enzymes, as glycerol can affect activity negatively. The reactions were stopped by enzyme inactivation according to the manufacturer. If the target DNA was a PCR product (3.2.3.1), the digested DNA fragment was directly purified from solution using the *NucleoSpin® Gel and PCR Clean-up Kit* (Macherey-Nagel). In case the target DNA was a plasmid, the fragments were incubated with calve intestinal alkaline phosphatase (New England Biolabs GmbH) for 1 h at 37 °C, before they were analyzed by agarose gel electrophoresis (3.2.2) and purified from the gel (3.2.5).

3.2.6.2 Ligation of DNA fragments with sticky ends

The digested plasmid and DNA fragment were mixed in a ratio of 1 to 3 in a total volume of 20 μ L with 1 U of T4-DNA ligase (New England Biolabs GmbH) and ligase buffer, and incubated overnight at 16 °C. Chemically competent cell were transformed with 5 to 10 μ L of the heat inactivated solution (3.1.4).

3.2.6.3 Ligation of DNA fragments with blunt ends

Blunt end ligations using the plasmid pJET2.1 were performed with the *CloneJET PCR Cloning Kit* following the instructions of the manufacturer. Inserts were either Strings DNA fragments (GeneArt, Regensburg) or PCR products. Chemically competent cells were transformed with 1 to 2 μL of the reaction mixture (3.1.4).

3.2.7 Simple Cloning

The principal of this cloning strategy from You and Zhang (2012) is depicted in Figure 7. Here, no restriction and ligation reactions are required. Instead, the plasmid and target gene are amplified by PCR with specific primers: insert-forward, insert-reverse, vector-forward, and vector-reverse. This yields DNA fragments with complementary ends, from which multimers are generated in a second, a prolonged overlap extension PCR. These multimers can be directly used for transformation of *E. coli*, which are capable to dissect the multimer into single cyclized plasmids.

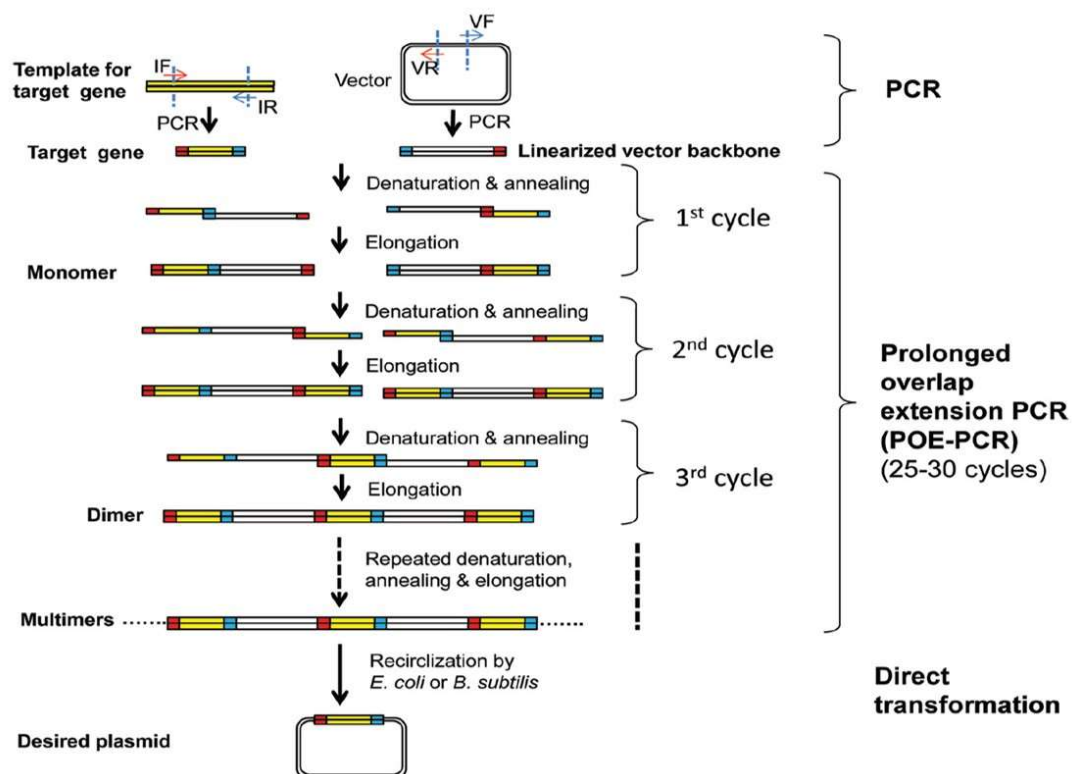


Figure 7: Simple Cloning strategy after You and Zhang (2012)

In a first PCR, the target gene and the plasmid are amplified with specific primers (insert forward, IF; insert reverse, IR; vector forward, VF; vector reverse, VR), generating complementary ends. In a second PCR, a prolonged overlap extension PCR, these can anneal and multimers are formed after several cycles. The multimers can be used to transform competent *E. coli* cells, which dissect and cyclize the multimers into single plasmids.

For the generation of DNA fragments with complementary ends, the PCR was performed in a total volume of 50 μL containing 8 to 50 ng DNA template, 0.5 mM of both primers, 0.2 mM of each dNTP, 1 U *Phusion*TM High Fidelity DNA polymerase, and 1x *Phusion*TM HF reaction buffer (with 1.5 mM MgCl_2). The reaction conditions are summarized in Table 7.

Table 7: PCR protocol for the generation of complementary ends

Stage	Temperature	Time	Number of cycles
Initial denaturation	98 °C	30 s	1x
Denaturation	98 °C	10 s	
Annealing	T _A °C	30 s	25x
Extension	72 °C	30 s/kB	
Final extension	72 °C	10 min	1x
Storage	16 °C	∞	

The second PCR, the prolonged overlap extension PCR was performed in a total volume of 40 µL with 2 ng/µL of the purified insert DNA from the first PCR and an equimolar amount of the purified vector DNA together with 0.2 mM of each dNTP, 1 U *Phusion*TM *High Fidelity* DNA polymerase, and 1x *Phusion*TM *HF* reaction buffer (with 1.5 mM MgCl₂). The reaction conditions are summarized in Table 8.

Table 8: PCR protocol for the generation of the plasmid multimer

Stage	Temperature	Time	Number of cycles
Initial denaturation	98 °C	30 s	1x
Denaturation	98 °C	10 s	
Annealing	60 °C	10 s	25x
Extension	72 °C	30 s/kB	
Final extension	72 °C	10 min	1x
Storage	16 °C	∞	

3 µL of the second PCR were directly used to transform chemically competent *E. coli* JM109 or DH10B (3.1.4).

3.2.8 Sequencing of DNA fragments

In order to verify the DNA sequences of the cloned genes, plasmids containing the corresponding sequences were sent to GATC Biotech, Köln, for sequencing.

3.3 Protein analytics

3.3.1 Determination of protein concentrations by UV spectroscopy

The concentration of purified proteins was determined by UV spectroscopy using a Multiskan (Thermo Fisher Scientific) or Nanophotometer (Implen). The molecular weight as well as the extinction coefficient of all proteins was calculated with the ProtParam tool (ExpASY). For the latter, the absorption of the aromatic amino acids tryptophan and tyrosine, as well as cystines (disulfide bridges) between 250 and 300 nm is taken into account. The extinction coefficient is then calculated by the following formula (Pace et al., 1995):

$$\epsilon_{280} = \sum Trp \cdot 5500 + \sum Tyr \cdot 1490 + \sum Cystine \cdot 125 \quad (7)$$

The protein concentration can then be assessed from the Lambert-Beer law:

$$c = \frac{A_{280}}{d \cdot \epsilon_{280}} * MW \quad (8)$$

c: Concentration [mg mL⁻¹]
*A*₂₈₀: Absorption at 280 nm
d: Optical path length [cm]

*ε*₂₈₀: Extinction coefficient [M⁻¹ cm⁻¹]
MW: Molecular weight [g mol⁻¹]

Absorption above 300 nm is caused by light scattering and an indication of protein aggregates.

In Table 9 the molecular weight, extinction coefficient and GenBank ID of all enzymes used in this work are listed.

Table 9: Molecular weight and extinction coefficients determined with the ProtParam tool (ExpASY), and GenBank ID of all proteins used.

MW: molecular weight (g mol⁻¹) including His₆-tag, *ε*₂₈₀: extinction coefficient at 280 nm (M⁻¹*cm⁻¹) assuming all cysteins are reduced

Protein	MW	ε ₂₈₀	GenBank ID
<i>bt</i> UGDH (no His ₆ -tag)	55136	49850	AAI50069.1
<i>ec</i> UGDH	45820	26820	BAA15860.1.
SpsADH-P	29111	11460	BAJ09322.1
SpsADH	29500	18450	BAP40335.1
NOX	51936	44810	CCB83530.1
UDH	31210	37930	DAA06454.1
GlucD	51010	64400	ABR75198.1
KdgD	34787	21890	ENV53020.1
ADHZ3 LND	38719	40910	U14003.1 (wildtype)
KgsalDH	57702	28420	AAN66880.1

3.3.2 Determination of protein concentrations with the Bradford assay

For the determination of protein concentrations with the Bradford assay (Bradford, 1976), the Roti®-Nanoquant Kit (Carl Roth GmbH & Co. KG, Karlsruhe) was used, whereby the instructions of the manufacturer were followed.

3.3.3 Determination of the FAD content of NADH oxidase

NOX non-covalently binds one molecule of FAD per subunit. The FAD in NOX preparations was determined photometrically at 450 nm (Multiskan, Thermo Fisher Scientific) with an external FAD standard. From the ratio of protein concentration (by Bradford, 3.3.2) to FAD concentration, the percentage of loaded NOX was calculated.

3.3.4 SDS polyacrylamide gel electrophoresis

Sodium dodecyl sulfate polyacrylamide gel electrophoresis (SDS-PAGE) was performed after the protocol of Laemmli (1970). The following solutions were used:

Ammonium persulfate (APS) stock solution, 10%

10% (w/v) APS were solved in ddH₂O and stored at 4 °C.

Coomassie staining solution

0.2% (w/v) Coomassie Brilliant Blue G250 und R250, 50% (v/v) ethanol, 10% (v/v) pure acetic acid.

The solution was stirred for 3 h before filtration and stored protected from light at room temperature.

4x SDS-PAGE separating gel buffer

0.8% (w/v) SDS, 1.5 M TRIS/HCl pH 8.8. The pH was adjusted with 37% (v/v) HCl.

4x SDS-PAGE stacking gel buffer

0.8% (w/v) SDS, 0.5 M TRIS/HCl, pH 6.8. The pH was adjusted with 37% (v/v) HCl.

10x SDS-PAGE buffer

1% (w/v) SDS, 0.25 M TRIS, 1.92 M glycine. The resulting pH of 8.5 must not be changed.

5x SDS loading dye

50% (v/v) glycerol; 12.5% (v/v) β-mercaptoethanol; 7.5% (w/v) SDS; 0.25 M TRIS, 0.25 g/L bromophenol blue, pH 6.8. The pH was adjusted with 37% (v/v) HCl.

The composition of the gels is summarized in Table 10. They were prepared using the Mini-Protean®3 *Multi-Casting Chamber* (Bio-Rad Laboratories GmbH).

Table 10: Preparation of gels for SDS-PAGE

The amounts given make 14 gels.

	Separation gel (80 mL) (12%)	Stacking gel (40 mL) (5 %)
Acrylamide/bisacrylamide solution (40% (w/v); 37.5:1)	24 mL	5.2 mL
Separation/stacking gel buffer (4x)	20 mL	10 mL
ddH ₂ O	34.32 mL	23.96 mL
SDS (10% (w/v))	800 µL	400 µL
The polymerization was initiated with		
Tetramethylethylenediamine (TEMED)	80 µL	40 µL
APS (10% (w/v))	800 µL	400 µL

Samples were first diluted with water, if necessary, and mixed with 5x loading dye to give a final concentration of 1x. After heating at 95 °C for 5 min, they were spun (Thermo Fischer Scientific Heraeus, Fresco 21 Centrifuge, 21.000 g, 10 s) and could then be stored at 4 °C for several days. In the latter case, the samples were heated and centrifuged again before 5 to 15 µL were applied to the gel using a microliter syringe and the electrophoresis was run at a constant current of 30 mA per gel for about 50 min (Bio-Rad Laboratories GmbH, *Mini-PROTEAN Tetra Cell*).

For detection of proteins, the gels were first stained with Coomassie Brilliant Blue for 15 min, whereas the detection limit lies around 0.2-0.5 µg/mm². For a first analysis, the gels destained in boiling water (microwave, three times) and afterwards the gels were further destained in water at room temperature overnight. Here, a paper towel was added to bind the dye.

3.3.5 Protein purification

3.3.5.1 Cell disruption by sonication

Cells of expression cultures (3.1.5.2) were resuspended (10 to 20% (w/v)) in binding buffer (50 mM potassium phosphate (KP) pH 8.0, 500 mM NaCl, 10% glycerol, 10 mM imidazole) and disrupted while cooled on ice by sonication: 80% amplitude, 0.6 ms pulse, 3x 5 min (UIS250v with sonotrode LS24d10, Hielscher Ultrasonics GmbH, Teltow). The soluble fraction was obtained by centrifugation (Sorvall RC 6+ Centrifuge, SS34 Rotor, 14.000 g, 45 min, 4 °C), from which the His-tagged proteins were purified by immobilized metal ion affinity chromatography.

3.3.5.2 Immobilized metal ion affinity chromatography

Immobilized metal ion affinity chromatography (IMAC) was performed using HisTrap™ FF columns (GE Healthcare, column volume (CV): 5 mL). Here, the His-tagged proteins bind to the column and can be eluted with imidazole. The ÄKTA™ purifier system (GE Healthcare) was used, whereby the following procedure was applied:

Flowrate:	5 mL/min	
Equilibration:	2 CV	binding buffer ^a
Loading:	5 mL/min	soluble fraction of the cell lysate
Wash:	3 CV	binding buffer ^a
Elution:	10 CV	gradient 0 to 100% elution buffer ^b
	2 mL fractions were collected.	
Column cleaning:	5 CV	elution buffer ^b
Column storage:	5 CV	ddH ₂ O
	3 CV	20% ethanol

^a: 50 mM KP pH 8,0, 500 mM NaCl, 10% glycerol, 10 mM imidazole

^b: 50 mM KP pH 8,0, 500 mM NaCl, 10 % glycerol, 500 mM imidazole

The complete procedure was monitored on-line by UV measurement at 280 nm. The collected fractions as well as the lysate and the flow through of the washing step were analyzed by SDS-PAGE (3.3.4). Fractions that contained the target protein in sufficient purity were pooled and desalted using the *HiPrep 26/10 Desalting* column (3.3.5.3).

For the regeneration of the column, the instructions of the manufacturer were followed.

3.3.5.3 Size exclusion chromatography for desalting of protein preparations

In order to switch buffers and remove salts, size exclusion chromatography of protein preparations was performed. Here, the ÄKTA™ purifier system (GE Healthcare) was used with the column *HiPrep 26/10 Desalting* (GE Healthcare).

The following procedure was applied:

Flow rate:	5-10 mL/min	
Equilibration:	2 CV	Exchange buffer ^a
Loading:	15 mL	Protein preparation
Elution:	2 CV	Exchange buffer ^a ; with manual collection of the fraction containing the protein (monitored by UV)
Column Cleaning:	2 CV	Exchange buffer ^a
Column storage:	2 CV	ddH ₂ O
	2 CV	20% ethanol

^a: for all proteins 50 mM ammonium bicarbonate buffer pH 7.9 was used, with exception of *ecUGDH*, where 50 mM glycine pH 8.9, 2 mM dithiothreitol (DTT) was applied.

3.3.6 Storage of protein preparations

Purified proteins were slowly dripped into liquid nitrogen resulting in aliquots of 20 to 50 µL. The globules were stored at -80 °C.

3.3.7 Determination of enzymatic activity

3.3.7.1 Photometric assay based on NADH detection

The activity of enzymes, which use NAD(P)/H as a cofactor, was measured photometrically by the detection of NADH at 340 nm using a photometer (Multiskan Spectrum or Varioskan, Thermo Fischer Scientific, or Infinite 200 pro, Tecan Group Ltd.). Clear flat bottom microtiter plates (Greiner Bio-One International GmbH, Austria) were used to measure triplicates and controls without enzyme or substrate, respectively, in a total volume of 200 µL each. The calculation of Michaelis–Menten kinetics for determination of K_m and V_{max} was carried out using SigmaPlot 11.0 (Systat Software). Detailed reaction conditions for each enzyme are outlined below:

btUGDH

The reaction conditions were adopted from Axelrod et al. (1957): 50 mM glycine pH 8.9 with 2 mM DTT at 25 °C were used.

For the determination of kinetic parameters with the native substrates, uridine diphosphate D-glucose (UDP-Glc) and NAD⁺, a final enzyme concentration of 0.56 µM was used and the substrate concentrations were varied between 0 to 2 mM UDP-Glc (2 mM NAD⁺) or 0 to 2 mM NAD⁺ (5 mM UDP-Glc), respectively.

For the determination of kinetic parameters with D-glucose a final enzyme concentration of 1.1 µM was applied and the substrate concentration was varied between 0- to 20 mM (2 mM NAD⁺), in absence and presence of uridine monophosphate (1 to 90 mM).

Activity with methyl-D-glucose (α - and β -, respectively) was measured at a substrate concentration of 50 mM with 2 mM NAD⁺.

ecUGDH

The assay mixture contained 50 mM glycine pH 8.9, 2 mM DTT and 3.3 μ M of enzyme. Reactions were measured at 25 °C.

For the determination of kinetic parameters, the substrates UDP-Glc and NAD⁺ were varied between 0 to 5 mM (5 mM NAD⁺) or 0 to 0.2 mM (10 mM UDP-Glc), respectively.

Activity with 0 to 250 mM D-glucose was tested at a constant NAD⁺ concentration of 5 mM.

SpsADH-P

The activity of SpsADH-P was measured in 50 mM ammonium bicarbonate (AbC) pH 7.9 at 25 °C using 1.6 to 6.5 μ M purified enzyme.

For the determination of kinetic parameters, the substrates D-gluconate and NADP⁺ were varied between 0 to 200 mM (0.5 mM NADP⁺) or 0 to 1 mM (150 mM D-gluconate), respectively.

Activity with 10 mM D-gluconate, D-galactonate, D-xylonate, L-arabonate, and D-mannonate, respectively, was tested at a constant NADP⁺ concentration of 1 mM.

Activity in dependence of pH was measured using either 50 mM triple buffer (consisting of $\frac{1}{3}$ acetate, $\frac{1}{3}$ KP, and $\frac{1}{3}$ glycine, pH 5.0 to 10.0) or 50 mM arginine buffer (pH 10.0 to 13.0) with 0.3 mM NADP⁺ and 10 mM D-gluconate.

For the measurement of the activity in various buffers, 50 mM of the corresponding buffer, 0.3 mM NADP⁺, and 10 mM D-gluconate were used.

SpsADH

The activity of SpsADH was measured in 50 mM AbC pH 7.9 at 25 °C using 0.3 to 163 μ M purified enzyme.

For the determination of kinetic parameters, the corresponding substrates were varied between 0 and 2.5 M with 1 mM NAD⁺.

Activity with various substrates (5 to 25 mM) was tested at a constant NAD⁺ concentration of 1 mM.

Activity in dependence of pH was measured using either 50 mM triple buffer (consisting of $\frac{1}{3}$ acetate, $\frac{1}{3}$ KP, and $\frac{1}{3}$ glycine, pH 5.0 to 10.0) or 50 mM arginine buffer (pH 10.0 to 13.0) with 1 mM NAD⁺ and 10 mM D-gluconate.

For the measurement of the activity in various buffers, 50 mM of the corresponding buffer, 1 mM NAD⁺, and 10 mM D-gluconate were used.

UDH

The activity of UDH was measured in 50 mM AbC pH 7.9 with 5 mM MgCl₂ at 25 °C using 0.03 μ M purified enzyme.

For the determination of kinetic parameters, the substrates D-glucuronate and NAD⁺ were varied between 0 to 100 mM (1 mM NAD⁺) or 0 to 1.2 mM (10 mM D-glucuronate), respectively.

KgsalDH

For the determination of kinetic parameters, reactions contained 50 mM AbC pH 7.9, 5 mM MgCl₂, and either 0 to 4 mM 2-ketoglutaric semialdehyde (Kgsa) (with 4 mM NAD⁺) or 0 to 4 mM NAD⁺ (with 2 mM Kgsa). Reactions were initiated by the addition of 0.13 to 0.26 μM purified enzyme.

Activity in dependence of pH was measured using 50 mM triple buffer (consisting of 1/3 acetate, 1/3 KP, and 1/3 glycine, pH 5.0 to 10.0) with 1 mM NAD⁺ and 10 mM butanal. Reactions were initiated by the addition of 6 μM purified enzyme.

For the measurement of the activity in various buffers, 50 mM of the corresponding buffer, 1 mM NAD⁺, and 10 mM butanal were used. Reactions were initiated by the addition of 6 μM purified enzyme.

KdgD, coupled with KgsalDH

KdgD activity was determined in a coupled assay with KgsalDH monitoring the increase of NADPH.

For the determination of kinetic parameters, reactions contained 50 mM AbC, 5 mM MgCl₂, 0.5 mM NADP⁺, 1 U KgsalDH, and 0 to 10 mM 5-keto-4-deoxyglucarate (5-Kdg). Reactions were initiated with 0.1 μM purified KdgD.

NOX

For the determination of kinetic parameters, reactions contained 50 mM AbC pH 7.9, 5 mM MgCl₂, and 0 to 0.24 mM NADH. Reactions were started by the addition of 0.03 μM purified enzyme.

3.3.7.2 Semicarbazide assay

GlucD activity was determined with a modified semicarbazide assay of Macgee and Doudoroff (1954). Product formation (5-Kdg) was quantified by detection of its semicarbazone in an end-point assay using the Liquid Handling Station (BRAND GmbH & Co. KG, Wertheim). The reaction (final volume of 1 mL) was initiated with 0.3 μM of purified enzyme and aliquots of 50 μL were mixed with 50 μL of 2N HCl every 1.2 min to stop the reaction. Then, 100 μL of 1% semicarbazide hydrochloride (with 1.5% sodium acetate trihydrate) was added and incubated for 30 min at room temperature before measuring the absorbance at 250 nm in UV-transparent microtiter plates. The extinction coefficient of Kdg-semicarbazone was experimentally determined to be 8900 M⁻¹cm⁻¹.

For the determination of kinetic parameters of GlucD, activity was measured in 50 mM AbC pH 7.9, supplemented with 5 mM MgCl₂ at 25 °C and D-glucarate was varied between 0 and 50 mM.

Activity in dependence of pH was measured using 50 mM triple buffer (consisting of 1/3 acetate, 1/3 KP, and 1/3 glycine, pH 5.0 to 10.0) with 5 mM MgCl₂ and 3.5 mM D-glucarate.

For the measurement of the activity in various buffers, 50 mM of the corresponding buffer, 5 mM MgCl₂, and 3.5 mM D-glucarate were used.

3.3.8 Determination of enzyme stability

3.3.8.1 Half-life and process stability

The half-life ($t_{1/2}$) of enzymes is defined as the time after which half of the initial activity is left. It was determined by measuring the activity after incubation for a specific time at specific conditions.

The half-life and the process stability were then calculated using formulas (2) to (4) given in 1.3.2.

3.3.8.2 *Temperature-induced unfolding*

The thermal stability of the enzymes was measured by differential scanning fluorimetry (DSF), using a real-time PCR detection system (CFX96 Touch, Bio-Rad) and the fluorescent dye SYPRO orange (Invitrogen) using the protocol of Niesen et al. (2007). In a total volume of 25 μ L, 0.2 mg/mL protein, 50 mM of various buffers, and 5x SYPRO Orange were mixed on ice in a clear 96-well plate. After 5 min at 5 $^{\circ}$ C, a temperature gradient from 5 to 95 $^{\circ}$ C with 0.5 $^{\circ}$ C increments was applied, maintaining each temperature for 5 s. Protein denaturation was monitored at 560–580 nm (excitation 450–490 nm). The data were analyzed with CFX Manager 3.1 (Bio-Rad) to determine the melting point (T_M), defined as the temperature at which 50% of the protein is denatured.

3.3.8.3 *Guanidine hydrochloride-induced unfolding*

The thermodynamic stability was determined by guanidine hydrochloride induced unfolding. Therefore, 100 μ L protein were incubated with various concentrations of guanidine hydrochloride (0–3.5 M) in 25 mM KP pH 8.0 for eight days at RT. The proteins were transferred into a 96-well optical-bottom plate (Thermo Fisher Scientific) and the fluorescence emission at 344 nm was measured after excitation at 278 nm in a Varioskan (Thermo Fisher Scientific).

3.4 **Single enzyme reactions**

3.4.1 **Analytical single enzyme reactions**

For product identification or verification, single enzyme reactions were performed to allow the analysis by HPLC, MS, or NMR (see 3.6).

3.4.1.1 *btUGDH*

In a final volume of 0.2 mL, 50 mM glycine pH 8.9, 2 mM DTT, 2 mM NAD^+ and 10 mM D-glucose were incubated with 0.05 U/mL *btUGDH*. For cofactor recycling 2 U/mL NOX (Sigma-Aldrich, Deisenhofen) were added. After one day at 37 $^{\circ}$ C, the reaction was stopped by filtration (10 kDa MWCO, modified PES; VWR), the sample was diluted and carboxylic acids were derivatized with 4-APEBA (3.6.1.2).

3.4.1.2 *SpsADH*

Reactions were conducted in a total volume of 100 μ L with 25 mM AbC pH 7.9, 5 mM NAD^+ , 25 mM substrate, 8.1 μ M *SpsADH*, and 0.9 μ M NOX for cofactor recycling. After one day at 25 $^{\circ}$ C, the reactions were stopped by filtration (10 kDa MWCO, modified PES; VWR), the samples were diluted and analyzed by HPLC. In detail: Aldonic and aldaric acids were analyzed by anion exchange chromatography (3.6.1.3), uronic acids and sugars were analyzed with the PMP method (3.6.1.1).

3.4.1.3 *ADHZ3 LND*

The reduction of Kgsa to 5-hydroxy-2-oxovalerate (Hov) by ADHZ3 LND was conducted at 25 °C in a total volume of 1 mL containing 10 mM Kgsa (3.4.2.2), 1 mM NADH, 10 mM ammonium formate, 6.2 µM ADHZ3 LND, and 0.2 mg/mL FDH from *Candida boidinii* (Sigma-Aldrich, Deisenhofen). Samples were taken after 1 h up to 48 h, diluted in water, filtered (10 kDa MWCO, modified PES; VWR), and analyzed by anion exchange chromatography (3.6.1.3).

3.4.2 Preparative single enzyme reactions

For the synthesis of compounds that were not commercially available, single enzyme reactions were performed in preparative scale and complete product formation was confirmed by HPLC.

3.4.2.1 *Synthesis of 5-keto-4-deoxyglucarate*

5-Kdg was prepared enzymatically with GlucD. Therefore, 120 mM D-glucarate (pH 6.5, titrated with NaOH) were converted by 3.7 U of enzyme in a total volume of 20 mL containing 0.5 mM AbC from the enzyme preparation supplemented with 5 mM MgCl₂. The reaction took place at room temperature and complete conversion of the substrate was confirmed by anion exchange chromatography (3.6.1.3). The reaction was then stopped by ultrafiltration with a VivaSpin column (10 kDa cut-off, GE Healthcare) and the flow through was stored at -20 °C.

The 5-Kdg preparation was used for the synthesis of Kgsa (3.5.2), as a standard for the semicarbazide assay (3.3.7.2), and for the calibration of the anion exchange column (3.6.1.3).

3.4.2.2 *Synthesis 2-ketoglutaric semialdehyde*

2-Ketoglutaric semialdehyde (Kgsa) was prepared from 5-Kdg (3.4.2.1) using KdgD. Here, 100 mM 5-Kdg were converted with 3.3 µM of enzyme in a total volume of 16.2 mL containing 3.8 mM AbC from enzyme preparations and 5 mM MgCl₂ from the 5-Kdg preparation. The reaction took place at room temperature and was titrated (Titroline 7750 or Titroline 7000, SI Analytics) with 3.7% HCl to keep the pH at 6.5 (final volume of added HCl was 1.484 mL). Samples were analyzed by anion exchange chromatography (3.6.1.3) to confirm complete conversion, before the enzyme was removed by ultrafiltration (VivaSpin column, 10K cut-off, GE Healthcare). The flow through was stored at -20 °C. The Kgsa preparation was used for enzymatic reactions and for the calibration to of the anion exchange column (3.6.1.3).

3.5 *In vitro* enzymatic cascade reactions

3.5.1 *Synthesis of 5-hydroxy-2-oxovalerate*

Hov synthesis from D-glucuronate or D-glucarate using the enzymes UDH, GlucD, KdgD, ADHZ3 LND, and FDH (if needed for cofactor recycling). Various conditions and setups were tested, which are indicated in the results section (4.3.1). In brief, different buffer systems, enzyme concentrations, cofactor concentrations/recycling and setups with and without titration were investigated.

3.5.2 Synthesis of α -ketoglutarate

α -ketoglutarate (aKG) was synthesized from D-glucuronate using the enzymes UDH, GlucD, KdgD, KgsalDH, and NOX for cofactor recycling. Reactions for determination of the necessary concentrations of NAD^+ and NOX were performed in a volume of 1.5 mL. Each mixture contained 50 mM AbC, 5 mM MgCl_2 , 50 mM D-glucuronate, and 2 U/mL of UDH, GlucD, KdgD, and KgsalDH, respectively. NOX concentrations were varied between 2 and 8 U/mL and NAD^+ concentrations were varied between 1 and 10 mM. Reactions were performed in closed vessels at 25 °C (water bath) with stirring.

Conversions in the small-scale bubble reactor were performed in vessels equipped with a septum. Gaseous, humidified oxygen was supplied through a cannula at 20 mL/min. The reactions took place at 25 °C (water bath) with stirring. In a volume of 5 mL, the mixtures contained 50 mM AbC, 5 mM MgCl_2 , 50 mM D-glucuronate, 2 U/mL of UDH, GlucD, KgsalDH, and NOX, respectively, 1 U/mL KdgD, and 5 mM NAD^+ . In the experiment with additional NOX supplementation, 2 U/mL NOX was added every 20 min for 1 h.

Samples for HPLC analysis (3.6.1.3) were filtrated with spin filters (10 kDa MWCO, modified PES; VWR) to remove enzymes and stop the reaction.

Inhibitory effects of the corresponding products and of the intermediates of the cascade on the single enzymes were tested as follows: 0.4 U/mL of each enzyme was incubated separately in 50 mM AbC pH 7.9, 5 mM MgCl_2 , 10 mM of the corresponding substrate/s, 1 mg/mL bovine serum albumin for simulation of a high protein load as in the cascade reaction, and either 0 or 10 mM of one of the following substances: D-glucuronate, D-glucarate, 5-Kdg, Kgsa, aKG, or NADH. All reactions were stopped after 15 min by removal of the enzymes by ultracentrifugation. The samples were diluted and analyzed by HPLC (3.6.1.3). Product formation in the sample without a potential inhibitor was then compared to the samples with an inhibitor.

3.6 Instrumental analytics

3.6.1 High performance liquid chromatography

3.6.1.1 PMP method

Reducable sugars and sugar derivatives can be analyzed by high performance liquid chromatography (HPLC) coupled with mass spectrometry (MS) as 1-phenyl-3-methyl-5-pyrazolone (PMP) derivatives using the method of Rühmann et al. (2014).

Samples were diluted in water and derivatized with 0.1 M PMP and 0.4% ammonium hydroxide in methanol. After 100 min at 70 °C the reaction was stopped with 16.7 mM acetic acid and filtered (Restek, 0.22 μm , PVDF). When elution of the sample was expected before 3 min, the sample was extracted with chloroform (three times) to reduce excess PMP and then filtered.

The HPLC system (UltiMate 3000RS, Dionex) was composed of a degasser (SRD 3400), a pump module (HPG 3400RS), an auto sampler (WPS 3000TRS), a column compartment (TCC3000RS), a diode array detector (DAD 3000RS), and an electrospray ionization (ESI) mass spectrometer (MS, Bruker). Data was collected and analyzed using Bruker HyStar software. The column (Gravity C18, 100

mm length, 2 mm i.d.; 1.8 μm particle size; Macherey-Nagel) was operated at 50 °C with a mobile phase A (5 mM ammonium acetate buffer, pH 5.6, with 15% acetonitrile) and a chromatographic flow rate of 0.6 mL/min. The gradient (mobile phase B containing pure acetonitrile) was as follows: start of mobile phase B at 1%, with an increase to 5% over 5 min, hold for 2 min, then increase to 18% over 1 min. The gradient was further increased to 40% over 0.3 min, held for 2 min, and returned within 0.2 min to starting conditions for 1.5 min. If samples were not extracted, the first 3 min of chromatographic flow were refused by a switch valve behind the UV detector (245 nm). Before entering ESI-MS the flow was split 1:20 (Accurate post-column splitter, Dionex). The temperature of the auto sampler was set to 20 °C and an injection volume of 10 μL was used.

ESI ion trap parameters: The ion trap operated in the ultra scan mode (26,000 m/z/s) from 50 to 1000 m/z. The ICC target was set to 200,000 with a maximum accumulation time of 50 ms and four averages. The ion source parameters were set as follows: capillary voltage 4 kV, dry temperature 325 °C, nebulizer pressure 40 psi, and dry gas flow 6 L/min. Auto MS mode with a smart target mass of 600 m/z and an MS/MS fragmentation amplitude of 0.5 V was used. Analysis was performed by using the extracted ion chromatograms of the m/z value corresponding to the protonated molecules.

3.6.1.2 4-APEBA method

Carboxylic acids as well as aldehydes can be derivatized with 2-(4-aminophenoxy)ethyl(4-bromophenethyl)-dimethylammoniumbromide hydrobromide (4-APEBA) and analyzed by HPLC/MS after the protocols of Eggink et al. (2010) and Kretschmer et al. (2011).

Derivatization of aldehydes:

200 μL 4-APEBA (150 mM in acetate buffer pH 5.7) and 50 μL sodium cyanoborohydride (NaBH_3CN , 0.5 g/L in methanol) were mixed with 250 μL of sample and incubated at 10 °C for 3 h.

Derivatization of carboxylic acids:

150 μL N-(3-dimethylaminopropyl)-N'-ethyl-carbodiimide-hydrochloride (EDC, 24 g/L in water) and 300 μL 4-APEBA (2 g/L in water) were mixed with 150 μL of sample (diluted with water pH 5) and incubated at 60 °C for 1 h.

The HPLC system (UltiMate 3000RS, Dionex) was composed of a degasser (SRD 3400), a pump module (HPG 3400RS), an auto sampler (WPS 3000TRS), a column compartment (TCC3000RS), a diode array detector (DAD 3000RS), and an ESI-MS (Bruker). Data was collected and analyzed using Bruker HyStar software. The column (Triart C18, 100 mm length, 2 mm i.d.; 1.9 μm particle size; YMC America Inc.) was operated at 60 °C and a flow rate of 0.4 mL/min with a mobile phase consisting of 75% A (0.1% formic acid) and 25% B (MeOH with 0.1% formic acid). After 7.5 min B increases to 40% for 0.5 min before equilibrating the column with the starting conditions for 2 min.

The elution was followed by UV (245 nm) and before entering ESI-MS the flow was split 1:4 (Accurate post-column splitter, Dionex). The temperature of the auto sampler was set to 20 °C and an injection volume of 10 μL was used.

ESI ion trap parameters: The ion trap operated in the ultra scan mode (26,000 m/z/s) from 50 to 1500 m/z. The ICC smart target was set to 200,000 with a maximum accumulation time of 50 ms and four averages. The ion source parameters were set as follows: capillary voltage 4 kV, dry temperature 325 °C, nebulizer pressure 20 psi, and dry gas flow 5 L/min. Auto MS mode with an MS/MS fragmentation

amplitude of 0.5 V was used. Analysis was performed by using the extracted ion chromatograms of the m/z value corresponding to the protonated molecules.

Data was collected and analyzed using Bruker HyStar software using the extracted ion chromatograms of the m/z value corresponding to the protonated molecules.

3.6.1.3 *Metrosep*

Carboxylic acids could also be analyzed without derivatization using an UltiMate 3000 HPLC system (Dionex, Idstein, Germany), equipped with auto sampler (WPS 3000TRS), a column compartment (TCC3000RS), and a diode array detector (DAD 3000RS). The anion exchange column Metrosep A Supp10–250/40 (250 mm, particle size 4.6 mm; Metrohm) at 65 °C was used for separation by isocratic elution with either 12 mM AbC pH 10.0 or 30 mM AbC pH 10.4 as the mobile phase at 0.2 mL/min. The column was washed with 30 mM AbC pH 10.4, if the elution buffer was 12 mM AbC pH 10.0 before returning to the starting conditions. Samples were diluted in water, filtered (10 kDa MWCO, modified PES; VWR, Darmstadt, Germany), and 10 μ L were applied to the column. Data was analyzed using the Dionex Chromeleon software.

3.6.2 **Mass spectroscopy**

Direct analysis of substances by MS was performed using a syringe with a pump module (10 μ L/min) for sample application. Data was collected and analyzed using Bruker HyStar software, whereby the MS parameters could be adjusted during the measurement.

3.6.3 **Nuclear magnetic resonance spectroscopy**

Nuclear magnetic resonance (NMR) spectroscopy allows the structural analysis of compounds with NMR active nuclei (^1H , ^{13}C , etc.). ^1H spectra were measured with a JEOL ECS 400 (Jeol Ltd., Akishima, Japan). Samples, which were solved in water, like products from enzymatic cascade reactions, were lyophilized (freeze-dryer Alpha 2-4 LD plus) and solved in D_2O or $\text{DMSO-}d_6$ (100 mM in 0.6 mL). Reference substances were either solved in 50 mM AbC buffer pH 7.9 and lyophilized (same procedure as samples) or directly solved in D_2O or $\text{DMSO-}d_6$ (100 mM in 0.6 mL). Chemical shifts were referenced via the residual solvent signal.

4 Results

4.1 Identification of enzymes for the oxidation of D-glucose to D-glucarate

For the oxidation of D-glucose to D-glucarate no short natural metabolic pathway is known. Therefore, enzymes for an artificial pathway need to be identified. The two shortest routes possible are depicted in Figure 8, box, whereas non-natural enzymatic activities are highlighted. In this section, results are shown for the investigation of enzymes either for the oxidation of D-glucose at C6 to form D-glucodialdose or for the oxidation of D-gluconate at C1 to form L-guluronate.

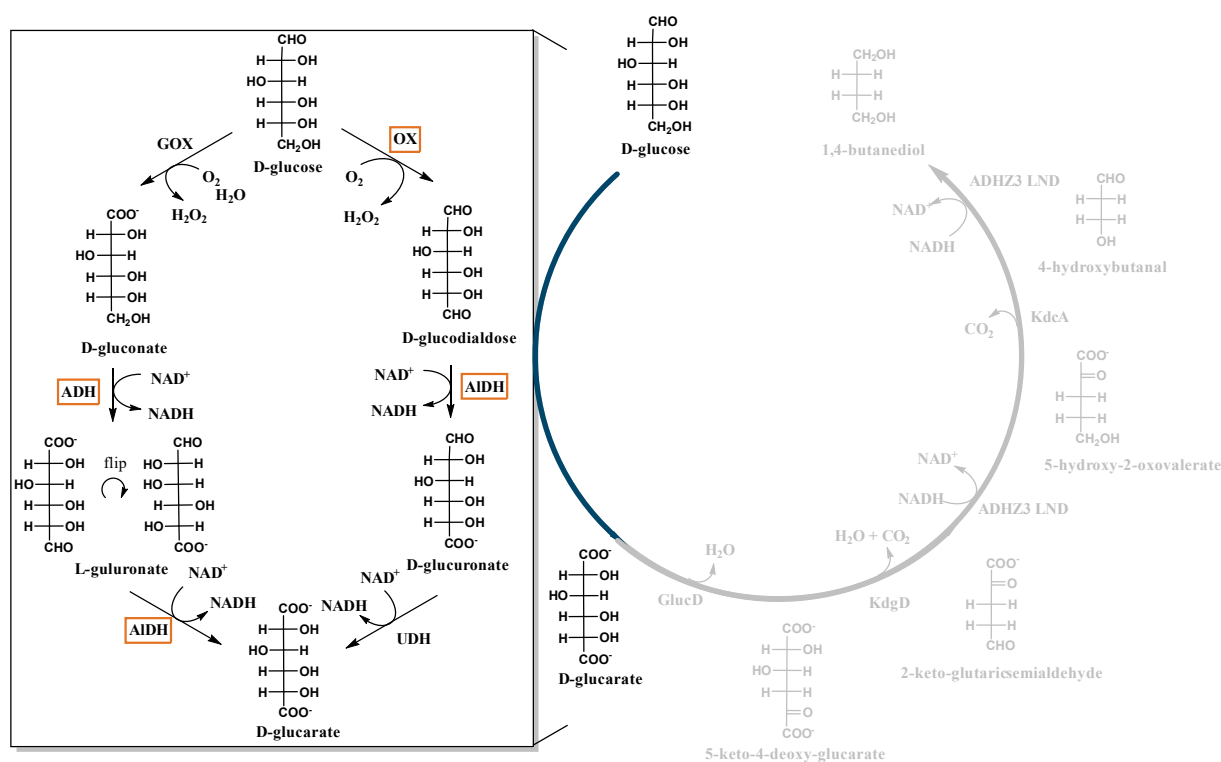


Figure 8: Enzymes to be identified for the oxidative module

For both possible routes from D-glucose to D-glucarate, enzymes need to be identified (red boxes). In the first pathway an alcohol dehydrogenase (ADH) and an aldehyde dehydrogenase need to be found (AIDH), whereas in the second pathway, an oxidase (OX) and an AIDH are necessary to perform the corresponding reactions.

4.1.1 UDP-glucose-6-dehydrogenases

Ascorbic acid can be produced by most organisms, prokaryotes as well as eukaryotes (humans are among others an exception). Along this metabolic pathway, D-glucose is activated with UDP to UDP-glucose and then oxidized to UDP-glucuronate. The enzyme catalyzing this double oxidation is UDP-glucose-6-dehydrogenase (UGDH). For the desired cascade reaction from D-glucose to 1,4-butanediol (BDO), this enzyme was tested for a side activity towards D-glucose, which is missing the UDP moiety compared to the native substrate. Three UGDHs from various species were chosen: UGDH from *Streptococcus pyogenes*, *E. coli*, and *Bos Taurus* (for gene sequences see appendix 6.1). However, only the latter two were analyzed, due to insoluble expression of *ugdh* from *Streptococcus pyogenes*.

4.1.1.1 UGDH from *E. coli*

The *ugdH* was amplified using genomic DNA from *E. coli* strain K-12. After cloning into pET28a, the gene was overexpressed and purified (*ec*UGDH). The enzymatic activity with the native substrate UDP-D-glucose was measured to assure that an active enzyme had been purified. Here, a V_{\max} of 2.3 ± 0.1 mU/mg, a K_m for UDP-glucose of 1.3 ± 0.1 mM and a K_m for NAD^+ of 0.10 ± 0.01 mM was observed. In the next step, D-glucose was used as a substrate. However, no activity toward this substrate analog was measurable and therefore, no further experiments were conducted.

4.1.1.2 UGDH from *Bos taurus*

UGDH from bovine liver (*bt*UGDH) was purchased from Sigma-Aldrich (Deisenhofen). A V_{\max} of 0.39 ± 0.003 U/mg (at pH 8.9 and room temperature) was measured, which was consistent with the description of the manufacturer, (0.33 U/mg, at pH 8.7 and 25 °C). Using a photometrical assay, an activity with D-glucose with a V_{\max} for the double oxidation of 14.6 ± 0.4 mU/mg and K_m of 77.0 mM was observed. Product formation, that is, either D-glucodialdose in case of a single oxidation or D-gluconate in case of a double oxidation, was analyzed by HPLC/MS. First, detection of the PMP derivate was chosen, where only aldehydes can be observed (3.6.1.1). However, no product was detected. Surprisingly, when using derivatization with 4-APEBA, where only carboxylic acids can be detected (3.6.1.2), D-gluconate was found as the product of the reaction (Figure 9). This means that D-glucose was oxidized at C1 instead of C6.

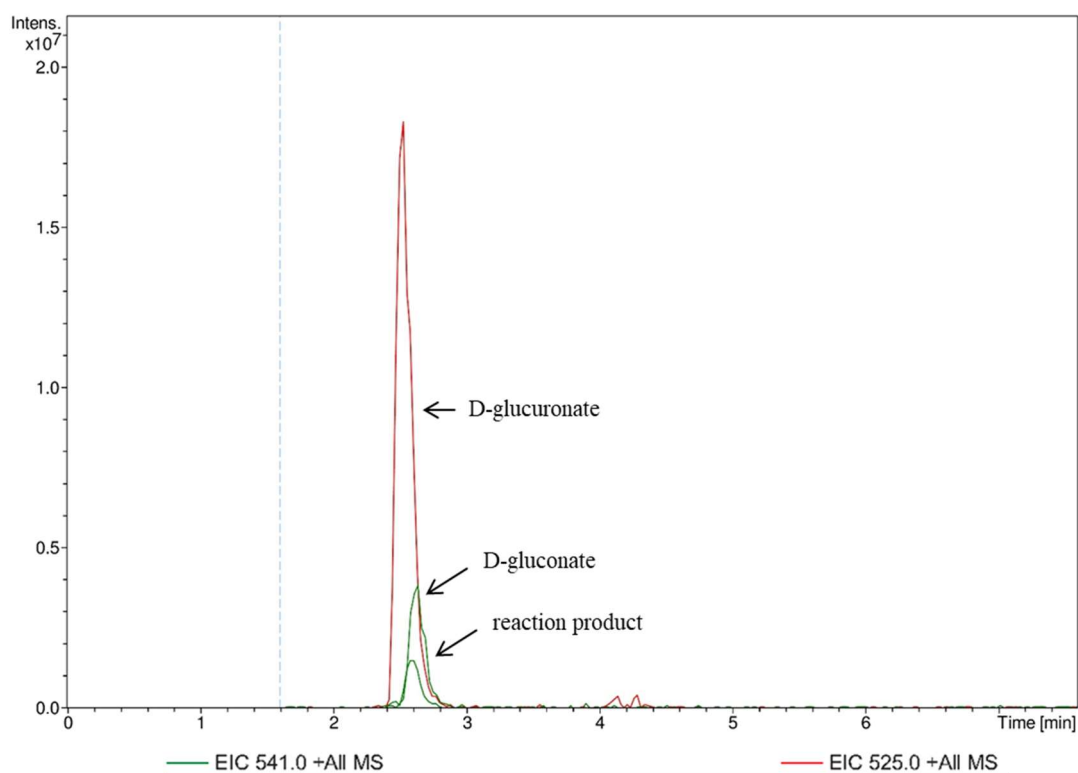


Figure 9: Product identification of *bt*UGDH

The reaction product of *bt*UGDH with D-glucose showed a retention time of 2.6 min and an m/z of 541.0 (green). This corresponds to gluconate (m/z 541.0, green) instead of D-gluconate (m/z 525.0, red). The two derivatives have the same retention time and can only be distinguished by their mass.

Since this finding suggested that D-glucose was not arranged appropriately in the active site of *bt*UGDH for oxidation of the C6, uridine monophosphate and uridine were added to the reaction, respectively, in order to assist the coordination of the substrate. However, instead, both the K_m for D-glucose and V_{max} were affected negatively. Finally, activity with D-glucose protected at C1, methyl-1-glucose, was tested, but no activity at all was detected. Therefore, it was anticipated that the measured activity of *bt*UGDH with D-glucose is either due to a glucose dehydrogenase side activity or, more likely, due to an impurity of the enzyme preparation with glucose dehydrogenase, an enzyme that is also present in bovine liver. In fact, other preparations of *bt*UGDH sold by Sigma Aldrich indicate the presence of glucose dehydrogenase.

4.1.2 Alcohol dehydrogenases from *Agrobacterium tumefaciens*

Various alcohol dehydrogenases from *Agrobacterium tumefaciens* have been shown to catalyze the reduction of 4-deoxy-L-erythro-5-hexulose uronate (Dehu) using NADPH as a cofactor (Kashiyama, 2012). The resulting 2-keto-3-deoxy-D-gluconate (2-Kdg) is a derivative of D-gluconate. Therefore, two enzymes from this patent, ADH1 and ADH2, were cloned and purified (Gansbiller, 2014). However, both exhibited too low activities to be investigated further.

4.1.3 Alcohol dehydrogenases from *Sphingomonas* species A1

Sphingomonas sp. strain A1 is an alginate assimilating bacterium. It degrades alginate through four lyase reactions. The resulting monosaccharide is first non-enzymatically converted to Dehu, which is then reduced by a short-chain dehydrogenase/reductase, here termed SpsADH, to 2-Kdg. It can then enter the main metabolism. Two isozymes of SpsADH are described in literature with different cofactor specificities for NADP⁺ (SpsADH-P) and NAD⁺ (SpsADH), respectively (Takase et al., 2014; Takase et al., 2010). Both of them were found to be able to oxidize D-gluconate at C6.

4.1.3.1 General characterization of two isozymes

Both isozymes (SpsADH-P and SpsADH) were not active in acidic solutions (pH 5 to 6) and exhibited their maximum activity at pH 10 (100% or 1.1 U/mg and 4.8 U/mg, respectively). In more basic solutions, the activity declined again, whereas SpsADH-P showed a plateau between pH 10.5 and 11.5, which is not seen with SpsADH (Figure 10 A and C, respectively). In addition, different buffer salts at pH 8 resulted in different relative activities of the two enzymes. While SpsADH-P was most active in phosphate buffers, potassium phosphate (KP) 100% (1.7 U/mg) and sodium phosphate (NaP) 90%, followed by ammonium bicarbonate (AbC) with 84%, arginine with 65%, TRIS with 47% and 2-(4-(2-hydroxyethyl)-1-piperazinyl)-ethansulfonic acid (HEPES) buffer with 56%; SpsADH was most active in AbC (1.8 U/mg, 100%), followed by HEPES (70%), NaP (65%), KP (65%), Arginine (38%), and TRIS buffer (35%) (Figure 10 B and D, respectively)

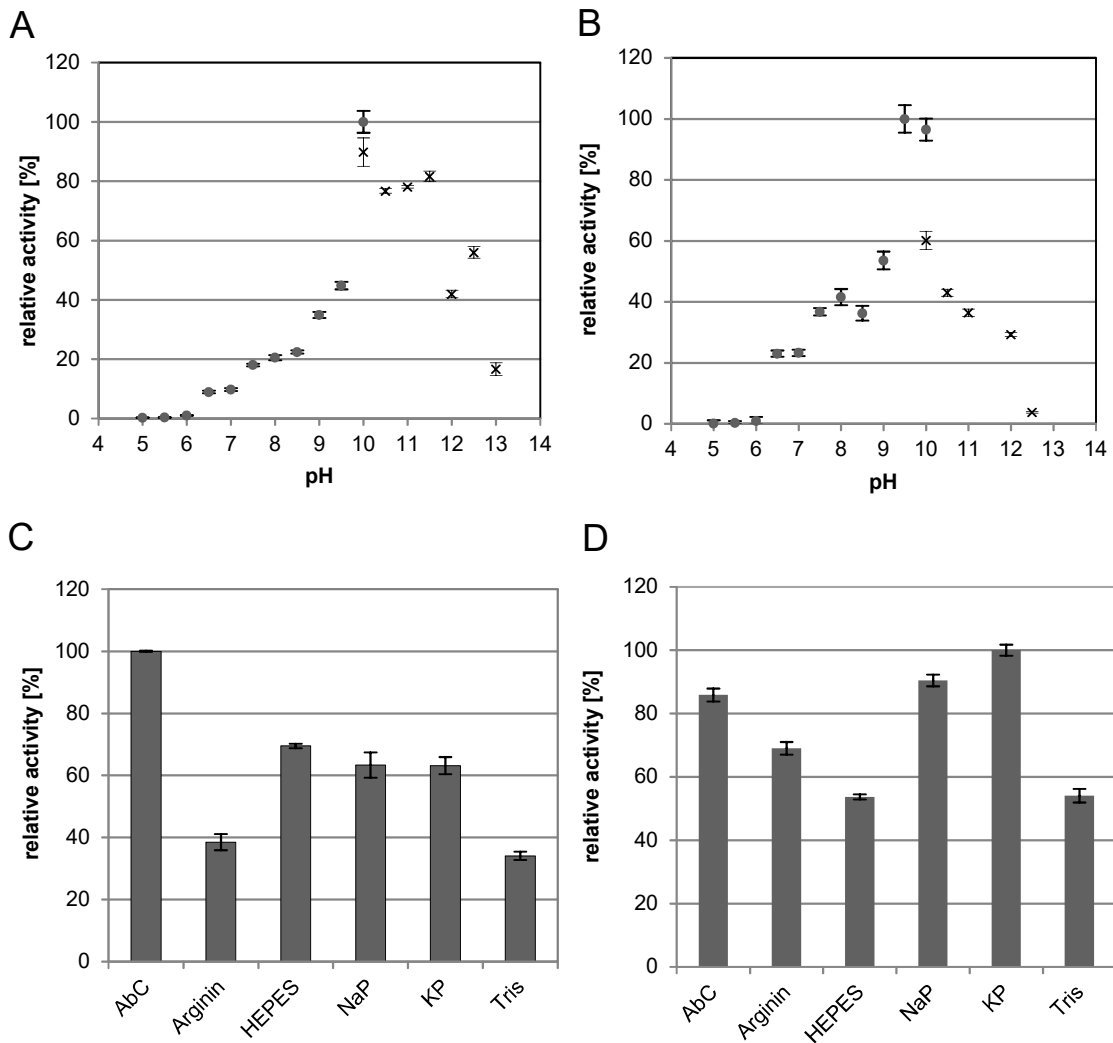


Figure 10: General properties of both SpsADH isozymes

SpsADH-P: relative activity (A) in dependence of pH (100% refers to 1.1 U/mg) using triple puffer (pH 5 to 10) and arginine buffer (pH 10 to 12.5), and (B) in dependence of buffer salts at pH 8 (100% refers to 1.7 U/mg). *SpsADH*: relative activity (C) in dependence of pH (100% refers to 4.8 U/mg) using triple puffer (pH 5 to 10) and arginine buffer (pH 10 to 12.5), and (D) in dependence of buffer salts at pH 8 (100% refers to 1.8 U/mg). Error bars indicate the standard deviation of three measurements.

SpsADH-P showed activity towards D-gluconate (0.9 U/mg), D-mannonate (0.7 U/mg), and D-galactonate, as well as D-xylonate (both around 0.4 U/mg).

Detailed experiments concerning the substrate scope were then conducted with the NAD^+ dependent *SpsADH* and are outlined in the following section.

4.1.3.2 Substrate scope of a dehydrogenase from *Sphingomonas* sp. A1 and its potential for the synthesis of rare sugars and sugar derivatives

Authors: Barbara Beer, André Pick, Manuel Döring, Petra Lommes, and Volker Sieber

In this publication, the substrate scope of SpsADH was analyzed in detail and the applicability of the enzyme for the synthesis of the rare sugar L-gulose from D-sorbitol was shown. Rare sugars and sugar derivatives that can be obtained from abundant sugars are of great interest to the pharmaceutical industry and for biochemical research. The finding of SpsADH catalyzing not only the oxidation of C6 of its native substrate 2-Kdg, but also C6 of the substrate analog D-gluconate, led to the question, which other substrates are recognized by SpsADH. Since biocatalysts are nowadays accepted and valued for their relaxed substrate specificity, a comprehensive analysis can open up new reaction pathways for target compounds. Therefore, C3 to C6 aldonates were synthesized in our lab and analyzed, drawing a picture of how the stereo configurations of the hydroxyl groups at C2 to C_{n-1} (with n = 4, 5, 6) influence the substrate specificity of SpsADH. Furthermore, the oxidation of polyols was tested, where two primary hydroxyl groups can be oxidized. Here, the stereoconfiguration at the two carbons adjacent to the carbon being oxidized were shown to be recognized by SpsADH. Most of these reactions hold the potential for the synthesis of high value compounds from cheap and available raw materials. One of them is the oxidation of D-sorbitol to the rare sugar L-gulose. In a lab-scale experiment (50 mL), it was possible to produce 300 mM of L-gulose within 234h, which corresponds to a space-time-yield of 4.0 gL⁻¹d⁻¹. This is above the range of published fermentation processes for the production of L-gulose.

Barbara Beer performed the cloning, designed the experiments and conducted part of them. She also analyzed the data and wrote the manuscript. André Pick contributed to the content and language of the manuscript. Manuel Döring conducted most substrate scope experiments as well as the synthesis of L-gulose, Petra Lommes synthesized and purified aldonic acids, and Volker Sieber contributed to the content and language of the manuscript.

The supplemental information for this publication can be found in the appendix, section 6.5.

The manuscript was submitted to Microbial Biotechnology on March 7th 2018.

Substrate scope of a dehydrogenase from *Sphingomonas* species A1 and its potential application in the synthesis of rare sugars and sugar derivatives

Barbara Beer,¹ André Pick,¹ Manuel Döring,¹ Petra Lommes¹ and Volker Sieber^{1,2,3,4,*} 

¹Chair of Chemistry of Biogenic Resources, Technical University of Munich, Schulgasse 16, 94315 Straubing, Germany.

²Catalysis Research Center, Technical University of Munich, Ernst-Otto-Fischer-Str. 1, 85748 Garching, Germany.

³Fraunhofer Institute of Interfacial Engineering and Biotechnology (IGB), Bio-, Electro- and Chemo Catalysis (BioCat) Branch, Schulgasse 11a, Straubing 94315, Germany.

⁴School of Chemistry and Molecular Biosciences, The University of Queensland, 68 Cooper Road, St. Lucia, 4072 Qld, Australia.

Summary

Rare sugars and sugar derivatives that can be obtained from abundant sugars are of great interest to biochemical and pharmaceutical research. Here, we describe the substrate scope of a short-chain dehydrogenase/reductase from *Sphingomonas* species A1 (SpsADH) in the oxidation of aldonates and polyols. The resulting products are rare uronic acids and rare sugars respectively. We provide insight into the substrate recognition of SpsADH using kinetic analyses, which show that the configuration of the hydroxyl groups adjacent to the oxidized carbon is crucial for substrate recognition. Furthermore, the specificity is demonstrated by the oxidation of D-sorbitol leading to L-gulose as sole product instead of a

mixture of D-glucose and L-gulose. Finally, we applied the enzyme to the synthesis of L-gulose from D-sorbitol in an *in vitro* system using a NADH oxidase for cofactor recycling. This study shows the usefulness of exploring the substrate scope of enzymes to find new enzymatic reaction pathways from renewable resources to value-added compounds.

Introduction

Sugars and sugar derivatives play an important role in biochemical research, pharmaceutical drug discovery and the food industry as they are involved in a myriad of metabolic processes, including signalling, cellular recognition and processes that are central to human health. However, only a small number of all possible monosaccharides, that is D-glucose, D-galactose, D-mannose, D-fructose, D-xylose, D-ribose and L-arabinose, according to the International Society of Rare Sugars (Granström *et al.*, 2004), are found in nature in sufficient amounts to allow their commercial exploitation. Consequently, the so-called rare sugars have to be produced by (bio)chemical processes starting from cheap and widely available substrates. Four enzyme classes that can be used for rare sugar production are aldolases, keto-aldol isomerases, epimerases and oxidoreductases (Izumori, 2006; Li *et al.*, 2015). Included in the last enzyme class are dehydrogenases/reductases (EC 1.1.-.-), which catalyse oxidations and corresponding reductions using different redox-mediating cofactors. They can be classified into short- (SDR), medium- (MDR) and long-chain (LDH) dehydrogenases/reductases according to the number of amino acids. SDRs consist of 250 to 300 amino acids and contain two domains; a cofactor-binding domain and a substrate-binding domain. While the cofactor-binding domain is usually conserved, the substrate-binding domain varies and determines the substrate specificity (Kavanagh *et al.*, 2008). SDR family enzymes use NADP(H) or NAD(H) as a cofactor and substrates include important metabolites such as sugars and their derivatives in carbohydrate metabolism (Koropatkin and Holden, 2005; Zhang *et al.*, 2009), steroids in signal transduction (Benach *et al.*, 2002; Sveglj *et al.*, 2012), and keto-acyl-(acyl carrier proteins) and enoyl-acyl-(acyl

Received 22 September, 2017; revised 31 March, 2018; accepted 2 April, 2018.

*For correspondence. E-mail sieber@tum.de; Tel. +49 9421 187 300; Fax +49 9421 187 310.

This work was conducted at the Chair of Chemistry of Biogenic Resources, Technical University of Munich, Schulgasse 16, 94315 Straubing, Germany.

Microbial Biotechnology (2018) 0(0), 1–12
doi:10.1111/1751-7915.13272

Funding Information

Funding of BB was provided by the Bavarian State Ministry of the Environment and Consumer Protection (grant number TGC01GCU-60345). Further funding was provided by the Technical University of Munich within the funding program Open Access Publishing and by the COST action CM1303 Systems Biocatalysis.

© 2018 The Authors. *Microbial Biotechnology* published by John Wiley & Sons Ltd and Society for Applied Microbiology. This is an open access article under the terms of the Creative Commons Attribution License, which permits use, distribution and reproduction in any medium, provided the original work is properly cited.

carrier proteins) in fatty-acid synthesis (Kim *et al.*, 2011; Blaise *et al.*, 2017). More than 170 000 enzymes in the SDR family are registered in UniProtKB (January 2018). New members of this superfamily are identified every year (there were almost 416 000 new entries in UniProt in 2017), further increasing the vast number of substances known to be metabolized.

Apart from their physiological role, many SDR enzymes are also known for their broad substrate scope (Hirano *et al.*, 2005; Pennacchio *et al.*, 2010; Stekhanova *et al.*, 2010; Ghatak *et al.*, 2017; Roth *et al.*, 2017). These non-native substrates can represent interesting starting points for products that are difficult to synthesize chemically. To identify these activities, enzymes can be isolated and exposed to reaction conditions or substrates not seen *in vivo* that will challenge their specificity, possibly forcing them to act on substrates they were not originally designed for. This lack of specificity of enzymes has become increasingly important in white biotechnology for the environmentally friendly synthesis of fine as well as bulk chemicals using enzymes as catalysts (Arora *et al.*, 2014). Here, new enzymatic activities are often required for the synthesis of non-native substances or for the conversion of non-native intermediates of an artificial metabolic pathway for both *in vivo* and *in vitro* applications. In the latter, with no constraints such as cell viability or transportation across cell boundaries, non-native substrates can be applied in a straightforward manner. Moreover, side reactions, which can be a disadvantage of using enzymes with lower specificity, can be controlled more easily *in vitro*, as only a limited and specified number of substances, that is, the substrate, the product, and possibly intermediates, are involved.

A NADH/NADPH-dependent SDR involved in alginate metabolism for the reduction in 4-deoxy-L-erythro-5-hexoseulose (DEHU) to 2-keto-3-deoxy-D-gluconate (KDG) has been identified in *Pseudomonas* (Preiss and

Ashwell, 1962) and *Vibrio splendidus* (Wargacki *et al.*, 2012), and recently characterized in detail from *Sphingomonas* species A1 (Takase *et al.*, 2010, 2014), *Flavobacterium* species strain UMI-01 (Inoue *et al.*, 2015), and abalone (Mochizuki *et al.*, 2015). The last two studies also addressed the question of substrate scope. However, no activity was observed for the reduction in other substrates apart from DEHU. Thus far, no study has examined the reverse reaction (the oxidation reaction) and challenged the specificity with non-native concentrations of substrates. Here, we provide a comprehensive picture of the substrate scope and specificity of the NAD⁺-dependent SDR from *Sphingomonas* species A1 (SpsADH, ID: SPH3227, PDB: 4TKM) for oxidation reactions. This enzyme consists of 258 amino acids, has 64% sequence similarity to its NADP⁺-dependent isoenzyme, and high sequence identity (40%–71%) to 3-ketoacyl-CoA-reductases. Some of the reactions we observed have not been found in nature and may be useful for the synthesis of rare sugars and sugar derivatives.

Results

Substrate scope

Oxidation of C6 of aldonates. SpsADH has been described for the reduction in DEHU to KDG, by reducing the terminal aldehyde (C6 in respect to KDG, Fig. 1). However, we were interested in oxidation reactions rather than reductions. Therefore, we first analysed SpsADH with its native substrate KDG. As expected from thermodynamics, the oxidation of KDG to DEHU was far less preferred compared to reduction, with a V_{\max} of $2.8 \pm 0.2 \text{ U mg}^{-1}$ and a K_m of $13 \pm 3 \text{ mM}$. For comparison, Takase *et al.* (2014) reported for the reduction in DEHU a V_{\max} of $462 \pm 33 \text{ U mg}^{-1}$ and a K_m of $4.8 \pm 0.6 \text{ mM}$. We then measured the kinetic parameters for the analog

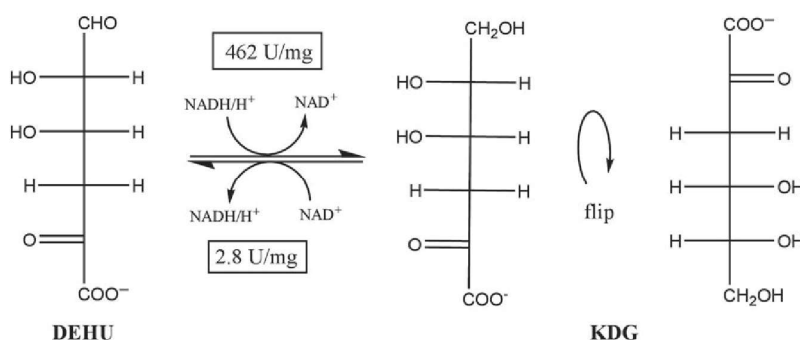


Fig. 1. Native reaction of SpsADH. SpsADH is involved in alginate metabolism for the reduction in 4-deoxy-L-erythro-5-hexoseulose (DEHU) to 2-keto-3-deoxy-D-gluconate (KDG).

D-gluconate, which has hydroxyl groups at C2 and C3 and obtained similar values as for KDG: $V_{\max} = 2.0 \pm 0.1 \text{ U mg}^{-1}$; $K_m = 12 \pm 2 \text{ mM}$. Encouraged by these positive results, we investigated the substrate specificity of SpsADH. Therefore, we synthesized and performed kinetic analyses with all C6- and C5-D-aldonates (except D-idonate, and D-gulonate, as neither the corresponding aldose nor the aldonates were commercially available) (Table 1). The catalytic efficiency (k_{cat}/K_m) for the various substrates compared to KDG followed this order: D-gluconate (79%), D-mannonate (37%), D-allonate (10%), D-altronate (8%), D-talonate (3%), D-xylonate (1%), D-ribonate (0.3%), and D-arabinonate, D-lyxonate, and D-galactonate (0.2%). The formation of the corresponding uronates could be proved by HPLC using the PMP method (Fig. S1). An activity with shorter aldonates, namely D-erythronate and D-threonate as well as D-glycerate was barely measurable; therefore, no kinetic analysis was possible. In addition, the evaluation of the reverse reactions was not possible, as the corresponding uronates are not commercially available or come in too low quantities.

Oxidation of polyols

The next group of substrates we tested was polyols. Here, the catalytic efficiencies for the tested polyols glycerol, meso-erythritol, D-ribitol, D-arabitol, D-xylitol, D-mannitol, and D-sorbitol were extremely low ranging from 8.7×10^{-5} to 1.5×10^{-5} for D-arabitol and D-sorbitol respectively (Table 1). As two primary hydroxyl groups are present in these molecules, here termed C_1 and C_{terminal} , that can be oxidized to form different aldoses, we analysed the products of the oxidation of D-sorbitol and D-arabitol using the PMP method (see Experimental section). The oxidation of D-sorbitol resulted in L-gulose as the sole product, which means that only C_{terminal} was oxidized by SpsADH. D-arabitol oxidation yielded D-lyxose as well as traces of D-arabinose (Fig. 2). The resulting aldoses of the other polyols have either D- or L-configuration depending on the carbon being oxidized. These could not be distinguished with this analytical method. The reverse reactions, that is, the reduction in aldoses was not measurable with C5 and C6 sugars, which is unsurprising, as the reduction in the aldehyde requires adoption by the aldoses of an open-chain configuration. Accordingly, the C4 sugars were better substrates. Here, only the activity at a fixed substrate concentration, 25 mM, was compared as follows: D-erythrose: 5 mU mg^{-1} , D-threose: 43 mU mg^{-1} , D-glyceraldehyde: 7 mU mg^{-1} , and L-glyceraldehyde: 346 mU mg^{-1} .

Other aldehydes lacking hydroxyl groups such as propanal, butanal, hexanal and 4-oxobutanoic acid were not

Substrate scope of a dehydrogenase 3

reduced by SpsADH. However, pyruvaldehyde, carrying a keto-group, and iso-butanal, having a methyl-side-chain at the carbon adjacent to the carbon being oxidized, were accepted with an activity of 25 mU mg^{-1} and 5.5 mU mg^{-1} , respectively, at 25 mM substrate concentration each.

Stability and total turnover

As SpsADH exhibits only very low activities towards non-native substrates, the stability of the enzyme is very important to ensure complete conversion by extended incubation. Therefore, we analysed the enzyme at 25°C in ammonium bicarbonate buffer pH 7.9 with 1 mM NAD^+ and found the half-life to be 20 h. In the case of oxidation of D-gluconate to L-gulonate, this gives a total turnover number of 28.300.

Production of L-gulose from D-sorbitol

We applied SpsADH for the synthesis of the rare and high-priced sugar L-gulose from available and cheap D-sorbitol in a proof-of-concept experiment. From the kinetic analysis, we found an extremely high K_m of $350 \pm 20 \text{ mM}$ and only a low V_{\max} of $11 \pm 0.2 \text{ mU mg}^{-1}$. Nonetheless, within 230 h, 300 mM L-gulose were produced, resulting in a space-time yield (STY) of 1.3 mM h^{-1} ($4.0 \text{ g L}^{-1} \text{ d}^{-1}$) (Fig. 3A). Although the theoretical V_{\max} was not reached here, as this value only reflects the activity without any product present, SpsADH seemed to be stabilized by sorbitol, as it has also been reported for various other proteins (Brennan *et al.*, 2003; Khajehzadeh *et al.*, 2016; Pazhang *et al.*, 2016). This allowed SpsADH to be active for an extended time period of approximately 230 h, resulting in this high yield.

During the purification procedure, glucose was found as an impurity of the D-sorbitol charge. Due to the similar properties of D-glucose and L-gulose, we converted D-glucose to D-gluconate using glucose dehydrogenase and catalase. Gluconate was then separated from L-gulose and D-sorbitol by anion exchange chromatography with a recovery of 95% of the L-gulose/D-sorbitol mixture. Subsequent purification of L-gulose was possible by cation exchange chromatography with a recovery of 66% pure L-gulose (Fig. 3B).

Discussion

'Where there is oxidation there will always be reduction' (Robins and Osorio-Lozada, 2012) is essentially the same as: where there is reduction, there will always be oxidation. The native reaction of SpsADH is the reduction in DEHU to KDG in alginate metabolism. Although

4 B. Beer et al.

Table 1. Kinetic parameters of SpsADH with various substrates. The kinetic parameters of SpsADH with D-aldonates with a carbon chain length of four to six were determined. Furthermore, polyols with a carbon chain length of three to six were investigated.

Structure	Substrate	K_m (mM)	V_{max} (mU mg ⁻¹)	k_{cat} (s ⁻¹)	k_{cat}/K_m (mM ⁻¹ s ⁻¹)	k_{cat}/K_m (%)
$ \begin{array}{c} \text{COO}^- \\ \\ \text{C}=\text{O} \\ \\ \text{H}-\text{C}-\text{H} \\ \\ \text{H}-\text{C}-\text{OH} \\ \\ \text{H}-\text{C}-\text{OH} \\ \\ \text{CH}_2\text{OH} \end{array} $	KDG	13 ± 3	2.8 × 10 ³ ± 0.2 × 10 ³	1.4 ± 0.08	10 × 10 ⁻² ± 3 × 10 ⁻²	100
$ \begin{array}{c} \text{COO}^- \\ \\ \text{H}-\text{C}-\text{OH} \\ \\ \text{HO}-\text{C}-\text{H} \\ \\ \text{H}-\text{C}-\text{OH} \\ \\ \text{H}-\text{C}-\text{OH} \\ \\ \text{CH}_2\text{OH} \end{array} $	D-gluconate	12 ± 1	2.0 × 10 ³ ± 0.6 × 10 ³	9.8 × 10 ⁻¹ ± 0.3 × 10 ⁻¹	8.2 × 10 ⁻² ± 0.9 × 10 ⁻²	79
$ \begin{array}{c} \text{COO}^- \\ \\ \text{HO}-\text{C}-\text{H} \\ \\ \text{HO}-\text{C}-\text{H} \\ \\ \text{H}-\text{C}-\text{OH} \\ \\ \text{H}-\text{C}-\text{OH} \\ \\ \text{CH}_2\text{OH} \end{array} $	D-mannonate	14 ± 1	1.1 × 10 ³ ± 0.2 × 10 ³	5.3 × 10 ⁻¹ ± 0.1 × 10 ⁻¹	3.8 × 10 ⁻² ± 0.4 × 10 ⁻²	37
$ \begin{array}{c} \text{COO}^- \\ \\ \text{H}-\text{C}-\text{OH} \\ \\ \text{H}-\text{C}-\text{OH} \\ \\ \text{H}-\text{C}-\text{OH} \\ \\ \text{H}-\text{C}-\text{OH} \\ \\ \text{CH}_2\text{OH} \end{array} $	D-allonate	16 ± 2	3.6 × 10 ² ± 0.1 × 10 ²	1.8 × 10 ⁻¹ ± 0.05 × 10 ⁻¹	1.1 × 10 ⁻² ± 0.2 × 10 ⁻²	10
$ \begin{array}{c} \text{COO}^- \\ \\ \text{HO}-\text{C}-\text{H} \\ \\ \text{H}-\text{C}-\text{OH} \\ \\ \text{H}-\text{C}-\text{OH} \\ \\ \text{H}-\text{C}-\text{OH} \\ \\ \text{CH}_2\text{OH} \end{array} $	D-altronate	24 ± 4	3.9 × 10 ² ± 0.2 × 10 ²	1.9 × 10 ⁻¹ ± 0.08 × 10 ⁻¹	8.0 × 10 ⁻³ ± 2 × 10 ⁻³	8
$ \begin{array}{c} \text{COO}^- \\ \\ \text{H}-\text{C}-\text{OH} \\ \\ \text{HO}-\text{C}-\text{H} \\ \\ \text{HO}-\text{C}-\text{H} \\ \\ \text{H}-\text{C}-\text{OH} \\ \\ \text{CH}_2\text{OH} \end{array} $	D-galactonate	50 ± 5	16 ± 1	7.9 × 10 ⁻³ ± 0.3 × 10 ⁻³	1.6 × 10 ⁻⁴ ± 0.2 × 10 ⁻⁴	0.2
$ \begin{array}{c} \text{COO}^- \\ \\ \text{HO}-\text{C}-\text{H} \\ \\ \text{HO}-\text{C}-\text{H} \\ \\ \text{HO}-\text{C}-\text{H} \\ \\ \text{H}-\text{C}-\text{OH} \\ \\ \text{CH}_2\text{OH} \end{array} $	D-talonate	6 ± 1	42 ± 2	2.1 × 10 ⁻² ± 0.1 × 10 ⁻²	3.4 × 10 ⁻³ ± 0.9 × 10 ⁻³	3

Substrate scope of a dehydrogenase 5

Table 1. (Continued)

Structure	Substrate	K_m (mM)	V_{max} (mU mg ⁻¹)	k_{cat} (s ⁻¹)	k_{cat}/K_m (mM ⁻¹ s ⁻¹)	k_{cat}/K_m (%)
$\begin{array}{c} \text{COO}^- \\ \\ \text{HO}-\text{C}-\text{H} \\ \\ \text{H}-\text{C}-\text{OH} \\ \\ \text{H}-\text{C}-\text{OH} \\ \\ \text{CH}_2\text{OH} \end{array}$	D-ribonate	16 ± 1	10 ± 0.2	5.2 × 10 ⁻³ ± 0.1 × 10 ⁻³	3.3 × 10 ⁻⁴ ± 0.3 × 10 ⁻⁴	0.3
$\begin{array}{c} \text{COO}^- \\ \\ \text{H}-\text{C}-\text{OH} \\ \\ \text{H}-\text{C}-\text{OH} \\ \\ \text{H}-\text{C}-\text{OH} \\ \\ \text{CH}_2\text{OH} \end{array}$	D-arabinonate	27 ± 3	10 ± 0.3	4.8 × 10 ⁻³ ± 0.1 × 10 ⁻³	1.8 × 10 ⁻⁴ ± 0.2 × 10 ⁻⁴	0.2
$\begin{array}{c} \text{CH}_2\text{OH} \\ \\ \text{COO}^- \\ \\ \text{H}-\text{C}-\text{OH} \\ \\ \text{HO}-\text{C}-\text{H} \\ \\ \text{H}-\text{C}-\text{OH} \\ \\ \text{CH}_2\text{OH} \end{array}$	D-xylonate	24 ± 2	66 ± 4	3.2 × 10 ⁻² ± 0.2 × 10 ⁻²	1.4 × 10 ⁻³ ± 0.2 × 10 ⁻³	1
$\begin{array}{c} \text{CH}_2\text{OH} \\ \\ \text{COO}^- \\ \\ \text{HO}-\text{C}-\text{H} \\ \\ \text{HO}-\text{C}-\text{H} \\ \\ \text{H}-\text{C}-\text{OH} \\ \\ \text{CH}_2\text{OH} \end{array}$	D-lyxonate	27 ± 2	8.6 ± 0.3	4.2 × 10 ⁻³ ± 0.1 × 10 ⁻³	1.6 × 10 ⁻⁴ ± 0.2 × 10 ⁻⁴	0.2
$\begin{array}{c} \text{CH}_2\text{OH} \\ \\ \text{CH}_2\text{OH} \\ \\ \text{H}-\text{C}-\text{OH} \\ \\ \text{HO}-\text{C}-\text{H} \\ \\ \text{H}-\text{C}-\text{OH} \\ \\ \text{H}-\text{C}-\text{OH} \\ \\ \text{CH}_2\text{OH} \end{array}$	D-sorbitol	3.5 × 10 ² ± 0.1 × 10 ²	11 ± 0.2	5.2 × 10 ⁻³ ± 0.09 × 10 ⁻³	1.5 × 10 ⁻⁵ ± 0.08 × 10 ⁻⁵	0.01
$\begin{array}{c} \text{CH}_2\text{OH} \\ \\ \text{CH}_2\text{OH} \\ \\ \text{H}-\text{C}-\text{OH} \\ \\ \text{HO}-\text{C}-\text{H} \\ \\ \text{H}-\text{C}-\text{OH} \\ \\ \text{H}-\text{C}-\text{OH} \\ \\ \text{CH}_2\text{OH} \end{array}$	D-mannitol	1.1 × 10 ² ± 0.1 × 10 ²	5.9 ± 0.3	2.9 × 10 ⁻³ ± 0.1 × 10 ⁻³	2.6 × 10 ⁻⁵ ± 0.4 × 10 ⁻⁵	0.03
$\begin{array}{c} \text{CH}_2\text{OH} \\ \\ \text{CH}_2\text{OH} \\ \\ \text{H}-\text{C}-\text{OH} \\ \\ \text{H}-\text{C}-\text{OH} \\ \\ \text{H}-\text{C}-\text{OH} \\ \\ \text{CH}_2\text{OH} \end{array}$	D-ribitol	16 × 10 ² ± 4 × 10 ⁻⁴	45 ± 6	2.3 × 10 ⁻² ± 0.3 × 10 ⁻²	1.5 × 10 ⁻⁵ ± 0.5 × 10 ⁻⁵	0.01
$\begin{array}{c} \text{CH}_2\text{OH} \\ \\ \text{CH}_2\text{OH} \\ \\ \text{HO}-\text{C}-\text{H} \\ \\ \text{H}-\text{C}-\text{OH} \\ \\ \text{H}-\text{C}-\text{OH} \\ \\ \text{CH}_2\text{OH} \end{array}$	D-arabitol	2.2 × 10 ² ± 0.2 × 10 ²	39 ± 1	19 × 10 ⁻³ ± 0.6 × 10 ⁻³	8.7 × 10 ⁻⁵ ± 1 × 10 ⁻⁵	0.08

Table 1. (Continued)

Structure	Substrate	K_m (mM)	V_{max} (mU mg ⁻¹)	k_{cat} (s ⁻¹)	k_{cat}/K_m (mM ⁻¹ s ⁻¹)	k_{cat}/K_m (%)
$\begin{array}{c} \text{CH}_2\text{OH} \\ \\ \text{H}-\text{C}-\text{OH} \\ \\ \text{HO}-\text{C}-\text{H} \\ \\ \text{H}-\text{C}-\text{OH} \\ \\ \text{CH}_2\text{OH} \end{array}$	D-xylitol	$14 \times 10^2 \pm 2 \times 10^2$	16 ± 1	$7.8 \times 10^{-3} \pm 0.6 \times 10^{-3}$	$5.5 \times 10^{-6} \pm 1 \times 10^{-6}$	0.01
$\begin{array}{c} \text{CH}_2\text{OH} \\ \\ \text{H}-\text{C}-\text{OH} \\ \\ \text{H}-\text{C}-\text{OH} \\ \\ \text{H}-\text{C}-\text{OH} \\ \\ \text{CH}_2\text{OH} \end{array}$	meso-Erythritol	$7.0 \times 10^2 \pm 1 \times 10^2$	39 ± 3	$1.9 \times 10^{-2} \pm 0.1 \times 10^{-2}$	$2.7 \times 10^{-5} \pm 0.6 \times 10^{-5}$	0.03
$\begin{array}{c} \text{CH}_2\text{OH} \\ \\ \text{H}-\text{C}-\text{OH} \\ \\ \text{H}-\text{C}-\text{OH} \\ \\ \text{H}-\text{C}-\text{OH} \\ \\ \text{CH}_2\text{OH} \end{array}$	Glycerol	$1 \times 10^2 \pm 0.1 \times 10^2$	11 ± 0.4	$5.6 \times 10^{-3} \pm 0.2 \times 10^{-3}$	$2.7 \times 10^{-5} \pm 0.6 \times 10^{-5}$	0.04

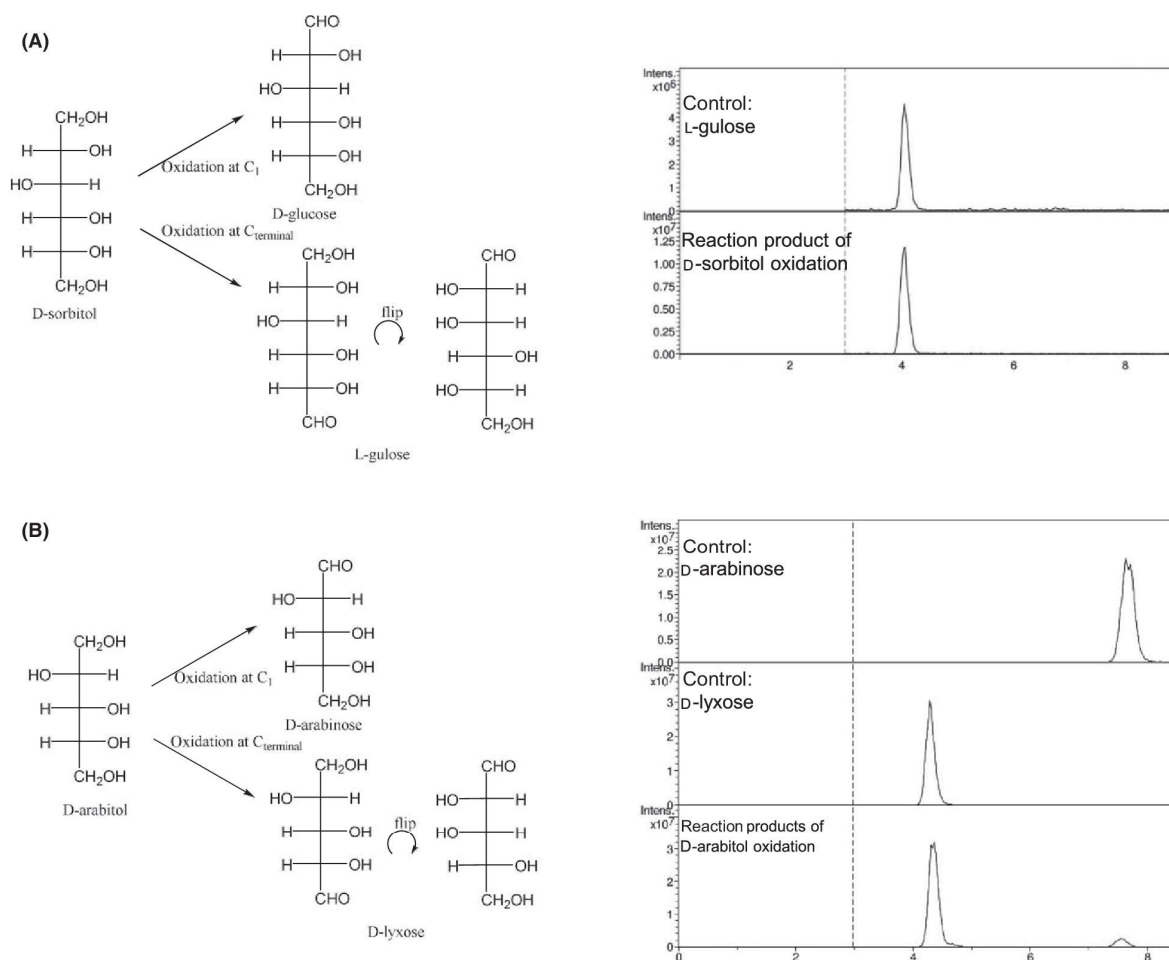


Fig. 2. Product identification of D-sorbitol and D-arabitol oxidation. In polyols, two primary hydroxyl groups are present, which could be oxidized by SpsADH, which would lead to different aldoses. For D-sorbitol, only L-gulose was detected (A), for D-arabitol (B), both D-lyxose as well as traces of D-arabinose were measurable.

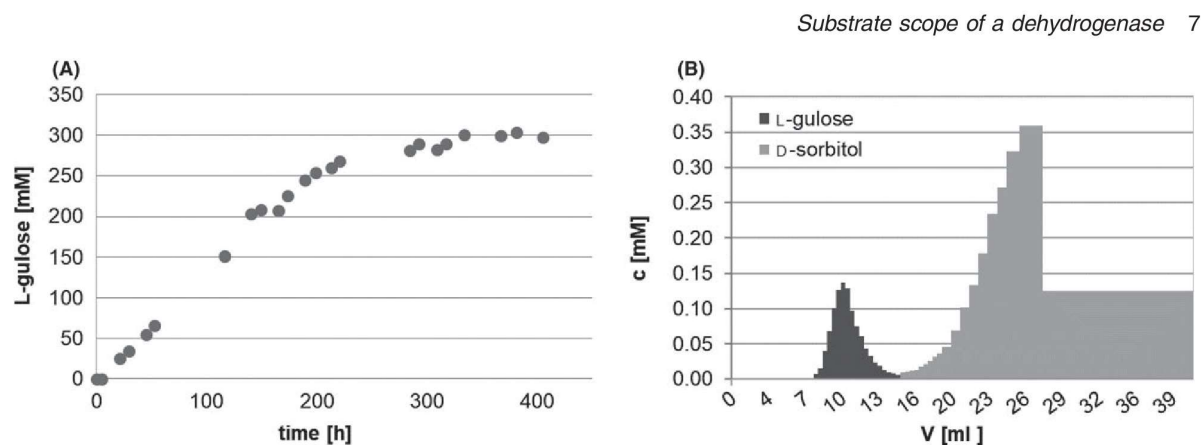


Fig. 3. Synthesis of L-gulose using SpsADH.

A. Starting from D-sorbitol, 300 mM L-gulose was produced by SpsADH within 234 h. This gives a space-time yield of 1.3 mM h^{-1} .

B. Purification of L-gulose by cation exchange chromatography. Multiple measurements were not conducted as this is only a proof-of-concept experiment.

this reaction is highly important for third-generation biomass utilization, where degradation of alginate from brown macro algae, for instance, plays a key role (Wargacki *et al.*, 2012; Mochizuki *et al.*, 2015), we were interested in the oxidation reaction, and beyond this, in the oxidation of other substrates apart from KDG.

The oxidation of KDG to DEHU is unfavourable compared to the reduction due to thermodynamics, and possibly also due to the physiological role of SpsADH as DEHU was indicated to be toxic to cells and therefore needs to be metabolized to non-hazardous KDG (Hashimoto *et al.*, 2010). Nonetheless, oxidation is possible at pH 8 and furthermore, SpsADH can also oxidize the analog D-gluconate with only 21% reduced catalytic efficiency. Here, C2 and C3 carry hydroxyl groups, whereas C1, C4, C5 and C6 are the same as in KDG. Interestingly, other C6-aldonates of the erythro-group, that is D-allonate, D-altronate, and D-mannonate, which differ only in the configuration of the hydroxyl groups at C2 and C3, show a sharp decrease in the catalytic efficiency. For D-aldonates from the threo-group (D-talonate and D-galactonate), as well as C5-D-aldonates, the catalytic efficiency decreases even further. A general rule to substrate recognition is that the carbon adjacent to the carbon being oxidized needs to carry a substituent (hydroxyl-, keto-, or methyl-group). Furthermore, from the specific oxidation of D-sorbitol to L-gulose instead of D-glucose, we conclude that the adjacent hydroxyl-group has to be in the D-conformation. This is also true for the reduction in glyceraldehyde, where the L-enantiomer is clearly preferred over D-glyceraldehyde, meaning that in the reverse reaction, glycerol only binds when the hydroxyl group at C2 is positioned in L-configuration. Furthermore, the position of the hydroxyl group at the next but one carbon also seems to play a role in substrate recognition, as D-arabitol was

mainly oxidized to D-lyxose with only traces of D-arabinose. It also shows in the preference for C6-D-aldonates of the erythro group over those of the threo-group. In general, the substrates are better recognized, if they are anionic: the catalytic efficiencies of aldonates always exceed those of the corresponding polyols. For D-gluconate, it is even about 5500 times higher than for the corresponding polyol D-sorbitol (8.2×10^{-2} and $1.5 \times 10^{-5} \text{ mM}^{-1} \text{ s}^{-1}$ respectively). Even though the activity was so low, we were able to produce the rare sugar L-gulose from D-sorbitol in an *in vitro* system with a STY of $4.0 \text{ g L}^{-1} \text{ d}^{-1}$. In comparison, another single-step conversion from D-sorbitol to L-gulose using a mannitol dehydrogenase from *Apium graveolens* in a recombinant *Escherichia coli* strain resulted in a STY of $0.9 \text{ g L}^{-1} \text{ d}^{-1}$ (Woodyer *et al.*, 2010). Furthermore, a glucose 6-phosphate isomerase from *Pyrococcus furiosus* was also assessed for the production of L-gulose from L-idose; however, incomplete conversion as well as formation of the side-product L-sorbose, is downsides of this reaction (Yoon *et al.*, 2009).

From other polyols tested here, the rare sugars L-erythrose (from meso-erythritol), L-ribose (from D-ribitol), D-lyxose (from D-arabitol) or L-xylose (from D-xylitol) could be obtained.

The aldonates can be converted to uronic acids, which could be further oxidized by uronate dehydrogenases (UDHs) to the corresponding aldonic acids, which are considered top value-added chemicals to be obtained from biomass (Werpy and Petersen, 2004). They can, for example, be used as building blocks for polymers and hyperbranched polyesters, and also for the metabolite α -ketoglutarate, for which an *in vitro* enzymatic cascade reaction has been established (Beer *et al.*, 2017). Here, glucuronate was used as a substrate, but glucose could also be converted using glucose dehydrogenase,

SpsADH and UDH. However, so far, UDHs are only known to participate in the oxidation of D-glucuronate, D-galacturonate and D-mannuronate (Pick *et al.*, 2015). Therefore, engineering of UDH, so that it is active with L-gulonate, is necessary here.

In summary, we showed that SpsADH exhibits a broad substrate scope, when challenged with non-native substrate concentrations. Research groups that previously investigated the substrate specificity of other DEHU reductases could not find any activity at a 1 mM substrate concentration (Inoue *et al.*, 2015; Mochizuki *et al.*, 2015). We believe that these enzymes could also show activity, if higher concentrations of substrates were used. Even with the very low (mU mg^{-1} range) activities found here, the long half-life of SpsADH allows conversion of significant amounts of substrate. In addition, these activities can be the starting point for enzyme engineering to enhance specific activities. The availability of the crystal structure (4TKM, Takase *et al.*, 2014) will facilitate this, as substrates of interest can be docked *in silico* into the binding pocket to find possible amino acid positions to be exchanged.

Experimental procedures

Reagents

Restriction enzymes, alkaline phosphatase, T4 ligase and Taq polymerase were obtained from New England Biolabs. Oligonucleotides were from biomers.net GmbH. All chemicals were of analytical grade or higher quality and purchased from Carbosynth, Sigma-Aldrich, Alfa Aesar, Serva, or Carl Roth. For protein purification, equipment (including columns) from GE Healthcare was used.

Preparation of aldonic acids and dehydrated aldonic acids

Aldonic acids were prepared from their corresponding sugars by oxidation using a gold catalyst (J213 XI/D 0.5%, 0.5% Au on Al_2O_3 powder, kindly provided by Evonik Industries, Germany). The procedure has been previously described for L-arabinose, D-xylose, D-galactose and D-glucose (Sperl *et al.*, 2016), as well as for D-ribose, D-lyxose, D-mannose, L-rhamnose and N-acetylglucosamine (Mirescu and Prüße, 2007), and could be adapted for the oxidation of D-allose, D-altrose, D-talose, D-arabinose, D-erythrose, D-threose, 2-deoxy-D-glucose and 3-deoxy-D-glucose. The results can be found in the supporting information. The procedure was as follows: reactions were carried out in a temperature controlled glass reactor (total volume 50 ml, initial reaction volume 30 ml) equipped with a reflux condenser, a pH electrode and a burette for base dosage, a 21 G needle as the

oxygen inlet, and a magnetic stirrer. Prior to the start of the reaction, the sugar solution was stirred at the desired pH value inside the reactor. This solution was heated to 50°C and oxygen was supplied at a flow rate of 40 ml min^{-1} . The reactions were then initiated by adding an appropriate amount of gold catalyst (see Supporting Information). During the reaction, the oxygen supply was maintained at the same flow rate and the pH value was kept constant with an automatic titrator (TitroLine 7000, SI Analytics, Germany) by adding aqueous NaOH. During the course of the reaction, the amount of added NaOH was monitored. Conversion and selectivity were checked with a HPLC system as described below.

For kinetic measurements, the aldonic acids were purified (preparative scale 200–1080 mg). For this, the resulting solution was loaded to a Dowex (1×8 , 200–400 mesh) anion exchange column, which was equilibrated with ammonium bicarbonate (AbC). The column was washed with three column volumes (CV) of H_2O and the sugar acids were eluted with 100 mM AbC (pH 10.4). The pooled fractions containing the sugar acids were lyophilized and dissolved in H_2O to give a concentration of 10 mg ml^{-1} . This solution was loaded to a Dowex (50Wx8-400, 200–400 mesh) cation exchange column in the Na^+ -form. Elution with H_2O and lyophilization gave the sugar acids as the sodium salt. Karl Fischer titrations were performed to analyse the water content and to calculate standard concentrations accordingly.

The keto-deoxy sugar KDG was obtained from D-glucuronate using the enzyme dihydroxy-acid dehydratase from *Sulfolobus solfataricus*. This detailed procedure is described by Sperl *et al.* (2016).

Construction of plasmid for overexpression

The DNA sequence encoding alcohol dehydrogenase from *Sphingomonas* species A1 (SpsADH, GenBank™ accession number BAP40335.1) was synthesized as a GeneArt®Strings DNA fragment with optimized codon usage for expression in *E. coli* and restriction sites for NdeI and XhoI (Life Technologies). The fragment was first cloned into pJET1.2 by blunt end ligation using a kit from Thermo Fisher Scientific. The gene was then cloned into pET-28a(+) (Novagen) with an N-terminal His₆-tag yielding the plasmid pET-28a-NHis-spsadh. Multiplication of the plasmids was performed in *E. coli* DH5 α (Stratagene) in LB medium containing 30 $\mu\text{g ml}^{-1}$ kanamycin.

Expression and purification

For small amounts, expression of *spsadh* was performed in *E. coli* BL21(DE3) (Novagen) containing the plasmid of interest in 1 L autoinduction medium that included

100 $\mu\text{g ml}^{-1}$ kanamycin (Studier, 2005). The preculture was incubated in 20 ml LB medium with 30 $\mu\text{g ml}^{-1}$ kanamycin at 37°C overnight on a rotary shaker (180 rpm). Expression cultures were inoculated with the overnight culture at an OD_{600} of 0.1. Incubation was performed in a shaking flask for 3 h at 37°C followed by incubation for 21 h at 16°C on a rotary shaker (120 rpm). Cells were harvested by centrifugation and stored at -20°C . For large amounts, expression of *sp-sadh* was performed using a 2 L Biostat Cplus bioreactor (Sartorius Stedim, Germany) in a batch cultivation process. The fermentation parameters were as follows: 2 L autoinduction medium containing 100 $\mu\text{g ml}^{-1}$ kanamycin was inoculated with 10% of a preculture grown overnight. The temperature was set at 37°C until an OD_{600} of 9 was reached, then it was decreased to 16°C for 24 h. The pH was held constant at 7 and the pO_2 at 30% with variable stirring speed and aeration. Cells were harvested by centrifugation and stored at -20°C .

For purification of SpsADH, cells were resuspended in 50 mM sodium phosphate buffer (pH 8.0, 20 mM imidazole, 500 mM NaCl, and 10% glycerol). Crude extracts were prepared on ice by ultrasonication (Hielscher Ultrasonics, sonotrode LS24d10): three cycles of 15-min pulsing (0.6 ms, 0.4 ms pause) at 80% amplitude. The insoluble fraction of the lysate was removed by centrifugation (20 000 rpm for 40 min at 4°C), and the supernatant was then applied to an IMAC affinity resin column (5 ml HisTrap™ FF) equilibrated with the resuspension buffer using the ÄKTA Purifier system. The column was washed with five column volumes of resuspension buffer and the His-tagged protein was eluted by a gradient of 10 column volumes of 0% to 100% elution buffer (50 mM sodium phosphate buffer; pH 8.0, 500 mM imidazole, 500 mM NaCl, and 10% glycerol). Aliquots of the eluted fractions were subjected to 12% SDS-PAGE as described by Laemmli (1970). The molecular weight was calculated using the ProtParam tool (Gasteiger 2005): this was 29 500 Da, including the additional amino acids of the N-terminal His₆-tag. The fractions containing the eluted protein were pooled and the protein was desalted using a HiPrep™ 26/10 Desalting column, which was preliminarily equilibrated with 50 mM AbC, pH 7.9. The protein concentration was determined by UV spectroscopy (NanoPhotometer, Implen) at 280 nm using the extinction coefficient (ϵ_{280}) calculated using the ProtParam tool (assuming all cysteines are reduced): 18 450 $\text{M}^{-1} \text{cm}^{-1}$. Aliquots of the protein solution were shock-frozen in liquid nitrogen and stored at -80°C .

Enzyme assays

The activity of SpsADH was determined photometrically by monitoring the increase/decrease in NADH at 340 nm

using the Infinite 200 PRO photometer (Tecan Group Ltd.). Reactions were performed at 25°C in triplicate using 96-well microtiter plates. For determination of the kinetic parameters, the reaction mixtures contained 50 mM AbC, pH 7.9, 0.3 mM NADH (or 1 mM NAD⁺), various concentrations of substrate, and an appropriate amount of purified enzyme. The initial reaction velocity was measured for 1 to 2 min and the calculation of Michaelis–Menten kinetics for determination of K_m and V_{max} was carried out using SigmaPlot 11.0 (Systat Software). One unit of enzyme activity was defined as the amount of protein that reduced (oxidized) 1 μmol of NAD (H) min^{-1} at 25°C.

For product identification, enzyme assays were performed overnight with the addition of the cofactor recycling enzyme NADH oxidase (NOX) from *Lactobacillus pentosus*. Expression, purification and activation with FAD were performed as described previously (Nowak *et al.*, 2015). Reaction mixtures contained 50 mM AbC, pH 7.9, 25 mM substrate, 5 mM NAD⁺ and purified SpsADH. Fresh NOX was added two more times during the incubation time due to stability issues (Beer *et al.*, 2017).

HPLC analysis

The synthesized aldonic acids were analysed by HPLC, using an UltiMate 3000 HPLC system (Dionex, Idstein, Germany), equipped with autosampler (WPS 3000TRS), a column compartment (TCC3000RS) and a diode array detector (DAD 3000RS). The Metrosep A Supp10–250/40 column (250 mm, particle size 4.6 mm; Metrohm, Filderstadt, Germany) at 65°C was used for separation by isocratic elution with 12 mM AbC, pH 10.0 as the mobile phase at 0.2 ml min^{-1} . Samples were diluted in water, filtered (10 kDa MWCO, modified PES; VWR, Darmstadt, Germany), and 10 μl were applied to the column. Data were analysed using Dionex Chromeleon software.

Uronic acids and aldoses were analysed by HPLC/MS as 1-phenyl-3-methyl-5-pyrazolone (PMP) derivatives using the method of Rühmann *et al.* (2014).

Samples were diluted in water and derivatized with 0.1 M PMP and 0.4% ammonium hydroxide in methanol. After 100 min at 70°C, the reaction was stopped with 16.7 mM acetic acid and filtered (Restek, 0.22 μm , PVDF). When elution of the uronic acid was expected before 3 min, the sample was extracted with chloroform (three times) to reduce excess PMP and then filtered.

The HPLC system (UltiMate 3000RS, Dionex) was composed of a degasser (SRD 3400), a pump module (HPG 3400RS), an autosampler (WPS 3000TRS), a column compartment (TCC3000RS), a diode array detector (DAD 3000RS) and an ESI ion trap unit (HCT, Bruker).

Data were collected and analysed using Bruker HyStar software. The column (Gravity C18, 100 mm length, 2 mm i.d.; 1.8 μm particle size; Macherey-Nagel) was operated at 50°C with a mobile phase A (5 mM ammonium acetate buffer, pH 5.6, with 15% acetonitrile) and a chromatographic flow rate of 0.6 ml min⁻¹. The gradient (mobile phase B containing pure acetonitrile) was as follows: start of mobile phase B at 1%, with an increase to 5% over 5 min, held for 2 min, then an increase to 18% over 1 min. The gradient was further increased to 40% over 0.3 min, held for 2 min, and returned within 0.2 min to starting conditions for 1.5 min. If samples were not extracted, the first 3 min of chromatographic flow were refused by a switch valve behind the UV detector (245 nm). Before entering ESI-MS, the flow was split 1:20 (Accurate post-column splitter, Dionex). The temperature of the autosampler was set to 20°C and an injection volume of 10 μl was used.

ESI ion trap parameters: The ion trap operated in the ultra scan mode (26 000 m/z/s) from 50 to 1000 m/z. The ICC target was set to 200 000 with a maximum accumulation time of 50 ms and four averages. The ion source parameters were set as follows: capillary voltage 4 kV, dry temperature 325°C, nebulizer pressure 40 psi, and dry gas flow 6 L min⁻¹. Auto MS mode with a smart target mass of 600 m/z and an MS/MS fragmentation amplitude of 0.5 V was used. Analysis was performed using the extracted ion chromatograms of the m/z value corresponding to the protonated molecules.

Production of L-gulose from D-sorbitol

Production of L-gulose was carried out in a volume of 50 ml in a two-necked round-bottom glass flask. One neck was used for drawing samples, and the second for supplementing gaseous, humidified oxygen through a cannula at 20 ml min⁻¹ once a day for 1 to 2 min. The reaction mixture contained 50 mM AbC, 1 mM NAD⁺, 1.5 M D-sorbitol and 0.04 U ml⁻¹ of SpsADH and NOX respectively. The kinetic parameters of NOX were determined in the presence of 1.5 M D-sorbitol in 50 mM AbC, and varying amounts of NADH.

The reaction took place at 25°C (water bath) with stirring. 0.04 U ml NOX was added multiple times over the entire duration of the experiment. Furthermore, to maintain the activity of SpsADH at V_{max} , 3.0 and 4.5 g D-sorbitol were added after 117 and 200 h respectively.

Samples for HPLC analysis were ultrafiltrated with spin filters (10 kDa MWCO, modified PES; VWR) to remove enzymes and stop the reaction. The experiment was stopped after there was no further rise in L-gulose concentrations.

Purification procedure: Due to an impurity of the used D-sorbitol charge, glucose had to be first removed. The

reaction mixture was consequently incubated with glucose oxidase and catalase to convert glucose to gluconate, which was then removed by anion exchange chromatography using a Dowex 1 \times 8, 200–400 mesh column. Pure L-gulose was then obtained by cation exchange chromatography (Dowex 50Wx8-400, 200–400 mesh column in the Na⁺-form).

Elution monitoring and quantification was performed using a HPLC system (Dionex, Sunnyvale, CA, USA) equipped with a Rezex ROA-H⁺ column (Phenomenex, Torrance, CA, USA), and a refractive index detector (RI-101, Shodex, Tokyo, Japan). The mobile phase (sulphuric acid, 2.5 mM) was set to a flow rate of 0.5 ml min⁻¹ at an oven temperature of 70°C. Quantitative calculations were referred to an external standard.

Acknowledgements

We thank Claudia Nowak for proofreading of the manuscript. Funding of BB was provided by the Bavarian State Ministry of the Environment and Consumer Protection (grant number TGC01GCU–60345). Further funding was provided by the Technical University of Munich within the funding program Open Access Publishing and by the COST action CM1303 Systems Biocatalysis. A patent application has been filed.

Conflict of interest

None declared.

References

- Arora, B., Mukherjee, J., and Gupta, M.N. (2014) Enzyme promiscuity: using the dark side of enzyme specificity in white biotechnology. *Sustain Chem Process* **2**: 25–34.
- Beer, B., Pick, A., and Sieber, V. (2017) *In vitro* metabolic engineering for the production of α -ketoglutarate. *Metab Eng* **40**: 5–13.
- Benach, J., Filling, C., Oppermann, U.C., Roversi, P., Bricogne, G., Berndt, K.D., *et al.* (2002) Structure of bacterial 3 β /17 β -hydroxysteroid dehydrogenase at 1.2 Å resolution: a model for multiple steroid recognition. *Biochemistry* **41**: 14659–14668.
- Blaise, M., Van Wyk, N., Banères-Roquet, F., Guérardel, Y., and Kremer, L. (2017) Binding of NADP⁺ triggers an open-to-closed transition in a mycobacterial FabG β -ketoacyl-ACP reductase. *Biochem J* **474**: 907–921.
- Brennan, J.D., Benjamin, D., DiBattista, E., and Gulceev, M.D. (2003) Using sugar and amino acid additives to stabilize enzymes within sol–gel derived silica. *Chem Mater* **15**: 737–745.
- Ghatak, A., Bharatham, N., Shanbhag, A.P., Datta, S., and Venkatraman, J. (2017) Delineating substrate diversity of disparate short-chain dehydrogenase reductase from *Debaryomyces hansenii*. *PLoS ONE* **12**: e0170202.

Substrate scope of a dehydrogenase 11

- Granström, T.B., Takata, G., Tokuda, M., and Izumori, K. (2004) Izumoring: a novel and complete strategy for bioproduction of rare sugars. *J Biosci Bioeng* **97**: 89–94.
- Hashimoto, W., Kawai, S., and Murata, K. (2010) Bacterial supersystem for alginate import/metabolism and its environmental and bioenergy applications. *Bioengineered Bugs* **1**: 97–109.
- Hirano, J., Miyamoto, K., and Ohta, H. (2005) Purification and characterization of the alcohol dehydrogenase with a broad substrate specificity originated from 2-phenylethanol-assimilating *Brevibacterium* sp. KU 1309. *J Biosci Bioeng* **100**: 318–322.
- Inoue, A., Nishiyama, R., Mochizuki, S., and Ojima, T. (2015) Identification of a 4-deoxy-L-erythro-5-hexoseulose uronic acid reductase, FIRed, in an alginolytic bacterium *Flavobacterium* sp. strain UMI-01. *Mar Drugs* **13**: 493–508, 416 pp.
- Izumori, K. (2006) Izumoring: a strategy for bioproduction of all hexoses. *J Biotechnol* **124**: 717–722.
- Kavanagh, K.L., Jornvall, H., Persson, B., and Oppermann, U. (2008) Medium- and short-chain dehydrogenase/reductase gene and protein families: the SDR superfamily: functional and structural diversity within a family of metabolic and regulatory enzymes. *Cell Mol Life Sci* **65**: 3895–3906.
- Khajehzadeh, M., Mehmejad, F., Pazhang, M., and Doustdar, F. (2016) Effects of sorbitol and glycerol on the structure, dynamics, and stability of *Mycobacterium tuberculosis* pyrazinamidase. *Int J Mycobacteriol* **5**: S138–S139.
- Kim, K.H., Ha, B.H., Kim, S.J., Hong, S.K., Hwang, K.Y., and Kim, E.E. (2011) Crystal structures of Enoyl-ACP reductases I (FabI) and III (FabL) from *B. subtilis*. *J Mol Biol* **406**: 403–415.
- Koropatkin, N.M., and Holden, H.M. (2005) Structure of CDP-D-glucose 4,6-dehydratase from *Salmonella typhi* complexed with CDP-D-xylose. *Acta Crystallogr D Biol Crystallogr* **61**: 365–373.
- Laemmli, U.K. (1970) Cleavage of structural proteins during the assembly of the head of Bacteriophage T4. *Nature* **227**: 680–685.
- Li, Z., Wu, X., Cai, L., Duan, S., Liu, J., Yuan, P., et al. (2015) Enzymatic synthesis of rare sugars with L-rhamnulose-1-phosphate aldolase from *Thermotoga maritima* MSB8. *Bioorg Med Chem Lett* **25**: 3980–3983.
- Mirescu, A., and Prüße, U. (2007) A new environmental friendly method for the preparation of sugar acids via catalytic oxidation on gold catalysts. *Appl Catal B* **70**: 644–652.
- Mochizuki, S., Nishiyama, R., Inoue, A., and Ojima, T. (2015) A novel aldo-keto reductase, HdRed, from the Pacific Abalone *Haliotis discus hannai*, which reduces alginate-derived 4-deoxy-L-erythro-5-hexoseulose uronic acid to 2-keto-3-deoxy-D-gluconate. *J Biol Chem* **290**: 30962–30974.
- Nowak, C., Beer, B.C., Pick, A., Roth, T., Lommes, P., and Sieber, V. (2015) A water-forming NADH oxidase from *Lactobacillus pentosus* and its potential application in the regeneration of synthetic biomimetic cofactors. *Front Microbiol* **6**: 957.
- Pazhang, M., Mehmejad, F., Pazhang, Y., Falahati, H., and Chaparzadeh, N. (2016) Effect of sorbitol and glycerol on the stability of trypsin and difference between their stabilization effects in the various solvents. *Biotechnol Appl Biochem* **63**: 206–213.
- Pennacchio, A., Giordano, A., Pucci, B., Rossi, M., and Raia, C.A. (2010) Biochemical characterization of a recombinant short-chain NAD(H)-dependent dehydrogenase/reductase from *Sulfolobus acidocaldarius*. *Extremophiles* **14**: 193–204.
- Pick, A., Schmid, J., and Sieber, V. (2015) Characterization of uronate dehydrogenases catalysing the initial step in an oxidative pathway. *Microb Biotechnol* **8**: 633–643.
- Preiss, J., and Ashwell, G. (1962) Alginic acid metabolism in bacteria. II. The enzymatic reduction of 4-deoxy-L-erythro-5-hexoseulose uronic acid to 2-keto-3-deoxy-D-gluconic acid. *J Biol Chem* **237**: 317–321.
- Robins, K., and Osorio-Lozada, A. (2012) Exploiting duality in nature: industrial examples of enzymatic oxidation and reduction reactions. *Catal Sci Technol* **2**: 1524–1530.
- Roth, S., Präg, A., Wechsler, C., Marolt, M., Fertlino, S., Lüdeke, S., et al. (2017) Extended catalytic scope of a well-known enzyme: asymmetric reduction of iminium substrates by glucose dehydrogenase. *ChemBioChem* **18**: 1703–1706.
- Rühmann, B., Schmid, J., and Sieber, V. (2014) Fast carbohydrate analysis via liquid chromatography coupled with ultra violet and electrospray ionization ion trap detection in 96-well format. *J Chromatogr* **1350**: 44–50.
- Sperl, J.M., Carsten, J.M., Guterl, J.-K., Lommes, P., and Sieber, V. (2016) Reaction design for the compartmented combination of heterogeneous and enzyme catalysis. *ACS Catal* **6**: 6329–6334.
- Stekhanova, T.N., Mardanov, A.V., Bezsudnova, E.Y., Gumerov, V.M., Ravin, N.V., Skryabin, K.G., and Popov, V.O. (2010) Characterization of a thermostable short-chain alcohol dehydrogenase from the hyperthermophilic archaeon *Thermococcus sibiricus*. *Appl Environ Microbiol* **76**: 4096–4098.
- Studier, F.W. (2005) Protein production by auto-induction in high-density shaking cultures. *Protein Expr Purif* **41**: 207–234.
- Svegelj, M.B., Stojan, J., and Rizner, T.L. (2012) The role of Ala231 and Trp227 in the substrate specificities of fungal 17beta-hydroxysteroid dehydrogenase and trihydroxynaphthalene reductase: steroids versus smaller substrates. *J Steroid Biochem Mol Biol* **129**: 92–98.
- Takase, R., Ochiai, A., Mikami, B., Hashimoto, W., and Murata, K. (2010) Molecular identification of unsaturated uronate reductase prerequisite for alginate metabolism in *Sphingomonas* sp. A1. *Biochim Biophys Acta* **1804**: 1925–1936.
- Takase, R., Mikami, B., Kawai, S., Murata, K., and Hashimoto, W. (2014) Structure-based conversion of the coenzyme requirement of a short-chain dehydrogenase/reductase involved in bacterial alginate metabolism. *J Biol Chem* **289**: 33198–33214.
- Wargacki, A.J., Leonard, E., Win, M.N., Regitsky, D.D., Santos, C.N., Kim, P.B., et al. (2012) An engineered microbial platform for direct biofuel production from brown macroalgae. *Science* **335**: 308–313.

- Werpy, T. and Petersen, G. (2004) Top Value Added Chemicals from Biomass: Volume I – Results of Screening for Potential Candidates from Sugars and Synthesis Gas. National Renewable Energy Lab., Golden, CO (US).
- Woodyer, R.D., Christ, T.N., and Deweese, K.A. (2010) Single-step bioconversion for the preparation of L-gulose and L-galactose. *Carbohydr Res* **345**: 363–368.
- Yoon, R.Y., Yeom, S.J., Park, C.S., and Oh, D.K. (2009) Substrate specificity of a glucose-6-phosphate isomerase from *Pyrococcus furiosus* for monosaccharides. *Appl Microbiol Biotechnol* **83**: 295–303.
- Zhang, Q., Peng, H., Gao, F., Liu, Y., Cheng, H., Thompson, J., and Gao, G.F. (2009) Structural insight into the catalytic mechanism of gluconate 5-dehydrogenase from

Streptococcus suis: crystal structures of the substrate-free and quaternary complex enzymes. *Protein Sci* **18**: 294–303.

Supporting information

Additional Supporting Information may be found online in the supporting information tab for this article:

Table S1. Synthesis of aldonic acids.

Fig. S1. Product identification of aldonate oxidation.

4.1.3.3 Finding of a promiscuous activity with uronic acids

The product from D-gluconate oxidation is L-gulonate. Since no reference compound of L-gulonate was available at the time of the now following analysis, the substrate decline was quantified instead of the product formation in a time course experiment. Surprisingly, SpsADH not only oxidized gluconate, but also the resulting L-gulonate, which yielded D-glucarate (Figure 11). In this experiment, 1.9 mM D-glucarate were produced from 5 mM gluconate. L-gulonate and residual gluconate could not be quantified, since only one other peak was present in the chromatogram, which could not be assigned to any of the two beyond doubt without an L-gulonate reference.

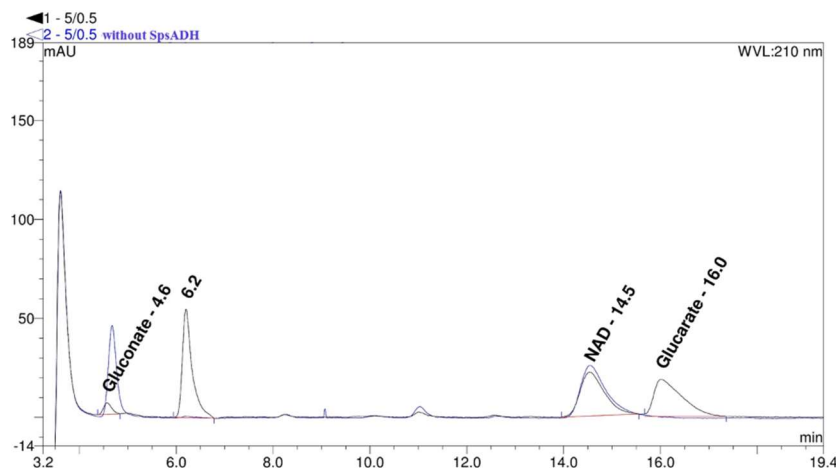


Figure 11: Analysis of SpsADH product formation by anion exchange chromatography

Chromatograms of isocratic elution with 30 mM AbC pH 10.4 of the reaction of SpsADH with 5 mM D-gluconate, 0.5 mM NAD⁺ and NOX overnight at 25 °C („5/0,5“, black) and of the control lacking SpsADH („5/0,5 without SpsADH“, blue) are shown. Comparing both, a substantial decline of gluconate (4.57 min) can be observed, as well as D-glucarate formation (16.0 min). The peak at 6.2 min probably arises from the enzyme preparation or from NAD⁺/NADH.

For further verification of D-glucarate formation, a cascade reaction involving glucarate dehydratase (GlucD) was conducted. Here, 5-keto-3-deoxyglucarate (5-Kdg) was indeed formed from D-gluconate: Within 119 h, 34.8 mM D-gluconate were converted with a yield of 5-Kdg of 25.2 mM (Figure 12). The intermediates L-gulonate and D-glucarate could not be quantified here.

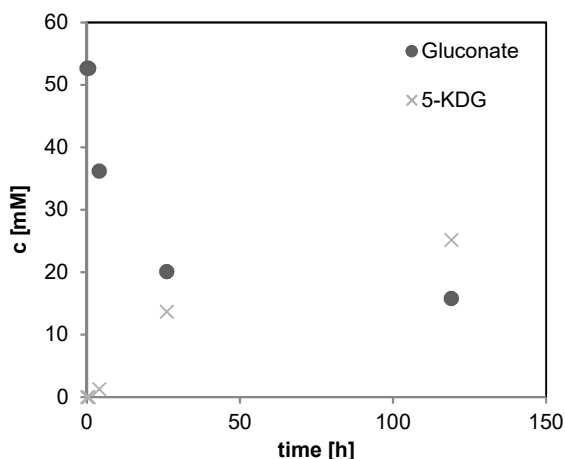


Figure 12: Synthesis of 5-Kdg from D-gluconate by SpsADH and GlucD

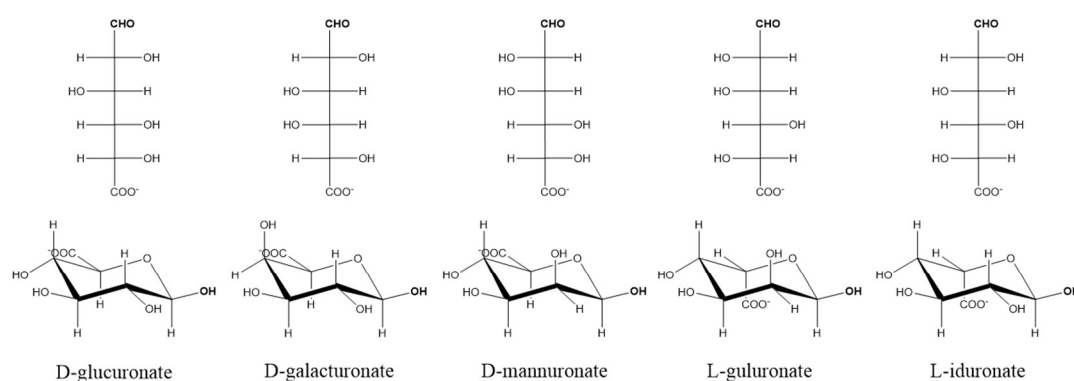
In the time course of the reaction a decline of gluconate (circle) from 53 mM to 16 mM and formation of 25 mM 5-Kdg (cross) was observed within 119 h.

Due to this finding, all reactions of aldonates with SpsADH were analyzed again, this time by anion exchange chromatography (Figure 23 to Figure 32 in section 6.2). The formation of the corresponding

aldaric acids was shown for all tested aldonates except for galactarate (from D-galactonate with the intermediate L-galacturonate).

To gain more insights into the reactivity of SpsADH with uronates, all available uronates, that is, D-glucuronate, D-galacturonate, D-mannuronate, L-guluronate, and L-iduronate (Figure 13), were tested in the reduction as well as in the oxidation reaction. Despite the assumption that the reduction would always be more favorable than the oxidation due to thermodynamics, D-glucuronate was an exception. At 25 mM substrate concentration the reduction of D-glucuronate was not measurable, while the oxidation proceeded with a V_{\max} of 0.81 ± 0.01 U/mg ($K_m = 2.5 \pm 0.2$ mM). Surprisingly, D-galacturonate was not accepted at all by SpsADH. For the other uronates only a very limited analysis was possible due to the high costs of these compounds. Here, only single measurements at a fixed substrate concentration of 25 mM were conducted. D-mannuronate and L-guluronate were reduced with a specific activity of 850 mU/mg and >3500 mU/mg, respectively, while the oxidation of D-mannuronate proceeded only at 17 mU/mg and for L-guluronate it was not measurable at all. The reduction of L-iduronate was slightly better than the oxidation with 30 mU/mg compared to 15 mU/mg.

From this analysis, however, no conclusion about the reaction equilibria can be drawn. A possible disproportionation of the uronates to the corresponding aldonates and aldarates was not analyzed and might reveal different reaction rates, especially concerning the first seconds of the reactions, which were not resolved in this experiment.



Reduction	n.m.	n.m.	850 mU/mg	> 3500 mU/mg	31 mU/mg
Oxidation	$V_{\max} = 810$ mU/mg $K_m = 2.5$ mM	n.m.	17 mU/mg	n.m.	15 mU/mg

Figure 13: Oxidation and reduction of uronates by SpsADH

The linear and the β -pyranurionate conformations of D-glucuronate, D-mannuronate, D-galacturonate, L-guluronate, and L-iduronate are depicted, where either an aldehyde or hydroxyl group are available for reduction and/or oxidation, respectively. Below the kinetic parameters or specific activities at 25 mM substrate concentration of SpsADH for the oxidation and reduction are given. n.m.: not measurable.

It should be pointed out here, that even though the oxidation of L-guluronate was not measurable with this experimental setup, it could be oxidized to D-glucuric acid. This can be explained by the presence of NOX in these reactions. It oxidized the cofactor NADH before SpsADH could use it for the reverse reaction. Therefore, and with the oxidation of L-guluronate to D-glucuric acid being essentially irreversible, the equilibrium of the reaction was shifted toward D-glucuric acid.

The finding of SpsADH catalyzing the oxidation of both D-glucuronate and L-guluronate to D-glucuric acid, neglected the need of identifying an AIDH for the cascade reaction from D-glucose to BDO.

4.2 Enzyme characterization and engineering

For the evaluation of separate modules of the cascade reaction, NAD(H) recycling is necessary. For NADH recycling the commercially available formate dehydrogenase (FDH) from *Candida boidinii* can be used, whereas for NAD⁺ recycling, a water-forming NADH oxidase (NOX) from *Lactobacillus pentosus* was characterized in this work. Furthermore, uronate dehydrogenase (UDH) from *Agrobacterium tumefaciens* was engineered for enhanced stability. In Figure 14 the investigated enzymes are highlighted.

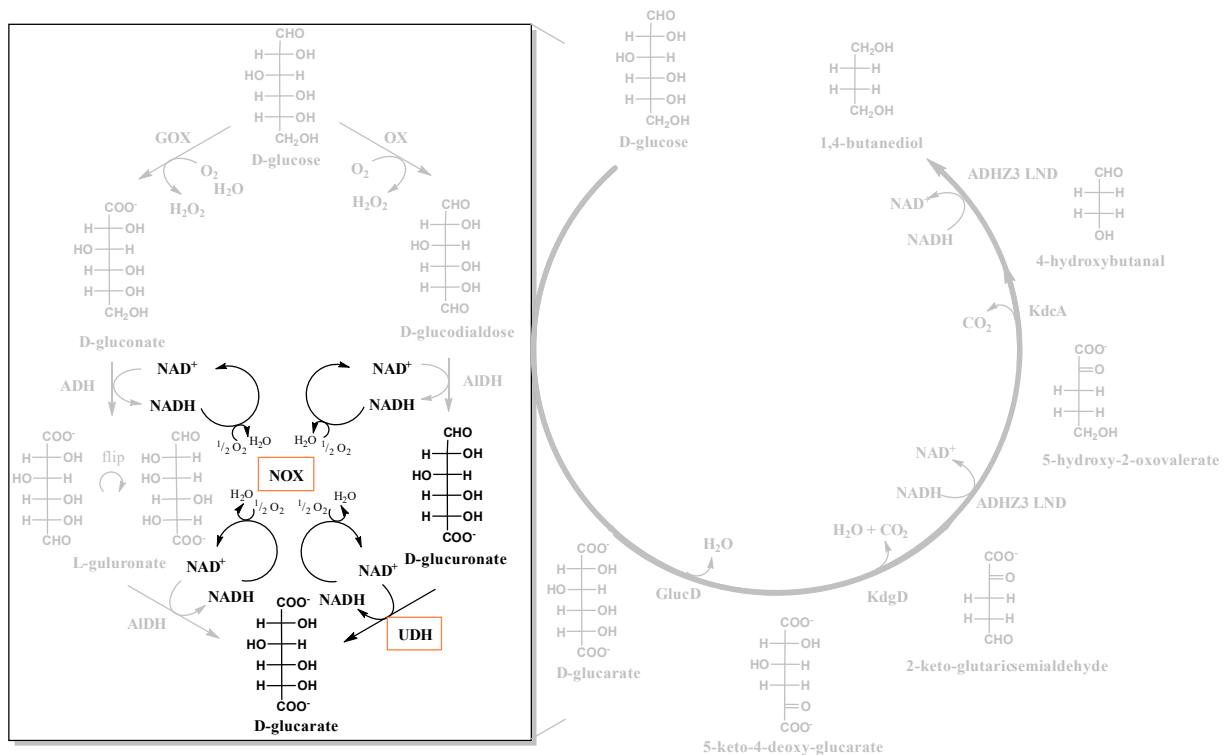


Figure 14: Enzymes that were newly characterized or engineered

For the evaluation of the oxidative module (box), an NAD⁺ recycling enzyme, namely NADH oxidase from *Lactobacillus pentosus* (NOX), was characterized. Furthermore, uronate dehydrogenase (UDH) from *Agrobacterium tumefaciens* was engineered for enhanced stability.

4.2.1 A water-forming NADH oxidase from *Lactobacillus pentosus* suitable for the regeneration of synthetic biomimetic cofactors

Authors: Claudia Nowak, Barbara Beer, André Pick, Teresa Roth, Petra Lommes, and Volker Sieber

Cofactor regeneration is of utmost importance for efficient and economically feasible biocatalytic processes. Water-forming NADH oxidases have emerged as regeneration enzymes for the cofactors NAD^+ and NADP^+ . They use the molecular oxygen dissolved in solution as the proton acceptor to yield the oxidized cofactor and water. However, even with regeneration systems at hand, the cofactor is still a cost-pushing factor. Therefore, biomimetic nicotinamide cofactors have been developed that are cheap and can easily be synthesized.

In this publication, a water-forming NOX from *Lactobacillus pentosus* is described for the regeneration of the natural cofactor NAD^+ as well as the biomimetics MNA^+ and BNA^+ . The enzyme could be activated by FAD, which is involved in the catalysis and usually bound intrinsically. Proposedly, overexpression leads to incomplete loading of NOX with FAD. The enzyme was next characterized in regard of its activity at various conditions, kinetic parameters with NADH and biomimetic cofactors, as well as stability and total turnover. Furthermore, it was found that free FAD is also able to act as a catalyst for the oxidation of the biomimetic cofactors, though the reaction product is hydrogen peroxide instead of water. With NOX, the first enzymatic regeneration system for biomimetic cofactors is described.

The two authors Claudia Nowak and Barbara Beer contributed equally to this publication. Barbara Beer designed all experiments for the general characterization of NOX with the natural cofactor. She also conducted the experiments for activation of NOX, thermal stability and total turnover measurements and wrote the manuscript. Claudia Nowak designed and conducted all experiments with the synthetic biomimetic cofactors and wrote the manuscript. André Pick assisted in the design of the experiments and read the manuscript. Teresa Roth conducted experiments with the natural cofactor. Petra Lommes synthesized the biomimetic cofactors, and Volker Sieber contributed to the content and language of the manuscript.

The supplemental information for this publication can be found in the appendix, section 6.6.



A water-forming NADH oxidase from *Lactobacillus pentosus* suitable for the regeneration of synthetic biomimetic cofactors

Claudia Nowak[†], Barbara Beer[†], André Pick, Teresa Roth, Petra Lommes and Volker Sieber*

Chair of Chemistry of Biogenic Resources, Straubing Centre of Science, Department Life Science Engineering, Technische Universität München, Straubing, Germany

OPEN ACCESS

Edited by:

Robert Kourist,
Ruhr-University Bochum, Germany

Reviewed by:

Frank Hollmann,
Delft University of Technology,
Netherlands
Matthias Höhne,
University of Greifswald, Germany

*Correspondence:

Volker Sieber,
Chair of Chemistry of Biogenic
Resources, Straubing Centre
of Science, Department Life Science
Engineering, Technische Universität
München, Schulgasse 16,
D-94315 Straubing, Germany
sieber@tum.de

[†]These authors have contributed
equally to this work.

Specialty section:

This article was submitted to
Microbiotechnology, Ecotoxicology
and Bioremediation,
a section of the journal
Frontiers in Microbiology

Received: 01 July 2015

Accepted: 28 August 2015

Published: 16 September 2015

Citation:

Nowak C, Beer B, Pick A, Roth T,
Lommes P and Sieber V (2015)
A water-forming NADH oxidase from
Lactobacillus pentosus suitable
for the regeneration of synthetic
biomimetic cofactors.
Front. Microbiol. 6:957.
doi: 10.3389/fmicb.2015.00957

The cell-free biocatalytic production of fine chemicals by oxidoreductases has continuously grown over the past years. Since especially dehydrogenases depend on the stoichiometric use of nicotinamide pyridine cofactors, an integrated efficient recycling system is crucial to allow process operation under economic conditions. Lately, the variety of cofactors for biocatalysis was broadened by the utilization of totally synthetic and cheap biomimetics. Though, to date the regeneration has been limited to chemical or electrochemical methods. Here, we report an enzymatic recycling by the flavoprotein NADH-oxidase from *Lactobacillus pentosus* (*LpNox*). Since this enzyme has not been described before, we first characterized it in regard to its optimal reaction parameters. We found that the heterologously overexpressed enzyme only contained 13% FAD. *In vitro* loading of the enzyme with FAD, resulted in a higher specific activity towards its natural cofactor NADH as well as different nicotinamide derived biomimetics. Apart from the enzymatic recycling, which gives water as a by-product by transferring four electrons onto oxygen, unbound FAD can also catalyze the oxidation of biomimetic cofactors. Here a two electron process takes place yielding H₂O₂ instead. The enzymatic and chemical recycling was compared in regard to reaction kinetics for the natural and biomimetic cofactors. With *LpNox* and FAD, two recycling strategies for biomimetic cofactors are described with either water or hydrogen peroxide as by-product.

Keywords: cofactor regeneration, H₂O-forming NADH oxidase, synthetic cofactors, biomimetic cofactors, *Lactobacillus pentosus*, flavin adenine dinucleotide, hydrogen peroxide

Introduction

The cell-free biocatalytic production of fine chemicals by oxidoreductases has continuously grown over the past years (Matsuda et al., 2009). When enzymes such as dehydrogenases that depend on the stoichiometric use of nicotinamide pyridine cofactors are involved, an integrated efficient recycling system is crucial to allow process operation under economic conditions (Weckbecker et al., 2010; Tauber et al., 2011). For a further increase of the profitability the variety of available cofactors for biocatalysis was recently broadened by the utilization of totally synthetic and cheap

biomimetics (Lutz et al., 2004; Ryan et al., 2008; Campbell et al., 2012; Paul et al., 2013). Hence, the cost for the cofactor in a cell-free process can be decreased enormously (Rollin et al., 2013). In most cases these biomimetic cofactors can easily be synthesized in one or two steps. First, the oxidized form is prepared within the reaction of nicotinamide and the corresponding alkyl halogenide. Subsequent reaction with sodium dithionite yields the reduced form of the derivative (Karrer and Stare, 1937; Mauzerall and Westheimer, 1955). Several biomimetics have been described in literature so far: 5-methyl-1,4-dihydro-*N*-benzylnicotinamide and 6-methyl-1,4-dihydro-*N*-benzylnicotinamide (Takeda et al., 1987; Hentall et al., 2001), *N*-methyl-1,4-dihyronicotinamide (MNAH) (Friedlos et al., 1992; Knox et al., 1995) and *N*-benzyl-1,4-dihyronicotinamide (BNAH) (Lutz et al., 2004; Ryan et al., 2008; Paul et al., 2013). Though, to date the regeneration of the oxidized biomimetic cofactors has been limited to chemical or electrochemical methods (Lutz et al., 2004; Ryan et al., 2008; Poizat et al., 2010; Kara et al., 2014). An enzymatic recycling system would have the advantage of being evolvable and thereby holds the potential of a most efficient recycling in the future. The main challenge researchers are facing at the moment lies in finding enzymes that have at least a minor activity with biomimetic cofactors. So far only a few examples are known from literature: Paul et al. (2013) showed that the enoate reductase from *Thermus scotoductus* could use BNAH to perform the asymmetric reduction of conjugated C=C double bonds. Another example is the hydroxylation of non-activated C-H bonds by cytochrome P450 BM-3 R966D/W1046S from *Bacillus megaterium* with BNAH instead of the natural cofactor 1,4-dihydro-nicotinamide adenine dinucleotide (NADH) or 1,4-dihydro-nicotinamide adenine dinucleotide phosphate (NADPH) (Ryan et al., 2008). Most of the enzymes described so far need a second cofactor like flavin adenine mononucleotide (FMN) or flavin adenine dinucleotide (FAD) to be active. These flavin derivatives act as a linker between substrate and nicotinamide pyridine cofactor and are supposed to facilitate the hydride transfer (Paul et al., 2014a). From this it can be concluded that also other enzymes carrying flavin adenine cofactors have the potential to accept biomimetic cofactors. In this context NADH oxidases, which are also flavo-enzymes that oxidize NAD(P)H to NAD(P)⁺ with simultaneous reduction of molecular oxygen to either hydrogen peroxide (H₂O₂) or water (H₂O), have attracted interest as suitable candidates for an efficient NAD⁺ cofactor recycling. In coupled enzyme reactions the four-electron reduction to benign H₂O is preferred over the two-electron reduction to H₂O₂, which, even in small amounts, can inactivate the enzymes of the production-regeneration cycle (Hernandez et al., 2012). The addition of catalase as a possible remedy increases the complexity of the system to the point where three enzymes have to be coupled and adjusted to their activity over time. Water-forming NADH oxidases are described from various *Cocci* and *Bacilli* species: *Enterococcus (Streptococcus) faecalis* (Schmidt et al., 1986), *Streptococcus pyogenes* (Gao et al., 2012), *Streptococcus mutans* (Higuchi et al., 1993), *Lactobacillus rhamnosus* (Zhang et al., 2012), *Lactobacillus brevis* (Geueke et al., 2003), *Lactococcus lactis* (Heux et al., 2006), *Lactobacillus sanfranciscensis* (Riebel et al., 2003) as well as from

Clostridium aminovalericum (Kawasaki et al., 2004) and from the hyperthermophile *Thermococcus profundus* (Jia et al., 2008). The sequence analysis of H₂O-forming NADH oxidases from different *Lactobacilli* reveals sequence identities with a putative NADH oxidase from *Lactobacillus pentosus* (LpNox) that range from 42.5% for the crystallographically defined NADH oxidases from *L. sanfranciscensis* (pdb identifier CDU2) (Lountos et al., 2006) to 46.3 and 87.2% for the NADH oxidases from *L. brevis* (Geueke et al., 2003) and *L. plantarum* (Park et al., 2011), respectively. In each case, the most highly conserved regions include the redox-active cysteine (Cys42 in all sequences) as well as the FAD and NAD(P)II binding domains (see Supplementary Figure S1). In the proposed reaction mechanism of H₂O-forming NADH oxidases the first NADP(H) transfers electrons onto FAD. FADH₂ reduces molecular oxygen to hydrogen peroxide, which is supposed to be trapped in the active site and motioned toward the thiolate moiety of Cys42. A nucleophilic attack of Cys42-S⁻ on H₂O₂ yields the first water molecule and generates the Cys42-SOH intermediate. The second NAD(P)H then reduces FAD, which transfers the electrons much faster onto Cys42-SOH than onto another oxygen. Thus, the sulfenic acid is converted back to the thiolate and the second water molecule is released.

Due to the high sequence similarity to crystallographically defined H₂O-forming NADH oxidases, we decided to investigate the putative NADH oxidase from *L. pentosus* MP-10 (LpNox) as a possible recycling enzyme in cell-free reactions. Furthermore, we tested the enzyme for the acceptance of the synthetic biomimetic cofactors MNAH and BNAH. The structures of all cofactors used are depicted in Figure 1. Interestingly, both LpNox and free FAD (Paul et al., 2014b, 2015) were capable of oxidizing the biomimetics and were therefore compared in regard of their kinetic parameters and the resultant by-products.

Materials and Methods

Reagents

All chemicals were purchased from Sigma-Aldrich, Merck or Carl Roth. All columns used for protein purification were from GE Healthcare (Munich, Germany).

Synthesis of the Oxidized Biomimetics

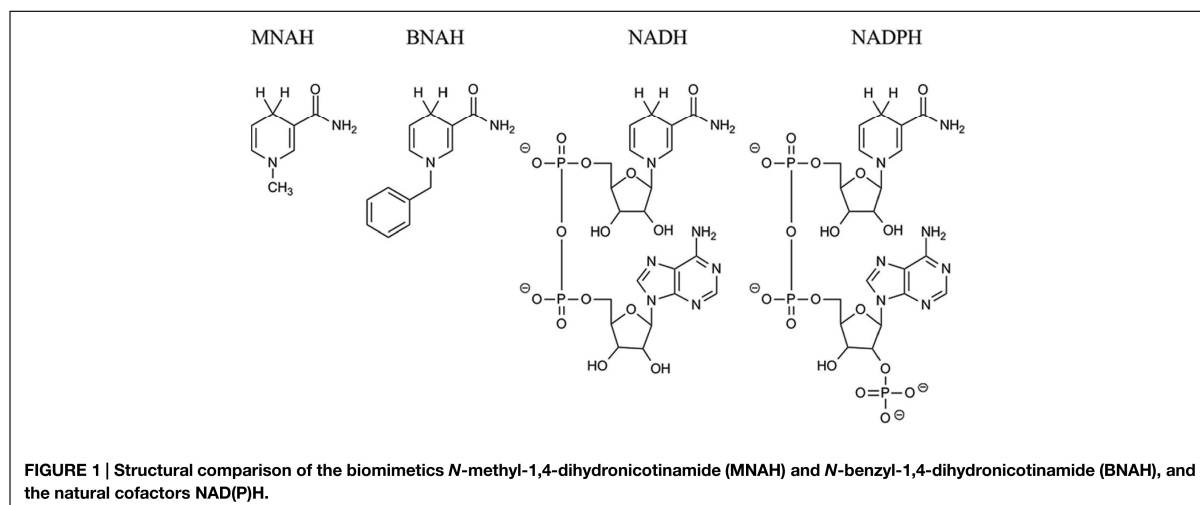
The synthesis was adapted from a former procedure (Karrer and Stare, 1937; Mauzerall and Westheimer, 1955).

MNA⁺

Nicotinamide (50 mmol) was dissolved in 30 mL methanol. Methyl iodide (150 mmol) was added and the reaction mixture was stirred for 27 h at room temperature. The yellow precipitate was filtered and washed twice with methanol. The crude product was recrystallized from 250 mL hot methanol. C₇H₉IN₂O; yellow solid; yield: 81%; ¹H NMR (400 MHz, DMSO) δ 9.3 (s, 1H), 9.0 (d, 1H), 8.8 (d, 1H), 8.5 (s, 1H), 8.2 (dd, 1H), 8.1 (s, 1H), 4.4 (s, 3H).

BNA⁺

Nicotinamide (120 mmol) was dissolved in 40 mL acetonitrile and heated to reflux. Benzyl chloride (120 mmol) was added



dropwise and the reaction mixture was stirred for further 12 h under reflux. After cooling to room temperature 120 mL diethyl ether was added, the precipitate was filtered and washed twice with diethyl ether. $C_{13}H_{13}ClN_2O$; white solid; yield: 86%; 1H NMR (400 MHz, D_2O) δ 9.2 (s, 1H), 8.9 (d, 1H), 8.8 (d, 1H), 8.1 (t, 1H), 7.4 (m, 5H), 5.8 (s, 2H).

Synthesis of the Reduced Biomimetics

The synthesis was adapted from a former procedure (Karrer and Stare, 1937; Mauzerall and Westheimer, 1955; Knox et al., 2000).

MNAH

MNA^+ (3.8 mmol) was dissolved in 250 mL water at 40°C under argon atmosphere. Sodium carbonate (24 mmol) and sodium bicarbonate (30 mmol) were added to the reaction mixture. Sodium dithionite (14 mmol) was added in portions and the mixture was stirred for further 30 min at 40°C. After cooling to room temperature an oily solid precipitated. The crude product was extracted three times with dichloromethane. The combined organic phases were washed once with water, dried over sodium sulfate and the solvent was removed by rotary evaporation. $C_7H_{10}N_2O$; yellow solid; yield: 25%; 1H NMR (400 MHz, $CDCl_3$) δ 7.0 (s, 1H), 5.7 (d, 1H), 5.4 (s, 2H), 4.7 (d, 1H), 3.1 (s, 2H), 2.9 (m, 3H).

BNAH

BNA^+ (20 mmol) was added to a solution of sodium bicarbonate (66 mmol) and sodium dithionite (60 mmol) at 50°C and stirred for 15 min. The reaction mixture was cooled to 0°C for another 15 min. The precipitating solid was then washed twice with 100 mL dichloromethane and dried over sodium sulfate. The crude product was recrystallized from water:ethanol (3:1) at 0°C for 2 h. $C_{13}H_{14}N_2O$; yellow solid; yield: 73%; 1H -NMR (400 MHz, $CDCl_3$), δ (ppm): 7.34–7.23 (m, 5H), 7.15–7.14 (d, 1H), 5.74–5.73 (dq, 1H), 5.40 (br s, 2H), 4.76–4.72 (m, 1H), 4.28 (s, 2H), 3.17–3.16 (m, 2H).

Cloning

For the cloning of the NADH oxidase (*LpNox*) from *L. pentosus* MP-10 (protein sequence GenBank™ CCB83530.1) genomic DNA was used as PCR template. It was isolated from cells of an overnight culture using the protocol of Chen and Kuo (1993). Three PCR reactions were performed to add an N-terminal, C-terminal or no His-Tag. For the N-terminal His-Tag the following primers were used: F-NheI-nox-*Lp* – GACAGGC TAGCATGAAAGTTATCGTAATTGGTTGTAC and R-XhoI-stop-nox-*Lp* – GCGACTCGAGTTATCCGTCACCTTTTTCAGCC, for the C-terminal His-Tag: F-BsaI-nox-*Lp*-CACGGTCTCGCATGAAAGTTATCGTAATTGGTTGTAC and R-XhoI-nox-*Lp*-GCGACTCGAGTTCCGTCACCTTTTTCAGCCGCG and for no His-Tag: F-BsaI-nox-*Lp*-CACGGTCTCGCATGAAAGTTATCGTAATTGGTTGTAC and R-XhoI-stop-nox-*Lp* – GCGACTCGAGTTATCCGTCACCTTTTTCAGCC. The restriction enzyme recognition sites are underlined and the start and stop codon is marked in bold. The PCR products were purified and ligated into pET28a (Novagen, Darmstadt, Germany). The multiplication of the plasmid was performed with *E. coli* DH5 α (Stratagene, La Jolla, CA, USA) in LB medium containing 30 μ g/mL kanamycin.

Expression and Purification

The expression of each variant of *LpNox* was performed with *E. coli* BL21 (DE3) in 200 mL autoinduction media with 100 μ g/mL kanamycin (Studier, 2005). The preculture was incubated in 20 mL of LB medium with 30 μ g/mL kanamycin at 37°C overnight on a rotary shaker (180 rpm). Expression cultures were inoculated with a 1:100 dilution of overnight cultures. Incubation was performed for 3 h at 37°C followed by incubation for 21 h at 16°C.

Subsequently, there was a separation in the handling for the His-tagged enzymes and the one without His-Tag. The treatment for both His-tagged enzymes was the same. Cells were harvested by centrifugation and resuspended in 50 mM sodium phosphate buffer (pH 8.0, 20 mM imidazole, 500 mM

NaCl, and 10% glycerol). Crude extracts were prepared by the use of a Basic-Z Cell Disrupter (IUL Constant Systems), subsequent addition of $MgCl_2$ to a final concentration of 2.5 mM in combination with DNase I (1 $\mu g/mL$) and a following incubation for 20 min at room temperature to degrade DNA. The insoluble fraction of the lysate was removed by centrifugation (20,000 rpm for 40 min at 4°C). The supernatant was filtered through a 0.45 μm syringe filter and applied to an IMAC affinity resin column, 5 mL HisTrap™ FF, equilibrated with the resuspension buffer using the ÄKTA Purifier-system. The column was washed with five column volumes of resuspension buffer and eluted in a gradient of 10 column volumes from 0 to 100% elution buffer (50 mM sodium phosphate buffer pH 8.0, 500 mM imidazole, 500 mM NaCl, and 10% glycerol). Aliquots of eluted fractions were subjected to 12% SDS-Page described by Laemmli (1970). The molecular weight of the His-tagged LpNox was calculated to be 51.94 kDa using the ProtParam tool (Artimo et al., 2012). The fractions containing the eluted protein were pooled and the protein was desalted using a HiPrep™ 26/10 Desalting column which was preliminary equilibrated with 50 mM Tris-HCl pH 7.5. Aliquots of the light yellow protein solution were frozen in liquid nitrogen and stored at $-80^\circ C$.

Cells containing the enzyme without His-Tag were harvested by centrifugation and resuspended in 50 mM potassium phosphate buffer pH 7.0. Crude extracts were prepared by the use of a Basic-Z Cell Disrupter (IUL Constant Systems), subsequent addition of $MgCl_2$ to a final concentration of 2.5 mM in combination with DNase I (1 $\mu g/mL$) and a following incubation for 20 min at room temperature to degrade DNA. The insoluble fraction of the lysate was removed by centrifugation (20,000 rpm for 40 min at 4°C). The supernatant was filtered through a 0.45 μm syringe filter and applied to an affinity resin column, 5 mL HiTrap Blue HP, equilibrated with the resuspension buffer using the ÄKTA Purifier-system. The column was washed with five column volumes of resuspension buffer and eluted in one step with elution buffer (50 mM potassium phosphate buffer pH 7.0 and 1.5 M KCl). Aliquots of the different fractions were subjected to 12% SDS-Page described by Laemmli (1970). The molecular weight was calculated to be 49.46 kDa.

Determination of Protein and FAD Concentration

The LpNox concentration was determined using a Bradford assay Roti®-nanoquant (Carl Roth) with BSA as standard. The FAD concentration was measured in microtiter plates at 450 nm and compared to a FAD standard (10–70 μM).

Enzyme Activation

The LpNox was incubated with an excess of FAD at 37°C for 15 min. After cooling the enzyme to 4°C precipitated protein was separated by centrifugation (20,000 rpm for 15 min at 4°C). Afterward unbound FAD was removed by size exclusion chromatography using a HiPrep™ 26/10 Desalting column, which had been preliminary equilibrated with 50 mM Tris-HCl pH 7.5. Aliquots of the protein were frozen in liquid nitrogen and stored at $-80^\circ C$.

General Characterization of LpNox

All enzyme assays were performed in triplicate with 50 mM buffer at the desired pH, concentration of NADH and at the desired temperature. The absorption of NADH was measured in microtiter plates (Greiner, flat bottom) at 340 nm using a Multiskan or Varioskan spectrophotometer (Thermo Fisher Scientific).

The pH activity profile was obtained at 25°C with 0.3 mM NADH in 50 mM triple buffer containing $1/3$ sodium citrate, $1/3$ potassium phosphate and $1/3$ glycine. The pH values were adjusted with HCl or KOH from pH 5.0 to 10.0.

The optimum temperature was studied by adding the enzyme solution to the preheated reaction mixture containing 50 mM Tris-HCl pH 7.0 and 0.3 mM NADH. A temperature range of 25–50°C was chosen.

The thermostability (T_{50}^{30}) was studied by incubating the enzyme at various temperatures for 30 min in 50 mM Tris-HCl pH 7.0 with and without 5 mM DTT. The residual activity was measured at 37°C with 0.6 mM NADH.

The kinetic parameters of LpNox with NADH were investigated with a substrate range from 0.01 to 0.4 mM in 50 mM Tris-HCl pH 7.0. The calculation of Michaelis–Menten kinetics for determination of K_m and v_{max} was done with SigmaPlot 11.0 (Systat Software).

The total turnover number was calculated from k_{cat}/k_{deact} , whereas k_{deact} was obtained from incubating the enzyme at 37°C in 50 mM Tris-HCl pH 7.0 with and without 5 mM DTT. At certain time points the residual activity was measured with 0.3 mM NADH in the same buffer. The data points were fitted to an exponential decay equation using SigmaPlot 11.0 (Systat Software).

Characterization of the LpNox with the Biomimetic Cofactors

Stock solutions of MNAH/BNAH were dissolved in DMSO freshly before use and added to the assay to give a final DMSO concentration of 5%.

The activity of the LpNox was measured in triplicates with 0.5 mM biomimetic in 50 mM Tris-HCl pH 7.0 at 37°C. The decrease of the absorbance of MNAH/BNAH was followed at 358 nm. The activity of an equivalent concentration FAD with the biomimetics was determined similarly.

The kinetic constants for the biomimetic cofactors were determined in triplicate with a fluorescence measurement. A solution of 20 μl 2 M potassium hydroxide, 20 μl 20% acetophenone in DMSO, and 45 μl H₂O was prepared in a polypropylene fluorescence microtiter plate. The enzymatic reaction in 50 mM Tris-HCl pH 7.0 containing LpNox and substrate ranging from 0 to 8 mM was incubated at 37°C. Every 2–3 min a 5 μl sample from the enzymatic reaction was added to the solution. Then 90 μl 88% formic acid was added and it was incubated for 30 min at room temperature. The samples were measured at the following conditions: MNA⁺: excitation: 386 nm, emission: 446 nm; BNA⁺ excitation: 380 nm, emission: 438 nm (Zhang et al., 2011). For the calculation of concentrations a standard was used (0–0.8 mM oxidized cofactor). The calculation of Michaelis–Menten kinetics for

determination of K_m and v_{max} was done with Sigma-Plot 11.0 (Systat Software).

Quantification of H₂O₂

The H₂O₂ concentration was determined in a microtiter plate using 100 μ L of the activity assay containing 1 mM MNAH/BNAH/NADH and 6 μ M LpNox/FAD in 50 mM Tris-HCl pH 7.0, which was incubated for 5 h at 37°C, and 100 μ L detection reagent containing 50 μ M DA-64 and 0.2 U/ml horseradish peroxidase in 50 mM Tris-HCl pH 7.0. The absorbance was measured at 727 nm and the quantities were calculated by a standard curve (0–40 μ M).

Results

Enzyme Purification and Activation with FAD

The attempt to use the HiTrap Blue HP column for purification of the untagged enzyme was not successful. The complete enzyme was found in the flow through. However, both enzymes with N-terminal or C-terminal His-Tag were soluble and could be purified as a yellowish solution due to the bound FAD. No major impurities were detected by SDS-PAGE (Supplementary Figure S2) and 84 mg of N-terminal LpNox were obtained from 1 L of culture. There was no significant difference in the catalytic activity of both tagged enzymes and therefore all experiments were conducted using the N-terminal His-Tag enzyme.

The activity of NADH oxidases depends on the cofactor FAD, which binds to the enzymes when it is translated and folded in the producing organism. We found that the overexpression in *E. coli* can result in poor activity of the LpNox due to missing FAD: 1 mole of purified LpNox contained between 0.12 and 0.2 mol of FAD. But the LpNox could be loaded with FAD, when the enzyme was incubated with an excess amount of free FAD. The incubation of 157 μ M LpNox (containing 13% FAD) with 200 μ M FAD at 37°C for 15 min and subsequent desalting to remove unbound FAD, resulted in 60 μ M LpNox with 57 μ M FAD (95%). The specific activity was 7.9 U/mg before activation and 50.1 U/mg after loading. Overall, a sevenfold improvement in FAD content and a 6 fold increase in specific activity were achieved.

General Characterization

LpNox was investigated for its suitability as a regeneration enzyme. Therefore, it was tested under various conditions to determine influences on the activity (Figure 2).

pH, Buffer, and Temperature Effect

The pH profile showed a sharp peak at pH 7.0 with 70% residual activity at pH 6.0 and 8.0 (Figure 2A). The highest activity at pH 7.0 was measured in potassium phosphate buffer. But since potassium phosphate reduces cofactor stability (Rover et al., 1998), all further experiments were done in Tris-HCl pH 7.0 (92% activity compared to potassium phosphate; Figure 2B). The temperature optimum of LpNox was between 35 and 40°C. Overall, no strong temperature dependence could be detected during the first 5 min after starting the reaction (Figure 2C).

Kinetics and Reaction Product

From kinetic studies in 50 mM Tris-HCl pH 7.0 at 37°C, a K_m for NADH of 17.9 μ M \pm 3 μ M and a v_{max} of 50.1 \pm 1.9 U/mg ($k_{cat} = 43.4 \text{ s}^{-1}$) for NADH were determined (Figure 2D). NADPH can be recognized as a substrate by LpNox, though the specific activity was only about 2% compared to NADH. Due to a conserved Cys residue at position 42 LpNox should be an H₂O-forming NADH oxidase. This hypothesis could be confirmed with an H₂O₂ assay, where less than 1% of the theoretical yield of hydrogen peroxide could be detected.

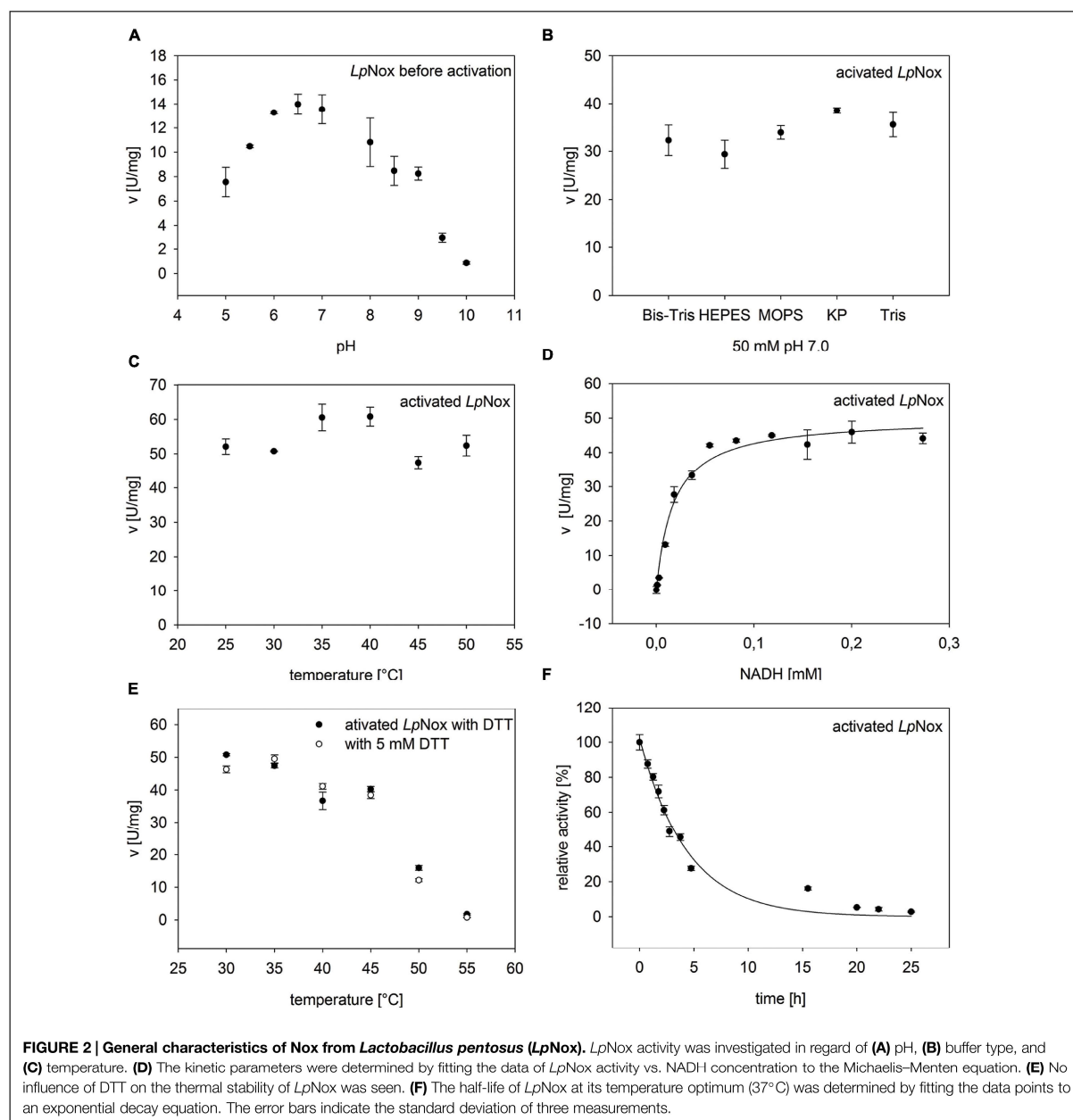
Thermal Stability and Total Turn Over

To determine the influence of temperature over a specific period of time, the thermal stability was tested by incubating the enzyme for 30 min at various temperatures and measuring the residual activity. The temperature, at which 50% of the activity was left compared to the activity before incubation (T_{50}^{30}), was 48.4°C. A similar result (48°C) was obtained when DTT was added to the enzyme during incubation (Figure 2E). The total turnover of an enzyme can be calculated from k_{cat}/k_{deact} . Therefore, the decrease in activity at 37°C until the enzyme was completely inactive was measured. The obtained values were fitted to an exponential function, giving a k_{deact} of $0.299 \pm 0.0237 \text{ h}^{-1}$ (Figure 2F). This resulted in a half-life of LpNox of 3 h and a total turnover number of $6.8 \cdot 10^5$. In order to see whether the loss of activity over time was due to a loss of FAD, the incubated enzyme solution was filtered (10 kDa cutoff). The flow through did not contain FAD, whereas the residue on the filter was yellow.

Activity with Biomimetic Cofactors

After the activation of the LpNox with FAD the activities with the biomimetic cofactors MNAH and BNAH could be increased by a factor of 4–6 (data not shown).

Recently, Paul et al. described the reaction of flavin mononucleotide (FMN) with the biomimetic cofactor BNAH under formation of H₂O₂ (Paul et al., 2014b, 2015). Accordingly, this chemical reaction was confirmed with FAD and the two biomimetics tested in this study (Table 1). In order to compare the enzymatic reaction to the reaction of free FAD, the turn over numbers (TON) were calculated with respect to the FAD content. With MNAH free FAD showed a slightly higher activity than the LpNox, while the activities with BNAH were equal. Since the LpNox is an FAD dependent enzyme the observed reaction could either be enzymatically or chemically catalyzed. To investigate this, the reaction products were determined. When incubating FAD with 1 mM of the biomimetic cofactors at 37°C for 5 h high quantities of H₂O₂ could be detected: $0.32 \pm 0.040 \text{ mM}$ for MNAH and $0.50 \pm 0.018 \text{ mM}$ for BNAH. In contrast, in the enzymatic reaction only small amounts of about $0.2 \cdot 10^{-3} \text{ mM}$ (MNAH) and $2.6 \cdot 10^{-3} \text{ mM}$ (BNAH) H₂O₂ were produced (Table 2). However, this could also be attributed to a possible catalase property of the LpNox. If LpNox is added after H₂O₂ production with free FAD, the concentration of hydrogen peroxide indeed decreases substantially but remains still significantly higher compared to the amount that was detected in the solely enzymatic reaction.



For the determination of the kinetic constants of *LpNox* with the biomimetic cofactors a fluorescence assay was used, because high concentrations of reduced cofactors exceeded the maximal absorbance for photometric measurements. Both could be fitted to the Michaelis–Menten equation (Figure 3). K_m and v_{max} (k_{cat}) of both cofactors are in the same range with BNAH showing a slightly lower K_m and higher v_{max} than MNAH. Therefore, k_{cat}/K_m for BNAH is 1.4 higher than for MNAH (Table 3).

Discussion

General Applicability of *LpNox* for the Regeneration of Oxidized Cofactors

With the NADH oxidase from *L. pentosus* (*LpNox*), we identified a regeneration system for the natural cofactor NAD^+ as well as for the biomimetic cofactors MNA^+ and BNA^+ . After expression and purification in *E. coli*, more than 80% of the enzyme was present in the apo-form and did not contain the essential cofactor

TABLE 1 | Comparison of the turn over number (TON) of LpNox and FAD with the biomimetics.

Cofactor	TON of free FAD [min^{-1}]	TON of LpNox [min^{-1}]
MNAH	2.23 ± 0.15	1.31 ± 0.05
BNAH	0.97 ± 0.07	0.79 ± 0.01

The activities of the enzymatic and chemical catalyst were investigated with the biomimetics MNAH and BNAH in a photometric assay (358 nm). The activities were compared concerning the FAD content. The standard deviation was calculated from three measurements.

TABLE 2 | Measurement of the by-product H_2O_2 .

Cofactor	FAD [$\text{mM H}_2\text{O}_2$]	LpNox [$\text{mM H}_2\text{O}_2$]	FAD/LpNox [$\text{mM H}_2\text{O}_2$]
MNAH	0.32 ± 0.04	$0.2^*10^{-3} \pm 0.1^*10^{-3}$	$16^*10^{-3} \pm 1^*10^{-3}$
BNAH	0.51 ± 0.18	$2.6^*10^{-3} \pm 0.9^*10^{-3}$	$25^*10^{-3} \pm 1^*10^{-3}$

H_2O_2 concentrations in the reactions of FAD or LpNox with 1 mM of the biomimetics MNAH and BNAH were detected with DA-64 and horseradish peroxidase. Firstly either FAD or the enzyme was added to the cofactor. Secondly a combined approach was performed with addition of LpNox after 1 h. The standard deviation was calculated from three measurements.

FAD. Incubation of the enzyme with an excess amount of FAD and subsequent desalting resulted in fully activated LpNox that did not lose the FAD during desalting or the activity tests. This is similar to the procedure described by Jiang and Bommarium (2004) and Tóth et al. (2008) and obviates the need of adding FAD to the reaction mixture, which is also common (Jiang et al., 2005; Rocha-Martin et al., 2011). The disadvantage of the latter only becomes obvious when using the biomimetic cofactors, where this leads to the formation of hydrogen peroxide. The activated LpNox was investigated in regard of its possible application in cell-free reaction systems. Therefore, the effect of pH, buffers, temperature, the reducing agent DTT and the thermal stability were determined. The enzyme's optimal activity range was from pH 5.5 to 8.0, a common range for NAD(P)H oxidases (Higuchi et al., 1993; Jiang et al., 2005; Park et al., 2011). The upper limit is compatible with most dehydrogenases, so appropriate coupling seems feasible. The amount of H_2O_2 released by LpNox during turnover is so low that it can be regarded as a water-forming NADH oxidase (Jiang et al., 2005; Lountos et al., 2006; Park et al., 2011). Deactivation of

TABLE 3 | Comparison of kinetic parameters of the biomimetics with LpNox.

Cofactor	K_m [mM]	v_{max} [mU/mg _{LpNox}]	k_{cat} [s^{-1}]	k_{cat}/K_m [$\text{s}^{-1} \text{mM}^{-1}$]
MNAH	1.6 ± 0.5	166.0 ± 16.9	0.14	0.09
BNAH	1.3 ± 0.4	198.9 ± 19.8	0.17	0.13

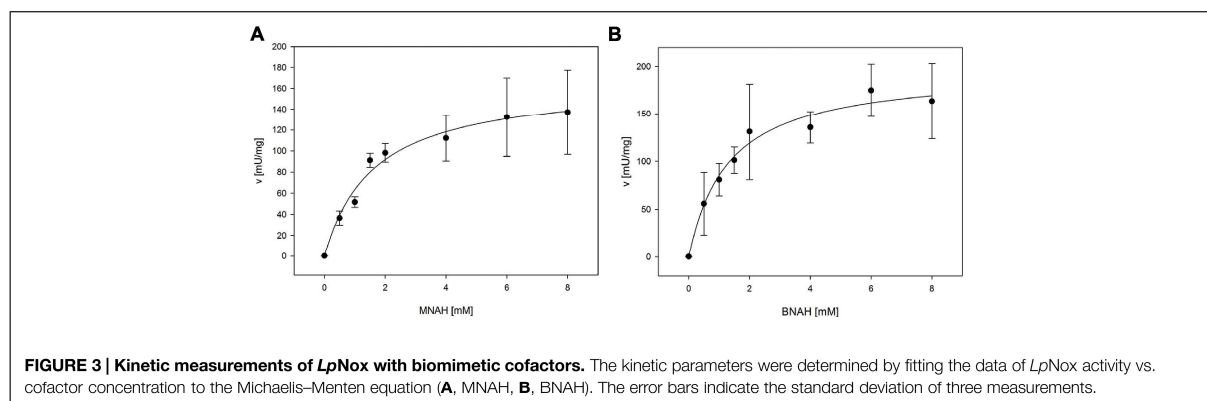
The enzymatic catalysis with MNAH and BNAH was characterized with a fluorescence assay. The kinetic parameters were determined by fitting the data of LpNox activity vs. cofactor concentration to the Michaelis–Menten equation. The standard deviation was calculated from three measurements.

NADH oxidases through over oxidation of the catalytically active Cysteine residue has been described among others for the Nox of *L. brevis* and could be avoided by adding a reducing agent such as DTT (Hummel and Riebel, 2003). For the LpNox no influence of DTT on activity or total turnover number was seen, neither positive nor negative. Together with the low influence of the buffer type on activity, this makes LpNox a flexible enzyme for coupled reactions. Room for improvement lies in the specific activity of LpNox, which is rather low compared to the H_2O -forming NADH oxidases from *Streptococcus pyogenes*: 344 U/mg (Gao et al., 2012) or *Lactobacillus brevis*: 116 U/mg (Hummel and Riebel, 2003). Also the rather low thermal stability at temperatures above 40°C could be improved by enzyme engineering.

Apart from NADH oxidases, an iron catalyzed oxidation of natural cofactors is possible (Maid et al., 2011). Here, also four electrons are transferred onto oxygen giving water as the by-product. Compared to the catalytic activity of LpNox, the metalloporphyrin is better in oxidizing NADPH (3.6 min^{-1}), but worse in oxidizing NADH (6.6 min^{-1}).

Enzyme-Catalyzed vs. FAD-Catalyzed Regeneration of Biomimetic Cofactors

LpNox and FAD are both capable of oxidizing the biomimetic cofactors MNAH and BNAH. The use of the catalyst decides on which by-product is formed. The chemical catalyst FAD produces H_2O_2 during the oxidation of the biomimetic proposedly by a two hydride transfer. However, in coupled redox reactions H_2O_2 should be avoided, since it can damage the



enzymes and substrates involved (Hernandez et al., 2012). The addition of a catalase would be possible, though this would add to the complexity of the system to the point where three catalysts (two enzymes and the chemical catalyst FAD) have to be matched. Therefore, using *LpNox* to regenerate biomimetic cofactors would be the superior choice over FAD, if it is optimized, e.g., by enzyme engineering. An exception is a case described by Paul et al. (2014b). Here the biomimetic cofactor BNAH plus FMN were used to specifically produce H₂O₂ *in situ* for the subsequent enzymatic reaction with a P450 peroxygenase. For this kind of application, both biomimetic cofactors tested in our study would be suitable. Apart from the stated example, inhibitions in the biotransformation of interest by H₂O₂ can be avoided using the *LpNox* for cofactor regeneration instead. The conserved Cys residue at position 42 presumably acts as a second redox center. Therefore, in total a four electron transfer is achieved and innocuous water is produced. The kinetic experiments suggest that BNAH could be oxidized slightly more efficiently compared to MNAH. Because of the hydrophobic benzyl group in BNAH, the recognition and coordination in the cofactor binding site of *LpNox* is possibly better than for the smaller cofactor MNAH. Generally, the activity with free FAD is higher than with the enzyme. However, it has to be considered that the *LpNox* could be improved by enzyme engineering. If the interactions of the *LpNox* with the biomimetic cofactors could be increased, a more efficient catalysis might be obtained. In this way the amount of catalysts can be kept low while simultaneously the activity and effectivity is improved.

Conclusion

In conclusion, we found a H₂O-forming NADH oxidase from *L. pentosus* (*LpNox*) that is able to oxidize the natural cofactor NADH as well as the biomimetic cofactors MNAH

and BNAH. The enzyme is highly active between pH 6.0 and 8.0, is independent of the buffer type and DTT, and has a temperature optimum of 35–40°C. The K_m for NADH is 17.9 μ M and k_{cat} is 43.4 s⁻¹, whereas for the biomimetic the K_m is 1.6 mM (1.3 mM) and k_{cat} is 0.14 s⁻¹ (0.17 s⁻¹) for MNAH (BNAH). Furthermore, we compared the reaction rates of the enzyme with the reaction rate of free FAD. Although, the *LpNox* has a lower or equal rate as free FAD, the reaction products differ. In case of *LpNox* innocuous water is formed, while with free FAD hydrogen peroxide is obtained. Considering the future application of biomimetic cofactors in cell-free coupled reaction systems with other enzymes, hydrogen peroxide would be hazardous and henceforth, the use of *LpNox* would be favorable. In order to enhance the activity of *LpNox* towards the synthetic cofactors, enzyme engineering could be performed.

Acknowledgments

BB was funded by the Bavarian State Ministry of the Environment and Consumer Protection. CN was funded by the Bavarian State Ministry of Economic Affairs and Media, Energy and Technology. We are also grateful to Patrick Westermann for constructing the plasmid for the N-terminal variant. This work was supported by the German Research Foundation (DFG) and the Technische Universität München within the funding program Open Access Publishing.

Supplementary Material

The Supplementary Material for this article can be found online at: <http://journal.frontiersin.org/article/10.3389/fmicb.2015.00957>

References

- Artimo, P., Jonnalagedda, M., Arnold, K., Baratin, D., Csardi, G., de Castro, E., et al. (2012). ExPASy: SIB bioinformatics resource portal. *Nucleic Acids Res.* 40, W597–W603. doi: 10.1093/nar/gks400
- Campbell, E., Meredith, M., Minter, S. D., and Banta, S. (2012). Enzymatic biofuel cells utilizing a biomimetic cofactor. *Chem. Commun.* 48, 1898–1900. doi: 10.1039/c2cc16156g
- Chen, W. P., and Kuo, T. T. (1993). A simple and rapid method for the preparation of gram-negative bacterial genomic DNA. *Nucleic Acids Res.* 21, 2260. doi: 10.1093/nar/21.9.2260
- Friedlos, F., Jarman, M., Davies, L. C., Boland, M. P., and Knox, R. J. (1992). Identification of novel reduced pyridinium derivatives as synthetic cofactors for the enzyme DT diophorase (NAD(P)H dehydrogenase (quinone), EC 1.6.99.2). *Biochem. Pharmacol.* 44, 25–31. doi: 10.1016/0006-2952(92)90033-f
- Gao, H., Tiwari, M. K., Kang, Y. C., and Lee, J.-K. (2012). Characterization of H₂O-forming NADH oxidase from *Streptococcus pyogenes* and its application in l-rare sugar production. *Bioorg. Med. Chem. Lett.* 22, 1931–1935. doi: 10.1016/j.bmcl.2012.01.049
- Geueke, B., Riebel, B., and Hummel, W. (2003). NADH oxidase from *Lactobacillus brevis*: a new catalyst for the regeneration of NAD. *Enzyme Microbial. Technol.* 32, 205–211. doi: 10.1016/S0141-0229(02)00290-9
- Hentall, P. L., Flowers, N., and Bugg, T. D. H. (2001). Enhanced acid stability of a reduced nicotinamide adenine dinucleotide (NADH) analogue. *Chem. Commun.* 2098–2099. doi: 10.1039/B107634P
- Hernandez, K., Berenguer-Murcia, A., Rodrigues, R. C., and Fernandez-Lafuente, R. (2012). Hydrogen peroxide in biocatalysis. A dangerous liaison. *Curr. Org. Chem.* 16, 2652–2672. doi: 10.2174/138527212804004526
- Heux, S., Cachon, R., and Dequin, S. (2006). Cofactor engineering in *Saccharomyces cerevisiae*: expression of a H₂O-forming NADH oxidase and impact on redox metabolism. *Metab. Eng.* 8, 303–314. doi: 10.1016/j.ymben.2005.12.003
- Higuchi, M., Shimada, M., Yamamoto, Y., Hayashi, T., Koga, T., and Kamio, Y. (1993). Identification of two distinct NADH oxidases corresponding to H₂O₂-forming oxidase and H₂O-forming oxidase induced in *Streptococcus mutans*. *J. Gen. Microbiol.* 139, 2343–2351. doi: 10.1099/00221287-139-10-2343
- Hummel, W., and Riebel, B. (2003). Isolation and biochemical characterization of a new NADH oxidase from *Lactobacillus brevis*. *Biotechnol. Lett.* 25, 51–54. doi: 10.1023/a:1021730131633
- Jia, B., Park, S.-C., Lee, S., Pham, B. P., Yu, R., Le, T. L., et al. (2008). Hexameric ring structure of a thermophilic archaeon NADH oxidase that produces predominantly H₂O. *FEBS J.* 275, 5355–5366. doi: 10.1111/j.1742-4658.2008.06665.x
- Jiang, R., and Bommarius, A. S. (2004). Hydrogen peroxide-producing NADH oxidase (nox-1) from *Lactococcus lactis*. *Tetrahedron Asymmetry* 15, 2939–2944. doi: 10.1016/j.tetasy.2004.07.057

- Jiang, R., Riebel, B. R., and Bommarius, A. S. (2005). Comparison of alkyl hydroperoxide reductase (AhpR) and water-forming NADH oxidase from *Lactococcus lactis* ATCC 19435. *Adv. Synth. Catalysis* 347, 1139–1146. doi: 10.1002/adsc.200505063
- Kara, S., Schrittwieser, J. H., Hollmann, F., and Ansorge-Schumacher, M. B. (2014). Recent trends and novel concepts in cofactor-dependent biotransformations. *Appl. Microbiol. Biotechnol.* 98, 1517–1529. doi: 10.1007/s00253-013-5441-5445
- Karrer, P., and Stare, F. J. (1937). N-Alkyl-o-dihydro-nicotinsäure-amide. *Helvetica Chimica Acta* 20, 418–423. doi: 10.1002/hlca.19370200167
- Kawasaki, S., Ishikura, J., Chiba, D., Nishino, T., and Niimura, Y. (2004). Purification and characterization of an H₂O-forming NADH oxidase from *Clostridium aminovalericum*: existence of an oxygen-detoxifying enzyme in an obligate anaerobic bacteria. *Arch. Microbiol.* 181, 324–330. doi: 10.1007/s00203-004-0659-653
- Knox, R. J., Friedlos, F., Jarman, M., Davies, L. C., Goddard, P., Anlezark, G. M., et al. (1995). Virtual cofactors for an *Escherichia coli* nitroreductase enzyme: relevance to reductively activated prodrugs in antibody directed enzyme prodrug therapy (ADEPT). *Biochem. Pharmacol.* 49, 1641–1647. doi: 10.1016/0006-2952(95)00077-d
- Knox, R. J., Jenkins, T. C., Hobbs, S. M., Chen, S. A., Melton, R. G., and Burke, P. J. (2000). Bioactivation of 5-(aziridin-1-yl)-2,4-dinitrobenzamide (CB 1954) by human NAD(P)H quinone oxidoreductase 2: a novel co-substrate-mediated antitumor prodrug therapy. *Cancer Res.* 60, 4179–4186.
- Laemmli, U. K. (1970). Cleavage of structural proteins during the assembly of the head of bacteriophage T4. *Nature* 227, 680–685. doi: 10.1038/227680a0
- Lountos, G. T., Jiang, R., Wellborn, W. B., Thaler, T. L., Bommarius, A. S., and Orville, A. M. (2006). The crystal structure of NAD (P)H oxidase from *Lactobacillus sanfranciscensis*: insights into the conversion of O₂ into two water molecules by the flavoenzyme. *Biochemistry* 45, 9648–9659. doi: 10.1021/bi060692p
- Lutz, J., Hollmann, F., Ho, T. V., Schnyder, A., Fish, R. H., and Schmid, A. (2004). Bioorganometallic chemistry: biocatalytic oxidation reactions with biomimetic NAD⁺/NADH co-factors and [Cp^{*}Rh(bpy)H]⁺ for selective organic synthesis. *J. Organomet. Chem.* 689, 4783–4790. doi: 10.1016/j.jorganchem.2004.09.044
- Maid, H., Böhm, P., Huber, S. M., Bauer, W., Hummel, W., Jux, N., et al. (2011). Iron catalysis for in situ regeneration of oxidized cofactors by activation and reduction of molecular oxygen: a synthetic metalloporphyrin as a biomimetic NAD(P)H oxidase. *Angew. Chem. Int. Ed. Engl.* 50, 2397–2400. doi: 10.1002/anie.201004101
- Matsuda, T., Yamanaka, R., and Nakamura, K. (2009). Recent progress in biocatalysis for asymmetric oxidation and reduction. *Tetrahedron Asymmetry* 20, 513–557. doi: 10.1016/j.tetasy.2008.12.035
- Mauzerall, D., and Westheimer, F. H. (1955). 1-Benzylidihydronicotinamide—a model for reduced DPN. *J. Am. Chem. Soc.* 77, 2261–2264. doi: 10.1021/ja01613a070
- Park, J. T., Hirano, J.-I., Thangavel, V., Riebel, B. R., and Bommarius, A. S. (2011). NAD(P)H oxidase V from *Lactobacillus plantarum* (NoxV) displays enhanced operational stability even in absence of reducing agents. *J. Mol. Catalysis B Enzymatic* 71, 159–165. doi: 10.1016/j.molcatb.2011.04.013
- Paul, C. E., Arends, I. W. C. E., and Hollmann, F. (2014a). Is simpler better? Synthetic Nicotinamide cofactor analogues for redox chemistry. *Acc Catalysis* 4, 788–797. doi: 10.1021/cs4011056
- Paul, C. E., Churakova, E., Maurits, E., Girhard, M., Urlacher, V. B., and Hollmann, F. (2014b). In situ formation of H₂O₂ for P450 peroxigenases. *Bioorg. Med. Chem.* 22, 5692–5696. doi: 10.1016/j.bmc.2014.05.074
- Paul, C. E., Gargiulo, S., Opperman, D. J., Lavandera, I., Gotor-Fernandez, V., Gotor, V., et al. (2013). Mimicking nature: synthetic nicotinamide cofactors for c-c bioreduction using enoate reductases. *Org. Lett.* 15, 180–183. doi: 10.1021/ol303240a
- Paul, C. E., Tischler, D., Riedel, A., Heine, T., Itoh, N., and Hollmann, F. (2015). Nonenzymatic regeneration of styrene Monooxygenase for catalysis. *Acc Catalysis* 5, 2961–2965. doi: 10.1021/acscatal.5b00041
- Poizat, M., Arends, I., and Hollmann, F. (2010). On the nature of mutual inactivation between Cp^{*}Rh(bpy)(H₂O) (2⁺) and enzymes - analysis and potential remedies. *J. Mol. Catalysis B Enzymatic* 63, 149–156. doi: 10.1016/j.molcatb.2010.01.006
- Riebel, B. R., Gibbs, P. R., Wellborn, W. B., and Bommarius, A. S. (2003). Cofactor regeneration of both NAD(+) from NADH and NADP(+) from NADPH : NADH oxidase from *Lactobacillus sanfranciscensis*. *Adv. Synth. Catalysis* 345, 707–712. doi: 10.1002/adsc.200303039
- Rocha-Martin, J., Vega, D., Bolivar, J. M., Godoy, C. A., Hidalgo, A., Berenguer, J., et al. (2011). New biotechnological perspectives of a NADH oxidase variant from *Thermus thermophilus* HB27 as NAD⁺-recycling enzyme. *BMC Biotechnol.* 11:101. doi: 10.1186/1472-6750-11-101
- Rollin, J. A., Tam, T. K., and Zhang, Y. H. P. (2013). New biotechnology paradigm: cell-free biosystems for biomanufacturing. *Green Chem.* 15, 1708–1719. doi: 10.1039/C3GC40625C
- Rover, L. Jr., Fernandes, J. C. B., Neto, G. D. O., Kubota, L. T., Katekawa, E., and Serrano, S. L. H. P. (1998). Study of NADH stability using ultraviolet-visible spectrophotometric analysis and factorial design. *Anal. Biochem.* 260, 50–55. doi: 10.1006/abio.1998.2656
- Ryan, J. D., Fish, R. H., and Clark, D. S. (2008). Engineering cytochrome p450 enzymes for improved activity towards biomimetic 1,4-NADH-cofactors. *ChemBioChem* 9, 2579–2582. doi: 10.1002/cbic.200800246
- Schmidt, H.-L., Stöcklein, W., Danzer, J., Kirch, P., and Limbach, B. (1986). Isolation and properties of an H₂O-forming NADH oxidase from *Streptococcus faecalis*. *Eur. J. Biochem.* 156, 149–155. doi: 10.1111/j.1432-1033.1986.tb09560.x
- Studier, F. W. (2005). Protein production by auto-induction in high-density shaking cultures. *Protein Exp. Purif.* 41, 207–234. doi: 10.1016/j.pep.2005.01.016
- Takeda, J., Ohta, S., and Hirobe, M. (1987). Steric and electronic effects of methyl substituents at 2- and 6-positions on N-Benzyl-1,4-dihydronicotinamide. *Chem. Pharm. Bull* 35, 2661–2667. doi: 10.1248/cpb.35.2661
- Tauber, K., Hall, M., Kroutil, W., Fabian, W. M. F., Faber, K., and Glueck, S. M. (2011). A highly efficient ADH-coupled NADH-recycling system for the asymmetric bioreduction of carbon-carbon double bonds using enoate reductases. *Biotechnol. Bioeng.* 108, 1462–1467. doi: 10.1002/bit.23078
- Tóth, K., Sedlak, E., Sprinzl, M., and Zoldak, G. (2008). Flexibility and enzyme activity of NADH oxidase from *Thermus thermophilus* in the presence of monovalent cations of Hofmeister series. *Biochim. Biophys. Acta* 1784, 789–795. doi: 10.1016/j.bbapap.2008.01.022
- Weckbecker, A., Gröger, H., and Hummel, W. (2010). “Regeneration of nicotinamide coenzymes: principles and applications for the synthesis of chiral compounds,” in *Biosystems Engineering I*, eds C. Wittmann and R. Krull (Berlin: Springer), 195–242.
- Zhang, R.-Y., Qin, Y., Lv, X.-Q., Wang, P., Xu, T.-Y., Zhang, L., et al. (2011). A fluorometric assay for high-throughput screening targeting nicotinamide phosphoribosyltransferase. *Anal. Biochem.* 412, 18–25. doi: 10.1016/j.ab.2010.12.035
- Zhang, Y.-W., Tiwari, M. K., Gao, H., Dhiman, S. S., Jeya, M., and Lee, J.-K. (2012). Cloning and characterization of a thermostable H₂O-forming NADH oxidase from *Lactobacillus rhamnosus*. *Enzyme Microb. Technol.* 50, 255–262. doi: 10.1016/j.enzmictec.2012.01.009

Conflict of Interest Statement: The authors declare that the research was conducted in the absence of any commercial or financial relationships that could be construed as a potential conflict of interest.

Copyright © 2015 Nowak, Beer, Pick, Roth, Lommes and Sieber. This is an open-access article distributed under the terms of the Creative Commons Attribution License (CC BY). The use, distribution or reproduction in other forums is permitted, provided the original author(s) or licensor are credited and that the original publication in this journal is cited, in accordance with accepted academic practice. No use, distribution or reproduction is permitted which does not comply with these terms.

4.2.2 **Thermostabilization of the uronate dehydrogenase from *Agrobacterium tumefaciens* by semi-rational design**

Authors: Teresa Roth, Barbara Beer, André Pick, and Volker Sieber

UDHs are relevant for exploitation of the production of aldaric acids as bio-based building blocks from waste biomass. Working with UDH from *Agrobacterium tumefaciens*, poor thermostability was encountered, but also the highest activity among UDHs identified so far.

In this publication it is described how the stability of this enzyme was improved using two different approaches. First, a semi-rational design based on structural data was applied. Here, the amino acids for substitution were chosen according to the B factor in combination with four additional knowledge-based criteria. Second, the best hits were combined with neutral mutations that were neither better nor worse in stability than the wildtype. Here, the triple variant A41P/H101Y/H236K showed the highest kinetic and thermodynamic stability with a T_{50}^{15} value of 62.2 °C (3.2 °C improvement) and a $\Delta\Delta G_U$ of 2.3 kJ/mol compared to wild type. With this, the power of the neutral drift approach for enzyme engineering was demonstrated.

The author Teresa Roth designed and conducted the experiments, and wrote the manuscript. Barbara Beer assisted in designing the experiments, in the lab, and in writing of the manuscript. André Pick and Volker Sieber contributed to the content and language of the manuscript.

ORIGINAL ARTICLE

Open Access



Thermostabilization of the uronate dehydrogenase from *Agrobacterium tumefaciens* by semi-rational design

Teresa Roth^{1,2}, Barbara Beer¹, André Pick¹ and Volker Sieber^{1,3,4*} **Abstract**

Aldaric acids represent biobased 'top value-added chemicals' that have the potential to substitute petroleum-derived chemicals. Until today they are mostly produced from corresponding aldoses using strong chemical oxidizing agents. An environmentally friendly and more selective process could be achieved by using natural resources such as seaweed or pectin as raw material. These contain large amounts of uronic acids as major constituents such as glucuronic acid and galacturonic acid which can be converted into the corresponding aldaric acids via an enzyme-based oxidation using uronate dehydrogenase (Udh). The Udh from *Agrobacterium tumefaciens* (UdhAt) features the highest catalytic efficiency of all characterized Udhs using glucuronic acid as substrate ($829 \text{ s}^{-1} \text{ mM}^{-1}$). Unfortunately, it suffers from poor thermostability. To overcome this limitation, we created more thermostable variants using semi-rational design. The amino acids for substitution were chosen according to the B factor in combination with four additional knowledge-based criteria. The triple variant A41P/H101Y/H236K showed higher kinetic and thermodynamic stability with a T_{50}^{15} value of 62.2 °C (3.2 °C improvement) and a $\Delta\Delta G_D$ of 2.3 kJ/mol compared to wild type. Interestingly, it was only obtained when including a neutral mutation in the combination.

Keywords: Uronate dehydrogenase, Glucuronic acid, *Agrobacterium tumefaciens*, Thermostability, B factor, Neutral drift

Introduction

The biocatalytic conversion of sugars from biomass-derived waste offers a promising route for the biotechnological production of fuels, chemicals and materials (Andberg et al. 2012). Next to sugars also sugar derivatives constitute an important building block of natural fibers and are therefore readily available.

Glucaric and other aldaric acids are considered top-value added chemicals to be obtained from biomass and have the potential for various applications such as a building block for polymers and hyperbranched polyesters (Werpy and Petersen 2004). Currently glucaric acid is produced from glucose using strong oxidants like nitric acid (Werpy and Petersen 2004). This process is expensive and

not selective. Higher selectivity could be achieved with an enzyme-based system for the production of glucaric acid. Moon et al. (2009) already constructed an enzyme-based pathway for the conversion of glucose to glucaric acid. The three enzymes *myo*-inositol-1-phosphate synthase, *myo*-inositol oxygenase and uronate dehydrogenase were recombinantly expressed in *E. coli*. However, only a yield of 17.4% (0.72 g/l) was achieved due to competition with the endogenous metabolism, which may limit carbon flux into the pathway for glucaric acid production. By inhibiting this flux through knockdown of phosphofructokinase an improvement up to a yield of 42% (1.56 g/l) could be achieved (Reizman et al. 2015). Due to the use of multiple enzymes this enzyme-based production of glucaric acid is still complex and insufficient. Instead of using glucose as the basic raw material the two ubiquitous sugar derivatives glucuronic acid and galacturonic acid would be more suitable to gain aldaric acids. Glucuronic acid is a component

*Correspondence: sieber@tum.de

¹ Chair of Chemistry of Biogenic Resources, Straubing Centre of Science, Technical University of Munich, Schulgasse 16, 94315 Straubing, Germany
Full list of author information is available at the end of the article

of hemicellulose, hyaluronic acid and seaweed, whereas the plant polysaccharide pectin largely consists of galacturonic acid (Ahn et al. 2012; Andberg et al. 2012). They can be oxidized to the corresponding aldaric acids by the enzyme uronate dehydrogenase (Udh, EC 1.1.1.203). For this conversion only the enzyme Udh would be required to obtain an enzyme-based system. The cell-based production of glucuronic acid by Moon et al. (2009) is further limited by the intracellular accumulation of the product and the resulting acidification. This problem could be avoided by using a cell-free biosystem. A cell-free production has further advantages, i.e. easy control of the process, no substrate or product toxicity, higher product titer and broad reaction conditions (Guterl et al. 2012; You and Zhang 2012). Moreover the necessary cofactor nicotinamide adenine dinucleotide could easily be recycled to allow process operation under economic conditions. The recently characterized NADH oxidase from *Lactobacillus pentosus* which only forms water as byproduct would be a suitable enzyme in this process (Nowak et al. 2015).

The oxidation of uronic acids to aldaric acids by Udh was first described in the phytopathogenic bacteria *Pseudomonas syringae* and *Agrobacterium tumefaciens* (Zajic 1959). Until now several Udh's of the following organisms have been characterized: *Agrobacterium tumefaciens*, *Fulvmarina pelagi*, *Oceanicola granulosus*, *Streptomyces viridochromogenes*, *Pseudomonas syringae*, *Pseudomonas putida*, *Pseudomonas mendocina*, *Pseudomonas fluorescens*, *Polaromonas naphthalenivorans* and *Chromohalobacter salixigens* (Boer et al. 2010; Pick et al. 2015; Yoon et al. 2009; Wagschal et al. 2014). The best characterized enzyme is the Udh from *Agrobacterium tumefaciens* (UdhAt), which belongs to the short-chain dehydrogenase/reductase (SDR) superfamily and accepts only NAD⁺ as cofactor (Pick et al. 2015). The enzyme forms a hexamer in which two monomers interact tightly through the contact of the α -helices 3 and 4 (PDB code: 3RFT). Three dimers are then more loosely packed to form the hexamer. Each monomer consists of a single domain with the typical Rossmann fold for cofactor binding (Parkkinen et al. 2011; Pick et al. 2015). In comparison to the other Udh's the one derived from *Agrobacterium tumefaciens* features the highest catalytic efficiency ($829 \text{ s}^{-1}\text{mM}^{-1}$) using glucuronic acid as substrate. Nevertheless, its short half-life of only 50 min at 37 °C is limiting its potential for industrial applications (Pick et al. 2015). Therefore the aim of this study was to overcome this limitation by improving the thermostability using enzyme engineering.

We chose a semi-rational design due to the availability of the crystal structure of the UdhAt. This helped to define positions for substitution, which could lead to a greater thermostability without losing or diminishing enzyme activity.

Systematic structural studies regarding mesophilic and thermophilic enzymes have shown that the latter are characterized by higher degrees of rigidity. This can be achieved by the accumulation of a variety of effects like hydrogen bonds or salt bridges. So, increasing the rigidity of the enzyme at appropriate sites should enhance thermostability (Reetz and Carballeira 2006). Therefore, the first and leading criterion was the B factor (atomic displacement parameter), which describes the movement of an atom around its mean position and therefore shows the flexibility and dynamics of the protein structure (Parthasarathy and Murthy 2000). The factor is determined for each atom in a protein structure during high-resolution X-ray crystallography. The average B factor for an amino acid position is then calculated by the program B-FITTER (Carballeira and Reetz 2007). Apart from this tool, informations on appropriate sites for mutagenesis can also be obtained from empirical studies that determine how amino acid side chains affect secondary or tertiary structures (Spector et al. 2000; Sriprapundh et al. 2000) or from looking at amino acid conservation (Anbar et al. 2012; Wijma et al. 2013). This rational approach for the selection of amino acids for mutagenesis is then combined with randomization using degenerated primers to find the best amino acid substitution at the specified positions. The generated smart enzyme libraries are small and can such easily be screened in a short period of time to find variants with improved thermostability.

Materials and methods

Reagents

All chemicals were of analytical grade or higher quality and purchased from Sigma-Aldrich, Molekula, Carl Roth, Alfa Aesar and VWR. For protein purification, equipment and columns, from GE Healthcare were used (Munich, Germany).

Strains and plasmid

The strains *E. coli* XL1 BLUE and *E. coli* BL21(DE3) were used during this work. Construction of the plasmid pCBB-*udh-A.t.* was described by Pick et al. (2015).

Enzyme expression and purification

Escherichia coli BL21(DE3) containing the plasmid of interest was grown in 250 ml autoinduction medium (Studier 2005). The preculture was incubated in 20 ml of LB medium with 30 $\mu\text{g/ml}$ kanamycin at 37 °C overnight on a rotary shaker (180 rpm). The expression culture was then inoculated to reach an $\text{OD}_{600 \text{ nm}}$ of 0.1. Incubation was performed for 4 h at 37 °C followed by incubation for 21 h at 16 °C. Cells were harvested by centrifugation and resuspended in 50 mM potassium phosphate buffer (KPi) pH 8.0 (10 mM imidazol, 500 mM NaCl and 10%

glycerol). Crude extracts were prepared with a Basic-Z Cell Disrupter (IUL Constant Systems) and subsequent incubation with $MgCl_2$ (2.5 mM) and DNaseI (1 $\mu g/ml$) for 20 min at room temperature to degrade DNA. The insoluble fraction of the lysate was removed by centrifugation (20,000 rpm for 40 min at 4 °C). The supernatant was applied to an IMAC affinity column, 5 ml HisTrap™ FF, equilibrated with the resuspension buffer using the ÄKTA Purifier-system. The column was washed with 20 ml of resuspension buffer and the enzyme was eluted with 50 mM KPi buffer pH 8.0 (500 mM imidazol, 500 mM NaCl and 10% glycerol). Elution was monitored by UV (280 nm) and fractions containing protein were subjected to 12% SDS-Page described by Laemmli (1970). The molecular weight of UdhAt was calculated to be 31.21 kDa (including the additional amino acids of the N-terminal His₆-tag) using the ProtParam tool (Expasy). Fractions containing the eluted target protein were pooled and desalted using a HiPrep™ 26/10 Desalting column which was preliminary equilibrated with 50 mM ammonium bicarbonate pH 7.9. Protein concentrations were determined using a NanoPhotometer (IMPLEN) with 50 mM ammonium bicarbonate pH 7.9 as the reference and an extinction coefficient of 37,930 $M^{-1}cm^{-1}$ (ProtParam, Expasy).

Enzyme assay

The Udh activity was determined photometrically by monitoring the increase of NADH at 340 nm with a Multiskan spectrum spectrophotometer (Thermo Fisher Scientific). The reaction mixture contained 25 mM KPi buffer pH 8.0, 1 mM NAD^+ , 5 mM $MgCl_2$ and 10 mM glucuronic acid. Measurements were performed at 25 °C after adding 20 μl of purified enzyme (9.1×10^{-5} mg/ml). One unit of enzyme activity was defined as the amount of protein that oxidizes 1 μmol of NADH/min at 25 °C.

Mutagenesis

Saturation mutagenesis libraries were generated using the QuikChange® mutagenesis strategy from Stratagene (USA). The degenerated primers used (Table 1) contained the codon NNK. High quality of the generated libraries was verified by sequencing five clones per library (GATC Biotech, Cologne, Germany).

Culture conditions for 96 deep-well plates

Escherichia coli BL21(DE3) containing the plasmid (plasmid libraries) of interest were used for expression in 96 well format. The colonies were picked using the Hudson Rapid Pick lite colony picker (Hudson Robotics Inc., Springfield, USA) and grown in 96 deep-well plates containing 1200 μl autoinduction medium (Studier 2005)

Table 1 Primers used for saturation mutagenesis

	Sequence 5'–3'
L38fw	GATCTGTCTCCG NNK GATCCGGCTGGTCCGAATGAAG
L38rv	CAGCCGGAT CMNN CGGAGACAGATCTGCCAGAC
A41fw	CCGCTGGATCCG NNK GGTCCGAATGAAGAATGTGTTC
A41rv	CTTCATTCCGACC MNN CGGATCCAGCGGAGACAGATC
E81fw	GCGTTGAAAAACCGTTT TNNK CAGATTCTGCAGGGTAACAT-TATTGGC
E81rv	CCCTGCAGAATCTG MNN AAACGGTTTTTCAACGCTAATGCCAC
H101fw	GCAGCACGTGC ANNK GGTCAGCCTCGTATTGTTTTGCAAG
H101rv	CAATACGAGGCTGACC MNN TGCACGTGCTGCTTCATACAG
H236fw	GCCTTTTCGTCG TNNK ATTACCGAAACCACACCCGCTCCG
H236rv	GGTGTGGTTTCGGTAAT MNN ACGACGAAAGGCTTCGCAT-TATCTTCGG
E239fw	GTCGTCATATTACC NNK ACCACACCCGCTCCGGATCCGAATG
E239rv	CCGGAGGGGGTGTGGT MNN GGTAATATGACGACGAAAGGCTTC

with 100 $\mu g/ml$ kanamycin, for 25 h at 37 °C on a rotary shaker (1000 rpm). 100 μl of the cultures were centrifuged (3000 rpm for 15 min at 4 °C), the supernatants discarded and the cell pellets frozen at –80 °C for at least 2 h. Afterwards 100 μl of 25 mM KPi pH 8.0 were added and the plates incubated for 1 h at 37 °C on a rotary shaker (700 rpm) for cell disruption.

Screening

The screening for thermostability was assessed based on the residual activity subsequent to the exposure to high temperatures. The supernatants were diluted (1:2000 in a total volume of 50 μl) in incubation mixture containing 25 mM KPi pH 8.0, 5 mM $MgCl_2$ and 100 mM glucuronic acid. Before incubation the initial activity was measured using an aliquot of 20 μl and adding 180 μl of reaction mixture (25 mM KPi pH 8.0 and 1 mM NAD^+). Heat treatment was performed for 15 min at 58 °C in a PCR thermocycler. After cooling to 4 °C another aliquot of 20 μl was used to measure the residual activity. Variants showing a residual activity greater than the wildtype enzyme plus standard deviation were considered as hits.

Kinetic stability

Kinetic stability can be described by T_{50}^{15} , the temperature at which 50% of the enzyme's initial activity is left after incubation for a defined time period. For this purpose, a gradient PCR thermocycler was used. The purified enzymes were incubated at 50–64 °C at the same enzyme concentration (9.1×10^{-5} mg/ml) with 25 mM KPi pH 8.0, 5 mM $MgCl_2$, 0.1 mg/ml BSA and 100 mM glucuronic acid.

Thermodynamic stability

The thermodynamic stability was determined by guanidine hydrochloride (GdmCl) induced unfolding. Therefore, 100 μ l protein were incubated with various concentrations of GdmCl (0–3.5 M) in 25 mM KPi pH 8.0 for 8 days at RT. The proteins were transferred into a 96-well optical-bottom plate (Thermo Fisher Scientific) and the fluorescence emission at 344 nm was measured after excitation at 278 nm in a Variskan (Thermo Fisher Scientific). The difference in free energy of unfolding of WT and the variants ($\Delta\Delta G_U$) was calculated using the following equation: $\Delta\Delta G_U = 0.5(m_{wild\ type} + m_{variant})\Delta[GdmCl]_{50\%}$, where m is the slope of the linear denaturation plot $-dAG_u/d[denaturant]$ and $\Delta[GdmCl]_{50\%}$ is the difference between $[GdmCl]_{50\%}$ for wild type and mutant (Kellis et al. 1989).

Determination of kinetic parameters

Kinetic parameters (k_{cat} and K_M) were determined for WT and purified variants. Measurements were performed in 25 mM KPi pH 8.0 at 25 °C with varying concentrations of glucuronate (0–10, 1 mM NAD⁺) or NAD⁺ (0–4, 10 mM glucuronate). The increase of NADH was monitored at 340 nm with a Multiskan spectrum spectrophotometer (Thermo Fisher Scientific). The data was fitted to the Michaelis–Menten equation using SigmaPlot 11.0.

Results

Identification of amino acid positions for mutagenesis

Site-saturation mutagenesis has proven to be a useful strategy to alter enzyme properties like thermal stability or substrate specificity when the amino acid positions are properly selected (Reetz and Carballeira 2006). Setting the B factor as a criterion was already suggested by Parthasarathy and Murthy (2000) and further successfully applied for thermal stabilization of *Bacillus subtilis* lipase (Reetz and Carballeira 2006) and an α -Amino ester hydrolase (Blum et al. 2012). Hence, we used the B factor as our leading criterion. In multiple studies the

B factor was combined with the structure-guided consensus method to reduce the number of amino acids to be mutated (Blum et al. 2012; Jochens et al. 2010). In our case a combination of those methods was not suitable because the consensus sequence of all known UdhS (using the recommended cut off of 80%) was identical to the sequence of the UdhAt. Therefore, we chose four other criteria in combination with a B factor greater than 25 Å²: first, the localization of amino acids within the protein was considered. Amino acids within elements of pronounced secondary structure were excluded for mutagenesis except when they have a low propensity for this type of secondary structure (Bommarius and Paye 2013; Lehmann and Wyss 2001). In addition amino acids that are within the cofactor and substrate binding sites or at the interface between the protein domains of the multimer (α -helices 3 and 4) were not considered. Second, amino acids that occur more often in proteins from thermophilic origin and are typically considered for protein stabilization such as proline, arginine and tyrosine were excluded from mutagenesis (Querol et al. 1996; Lehmann and Wyss 2001). Furthermore, conserved amino acids as well as amino acids that are probably involved in a hydrogen bonding network (PyMOL) were excluded. Conserved amino acids are advantageous for the protein and “survived” during evolution (survival of the fittest) (Bommarius and Paye 2013). Therefore, sequence and structure alignments of all known UdhS and enzymes that had a sequence similarity greater than 60% compared to the UdhAt were created. From these alignments consensus sequences with coverage of 95 or 80% were created (BioEdit and PROMALS) and all amino acids that showed conservation were excluded from mutagenesis. An overview of these five criteria and the amino acids considered for mutagenesis is shown in Table 2. Six amino acids fulfilled all five criteria: L38, A41, E81, H101, H236 and E239. They were subjected to site-directed mutagenesis via QuikChange PCR using degenerated primers with an NNK motif, covering at least one codon of all canonical amino acids.

Table 2 The five criteria for selecting the amino acid positions for mutagenesis

Criterion	Amino acids
B factor >25 Å ²	K4, Q14, R17, E21, A24, P25, M26, E28, S36, P37, L38, D39, P40, A41, G42, P43, N44, E45, E46, Q49, A63, P79, E81, H101, G134, F154, C166, T167, P168, E169, N171, F180, S181, E190, H218, G223, K227, R235, H236, T238, E239, T240, T241, P242, P243, P244
Location	K4, M26, P37, L38, D39, P40, A41, G42, P43, N44, E45, A63, P79, E81, H101, T167, P168, E169, N171, F180, E190, K227, H236, T238, E239, P242, P243, P244
Occurrence in thermostable proteins	K4, M26, L38, D39, A41, G42, N44, E45, A63, E81, H101, T167, E169, N171, F180, E190, K227, H236, T238, E239
Conservation	M26, L38, D39, A41, G42, N44, A63, E81, H101, E169, N171, F180, E190, K227, H236, T238, E239
Part of hydrogen bonding network	L38, A41, E81, H101, H236, E239

Screening of mutant libraries

The stability of proteins can be judged by three types of criteria: kinetic, thermodynamic and process stability (Bommarius and Paye 2013).

Fast screening to examine improved thermostability in the initial six libraries was performed in 96-well PCR plates by heating the enzyme solutions (diluted supernatants) to 58 °C for 15 min in a thermocycler. The temperature of 58 °C was chosen because it reduced WT activity to 10% (standard deviation of 2%) allowing a fast identification of positive hits. In library H236 three variants showed a higher stability: H236K, H236I and H236R. All other enzyme variants in all other libraries showed lower thermostability than WT with exception of the variants A41P, H101Y and H101N, which were as stable as wild type enzyme. With only one position giving rise to improvements no combination of improved variants for possible additive or even synergistic effects was possible. However, recently several interesting studies had shown the importance of neutral drift on the evolution of enzymes (Gupta and Tawfik 2008; Smith et al. 2011). This led us to combine the mutations that were positive in the screen with the ones that at least did not show any decrease in activity. We created a series of double and triple variants in addition to the single variants H236K, H236I and H236R (see Table 3).

Again, the residual activity after incubation at 58 °C was measured (data not shown). Only the double variant A41P/H236R showed a reduced thermostability in the screen. The remaining 17 variants were purified and their kinetic and thermodynamic stability was compared as well as their kinetic parameters determined.

Kinetic stability

The T_{50}^{15} value was defined as the temperature required to reduce the initial enzyme activity to 50% within 15 min. The T_{50}^{15} of the purified WT enzyme was 59.0 °C. In Fig. 1 the T_{50}^{15} of WT and variants are shown. All variants had an improved or equal kinetic stability compared to WT. The highest improvement of kinetic stability was observed for the triple variant A41P/H101Y/H236 K with a T_{50}^{15} value of 62.2 °C, resulting in a ΔT_{50}^{15} of 3.2 °C compared to WT.

Thermodynamic stability

The thermodynamic stability was determined by GdmCl-induced protein unfolding. The differences in free energy of unfolding of the single and triple variants compared to WT ($\Delta\Delta G_U$) are shown in Fig. 2. The single variants all showed negative $\Delta\Delta G_U$ compared to the wildtype, except H236K and H236I. However, the $\Delta\Delta G_U$ of all double and triple variants—with exception of A41P/H101Y/H236R—were positive, which indicates that these variants have a higher thermodynamic stability than WT. Moreover, this stabilization is non-additive, as the single variants that were neutral in the screening, showed even lower stability than the WT when tested in the purified form. The best variant was the triple variant A41P/H101Y/H236K with a $\Delta\Delta G_U$ of 2.3 kJ/mol. In Fig. 3 the unfolding curves of WT, the single variant H236K and the best variant A41P/H101Y/H236K are shown.

Kinetic parameters

The kinetic parameters v_{max} , K_m and k_{cat}/K_m for the substrate glucuronic acid and the cofactor NAD⁺ were determined for the eight best variants. WT had a specific activity of 390 U/mg, a K_m of 0.71 mM and a catalytic efficiency of 287 s⁻¹mM⁻¹. In comparison, the variants had a slightly reduced specific activity and a higher K_m value (Table 4) resulting also in a reduced catalytic efficiency (40–60% compared to WT).

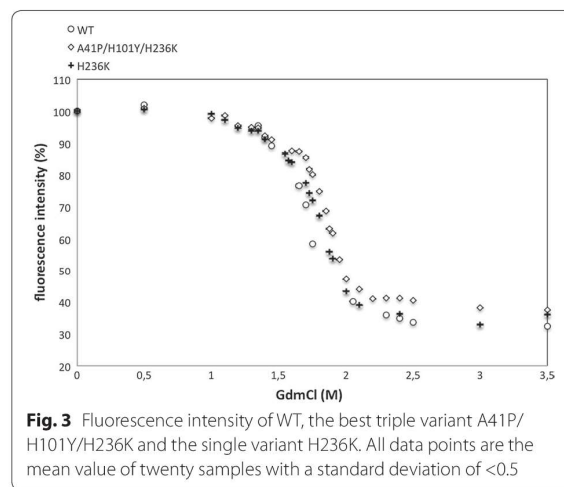
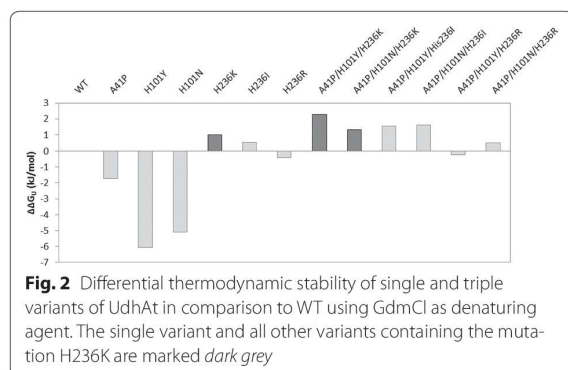
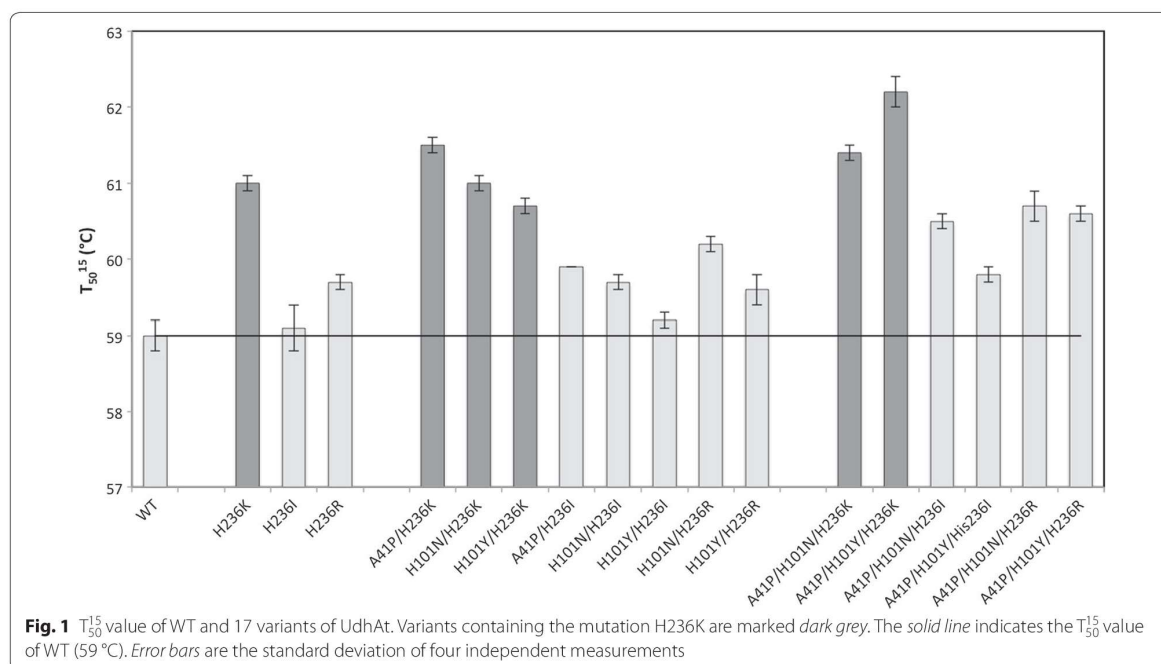
Discussion

With the enzyme uronate dehydrogenase a selective one-step enzyme-based production of aldaric acids from waste biomass could be possible. The uronate dehydrogenase from *Agrobacterium tumefaciens* (UdhAt) features the highest efficiency among all known Udh using glucuronic acid as substrate. However, the enzyme lacks stability with only a half-life of 50 min at 37 °C (Pick et al. 2015). This limits its potential for industrial application. As no Udh is known from thermophilic organisms, we developed more thermostable variants by enzyme engineering.

This was achieved through the combination of an effective selection method for the amino acid positions to be mutated and the accumulation of advantageous mutations.

Table 3 Created single, double and triple variants of UdhAt to test for additive or synergistic effects

Single variants	Double variants, combining single variants and:			Triple variants, combining single variants and:	
	A41P	H101Y	H101N	A41P/H101Y	A41P/H101N
H236K	A41P/H236K	H101Y/H236K	H101N/H236K	A41P/H101Y/H236K	A41P/H101N/H236K
H236I	A41P/H236I	H101Y/H236I	H101N/H236I	A41P/H101Y/H236I	A41P/H101N/H236I
H236R	A41P/H236R	H101Y/H236R	H101N/H236R	A41P/H101Y/H236R	A41P/H101N/H236R



The selection method for the amino acids was based on the B factor and four further criteria leading to the positions: L38, A41, E81, H101, H236 and E239. In the library H236 the three variants H236K, H236I and H236R had a greater thermostability than WT. The variants A41P, H101Y and H101N showed no change (positive or negative) and were therefore used to test for additivity. The triple variant A41P/H101Y/H236K showed the highest kinetic ($\Delta T_{50}^{15} = 3.2$ °C) and thermodynamic stability ($\Delta\Delta G_U = 2.3$ kJ/mol) compared to WT. When two or more point mutations are introduced, the question arises whether they interact additively or non-additively. In the latter case they can cause either cooperative (positive) or

antagonistic (negative) effects. It was suggested (Reetz 2013; Skinner and Terwilliger 1996) that additive effects might occur when the locations of mutations are well-separated. Whereas when the side chains of two residues are in close contact with one another their effects are generally non-additive. Our best variant A41P/H101Y/H236K showed non-additive synergistic cooperative effects, because the increase in thermostability was greater than the sum of the three single variants although the positions

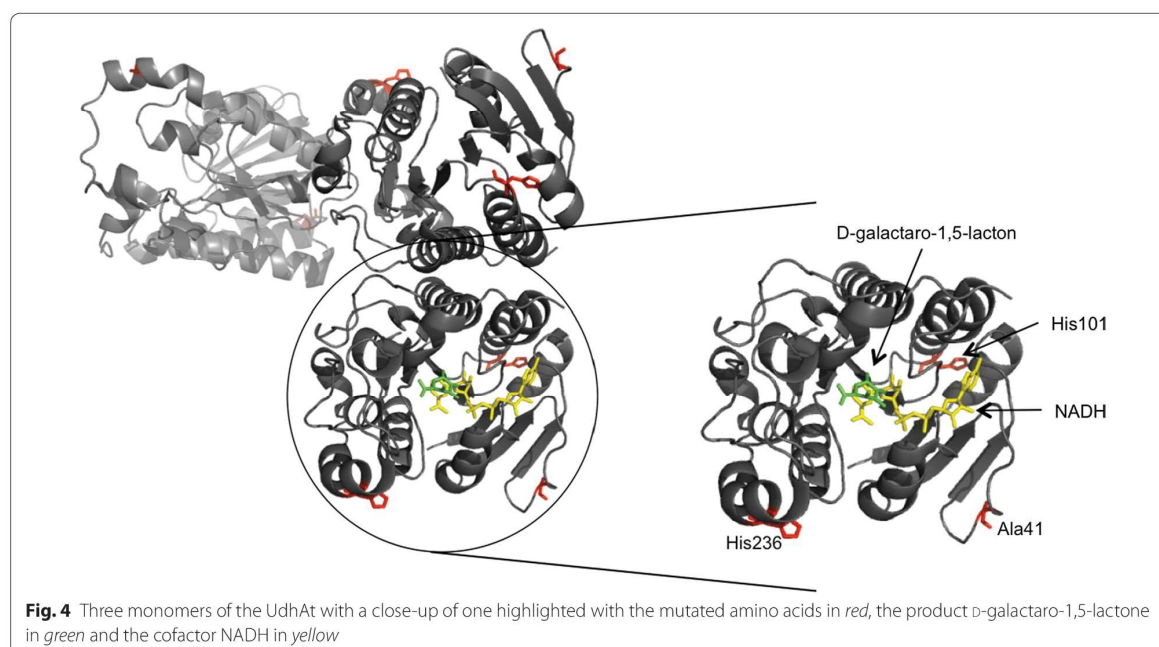
Table 4 Kinetic parameters of the eight best variants and WT for glucuronic acid including the standard deviation of three measurements

Variant	Specific activity (U/mg)	K_m (mM)	Catalytic efficiency	
			($s^{-1}mM^{-1}$)	(%)
WT	391 ± 17	0.7 ± 0.1	286.4 ± 13.0	100
H236K	234 ± 5	1.3 ± 0.1	97.5 ± 2.2	34.0
A41P/H236K	407 ± 8	1.2 ± 0.0	179.5 ± 3.5	62.7
H101Y/H236K	218 ± 6	1.0 ± 0.1	116.7 ± 3.4	40.8
H101N/H236K	228 ± 5	0.9 ± 0.1	139.7 ± 3.2	48.8
A41P/H101Y/H236K	280 ± 6	0.9 ± 0.1	167.3 ± 3.6	58.4
A41P/H101Y/H236R	302 ± 4	1.0 ± 0.1	160.5 ± 2.0	56.0
A41P/H101N/H236K	248 ± 4	0.9 ± 0.1	149.7 ± 2.25	52.3
A41P/H101N/H236R	330 ± 3	1.0 ± 0.0	170.0 ± 1.7	59.3

are not in close proximity ($>20 \text{ \AA}^2$). Istomin et al. (2008) have obtained new insights concerning this topic. They concluded that a statistically significant bias toward non-additivity occurs whenever the residues, although not in direct contact, are located within the same rigid cluster. Additivity can be expected when they are in different clusters. Also Reetz et al. (2009) could show that the hyperthermophilic mutant XI of the lipase from *Bacillus subtilis* had cooperative non-additive effects between five distal residues. The stabilization was performed by the formation of an extensive H-bond/salt-bridge network on the surface

of the enzyme. This could be the same case here because all three amino acid positions A41, H101 and H236 are located on the surface of the enzyme (Fig. 4). Furthermore, the substitution A41P helped to regain the catalytic function of the H236 mutation. The catalytic efficiency of the single variant H236K decreased to 34% of the wildtype activity, but was reconstituted to 63% in the double variant A41P/H236K. The triple variant A41P/H101Y/H236K with the highest stability still showed 56% of the wildtype activity (Table 4). This finding nicely demonstrates the potential of neutral drift mutations that have gained interest in the last decade (Bershtein et al. 2008; Bloom and Arnold 2009; Smith et al. 2011).

The mutation H236K had the greatest influence on thermostability of the UdhAt. The amino acid histidine at the position 236 had a high B factor (31.53 \AA^2) and was located in an α -helix. Histidine is not a good helix builder whereas the introduced amino acid lysine is. Interestingly, when we applied the strategy of Blum et al. (2012), who showed that consensus sequences with a rather low cut-off could lead to thermally more stable enzyme variants, Lysine 236 was indeed conserved (at a cut-off of 30%). In this consensus sequence 64 amino acids not identical to the UdhAt were conserved, i.e. E239A. Our screening assay did not find a preferable amino acid exchange at this position. At the positions A41, E81 and H101 wild type amino acid of UdhAt was conserved. This confirms the strategy of Blum et al. (2012) combining the B factor with the structure-guided consensus (SGC) concept: they



chose WT positions that were not consensus and did not fit a number of structural guidelines and also amino acid positions with a high B factor and replaced them by the consensus amino acid. Thereby they could improve the thermostability of α -amino ester hydrolase by 7 °C. This strategy has also the advantage of small libraries and therefore less screening effort. Our strategy of choosing the amino acid positions for mutagenesis was also successful. Furthermore, we found the triple variant A41P/H101Y/H236K showing better thermostability than WT, which would not be detected by the SGC. It would be interesting to know if both methods—structure guided consensus concept with a low cut-off of 50% and applying our five criteria—would lead to the same results for thermostabilization when transferred to another Udh. For this purpose the Udh of *Chromohalobacter salexigens* would be suitable because a crystal structure is already available (Ahn et al. 2012).

In summary, we have shown that the combination of the B factor with knowledge and structure-based criteria is successful for generating thermostable proteins of the UdhAt. The best UdhAt triple variant (A41P/H101Y/H236K) showed an improved T_{50}^{15} value of 3.2 °C and a higher thermodynamic stability ($\Delta\Delta G_U = 2.3$ kJ/mol). With this approach for improving the stability the UdhAt has been made available for biotechnological applications i.e. for the cell-free production of glucaric or galactaric acid.

Abbreviations

Udh: uronate dehydrogenase; UdhAt: uronate dehydrogenase from *Agrobacterium tumefaciens*; SDR: short-chain dehydrogenase/reductase; WT: wild type; SGC: structure-guided consensus; *E. coli*: *Escherichia coli*; KPi: potassium phosphate; GdmCL: guanidine hydrochloride.

Authors' contributions

All authors read and approval the final manuscript.

Author details

¹ Chair of Chemistry of Biogenic Resources, Straubing Centre of Science, Technical University of Munich, Schulgasse 16, 94315 Straubing, Germany. ² Present Address: Roche Diagnostics GmbH, Nonnenwald 2, 82377 Penzberg, Germany.

³ TUM Catalysis Research Center, Ernst-Otto-Fischer-Straße 1, 85748 Garching, Germany. ⁴ Fraunhofer Institute for Interfacial Engineering and Biotechnology IGB, Bio, Electro and Chemocatalysis BioCat, Straubing Branch, Schulgasse 11a, 94315 Straubing, Germany.

Competing interests

The authors declare that they have no competing interests.

Availability of data and materials

The data on which the conclusions are made are all presented in this paper.

Ethical statement

This article does not contain any studies with human participants or animals performed by any of the authors.

Funding

BB was funded by the Bavarian State Ministry of the Environment and Consumer Protection (Grant Number TGC01/GCU-60345). This work was supported

by the Technical University of Munich within the funding program Open Access Publishing.

Publisher's Note

Springer Nature remains neutral with regard to jurisdictional claims in published maps and institutional affiliations.

Received: 14 April 2017 Accepted: 17 May 2017

Published online: 23 May 2017

References

- Ahn J-W, Lee SY, Kim S, Kim SM, Lee SB, Kim K-J (2012) Crystal structure of glucuronic acid dehydrogenase from *Chromohalobacter salexigens*. *Proteins* 80(1):314–318
- Anbar M, Gul O, Lamed R, Sezerman UO, Bayer E (2012) Improved thermostability of *Clostridium thermocellum* endoglucanase Cel8A by using consensus-guided mutagenesis. *Acad Emerg Med* 78(9):3458–3464
- Andberg M, Maaheimo H, Boer H, Penttilä M, Koivula A, Richard P (2012) Characterization of a novel *Agrobacterium tumefaciens* galactarolactone cycloisomerase enzyme for direct conversion of D-galactarolactone to 3-deoxy-2-keto-L-threo-hexarate. *J Biol Chem* 287(21):17662–17671
- Bershtein S, Goldin K, Tawfik DS (2008) Intense neutral drifts yield robust and evolvable consensus proteins. *J Mol Biol* 379(5):1029–1044
- Bloom JD, Arnold FH (2009) In the light of directed evolution: pathways of adaptive protein evolution. *Proc Natl Acad Sci USA* 106(Suppl):9995–10000
- Blum JK, Ricketts MD, Bommaris AS (2012) Improved thermostability of AEF by combining B-FIT analysis and structure-guided consensus method. *J Biotechnol* 160(3–4):214–221
- Boer H, Maaheimo H, Koivula A, Penttilä M, Richard P (2010) Identification in *Agrobacterium tumefaciens* of the D-galacturonic acid dehydrogenase gene. *Appl Microbiol Biotechnol* 86(3):901–909
- Bommaris AS, Paye MF (2013) Stabilizing biocatalysts. *Chem Soc Rev* 42(15):6534–6565
- Carballeira D, Reetz MT (2007) Iterative saturation mutagenesis (ISM) for rapid directed evolution of functional enzymes. *Nat Protoc* 2(4):891–903
- Gupta RD, Tawfik DS (2008) Directed enzyme evolution via small and effective neutral drift libraries. *Nat Methods* 5(11):939–942
- Guterl J-K, Garbe D, Carsten J, Steffler F, Sommer B, Reiß S, Sieber V (2012) Cell-free metabolic engineering: production of chemicals by minimized reaction cascades. *ChemSuschem* 5(11):2165–2172
- Istomin A, Gromiha M, Vorov O, Jacobs D, Livesay D (2008) New insight into long-range nonadditivity within protein double-mutant cycles. *Proteins* 70(2):311–319
- Jochens H, Aerts D, Bornscheuer UT (2010) Thermostabilization of an esterase by alignment-guided focussed directed evolution. *Protein Eng Des Sel* 23(12):903–909
- Kellis JT, Nyberg K, Fersht R (1989) Energetics of complementary side-chain packing in a protein hydrophobic core. *Biochemistry* 28(11):4914–4922
- Laemmli UK (1970) Cleavage of structural proteins during the assembly of the head of bacteriophage T4. *Nature* 227:680–685
- Lehmann M, Wyss M (2001) Engineering proteins for thermostability: the use of sequence alignments versus rational design and directed evolution. *Curr Opin Biotechnol* 12(4):371–375
- Moon TS, Yoon S, Lanza AM, Roy-Mayhew JD, Prather KJL (2009) Production of glucaric acid from a synthetic pathway in recombinant *Escherichia coli*. *Appl Environ Microbiol* 75(3):589
- Nowak C, Beer B, Pick A, Roth T, Lommes P, Sieber V (2015) A water-forming NADH oxidase from *Lactobacillus pentosus* suitable for the regeneration of synthetic biomimetic cofactors. *Front Microbiol* 6(957):1–9
- Parkkinen T, Boer H, Jänis J, Andberg M, Penttilä M, Koivula A, Rouvinen J (2011) Crystal structure of uronate dehydrogenase from *Agrobacterium tumefaciens*. *J Biol Chem* 286(31):27294–27300
- Parthasarathy S, Murthy MR (2000) Protein thermal stability: insights from atomic displacement parameters (B values). *Protein Eng* 13(1):9–13
- Pick A, Schmid J, Sieber V (2015) Characterization of uronate dehydrogenases catalysing the initial step in an oxidative pathway. *Microbiol Biotechnol* 8(4):633–643

- Querol E, Perez-Pons J, Mozo-Villarias A (1996) Analysis of protein conformational characteristics related to thermostability. *Protein Eng* 9(3):265–271
- Reetz MT (2013) The importance of additive and non-additive mutational effects in protein engineering. *Angew Chem Int Ed* 52(10):2658–2666
- Reetz MT, Carballeira JD (2006) Iterative saturation mutagenesis on the basis of B factors as a strategy for increasing protein thermostability. *Angew Chem Int Ed* 45:7745–7751
- Reetz MT, Soni P, Acevedo JP, Sanchis J (2009) Creation of an amino acid network of structurally coupled residues in the directed evolution of a thermostable enzyme. *Angew Chem Int Ed* 48(44):8268–8272
- Reizman IMB, Stenger AR, Reisch CR, Gupta A, Connors NC, Prather KLJ (2015) Improvement of glucaric acid production in *E. coli* via dynamic control of metabolic fluxes. *Metab Eng Commun* 2:109–116
- Skinner MM, Terwilliger TC (1996) Potential use of additivity of mutational effects in simplifying protein engineering. *Proc Natl Acad Sci USA* 93(20):10753
- Smith WS, Hale JR, Neylon C (2011) Applying neutral drift to the directed molecular evolution of a β -glucuronidase into a β -galactosidase: two different evolutionary pathways lead to the same variant. *BMC Res Notes* 4(1):138
- Spector S, Wang M, Carp S, Robblee J, Hensch ZS, Fairman R, Raleigh DP (2000) Rational modification of protein stability by the mutation of charged surface residues. *Biochem* 39(5):872–879
- Sriprapundh D, Vieille C, Zeikus JG (2000) Molecular determinants of xylose isomerase thermal stability and activity: analysis of thermozymes by site-directed mutagenesis. *Protein Eng* 13(4):259–265
- Studier FW (2005) Protein production by auto-induction in high density shaking cultures. *Protein Expr Purif* 41(1):207–234
- Wagschal K, Jordan DB, Lee CC, Younger A, Braker JD, Chan VJ (2014) Biochemical characterization of uronate dehydrogenases from three *Pseudomonads*, *Chromohalobacter salixigens*, and *Polaromonas naphthalenivorans*. *Enzyme Microb Technol* 69:62–68
- Werpy T, Petersen G (2004) Top value added chemicals from biomass volume I—results of screening for potential candidates from sugars and synthesis gas. Department of Energy, Washington, DC
- Wijma HJ, Floor RJ, Janssen DB (2013) Structure- and sequence-analysis inspired engineering of proteins for enhanced thermostability. *Curr Opin Struct Biol* 23(4):588–594
- Yoon S-H, Moon TS, Iranpour P, Lanza AM, Prather KJ (2009) Cloning and characterization of uronate dehydrogenases from two *Pseudomonads* and *Agrobacterium tumefaciens* strain C58. *J Bacteriol* 191(5):1565–1573
- You C, Zhang YHP (2012) Cell-free biosystems for biomanufacturing. *Adv Biochem Eng Biotechnol* 123:127–141
- Zajic JE (1959) Hexuronic dehydrogenase of *Agrobacterium tumefaciens*. *J Bacteriol* 78(5):734

4.3 Evaluation of *in vitro* enzymatic cascade reactions toward BDO

4.3.1 *In vitro* enzymatic cascade reaction to 5-hydroxy-2-oxovalerate

For the screening of branched-chain ketoacid decarboxylase (KdcA) variants with increased activity toward 5-hydroxy-2-oxovalerate (Hov), the substrate was not available commercially. Therefore, it should be synthesized from D-glucuronate using the enzymes uronate dehydrogenase (UDH), glucarate dehydratase (GlucD), 5-keto-4-deoxyglucarate dehydratase (KdgD), and the triple variant of ADHZ3 from *E. coli* with the amino acid substitutions S199L/S200N/N201D (ADHZ3 LND) in a cascade reaction (Figure 15).

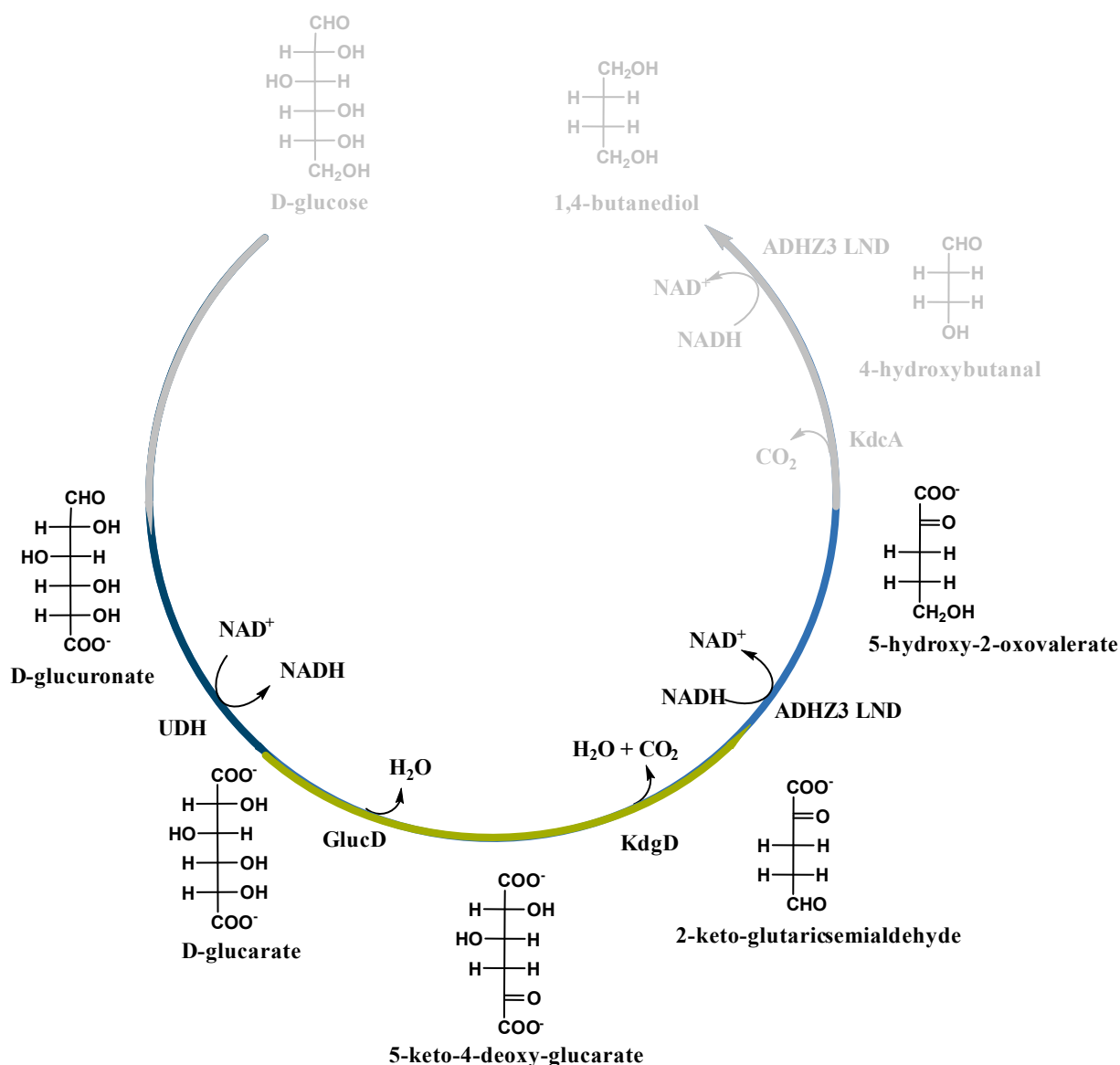


Figure 15: *In vitro* enzymatic cascade reaction for the synthesis of Hov

The cascade reaction from D-glucuronate to 5-hydroxy-2-oxovalerate was comprised of the enzymes uronate dehydrogenase (UDH), glucarate dehydratase (GlucD), 5-keto-4-deoxy-glucarate dehydratase (KdgD), and the triple variant of ADHZ3 with the amino acid substitutions S199L/S200N/N201D (ADHZ3 LND).

D-glucuronate was oxidized poorly by UDH within the enzymatic cascade reaction (Table 11, line 1), while in the single reaction, high activity was observed. Analyzing UDH stability revealed that it exhibits only a low half-life of 50 min at 37 °C (Pick et al., 2015). This led to the decision to engineer UDH to enhance its stability (4.2.2). Meanwhile, it was left out of this cascade reaction, which allowed to converting D-glucurate quantitatively, whereby Hov was detected as the sole product (line 2). At the same time, a pH shift assay had been under development for the screening of KdcA variants for enhanced activity with Hov. This assay required low and defined amounts of buffer. Therefore, the reaction conditions were changed stepwise until it was possible to perform the reaction with cofactor recycling by FDH in an unbuffered solution using a titrator to maintain the pH at 7.2 and to monitor the reaction on-line (lines 2-6). However, activity of KdcA with the Hov preparation was only observed once using an unfinished reaction; after the reaction was complete, judged by the end of the titration, no activity could be detected anymore (line 7). Therefore, it was anticipated that Hov was unstable and stopped further investigations.

Until then, the analysis of this enzymatic cascade reaction was limited to an HPLC/MS method that required derivatization with 4-APEBA (3.6.1.2). The method using anion exchange chromatography, which was applied for the analysis of the enzymatic cascade reaction to α -ketoglutarate (aKG) (3.6.1.3), had not been developed at that time. With the 4-APEBA method, 5-Kdg detection (or derivatization) was too poor for quantification (appendix, Figure 33) and 2-keto-glutaric semialdehyde (Kgsa) had not been available then for analysis. Finally, when the Metrosep method was available for analysis, it could be shown that actually only very little Hov was produced, while Kgsa had accumulated (line 8). In a final experiment, it was possible to convert 10 mM of the intermediate Kgsa to Hov (line 9).

Another interesting target compound that can be synthesized from D-glucuronate is aKG. For this, only ADHZ3 LND needs to be replaced with Kgsa dehydrogenase (KgsalDH) from *Pseudomonas putida* (Aghaie et al., 2008; Koo and Adams, 1974) in the last step. In this cascade reaction, two NAD^+ are consumed and regeneration of the cofactor needs to be accomplished with NOX. This reaction was examined next to gain insights into a setup, which is in part comprised of enzymes of the final cascade reaction and which is also dependent on oxygen like the reaction to BDO.

Table 11: Conditions and results of the enzymatic cascade reaction for the synthesis of Hov.

The enzymes and reaction conditions of various setups are given along with details of the HPLC analysis and activity measurements of branched-chain ketoacid decarboxylase (KdcA) with the corresponding 5-hydroxy-2-oxovalerate (Hov) preparation. Further information on the reaction conditions or other observations are supplied in the comments section.

	Enzymes	Conditions	HPLC analysis method	KdcA	Comment
1	5 µg/mL each corresponding to: 0.23 µM UDH, 0.14 µM GlucD, 0.21 µM KdgD, 0.19 µM ADHZ3 LND	50 mM MOPS pH 6.5 10 mM D-glucuronate 30 °, overnight	<i>4-APEBA</i> Almost no conversion of D-glucuronate; No Hov detected <i>Metrosep</i> -	n.d.	Internal cofactor recycling
2	0.6 mg/mL each corresponding to: 11.7µM GlucD, 17.1 µM KdgD, 15.5 µM ADHZ3 LND	50 mM MOPS, pH 6.5, 10-50 mM D-glucuronate/NADH rt, various time points	<i>4-APEBA</i> Detection of Hov <i>Metrosep</i> -	No	No cofactor recycling; D-glucuronate converted after 5 min in each case.
3	1 µM of each, GlucD, KdgD, and ADHZ3 LND	AbC pH 7.9 20 mM D-glucuronate/NADH; and w/o buffer pH 7.2 20 mM D-glucuronate/NADH rt, overnight	<i>4-APEBA</i> Detection of Hov less D-glucuronate remaining in reaction w/o buffer <i>Metrosep</i> -	n.d.	No cofactor recycling; No pH monitoring
4	1 µM of each, GlucD, KdgD, ADHZ3 LND; 0.025 mg/mL FDH	w/o buffer pH 7.2 40 mM D-glucuronate, 5 mM NADH rt, various time points	<i>4-APEBA</i> Only Hov after 1.5 h; decline of Hov after 47 h <i>Metrosep</i> -	n.d.	No pH monitoring; Cofactor recycling with FDH
5	2 µM of each in 15 mL, GlucD, KdgD, ADHZ3 LND; 0.32 mg/mL FDH	w/o buffer pH 7.2 40 mM D-glucuronate, 5 mM NADH rt, overnight	<i>4-APEBA</i> Only Hov; decline of Hov after lyophilization <i>Metrosep</i> -	n.d.	pH constant at 7.2 (titrator) until 6.7 h, then acidification to pH 7.0
6	2 µM of each in 300 mL GlucD, KdgD, ADHZ3 LND; 0.02 mg/mL FDH	w/o buffer pH 7.2 40 mM D-glucuronate, 5 mM NADH rt, overnight	<i>4-APEBA</i> Only Hov <i>Metrosep</i> -	No	Acidification after 16.5 h;
7	3.9 µM GlucD, 2.9 µM KdgD, 0.8µM mg/mL ADHZ3 LND, 0.2 mg/mL FDH	w/o buffer pH 7.2 100 mM D-glucuronate, 1 mM NADH Rt, various time points	<i>4-APEBA</i> Only Hov <i>Metrosep</i> -	Yes*	Acidification of the reaction after 7.5 h

	Enzymes	Conditions	HPLC analysis method	KdcA	Comment
8	4.7 μ M GlucD, 4.6 μ M KdgD. 1.3 μ M ADHZ3 LND, 0.2 mg/mL FDH	w/o buffer pH 7.2 100 mM D-glucarate, 1 mM NADH Rt, various time points	<i>4-APEBA</i> n.d. <i>Metrosep</i> Detection of Kgsa as main product, of a small peak for Hov, and of an unidentified peak	n.d.	D-glucarate is fully converted, however, Kgsa accumulated.
9	0.6 μ M ADHZ3 LND, 0.2 mg/mL FDH	w/o buffer pH 7.2 10 mM Kgsa, 1 mM NADH Rt, various time points	<i>4-APEBA</i> n.d. <i>Metrosep</i> Detection of Kgsa decline and Hov production over 48 h	n.d.	Full conversion of Kgsa after 48 h

rt: room temperature (20-25 °)

-: was not available at the time of analysis

n.d.: not determined

w/o: without

* KdcA was only active with a sample taken after 3.3 h. The sample could be stored at 4°C and RT without loss of activity. However, KdcA was not active with samples taken after the reaction was stopped after 17.6 h.

4.3.2 *In vitro* metabolic engineering for the production of α -ketoglutarate

Authors: Barbara Beer, André Pick, and Volker Sieber

Producing valuable industrial compounds from renewable resources via fermentation or biocatalysis is an essential element of a more sustainable economy. Understanding existing metabolic pathways and networks helps in manipulating living cells for our purposes. To overcome limitations that are often encountered when using living organisms, such as complex regulation machineries or downstream processing issues, metabolic pathways can also be established *in vitro* with purified enzymes. One major drawback of this approach can be the need to supply cofactors, such as ATP, CoASH or NADH and to balance the redox state. In this publication, a pathway that requires only one cofactor, which can easily be recycled enzymatically, was established. This *in vitro* metabolic pathway is derived from the oxidative conversion of uronic acids that is composed of four enzymes leading to α -ketoglutarate. It only depends on the cofactor NAD^+ , which is recycled by a water-forming NOX. The five enzymes were first investigated individually to define optimal reaction conditions for the cascade reaction: Ammonium bicarbonate buffer pH 7.9 at 25 °C. Then, the kinetic parameters were determined under these conditions and the inhibitory effects of substrate, intermediates, and product were evaluated. The initial concentration of NAD^+ as well as the concentration of NOX were found to be crucial for high product yield. Furthermore, oxygen supplementation lead to a significant acceleration of the overall cascade reaction from 150 h to 5 h. Finally, it was possible to convert 10 g/L D-glucuronate with 92% yield of aKG within 5 h. The maximum productivity of 2.8 g L⁻¹ h⁻¹ is the second highest reported in the biotechnological synthesis of aKG.

The author Barbara Beer designed and conducted the experiments, analyzed the data and wrote the manuscript. André Pick cloned the genes for GlucD and KdgD. André Pick and Volker Sieber contributed to the content and language of the manuscript.

The supplemental information for this publication can be found in the appendix, section 6.7.



Contents lists available at ScienceDirect

Metabolic Engineering

journal homepage: www.elsevier.com/locate/ymbenIn vitro metabolic engineering for the production of α -ketoglutarateBarbara Beer^a, André Pick^a, Volker Sieber^{a,b,*}^a Chair of Chemistry of Biogenic Resources, Technical University of Munich, Schulgasse 16, 94315 Straubing, Germany^b Catalysis Research Center, Technical University of Munich, Ernst-Otto-Fischer-Str. 1, 85748 Garching, Germany

ARTICLE INFO

Keywords:

In vitro reaction
Enzyme cascade reaction
 α -ketoglutarate
Bubble reactor
Systems biocatalysis

ABSTRACT

α -Ketoglutarate (aKG) represents a central intermediate of cell metabolism. It is used for medical treatments and as a chemical building block. Enzymatic cascade reactions have the potential to sustainably synthesize this natural product. Here we report a systems biocatalysis approach for an *in vitro* reaction set-up to produce aKG from glucuronate using the oxidative pathway of uronic acids. Because of two dehydrations, a decarboxylation, and reaction conditions favoring oxidation, the pathway is driven thermodynamically towards complete product formation. The five enzymes (including one for cofactor recycling) were first investigated individually to define optimal reaction conditions for the cascade reaction. Then, the kinetic parameters were determined under these conditions and the inhibitory effects of substrate, intermediates, and product were evaluated. As cofactor supply is critical for the cascade reaction, various set-ups were tested: increasing concentrations of the recycling enzyme, different initial NAD⁺ concentrations, as well as the use of a bubble reactor for faster oxygen diffusion. Finally, we were able to convert 10 g L⁻¹ glucuronate with 92% yield of aKG within 5 h. The maximum productivity of 2.8 g L⁻¹ h⁻¹ is the second highest reported in the biotechnological synthesis of aKG.

1. Introduction

α -Ketoglutaric acid (aKG) is an important intermediate of the tricarboxylic acid cycle and amino acid metabolism. Additionally, aKG plays a central role in nitrogen assimilation and storage. Besides its importance in cell metabolism, it is of particular industrial interest due to its broad range of applications, namely, as a dietary supplement, component of infusion solutions or wound healing compounds, and as a building block for the chemical synthesis of heterocycles (Chernyavskaya et al., 2000; Huang et al., 2006; Stottmeister et al., 2005; Verseck et al., 2009). D-glutamic acid, a pharmaceutical for bowel disorder, can be produced from aKG using D-aminotransferases (Taylor et al., 1998). In addition, it is used together with 5-hydroxymethylfurfural for the production of an agent that protects humans and animals from oxidative stress by increasing the antioxidant capacity (Moser et al., 2007). A potential application in biomedicine was described by Barrett and Yousaf (2008). By thermal polycondensation of aKG and one of the triols, glycerol, 1,2,4-butanetriol, or 1,2,6-hexanetriol, elastomers [poly(triol- α -ketoglutarate)] with a wide range of mechanical and chemical properties were provided, which could potentially be used for tissue engineering or drug delivery. Currently, aKG is chemically synthesized from succinic acid and oxalic acid diethyl esters

with cyanohydrines with a yield of 75% or by hydrolysis of acyl cyanides (Stottmeister et al., 2005). These multi-step synthetic processes have numerous disadvantages, such as the use of hazardous chemicals (e.g., cyanides), generation of toxic waste, presence and disposal of a catalyst containing copper, or low product selectivity due to the formation of various side products such as glycine and other organic acids (Cooper et al., 1983; Evans and Wiselogle, 1945; Stottmeister et al., 2005; Verseck et al., 2009).

Biocatalysis has emerged as an alternative to chemical synthesis due to reduced environmental pollution and the availability of different starting materials. So far, the focus for aKG production has been on fermentation-based techniques. In particular, the yeast *Yarrowia lipolytica* has been studied and metabolically engineered for the production of aKG since the 1960s (Otto et al., 2011; Tsugawa et al., 1969a, 1969b; Tsugawa and Okumura, 1969). Although great progress has been made in recent decades, cultivation conditions to achieve aKG overproduction have to be adjusted very carefully with respect to thiamine and nitrogen concentration, pH, and aeration (Guo et al., 2014; Otto et al., 2011; Yovkova et al., 2014). Nonetheless, by-products, especially pyruvate and other organic acids, hamper the industrial production of aKG using a whole-cell catalyst (Guo et al., 2014; Holz et al., 2011; Otto et al., 2012). These disadvantages of cell-

Abbreviations: AbC, ammonium bicarbonate; aKG, α -ketoglutarate; GlucD, glucuronate dehydratase; Kdg, 5-keto-4-deoxyglucuronate; KdgD, Kdg dehydratase; Kgsa, α -ketoglutaric semialdehyde; KgsalDH, Kgsa dehydrogenase; KP, potassium phosphate; NOX, NADH oxidase; UDH, uronate dehydrogenase

* Corresponding author at: Chair of Chemistry of Biogenic Resources, Technical University of Munich, Schulgasse 16, 94315 Straubing, Germany.

E-mail address: sieber@tum.de (V. Sieber).

<http://dx.doi.org/10.1016/j.ymben.2017.02.011>

Received 30 December 2016; Received in revised form 16 February 2017; Accepted 21 February 2017

Available online 22 February 2017

1096-7176/© 2017 The Authors. Published by Elsevier Inc. on behalf of International Metabolic Engineering Society. This is an open access article under the CC BY license (<http://creativecommons.org/licenses/by/4.0/>).

based synthesis, namely, a large number of metabolic pathways with many options to adjust and alter without knowledge of the consequences for the cell's energetics, metabolic bypasses, or improvement of product formation (Petzold et al., 2015; Zadran and Levine, 2013), are not new. Therefore, many researchers have focused on *in vitro* metabolic pathways, also called "systems biocatalysis" (Fessner, 2015; Guterl et al., 2012; Krutsakorn et al., 2013; Myung et al., 2014; Tessaro et al., 2015; Zhu and Zhang, 2016). Here, the reaction route can be set up according to natural metabolic pathways, but it can also be completely artificial. The simpler the pathway, the more easily it can be adjusted and improved. Therefore, the number of enzymes, mandatory cofactors for enzyme activity, and cofactor balance as well as thermodynamic equilibrium of the reaction have to be considered, when developing an *in vitro* metabolic pathway. During route scouting, the substrate also plays a critical role. It should be readily available, cheaper than the product, and, with the goal of making industrial processes more sustainable, derived from a renewable resource.

Among the vast number of natural metabolic pathways, the oxidative pathway of C₆ uronic acids holds potential for α -ketoglutarate synthesis in an *in vitro*-system. The number of enzymes involved is low (four enzymes), only one cofactor is needed (NAD⁺) and the substrate could be obtained from industrial wastes of renewable resources. The pathway has been identified in various *Pseudomonas* species and *Agrobacterium tumefaciens* (Aghaie et al., 2008; Andberg et al., 2012) and is similar to an alternative utilization of C₅-carbohydrate as identified for xylose, arabinose, and lyxonate (Stephens et al., 2007; Watanabe et al., 2006a, 2006b). C₆ uronic acids such as glucuronate and galacturonate are omnipresent sugar derivatives. They constitute monomeric building blocks of structural polysaccharides such as hemicellulose and pectin (Saha, 2003). They are also present in seaweed macroalgae and microalgae, which are considered as feedstock of third-generation biorefineries (Jung et al., 2013; Lahaye and Robic, 2007). Additionally, they are components of extracellular polymeric substances responsible for microbial biofilm formation (Sutherland, 2001). The pathway toward α KG includes the following steps: First, the uronic acid, namely, glucuronic acid, is oxidized by an NAD⁺-dependent uronate dehydrogenase (UDH) to yield glucarate. The aldaric acid is dehydrated to 5-keto-4-deoxyglucarate (Kdg), which is then converted by Kdg dehydratase, a decarboxylating dehydratase that gives α -ketoglutaric semialdehyde (Kgsa). The final step is another NAD⁺-dependent oxidation by α -ketoglutaric semialdehyde dehydrogenase (KgsalDH). The thermodynamic equilibrium of the reaction strongly favors the product due to the irreversible decarboxylation and the essentially irreversible oxidation of two aldehyde groups to carboxylic acids. To balance the NAD⁺ consumption in an *in vitro* system, an NADH oxidase, preferably a water-forming one, has to be included in the process (Kroutil et al., 2004; Nowak et al., 2015; Ödman et al., 2004). In total, five enzymes, one cofactor, and a catalytic amount of Magnesium-ions are necessary to convert the renewable resource glucuronic acid to the industrially relevant compound α -ketoglutarate.

We investigated whether this pathway can be set up in an *in vitro* system with enzymes from different species. Therefore, the reaction conditions (pH, buffer, and temperature) play a critical role in ensuring high activity of each enzyme as well as sufficient enzyme and cofactor stability. Information on enzyme activity is usually given by their kinetic parameters (v_{\max} and K_m). However, as the Michaelis-Menten model only considers the very start of the reaction, the overall speed of the reaction could be very different from v_{\max} . In addition, substrate and product inhibition as well as pathway intermediates can affect the velocity and completion of the reaction. As the *in vitro* system is defined very precisely and only a small number of enzymes are involved in this pathway, these parameters can be obtained for each biocatalyst rather quickly. In contrast, cell-based approaches lack the ability to define these parameters as the reaction conditions are not defined and the cell's regulatory systems are often unknown. This makes the optimization time-consuming and unpredictable. The *in vitro* reaction

pathway, on the other hand, can be tuned very easily by varying single variables (enzyme concentrations, cofactor concentrations, temperature, etc.) until the bottlenecks of the reaction are eliminated.

2. Materials and methods

2.1. Reagents

Restriction enzymes, alkaline phosphatase, Phusion[®] high-fidelity DNA polymerase, T4 ligase, and Taq polymerase were obtained from New England Biolabs (Frankfurt, Germany). Oligonucleotides were from Thermo Scientific (Germany) or biomers.net GmbH (Germany). DNaseI was obtained from Serva (Heidelberg, Germany). All chemicals were of analytical grade or higher quality and purchased from Sigma-Aldrich, Molekula, or Carl Roth. For protein purification, equipment (including columns) from GE Healthcare was used (Munich, Germany).

2.2. Strains and plasmids

The following strains were used during this work: *Escherichia coli* DH5 α , *E. coli* BL21 (DE3), and *Pseudomonas putida* KT2440. The genomic DNA from *P. putida* KT2440 was isolated from cells of an overnight culture using the protocol of Chen and Kuo (1993).

DNA sequences for the corresponding genes of uronate dehydrogenase (*udh*) from *A. tumefaciens* C58 (protein sequence GenBank[™] DAA06454.1), glucarate dehydratase *glucD* from *Actinobacillus succinogenes* 130Z (protein sequence GenBank[™] ABR75198.1), and 5-keto-4-deoxyglucarate dehydratase (*kdgD*) from *Acinetobacter baylyi* DSM 14961 (protein sequence GenBank[™] ENV53020.1) were synthesized with optimized codon usage for expression in *E. coli* (Life Technologies, Regensburg, Germany). Cloning of *glucD* was performed according to the procedure for *udh* and *kdgD*, which is described elsewhere (Pick et al., 2016, 2015). Briefly, the genes *udh*, *gdh*, and *kdgD* were cloned into pCBRHisN, a pET28a derivative (Guterl et al., 2012). After ligation and transformation, the following plasmids were obtained: pCBRHisN-*udh*-A.t., pCBRHisN-*glucD*-A.s., and pCBRHisN-*kdgD*-A.b. For cloning of the *kgsalDH* gene from *Pseudomonas putida* KT2440 (protein sequence GenBank[™] AAN66880.1), genomic DNA was used as the PCR template. PCR reactions were performed with the following primers: *kgsalDH*Pp F-*NdeI*-*kgsalDH*-P.p – CGACAGCATATGCCTGAGATCCTCGGCCATAA CTTC and R-Stop-*kgsalDH*-P.p. – GACGATCTCGAGTCAGATCGCCCCGT CACTCCACTGACC. The restriction enzyme recognition sites for *NdeI*/*XhoI* are underlined and the start/stop codons are marked in bold. The gene was cloned into pET28a with an N-terminal His-tag, yielding the plasmid pET28a-NHis-*kgsalDH*-P.p. The cloning of the plasmid pET28a-NHis-*nox*-L.p. was performed accordingly using genomic DNA from *Lactobacillus pentosus* as a PCR template. The detailed procedure is described elsewhere (Nowak et al., 2015). Multiplication of the plasmids was performed with *E. coli* DH5 α (Stratagene) in Luria-Bertani medium containing 30 μ g/mL kanamycin.

2.3. Expression and purification of enzymes

Expression of *udh*, *kgsalDH*, and *nox* was performed with *E. coli* BL21(DE3) containing the plasmid of interest in 200 mL of autoinduction medium containing 100 μ g/mL kanamycin (Studier, 2005). The preculture was incubated in 10 mL of LB medium with 30 μ g/mL kanamycin at 37 °C overnight on a rotary shaker (180 rpm). Expression cultures were inoculated with the overnight culture at an OD₆₀₀ of 0.1. Incubation was performed for 3 h at 37 °C followed by incubation for 21 h at 16 °C.

Expression of *glucD* and *kdgD* was performed with *E. coli* BL21(DE3) containing the plasmid of interest in 200 mL of terrific broth medium containing 1 M sorbitol, 5 mM betaine, and 100 μ g/mL kanamycin (Studier, 2005). The preculture was incubated in 10 mL of the same medium at 37 °C overnight on a rotary shaker (180 rpm).

Expression cultures were then inoculated with the overnight culture at an OD_{600} of 0.1. Incubation was performed at 37 °C until cultures reached an OD_{600} of 0.6–0.8. After cooling to 16 °C, expression was induced with 1 mM isopropyl β -D-1-thiogalactopyranoside (IPTG) followed by incubation for 21 h at 16 °C.

The following procedure was the same for all proteins: Cells were harvested by centrifugation and resuspended in 50 mM sodium phosphate buffer (pH 8.0, 20 mM imidazole, 500 mM NaCl, and 10% glycerol). Crude extracts were prepared on ice by ultrasonication (Hielscher Ultrasonics, sonotrode LS24d10): three cycles of 15 min pulsing (0.6 ms, 0.4 ms pause) at 80% amplitude. The insoluble fraction of the lysate was removed by centrifugation (20,000 rpm for 40 min at 4 °C) and the supernatant was then applied to an IMAC affinity resin column (5 mL of HisTrap™ FF) equilibrated with the resuspension buffer using the ÄKTA Purifier-system. The column was washed with 5 column volumes (CV) of resuspension buffer and eluted in a gradient of 10 CV from 0% to 100% elution buffer (50 mM sodium phosphate buffer pH 8.0, 500 mM imidazole, 500 mM NaCl, and 10% glycerol). Aliquots of the eluted fractions were subjected to 12% SDS-Page described by Laemmli (1970). The molecular weight was calculated using the ProtParam tool (Gasteiger E, 2005): 31.21 kDa for UDH, 51.01 kDa for GlucD, 34.79 kDa for KdgD, 57.70 kDa for KgsalDH, and 51.94 kDa for NOX, including the additional amino acids of the N-terminal His₆-tags. The fractions containing the eluted protein were pooled and the protein was desalted using a HiPrep™ 26/10 Desalting column, which was preliminarily equilibrated with 50 mM ammonium bicarbonate (AbC) pH 7.9. Protein concentrations of UDH, GlucD, KdgD, and KgsalDH were determined by UV-spectroscopy (Nanophotometer, Implen) at 280 nm using extinction coefficients (ϵ_{280}) calculated with the ProtParam tool (assuming all cysteines are reduced): UDH = 37,930 M⁻¹ cm⁻¹, GlucD = 64,400 M⁻¹ cm⁻¹, KdgD = 21,890 M⁻¹ cm⁻¹, KgsalDH = 28,420 M⁻¹ cm⁻¹. NOX concentration and FAD content were measured as described elsewhere (Nowak et al., 2015). Aliquots of the proteins were frozen in liquid nitrogen and stored at -80 °C.

2.4. Preparation of Kdg and Kgsa

5-Keto-4-deoxyglucuronate (Kdg) was prepared enzymatically with glucuronate dehydratase. Then, 120 mM D-glucuronate (pH 6.5, titrated with NaOH) was converted by 3.7 units (U) of enzyme in a total volume of 20 mL containing 0.5 mM ammonium bicarbonate from the enzyme preparation supplemented with 5 mM MgCl₂. The reaction took place at room temperature and was stopped after complete conversion of the substrate by ultrafiltration with a VivaSpin column (10 kDa cut-off, GE Healthcare). The flowthrough was stored at -20 °C.

α -Ketoglutaric semialdehyde (Kgsa) was prepared from Kdg using KdgD. Here, 100 mM Kdg was converted with 22 U of enzyme in a total volume of 16.2 mL containing 3.8 mM ammonium bicarbonate from enzyme preparations and 5 mM MgCl₂ from the Kdg preparation. The reaction took place at room temperature and was titrated (Titroline 7750 or Titroline 7000, SI Analytics) with 3.7% HCl to keep the pH at 6.5 (final volume of added HCl was 1.484 mL). Samples were analyzed by HPLC to confirm complete conversion. The enzymes were removed by ultrafiltration with a VivaSpin column (10 K cut-off, GE Healthcare) and the flowthrough was stored at -20 °C.

2.5. Enzyme stability

The thermal stability of the enzymes was measured by differential scanning fluorimetry (DSF), using a real-time PCR detection system (CFX96 Touch, Bio-Rad) and the fluorescent dye SYPRO orange (Invitrogen). In a total volume of 25 μ L, 0.2 mg/mL protein, 50 mM of various buffers, and 5x SYPRO Orange were mixed on ice in a clear 96-well plate. After 5 min at 5 °C, a temperature gradient from 5 to 95 °C with 0.5 °C increments was applied, maintaining each tempera-

ture for 5 s. Protein denaturation was monitored at 560–580 nm (excitation 450–490 nm). The data were analyzed with CFX Manager 3.1 (Bio-Rad) to determine the melting point (T_M), defined as the temperature at which 50% of the protein is denatured.

2.6. Enzyme assays

The general assay procedure for the various enzymes is described first, followed by the detailed reaction conditions according to the parameter under investigation.

2.6.1. UDH activity assay

Uronate dehydrogenase activity was determined photometrically by monitoring the increase of NADH at 340 nm using a Multiskan or Varioskan Photometer (Thermo Scientific). Reactions were performed at 25 °C in triplicate using 96-well microtiter plates.

For the determination of kinetic parameters, reactions contained 50 mM ammonium bicarbonate pH 7.9, 5 mM MgCl₂, and either 0–100 mM D-glucuronate (with 1 mM NAD⁺) or 0–1.2 mM NAD⁺ (with 10 mM D-glucuronate). Reactions were started by the addition of 0.174 μ g of UDH. Calculation of Michaelis-Menten kinetics for the determination of K_m and v_{max} was performed with Sigma-Plot 11.0 (Systat Software).

2.6.2. GlucD activity assay

Glucuronate dehydratase activity was determined with a modified assay of Macgee and Doudoroff (1954). Product formation (5-keto-4-deoxyglucuronate, KdG) was quantified by detection of its semicarbazone in an end-point assay using the Liquid Handling Station (BRAND). The reaction (final volume of 1 mL) was initiated by the addition of 7.3 μ g of purified enzyme and aliquots of 100 μ L were mixed with 100 μ L of 2N HCl every 1.2 min to stop the reaction. After six samples, 100 μ L of 0.1 M semicarbazide hydrochloride (containing 1.5% sodium acetate trihydrate) was added and incubated for 30 min at room temperature before measuring the absorbance at 250 nm in UV-transparent microtiter plates. The extinction coefficient of Kdg-semicarbazone was experimentally determined to be 8900 M⁻¹ cm⁻¹.

pH-dependent reactions contained 50 mM of a mixture of three buffers (16.7 mM potassium acetate, 16.7 mM potassium phosphate, and 16.7 mM glycine), with pH between 5 and 10 (0.5 intervals), supplemented with 5 mM MgCl₂ and 3.5 mM D-glucuronate.

Buffer-dependent reactions were performed using various buffers at pH 8.0 (50 mM each), supplemented with 5 mM MgCl₂ and 3.5 mM D-glucuronate.

For the determination of kinetic parameters, reactions contained 50 mM ammonium bicarbonate pH 7.9, 5 mM MgCl₂, and 0.05–50 mM D-glucuronate. Calculation of Michaelis-Menten kinetics for the determination of K_m and v_{max} was performed with Sigma-Plot 11.0 (Systat Software).

2.6.3. KdgD activity assay

Kdg dehydratase activity was determined in a coupled assay with KgsalDH monitoring the increase of NADPH at 340 nm using a Multiskan or Varioskan Photometer (Thermo Scientific). The reactions were performed at 25 °C in triplicate using 96-well microtiter plates.

For the determination of kinetic parameters, reactions contained 50 mM ammonium bicarbonate, 5 mM MgCl₂, 0.5 mM NADP⁺, 1 U KgsalDH, and 0–10 mM Kdg. Reactions were initiated by the addition of 64 ng of KdgD (final concentration of 0.1 μ M). Calculation of Michaelis-Menten kinetics for the determination of K_m and v_{max} was performed with Sigma-Plot 11.0 (Systat Software).

2.6.4. KgsalDH activity assay

KgsalDH activity was determined photometrically by monitoring the increase of NADH at 340 nm using a Multiskan or Varioskan Photometer (Thermo Scientific). The reactions were performed at 25 °C

in a volume of 200 μL in 96-well microtiter plates in triplicate.

pH-dependent reactions contained 50 mM of a mixture of three buffers (16.7 mM potassium acetate, 16.7 mM potassium phosphate, and 16.6 mM glycine), with pH between 5 and 10 (0.5 intervals), supplemented with 1 mM NAD^+ and 10 mM butanal. Reactions were initiated by the addition of 7 μg of KgsalDH.

Buffer-dependent reactions were performed using various buffers at pH 8.0 (50 mM each), supplemented with 1 mM NAD^+ and 10 mM butanal. Reactions were initiated by the addition of 7 μg of KgsalDH.

For the determination of kinetic parameters, reactions contained 50 mM ammonium bicarbonate pH 7.9, 5 mM MgCl_2 , and either 0–4 mM KGSA (with 4 mM NAD^+) or 0–4 mM NAD^+ (with 2 mM KGSA). Reactions were initiated by the addition of 0.15–0.3 μg of KgsalDH. Calculation of Michaelis-Menten kinetics for the determination of K_m and v_{max} was performed with Sigma-Plot 11.0 (Systat Software).

2.6.5. NOX activity assay

NOX activity was measured photometrically by monitoring the decrease of NADH at 340 nm using a Multiskan or Variokan Photometer (Thermo Scientific). The reactions were performed at 25 $^{\circ}\text{C}$ in a volume of 100 or 200 μL in 96-well microtiter plates in triplicate.

For the determination of kinetic parameters, reactions contained 50 mM ammonium bicarbonate pH 7.9, 5 mM MgCl_2 , and 0–0.24 mM NADH. Reactions were started by the addition of 0.32 μg of NOX. Calculation of Michaelis-Menten kinetics for the determination of K_m and v_{max} was performed with Sigma-Plot 11.0 (Systat Software).

2.7. Inhibition tests

Inhibitory effects of the corresponding products and of the intermediates of the cascade on the single enzymes were tested as follows: 0.4 U/mL of each enzyme was incubated separately in 50 mM AbC pH 7.9, 5 mM MgCl_2 , 10 mM of the corresponding substrate/s, 1 mg/mL bovine serum albumin (simulation of high protein load as in the cascade reaction), and either 0 or 10 mM of one of the following substances: D-glucuronate, D-glucarate, Kdg, Kgsa, aKG, or NADH. All reactions were stopped after 15 min by removal of the enzymes by ultracentrifugation. The samples were diluted and analyzed by HPLC. Product formation in the sample without a potential inhibitor was then compared to the samples with an inhibitor.

2.8. Cascade reactions

Reactions for determination of the necessary concentrations of NAD^+ and NOX were performed in a volume of 1.5 mL. Each mixture contained 50 mM ammonium bicarbonate, 5 mM MgCl_2 , 50 mM sodium D-glucuronate, and 2 U/mL of UDH, GlucD, KdgD, and KgsalDH, respectively. NOX concentrations were varied between 2 and 8 U/mL and NAD^+ concentrations were varied between 1 and 10 mM. Reactions were performed in closed vessels at 25 $^{\circ}\text{C}$ (water bath) with stirring.

Conversions in the small-scale bubble reactor were performed in vessels equipped with a septum. Gaseous, humidified oxygen was supplied through a cannula at 20 mL/min. The reactions took place at 25 $^{\circ}\text{C}$ (water bath) with stirring. In a volume of 5 mL, the mixtures contained 50 mM ammonium bicarbonate, 5 mM MgCl_2 , 50 mM D-glucuronate, 2 U/mL of UDH, GlucD, KgsalDH, and NOX, respectively, 1 U/mL KdgD, and 5 mM NAD^+ . In the experiment with additional NOX supplementation, 2 U/mL NOX was added every 20 min for 1 h.

Samples for HPLC analysis were ultrafiltrated with spin filters (10 kDa MWCO, modified PES; VWR) to remove enzymes and stop the reaction.

2.9. HPLC analysis

D-glucuronate, D-glucarate, 5-keto-4-deoxyglucarate, α -ketoglutaric semialdehyde, and α -ketoglutarate were separated by HPLC, using an Ultimate-3000 HPLC system (Dionex, Idstein, Germany), equipped with an autosampler (WPS 3000f OTRS), a column compartment (TCC3000RS), and a diode array detector (DAD 3000RS). The column Metrosep A Supp10–250/40 column (250 mm, particle size 4.6 mm; Metrohm, Filderstadt, Germany) at 65 $^{\circ}\text{C}$ was used for separation by isocratic elution with 30 mM ammonium bicarbonate (pH 10.4) as a mobile phase at 0.2 mL/min. Samples were diluted in water, filtered (10 kDa MWCO, modified PES; VWR, Darmstadt, Germany), and 10 μL of them were applied on the column. Data were analyzed with Dionex Chromeleon software.

3. Results

3.1. Overview of the pathway

The oxidative pathway from D-glucuronate (glucuronate) to aKG consists of four enzymes. A fifth enzyme is required for cofactor regeneration (Fig. 1).

The first step is the conversion of glucuronate to D-glucarate (glucarate) by uronate dehydrogenase from *Agrobacterium tumefaciens* (UDH). The enzyme has been described as a galacturonate and glucuronate dehydrogenase, but also shows activity towards mannuronate. NAD^+ is strongly preferred over NADP^+ , with more than 1000-fold greater activity (Pick et al., 2015).

The following dehydration is catalyzed by glucarate dehydratase from *Actinobacillus succinogenes* (GlucD). As it has not been described in the literature yet, we included Supplementary Information on all performed experiments (Figs. S2, S4C, and Table S1).

The second dehydratase is Kdg dehydratase from *Acinetobacter baylyi* (KdgD). It has been described by Aghaie et al. (2008) and also performs the decarboxylation, yielding the intermediate α -ketoglutaric semialdehyde (Kgsa). Both dehydratases are Mg^{2+} -dependent.

The final reaction is catalyzed by Kgsa dehydrogenase from *Pseudomonas putida* DSM 50,198 (KgsalDH). KgsalDH utilizes both NAD^+ and NADP^+ with a preference for NADP^+ (Koo 1974).

NAD^+ regeneration is achieved with an NADH oxidase from *Lactobacillus pentosus* (NOX). It has been described by our group to be a water-forming, FAD-dependent oxidase (Nowak et al., 2015).

All enzymes were produced heterologously in *E. coli* with an N-terminal His-tag for easy purification by affinity chromatography.

The single reactions of the pathway add up to a Δ_rG° of -1073.2 ± 30.4 kJ/mol (Table 1) caused by the nature of the reactions. Although this value cannot account for the true thermodynamics during the cascade reaction, the flux through the pathway is driven by (1) the irreversible reduction of oxygen, (2) the irreversible decarboxylation step, (3) the removal of the reaction product NADH by NOX, and (4) the virtually irreversible oxidation of aldehyde groups to carboxylic acids.

3.2. Definition of reaction conditions

As the reaction cascade should take place in a single reaction vessel, the buffer, pH, temperature, and cofactors have to be chosen carefully. Since both dehydratases are Mg^{2+} -dependent, 5 mM MgCl_2 was added to all activity assays (also if no dehydratase but dehydrogenase or oxidase activity was measured). As both dehydrogenases can utilize NAD^+ , no other cofactors were necessary. Further, the activity profile for each enzyme (except KdgD due to the enzyme assay) was determined with respect to pH and buffer salt (Table 2).

The best buffer for the enzymes to work in concert is potassium phosphate (KP) buffer at pH 8. However, since the cofactor NADH is prone to degradation in phosphate buffers (Rover et al., 1998), we used

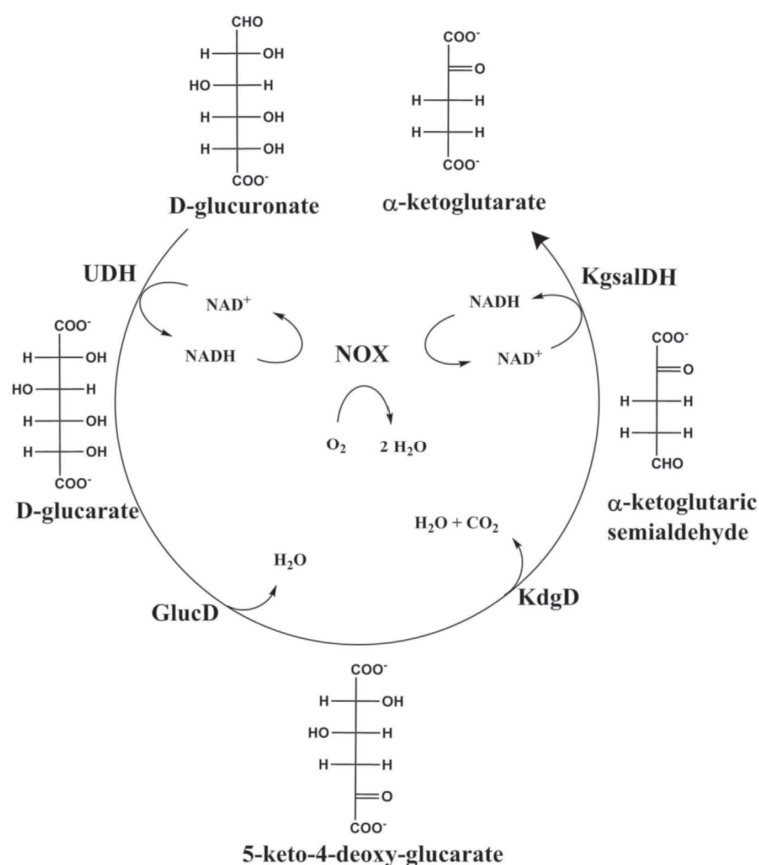


Fig. 1. *In vitro* oxidative pathway for the synthesis of α -ketoglutarate. The first enzyme of the *in vitro* oxidative pathway is uronate dehydrogenase (UDH). It oxidizes glucuronate to give glucarate, which is then dehydrated twice by glucarate dehydratase (GlucD) and 5-keto-4-deoxyglucarate dehydratase (KdgD). KdgD also performs a decarboxylation, which yields the intermediate α -ketoglutaric semialdehyde. In the final step, an aldehyde dehydrogenase (KgsalDH) produces α -ketoglutarate. Both the first and the last enzymes are NAD^+ -dependent. Therefore, a water-forming NADH oxidase is included to recycle the cofactor.

Table 1
: $\Delta_r G'^{\circ}$ values.

$\Delta_r G'^{\circ}$ is the change in Gibbs free energy due to a chemical reaction at pH 8.0 and ionic strength of 0.2 M. The values for the reactions indicated in Fig. 1 were calculated using eQuilibrator (Fiamholz et al., 2012). The reaction of NOX takes place twice, therefore it is included two times, indicated as recycling 1 and 2.

	$\Delta_r G'^{\circ}$ [kJ/mol]
UDH	-41.2 ± 4.6
GlucD	-42.0 ± 2.4
KdgD	-47.0 ± 6.4
KgsalDH	-48.4 ± 4.0
NOX (Recycling 1)	-447.3 ± 6.5
NOX (Recycling 2)	-447.3 ± 6.5
overall	-1073.2 ± 30.4

ammonium bicarbonate (AbC), which was the only other buffer tested, where we could detect any KgsalDH activity at all (30% compared to activity in KP). NADH degradation did not take place at 25 °C over a period of one week in 50 mM AbC pH 7.9 (Fig. S1A).

Since temperature plays a critical role in catalysis, but also in enzyme stability, we analyzed the thermal stability of all enzymes by thermal unfolding (Fig. S3). UDH, GlucD, KdgD, KgsalDH, and NOX have melting temperatures of 52.5, 57.0, 71.0, 51.5, and 40 °C,

Table 2
Activity profile for each enzyme with respect to pH and buffer.

Each enzyme was tested at pH values from 5 to 10. Buffers tested included potassium phosphate (KP), ammonium bicarbonate (AbC), tris-hydroxymethyl-aminomethane (Tris), and 2-[4-(2-hydroxyethyl)piperazin-1-yl]ethanesulfonic acid (HEPES) at pH 8.0.

	pH optimum % activity at	Buffer pH 8.0, activity [%]
UDH	optimum: 8.0 ^a	KP: 100 ^a AbC: 58
GlucD	optimum 7.0 pH 8.0: 94%	KP: 100 AbC: 80
KdgD	n.d.	n.d.
KgsalDH	optimum: pH 10 pH 8: 50%	KP: 100 AbC: 31
NOX	optimum: 7.0 ^b pH 8.0: 80%	KP: 100 AbC: 57

^a Pick et al., (2015).

^b Nowak et al., (2015).

respectively. Because of the rather low thermal stability of NOX, the temperature for the enzyme cascade was set to 25 °C.

3.3. Kinetic characterization

The kinetic behaviors of all five enzymes were characterized at the

Table 3
Kinetic parameters in 50 mM AbC pH 7.9 at 25 °C.

	Substrate/ comment	K_m [mM]	V_{max} [U/mg]	k_{cat}/K_m [mM ⁻¹ s ⁻¹]
UDH	Glucuronate	0.50 ± 0.01	193.9 ± 1.2	201.7 ± 6.5
	NAD ⁺	0.09 ± 0.01	220.8 ± 4.1	1276.1 ± 123.0
GlucD		0.29 ± 0.05	8.7 ± 0.5	24.7 ± 5.4
KdgD		0.47 ± 0.03	5.1 ± 0.1	6.3 ± 0.5
KgsalDH	Kgsa	0.10 ± 0.01	33.0 ± 0.7	317.4 ± 38.5
	NAD ⁺	0.71 ± 0.10	42.6 ± 2.3	57.7 ± 11.2
NOX	Before activation	0.03 ± 0.00	5.1 ± 0.1	151.9 ± 10.0
	After activation	0.06 ± 0.01	47.0 ± 3.4	739.1 ± 200.9

defined reaction conditions: 50 mM AbC pH 7.9 supplemented with 5 mM MgCl₂ at 25 °C. All kinetics followed the Michaelis-Menten model and no substrate inhibition could be observed within the range of tested concentrations (Table 3 and Fig. S4).

UDH exhibits the highest activity (~200 U/mg) with a moderately low K_m for glucuronate (0.5 mM) and a very high affinity for NAD⁺ ($K_m=0.09$ mM). In contrast, KgsalDH has a rather low affinity for NAD⁺ with a K_m of 0.71 mM. KdgD has only a K_m of 0.5 mM and v_{max} of 5.1 U/mg, making this enzyme the one with the lowest catalytic efficiency (6.3 mM⁻¹ s⁻¹). The second dehydratase GlucD is just slightly more efficient, with 24.7 mM⁻¹ s⁻¹. The NADH recycling enzyme NOX has moderate activity with 5.1 U/mg, after production in *E. coli* and purification by affinity chromatography, but it could be activated by FAD (Nowak et al., 2015). The fully loaded enzyme exhibits a v_{max} of 47.0 U/mg.

3.4. Test of inhibition by products or intermediates

In addition to product inhibition, the effect of the different intermediates was investigated, as product inhibition or regulation could occur (Liu et al., 2013; Ödman et al., 2004). Inhibitory effects of 10 mM glucuronate, glucarate, Kdg, Kgsa, aKG, and NADH, respectively, were tested by comparing the initial reaction rates in the presence of these compounds to the reaction rates without them. Generally, only small effects on the activity were observed. Negative effects (relative initial rate of conversion of 80% or less) were only seen for UDH and KdgD in the presence of 10 mM NADH, for KdgD in the presence of 10 mM aKG, and for NOX in the presence of 10 mM glucarate (Fig. 2). In the cascade reaction, high concentrations of NADH should therefore be avoided by using only low amounts of NAD⁺ to avoid the possible inhibition of UDH and KdgD. Lower activity of

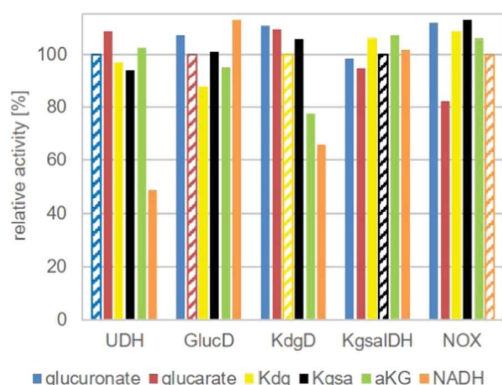


Fig. 2. Inhibitory effects of the intermediates. The relative activities of UDH, GlucD, KdgD, KgsalDH, and NOX were tested without inhibitors (dashed bars) and in the presence of 10 mM glucuronate (blue), glucarate (red), Kdg (yellow), Kgsa (black), aKG (green), or NADH (orange). (For interpretation of the references to color in this figure legend, the reader is referred to the web version of this article.)

KdgD is expected towards the end of the reaction, when high concentrations of aKG are reached.

3.5. Set-up of full cascade

3.5.1. Optimizing concentrations of NOX and NAD⁺

To establish the full cascade reaction, all enzymes were combined with an activity of 2 U/mL each. This corresponds to a total enzyme load of 1 mg/mL and, in theory, the reaction should be finished in 0.5 h given a substrate concentration of 50 mM (1 mM NAD⁺ was used). However, hardly any product formation (5%) could be observed. The conversion of glucuronate was only 20%, which made us wonder whether regeneration of the oxidized cofactor could be limiting. We therefore increased the amount of NOX to 4 and 8 U/mL. Using 4 U/mL NOX already gave 35% conversion with 20% product yield and quadrupling the amount of NOX to 8 U/mL resulted in full conversion of glucuronate within 50 h and a yield of 76% of aKG (33.6 mM) (Fig. 3A). As increasing the cofactor regenerating enzyme had such a major effect on conversion and yield, we thought that increasing the cofactor concentration itself could also have a significant influence. We therefore doubled the initial amount of NAD⁺ to 2 mM (keeping NOX at 2 U/mL) and also obtained full conversion with a yield of aKG of 75% (37.5 mM) within 145 h. When we tested set-ups with even higher initial amounts of NAD⁺ (5 or 10 mM), no further improvement could be observed (Fig. 3B). In all of these reaction set-ups, glucarate accumulated temporarily up to 15–20 mM, Kdg was never above the detection limit, and Kgsa was only seen in small amounts (< 5 mM) (Fig. S5).

3.5.2. Oxygen supplementation with bubble reactor

Since NOX is an oxygen-dependent enzyme, oxygen diffusion from the air into the reaction solution can be a limiting factor. Consequently, we constructed a small-scale bubble reactor, where oxygen was supplied in gaseous form at 20 mL/min. With this, the oxidation of NADH by NOX could be accelerated 27 times (Fig. 4).

Next, the entire cascade reaction was performed in the bubble reactor (Fig. 5A). Here, the reaction rate of UDH in the first 30 min was 51.4 mM/h, instead of 0.5–1 mM/h without oxygen supply. However, after half an hour, all NAD⁺-dependent reactions stagnated, leading to the accumulation of Kgsa. Adding new NOX (2 U/mL) resulted in a restart of the cascade, although again after 30 min no further conversions could be observed. In total, 25% glucuronate was left with a yield of aKG of 52% and 16% glucarate accumulation.

To optimize the yield and avoid the accumulation of intermediates, a new experiment was performed in which NOX was added at a time interval of 20 min over a period of 1 h (Fig. 5B). In approximately 30 min, glucuronate was fully converted to glucarate with a reaction rate of 98.4 mM/h. Overall, 46 ± 5 mM aKG (92 ± 8%) was obtained after 5 h (reaction rate of complete cascade: 9 mM/h, and an initial rate of 20 mM in the first hour). The rate-limiting step of the cascade reaction was glucarate dehydratase, with an observed deactivation rate of 0.03 min⁻¹ (for the calculations, see Figure S6). In order to exclude the possibility that NADH is degraded in the bubble reactor, we test its stability over a period of 5 h (according to the duration of the cascade reaction). However, no degradation was observed (Figure S1B).

4. Discussion

We demonstrate a short *in vitro* metabolic pathway for the production of α -ketoglutarate from glucuronate, a major constituent of renewable resources. The oxidative pathway of uronic acids is highly suitable for this purpose as it involves only a small number of enzymes compared with cell-based approaches that utilize *n*-paraffins, ethanol, or glycerol as feedstock. As every reaction of the oxidative pathway is driven thermodynamically toward aKG with a ΔG° of -1073.2 kJ/mol, high yields of aKG were possible (> 90%). In contrast, the *in vitro*

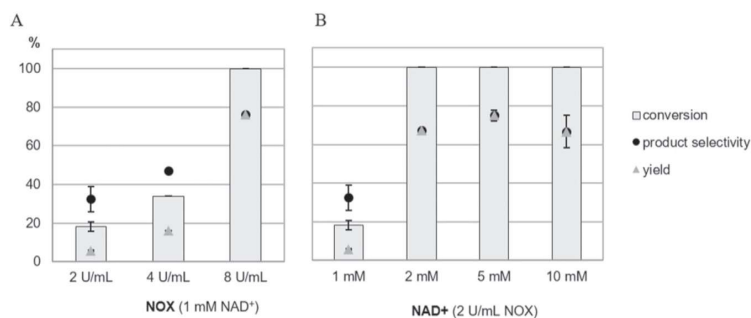


Fig. 3. Optimization of NOX and NAD⁺ concentrations. Conversion of glucuronate (gray bars), product selectivity (black circles), and yield of aKG (gray triangles) (A) at different NOX concentrations with an initial NAD⁺ concentration of 1 mM, and (B) at different NAD⁺ concentrations at an initial NOX concentration of 2 U/mL. The values were taken after 150 h reaction time. The corresponding time courses are included in the Supplemental Information (Fig. S5).

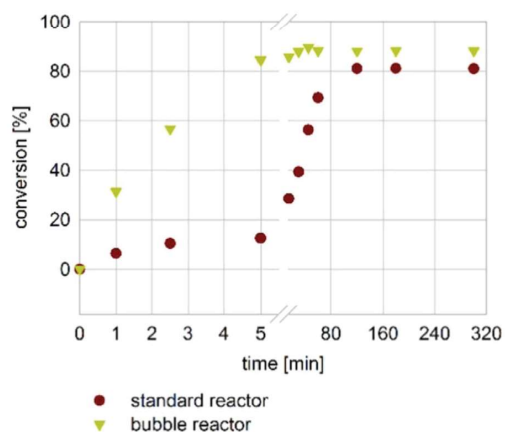


Fig. 4. NOX reaction in a standard reactor and in a bubble reactor. It was found that 10 U NOX could convert 24- to 27 μmol NADH in both reactors. In the bubble reactor, the reaction was already complete after 5 min (reaction rate of 5.4 $\mu\text{mol}/\text{min}$), whereas in the standard reactor, it took 120 min (reaction rate of 0.2 $\mu\text{mol}/\text{min}$). This corresponds to a 27-fold enhancement.

route from glutamate to α -ketoglutarate using glutamate dehydrogenase (GluDH) has a reaction equilibrium with a positive $\Delta G'^{\circ}$ of +31.0 kJ/mol (Flamholz et al., 2012). Two groups investigated this route for *in vitro* aKG production. Only low concentrations of glutamate (5 mM) could be fully converted to aKG, whereas higher concentrations (25 or 50 mM) only reached 25% or < 50% conversion, respectively (Greschner et al., 2014; Ödman et al., 2004). This was also due to product inhibition, which was a major obstacle observed with GluDHs as well as with the alternative deamination route using an L-amino acid deaminase (Liu et al., 2013). The enzymes of our oxidative pathway were mainly impaired by high concentrations of NADH, especially UDH and Kgd. Therefore, a low initial concentration of NAD⁺ and efficient recycling of NADH are important. Furthermore, NOX was inhibited by 10 mM glucarate (20% loss of activity). As glucarate accumulated during the reaction of glucuronate to aKG, NOX was probably not fully active. However, with glucarate concentrations as high as 27 mM, 4 U/mL NOX could still supply 55 mM NAD⁺ within 30 min for the reactions of UDH and KgsalDH (when added stepwise and supplemented with oxygen). Overall, the productivity of 19.3 mM/h (2.8 g L⁻¹ h⁻¹) was remarkably higher than that reached in the glutamate route reported by Ödman et al. (2004), with 1.0 g L⁻¹ d⁻¹. In addition, cell-based processes using the yeast *Yarrowia lipolytica* only

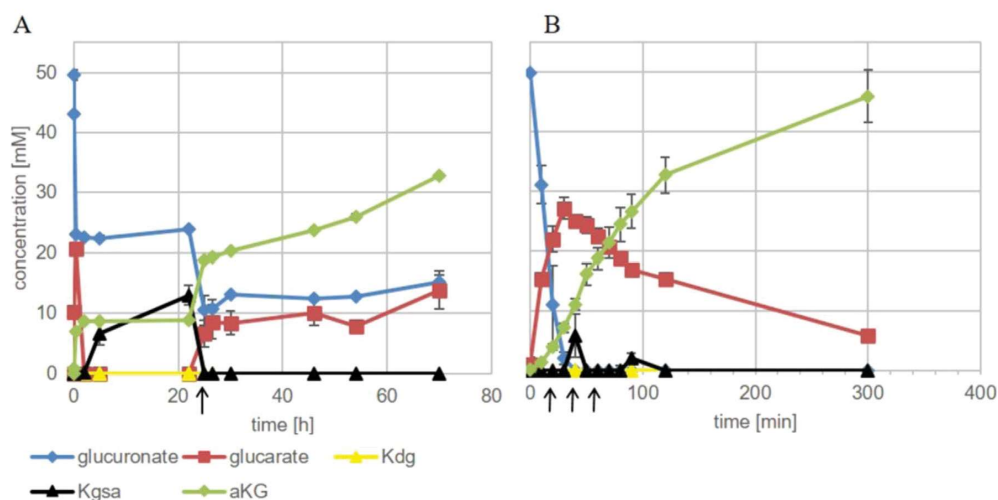


Fig. 5. Cascade reaction in the bubble reactor. (A) Use of the bubble reactor led to great acceleration of the cascade. UDH could convert approximately 50% of glucuronate in the first 20 min. However, all NAD⁺-dependent reactions stopped after 20 min, leading to an accumulation of Kgsa. Addition of a fresh aliquot of NOX after 24 h reactivated the cascade reaction for another 20 min. At this time, glucarate was hardly converted anymore. (B) Cascade reaction in the bubble reactor with multiple NOX additions (arrows) in the first hour. As NOX stability seemed to be very low in the bubble reactor, it was added repeatedly. This procedure led to full conversion of glucuronate in 30 min and a yield of aKG of almost 100% within 5 h. The rate-limiting step of the cascade reaction is GlucD, which seems to be inactivated with an observed deactivation rate of 0.04 min⁻¹.

reached productivities up to $1.75 \text{ g L}^{-1} \text{ h}^{-1}$ (Yovkova et al., 2014). Significantly higher values were only reached with the enzymatic production from L-glutamate using glutamate oxidase (Niu et al., 2014). Here, a productivity of $4.3 \text{ g L}^{-1} \text{ h}^{-1}$ was reported, with an initial productivity of $8.6 \text{ g L}^{-1} \text{ h}^{-1}$.

To reduce the enzyme load of the cascade reaction and to create an efficient process, the inhibition of NOX has to be avoided by reducing glucarate accumulation and finding the lowest NOX concentration necessary to ensure NAD^+ supply for both oxidation reactions.

As we were able to accelerate the cascade reaction from 150 h to 5 h by aeration and adding NOX at 20 min time intervals in the beginning of the reaction, degradation of NADH might not be as critical any more. Therefore, the cascade reaction could also be conducted in potassium phosphate instead of ammonium bicarbonate. This would decrease the enzyme load, as all enzymes of the cascade reaction have higher activities in potassium phosphate than in ammonium bicarbonate buffer. However, having the potential application of this cascade in a process in mind, ammonium bicarbonate might still be the better choice as it is a volatile buffer, which simplifies downstream processes and product purification. All of the above-mentioned factors (cofactor stability, enzyme load, and downstream processes) play a critical role in commercial processes and have to be evaluated carefully (Faber et al., 2015). Since this is an *in vitro* cascade reaction, a change of the reaction conditions is easy, predictable, and not as time-consuming as for cell-based reactions. Even though the cell-based production of aKG is already very successful, with high titers around 190 g/l ($=1.3 \text{ M}$) (Otto et al., 2011; Yovkova et al., 2014), we believe that this *n* route is highly promising for the production of aKG. Its major advantages compared with cell-based routes are the high purity of the product (no by-products such as pyruvate or other organic acids) and the fast optimization possibilities (no need to consider culture conditions or regulatory cell mechanisms, etc.). Important improvements include the reduction of enzyme load, which is still a cost driver when working with purified enzymes. However, prices are already decreasing as reported by Zhang et al. (2016) with $\$50\text{--}500/\text{kg}$. As GlucD seems to be the bottleneck of the cascade reaction, further experiments with the isolated enzyme should elucidate the low activity within the cascade. For instance, stability might be an issue, especially at oxygen saturation in the bubble reactor. NOX stability should also be addressed, as it has already been shown to have a rather low half-life of 3 h in KP pH 7.0 at 37°C (Nowak et al., 2015). Possible ways to address stability issues include lowering the reaction temperature, engineering the enzymes, or identifying more stable natural variants and most importantly enzyme immobilization. In addition, mathematical modeling can provide valuable information about how the cascade reaction could be optimized (Banta et al., 2002; Hold et al., 2016; Palacio et al., 2016; Zhong et al., 2017).

Conflict of interest statement

The authors declare that the research was conducted in the absence of any commercial or financial relationships that could be construed as a potential conflict of interest.

Funding

Barbara Beer was funded by the Bavarian State Ministry of the Environment and Consumer Protection (grant number TGC01GCU – 60345).

Further funding was provided by the Technical University of Munich within the funding program Open Access Publishing and by the COST action CM1303 Systems Biocatalysis.

Acknowledgments

We would like to thank Petra Lommes for performing experiments

with the bubble reactor, Manuel Döring for reproducing NADH stability tests, and Claudia Nowak for proofreading the manuscript.

Appendix A. Supplementary material

Supplementary data associated with this article can be found in the online version at doi:10.1016/j.ymben.2017.02.011.

References

- Aghaie, A., Lechaplais, C., Sirven, P., Tricot, S., Besnard-Gonnet, M., Muselet, D., de Berardinis, V., Kreimeyer, A., Gyapay, G., Salanoubat, M., Perret, A., 2008. New insights into the alternative D-glucarate degradation pathway. *J. Biol. Chem.* 283, 15638–15646.
- Andberg, M., Maaheimo, H., Boer, H., Penttilä, M., Koivula, A., Richard, P., 2012. Characterization of a novel *Agrobacterium tumefaciens* galactarolactone cycloisomerase enzyme for direct conversion of D-galactarolactone to 3-deoxy-2-keto-L-threo-hexarate. *J. Biol. Chem.* 287, 17662–17671.
- Banta, S., Boston, M., Jarnagin, A., Anderson, S., 2002. Mathematical modeling of *in vitro* enzymatic production of 2-keto-L-gulonic acid using NAD(H) or NADP(H) as cofactors. *Metab. Eng.* 4, 273–284.
- Barrett, D.G., Yousaf, M.N., 2008. Poly(triol α -ketoglutarate) as biodegradable, chemoselective, and mechanically tunable elastomers. *Macromolecules* 41, 6347–6352.
- Chen, W.-p., Kuo, T.-t., 1993. A simple and rapid method for the preparation of gram-negative bacterial genomic DNA. *Nucleic Acids Res.* 21, 1.
- Chernyavskaya, O.G., Shishkanova, N.V., Il'chenko, A.P., Finogenova, T.V., 2000. Synthesis of alpha-ketoglutaric acid by *Yarrowia lipolytica* yeast grown on ethanol. *Appl. Microbiol. Biotechnol.* 53, 152–158.
- Cooper, A.J.L., Ginos, J.Z., Meister, A., 1983. Synthesis and properties of the alpha-keto acids. *Chem. Rev.* 83, 321–358.
- Evans, R.C., Wiselogle, F.Y., 1945. Studies in the pyridazine series. The absorption spectrum of pyridazine. *J. Am. Chem. Soc.* 67, 60–62.
- Faber, K., Fessner, W.-D., Turner, N., 2015. Science of Synthesis: Biocatalysis in Organic Synthesis. Thieme, Stuttgart.
- Fessner, W.D., 2015. Systems biocatalysis: development and engineering of cell-free "artificial metabolisms" for preparative multi-enzymatic synthesis. *Nat. Biotechnol.* 32, 658–664.
- Flamholz, A., Noor, E., Bar-Even, A., Milo, R., 2012. EQuilibrator—the biochemical thermodynamics calculator. *Nucleic Acids Res.* 40, D770–D775.
- Gasteiger E, H.C., Gattiker, A., Duvaud, S., Wilkins, M.R., Appel, R.D., Bairoch, A., 2005. Protein identification and analysis tools on the ExpASY server. *The Proteomics Protocols Handbook*. Humana Press, 571–607.
- Greschner, W., Lanzerath, C., Reiß, T., Tenbrink, K., Borchert, S., Mix, A., Hummel, W., Gröger, H., 2014. Artificial cofactor regeneration with an iron(III)porphyrin as NADH-oxidase mimic in the enzymatic oxidation of L-glutamate to α -ketoglutarate. *J. Mol. Catal. B: Enzym.* 103, 10–15.
- Guo, H., Madzak, C., Du, G., Zhou, J., Chen, J., 2014. Effects of pyruvate dehydrogenase subunits overexpression on the alpha-ketoglutarate production in *Yarrowia lipolytica* WSH-Z06. *Appl. Microbiol. Biotechnol.* 98, 7003–7012.
- Guterl, J.K., Garbe, D., Carsten, J., Steffler, F., Sommer, B., Reisse, S., Philipp, A., Haack, M., Ruhmann, B., Koltermann, A., Kettling, U., Bruck, T., Sieber, V., 2012. Cell-free metabolic engineering: production of chemicals by minimized reaction cascades. *ChemSusChem* 5, 2165–2172.
- Hold, C., Billerbeck, S., Panke, S., 2016. Forward design of a complex enzyme cascade reaction. *Nat. Commun.* 7, 12971.
- Holz, M., Otto, C., Kretzschmar, A., Yovkova, V., Aurich, A., Potter, M., Marx, A., Barth, G., 2011. Overexpression of alpha-ketoglutarate dehydrogenase in *Yarrowia lipolytica* and its effect on production of organic acids. *Appl. Microbiol. Biotechnol.* 89, 1519–1526.
- Huang, H.J., Liu, L.M., Li, Y., Du, G.C., Chen, J., 2006. Redirecting carbon flux in *Torulopsis glabrata* from pyruvate to alpha-ketoglutaric acid by changing metabolic co-factors. *Biotechnol. Lett.* 28, 95–98.
- Jung, K.A., Lim, S.R., Kim, Y., Park, J.M., 2013. Potentials of macroalgae as feedstocks for biorefinery. *Bioresour. Technol.* 135, 182–190.
- Kroutil, W., Mang, H., Edegger, K., Faber, K., 2004. Recent advances in the biocatalytic reduction of ketones and oxidation of sec-alcohols. *Curr. Opin. Chem. Biol.* 8, 120–126.
- Krutsakorn, B., Honda, K., Ye, X., Imagawa, T., Bei, X., Okano, K., Ohtake, H., 2013. *In vitro* production of n-butanol from glucose. *Metab. Eng.* 20, 84–91.
- Laemmli, U.K., 1970. Cleavage of structural proteins during the assembly of the head of bacteriophage T4. *Nature* 227, 680–685.
- Lahaye, M., Robic, A., 2007. Structure and functional properties of ulvan, a polysaccharide from green seaweeds. *Biomacromolecules* 8, 1765–1774.
- Liu, L., Hossain, G.S., Shin, H.-d., Li, J., Du, G., Chen, J., 2013. One-step production of α -ketoglutaric acid from glutamic acid with an engineered L-amino acid deaminase from *Proteus mirabilis*. *J. Biotechnol.* 164, 97–104.
- Magee, J., Doudoroff, M., 1954. A new phosphorylated intermediate in glucose oxidation. *J. Biol. Chem.* 210, 617–626.
- Moser, P. M., Greilberger, J., Maier, A., Juan, H., Bücherl-Harrer, C., Kager, E., 2007. Verwendung von Alpha-Ketoglutarat und 5-Hydroxy-methylfurfural zur Reduktion von oxidativem Stress. C.Y.L. Pharmazeutika GmbH.
- Myung, S., Rollin, J., You, C., Sun, F., Chandrayan, S., Adams, M.W.W., Zhang, Y.H.P.,

2014. *In vitro* metabolic engineering of hydrogen production at theoretical yield from sucrose. *Metab. Eng.* 24, 70–77.
- Niu, P., Dong, X., Wang, Y., Liu, L., 2014. Enzymatic production of α -ketoglutaric acid from L-glutamic acid via L-glutamate oxidase. *J. Biotechnol.* 179, 56–62.
- Nowak, C., Beer, B.C., Pick, A., Roth, T., Lommers, P., Sieber, V., 2015. A water-forming NADH oxidase from *Lactobacillus pentosus* and its potential application in the regeneration of synthetic biomimetic cofactors. *Front. Microbiol.* 6, 957.
- Ödman, P., Wellborn, W.B., Bommarius, A.S., 2004. An enzymatic process to α -ketoglutarate from l-glutamate: the coupled system l-glutamate dehydrogenase/NADH oxidase. *Tetrahedron: Asymmetry*. 15, 2933–2937.
- Otto, C., Yovkova, V., Aurich, A., Mauersberger, S., Barth, G., 2012. Variation of the by-product spectrum during alpha-ketoglutaric acid production from raw glycerol by overexpression of fumarase and pyruvate carboxylase genes in *Yarrowia lipolytica*. *Appl. Microbiol. Biotechnol.* 95, 905–917.
- Otto, C., Yovkova, V., Barth, G., 2011. Overproduction and secretion of alpha-ketoglutaric acid by microorganisms. *Appl. Microbiol. Biotechnol.* 92, 689–695.
- Palacio, C.M., Crismaru, C.G., Bartsch, S., Navickas, V., Ditrich, K., Breuer, M., Abu, R., Woodley, J.M., Baldenius, K., Wu, B., Janssen, D.B., 2016. Enzymatic network for production of ether amines from alcohols. *Biotechnol. Bioeng.* 113, 1853–1861.
- Petzold, C., Chan, L.J., Nhan, M., Adams, P., 2015. Analytics for metabolic engineering. *Front. Bioeng. Biotechnol.* 3, 135.
- Pick, A., Beer, B., Hemmi, R., Momma, R., Schmid, J., Miyamoto, K., Sieber, V., 2016. Identification and characterization of two new 5-keto-4-deoxy-D-glucarate dehydratases/decarboxylases. *BMC Biotechnol.* 16, 80.
- Pick, A., Schmid, J., Sieber, V., 2015. Characterization of uronate dehydrogenases catalysing the initial step in an oxidative pathway. *Microb. Biotechnol.* 8, 633–643.
- Rover, L., Jr, Fernandes, J.C.B., Neto, G. d.O., Kubota, L.T., Katekawa, E., Serrano, S. L.H.P., 1998. Study of NADH stability using ultraviolet-visible spectrophotometric analysis and factorial design. *Anal. Biochem.* 260, 50–55.
- Saha, B.C., 2003. Hemicellulose bioconversion. *J. Ind. Microbiol. Biotechnol.* 30, 279–291.
- Stephens, C., Christen, B., Fuchs, T., Sundaram, V., Watanabe, K., Jenal, U., 2007. Genetic analysis of a novel pathway for D-xylose metabolism in caulobacter crescentus. *J. Bacteriol.* 189, 2181–2185.
- Stottmeister, U., Aurich, A., Wilde, H., Andersch, J., Schmidt, S., Sicker, D., 2005. White biotechnology for green chemistry: fermentative 2-oxocarboxylic acids as novel building blocks for subsequent chemical syntheses. *J. Ind. Microbiol. Biotechnol.* 32, 651–664.
- Studier, F.W., 2005. Protein production by auto-induction in high-density shaking cultures. *Protein Expr. Purif.* 41, 207–234.
- Sutherland, I., 2001. Biofilm exopolysaccharides: a strong and sticky framework. *Microbiology* 147, 3–9.
- Taylor, P.P., Pantaleone, D.P., Senkpeil, R.F., Fotheringham, I.G., 1998. Novel biosynthetic approaches to the production of unnatural amino acids using transaminases. *Trends Biotechnol.* 16, 412–418.
- Tessaro, D., Pollegioni, L., Piubelli, L., D'Arrigo, P., Servi, S., 2015. Systems Biocatalysis: an artificial metabolism for interconversion of functional groups. *ACS Catal.* 5, 1604–1608.
- Tsugawa, R., Nakase, T., Kobayashi, T., Yamashita, K., Okumura, S., 1969a. Fermentation of n-paraffins by yeas. *Agric. Biol. Chem.* 33, 158–167.
- Tsugawa, R., Nakase, T., Kobayashi, T., Yamashita, K., Okumura, S., 1969b. Fermentation of n-paraffins by yeast. *Agric. Biol. Chem.* 33, 929–938.
- Tsugawa, R., Okumura, S., 1969. Fermentation of n-paraffins by yeast. *Agric. Biol. Chem.* 33, 676–682.
- Verseck, S., Karau, A., Weber, M., 2009. Fermentative Herstellung von alpha-Ketoglutarinsäure. *Evonik Degussa GmbH*.
- Watanabe, S., Kodaki, T., Makino, K., 2006a. A novel α -ketoglutaric Semialdehyde dehydrogenase: evolutionary insight into an alternative pathway of bacterial l-arabinose metabolism. *J. Biol. Chem.* 281, 28876–28888.
- Watanabe, S., Shimada, N., Tajima, K., Kodaki, T., Makino, K., 2006b. Identification and characterization of l-arabonate dehydratase, l-2-Keto-3-deoxyarabonate dehydratase, and l-arabinolactonase involved in an alternative pathway of l-arabinose metabolism. *J. Biol. Chem.* 281, 33521–33536.
- Yovkova, V., Otto, C., Aurich, A., Mauersberger, S., Barth, G., 2014. Engineering the alpha-ketoglutarate overproduction from raw glycerol by overexpression of the genes encoding NADP(+)-dependent isocitrate dehydrogenase and pyruvate carboxylase in *Yarrowia lipolytica*. *Appl. Microbiol. Biotechnol.* 98, 2003–2013.
- Zadran, S., Levine, R.D., 2013. Perspectives in metabolic engineering: understanding cellular regulation towards the control of metabolic routes. *Appl. Biochem. Biotechnol.* 169, 55–65.
- Zhang, Y.-H.P., Sun, J., Ma, Y., 2016. Biomanufacturing: history and perspective. *J. Ind. Microbiol. Biotechnol.*, 1–12.
- Zhong, C., Wei, P., Zhang, Y.-H.P., 2017. A kinetic model of one-pot rapid biotransformation of cellobiose from sucrose catalyzed by three thermophilic enzymes. *Chem. Eng. Sci.* 161, 159–166.
- Zhu, Z., Zhang, Y.H.P., 2016. *In vitro* metabolic engineering of bioelectricity generation by the complete oxidation of glucose. *Metab. Eng.* 39, 110–116.

4.3.3 Identification of a side product formed from Kgsa

When the cascade reaction stopped at Kgsa, for instance, when no KgsalDH was added, a subsequent decline of Kgsa was observed. However, Kgsa preparations, which were synthesized from D-glucarate in water with only low amounts of AbC buffer (in total 3.8 mM deriving from enzyme preparations of GlucD and KdgD, 3.4.2) remained stable for several weeks at 4 to 10°C, and also at 25 °C for at least 48 h. It was hypothesized that the aldehyde moiety of Kgsa reacts with amino acid side chains of the protein and/or with the ammonium of the buffer. Indeed, after incubation with 1 mg/mL BSA over a period of three days at 25 °C, 40 % of Kgsa was lost (Figure 16). Incubation of Kgsa with 50 mM AbC buffer over a period of three days resulted in a decline of 80%.

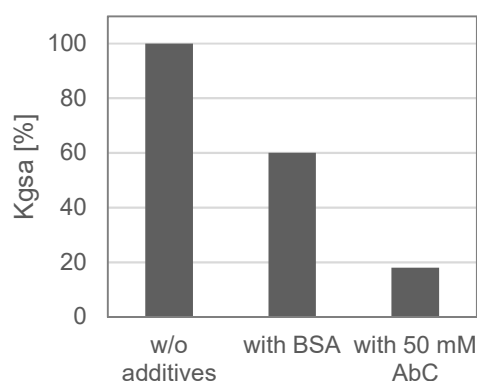


Figure 16: Influence of BSA and AbC buffer on Kgsa decline

Relative amount of Kgsa left after incubation at 25 °C without additives and with 1 mg/mL BSA over a period of two days as well as with 50 mM AbC buffer for a period of three days.

The reaction of Kgsa with AbC was further analyzed to identify the product formed from this reaction. Here, the formation of pyrrol-2-carboxylic acid (ammonium salt) could be proven by comparison to the reference compound using HPLC (see 3.6.1.3, retention time: 29.1 min), MS (see 3.6.2, negative mode: m/z 110) and NMR (see 3.6.3, ¹H NMR (400 MHz, DMSO-d₆) δ 11.0(s,1H), 6.7(m,1H), 6.4(m,1H), 5.9(m,1H), 3.3(m,4H, residual Kgsa). The reaction mechanism of pyrrole formation after Paal-Knorr is depicted in Figure 17.

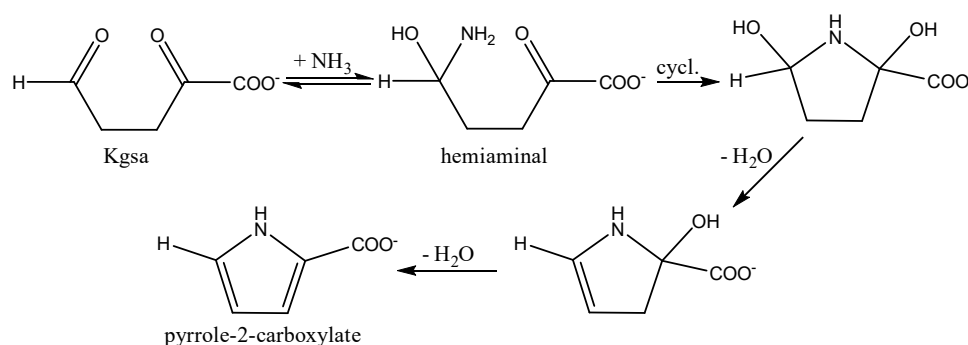


Figure 17: Proposed Paal-Knorr reaction mechanism of Kgsa to pyrrole-2-carboxylate

Kgsa and ammonia form a hemiaminal, which cyclizes spontaneously to the saturated pyrrole derivative. Subsequent dehydrations lead to pyrrole-2-carboxylate (Amarnath et al., 1995; Cho et al., 2015).

The formation of pyrrole-2-carboxylic acid from Kgsa is potentially useful for the synthesis of this compound and derivatives thereof from renewable resources. However, enzymatic cascade reactions including Kgsa as an intermediate have to be designed carefully to avoid its accumulation and the formation of pyrrole-2-carboxylic acid.

5 Discussion and Outlook

5.1 From D-glucose to D-glucarate with two enzymes

For the oxidation of D-glucose to D-glucarate nine enzymes are necessary in mammals (Linster and Van Schaftingen, 2007) (Figure 18 A). A considerably shorter route, depicted in Figure 18 B, with five enzymes was introduced into *E. coli* by Moon et al. (2009). Here, D-glucose is imported into *E. coli* through the native phosphotransferase system, generating D-glucose-6-phosphate. It is then isomerized to myo-inositol-1-phosphate by myo-inositol-1-phosphate synthase from *Saccharomyces cerevisiae*. An endogenous phosphatase dephosphorylates myo-inositol-1-phosphate to obtain myo-inositol, which is oxidized to D-glucuronic acid by myo-inositol oxygenase from *M. musculus*. D-glucuronate is finally oxidized by UDH from *P. syringae* to produce glucaric acid. Titters of 1 g/L and 2.5 g/L (using a scaffold for enzyme co-localization) were reported (T. S. Moon et al., 2010). The performance was improved by supplying myo-inositol instead of D-glucose (4.85 g/L) (Shiue and Prather, 2014).

In this thesis an approach, which reduces the number of enzymes to three was investigated (Figure 6, box). Both proposed reaction pathways contained only one known enzymatic activity, while no natural enzymes are capable of the other two oxidations. Therefore, it was necessary to identify biocatalysts with an activity for the oxidation of D-glucose to D-glucodialdose and to D-glucuronate or for the oxidation of D-gluconate to L-guluronate and to D-glucarate. For this task, enzymes converting similar substrates were investigated in order to identify those with a side activity towards the target compounds. Bioinformatic tools for finding such promiscuous activities in enzymes are also available (e.g., SABER) (Nosrati and Houk, 2012), however limited to enzymes with known crystal structures. In addition, the general feasibility of these fairly new *in silico* approaches remains to be shown.

For D-glucose oxidation, UDP-glucose-6-dehydrogenase from bovine liver seemed to be active. However, D-gluconate instead of glucodialdose or D-glucuronate was detected. It is believed that an impurity of the enzyme preparation with D-glucose dehydrogenase – an enzyme also found in bovine liver – caused the observed activity, since the UGDH from *E. coli* showed no activity toward D-glucose (section 4.1.1.1).

Another enzyme for the oxidation of D-glucose at C6 described in literature is a galactose oxidase variant (Lippow et al., 2010; Tae Seok Moon et al., 2009). However, the enzyme exhibits a very long lag phase and the authors state that further improvements of the enzyme seem to be hampered by the active site architecture. Here, the catalytically important Y495 probably poses a steric hindrance for the C-4 hydroxyl of D-glucose, forcing D-glucose into a twisted conformation, which decreases transition state planarity and likely contributes to decreased catalytic efficiency (Lippow et al., 2010). Although this enzyme was also tested and it was indeed active with D-glucose (data not shown), no further experiments were conducted, because an NAD⁺-dependent as well as an NADP⁺-dependent alcohol dehydrogenase from *Sphingomonas* species A1 (SpsADH and SpsADH-P, respectively) were identified in parallel. With these two isozymes, described for the reduction of 4-deoxy-L-erythro-5-hexulose uronate (Dehu) to 2-keto-3-deoxy-D-gluconate (2-Kdg) (Takase et al., 2014; Takase et al., 2010), two suitable enzymes for the designed pathway were identified. Since this pathway solely depends on NAD⁺ as a cofactor, the NAD⁺ dependent SpsADH was analyzed in more detail. Apart from 2-Kdg and gluconate, it exhibits a very broad substrate scope toward D-aldonates, C3- and C4-sugars as well as some polyols. However,

most striking is the oxidation of uronates to aldarates, abandoning the need of a third enzyme for the reaction pathway to D-glucarate. No literature describing such an enzymatic activity could be found.

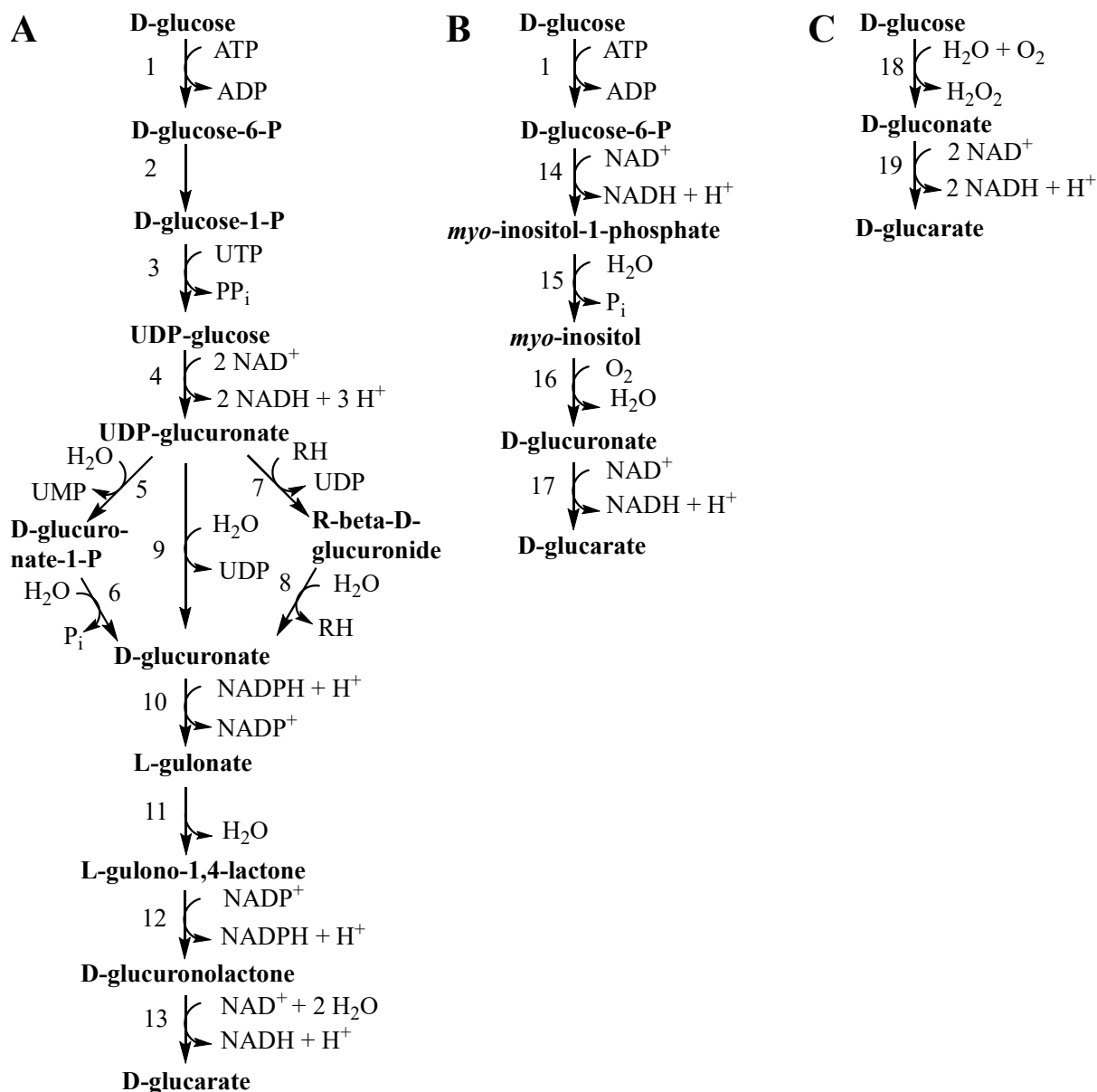


Figure 18: Natural and artificial pathways from D-glucose to D-glucarate

(A) The natural pathway from D-glucose to D-glucarate in mammals consists of at least nine enzymes: 1 hexokinase, 2 phosphoglucosmutase, 3 UTP-glucose-1-P-uridylyltransferase, 4 UDPG dehydrogenase, 5 glucuronate-1-P-uridylyltransferase, 6 glucuronokinase, 7 glucuronosyltransferase, 8 *b*-glucuronidase, 9 UDP-glucuronidase, 10 glucuronate reductase, 11 gulono-3-lactonase, 12 glucuronolactone reductase, and 13 aldehyde dehydrogenase.

(B) An artificial pathway, introduced into *E. coli* by Moon et al. (2009) only involves five enzymes: 1 hexokinase, 14 myo-inositol-1-phosphate synthase, 15 phosphatase, 16 myo-inositol oxygenase, 17 uronate dehydrogenase.

(C) A potential route with only two enzymes was identified in this work: 18 D-glucose oxidase and 19 NAD⁺-dependent alcohol dehydrogenase from *Sphingomonas* species A1 (*SpsADH*).

The mechanism of oxidation of uronates by *SpsADH* is so far not clear. Even though the substrate scope towards various primary alcohols was very broad, substrate promiscuity, i.e., activity toward different chemical groups, was only observed with uronates and aldehydes, which carry a substituent at the carbon

adjacent to the one being attacked. Proposedly, such a substituent, e.g., a hydroxyl-, methyl- or keto-group, is necessary for recognition by SpsADH.

Uronates can be present in various conformations: linear, as hemiacetal, or lactone (Figure 19A). The preferred form is the six-membered hemiacetal ring, while the linear form attributes to less than 1%. The lactone is not believed to be the active conformation for oxidation by SpsADH as lactone formation does not occur spontaneously, which is for example evidenced by the commercial availability of the linear form of D-glucuronate as well as its lactone. In the linear form, an aldehyde at C1 is available, whereas in the hemiacetal there is a secondary alcohol. To elucidate whether SpsADH is able to oxidize the aldehyde or the secondary alcohol, one could test analogs that are only present in one of these conformations, like 4-deoxy-L-erythro-5-hexulose uronate (Dehu) or D-quinic acid (Fig 19B), respectively. The former, Dehu, can be synthesized from alginate using alginate lyase Atu3025 (Takase et al., 2014).

Promiscuous functions have been the starting point for directed evolution to improve the promiscuous activity, as described, for instance, for a phosphotriesterase (Colin et al., 2015), human glutathione transferase (Norrgård and Mannervik, 2011), or sortase A from *Staphylococcus aureus* (Bigley et al., 2013). In order to also enhance the promiscuous activity of SpsADH for the conversion of D-glucuronate to D-glucarate, it will be helpful to identify the mechanism, by which uronates are recognized and oxidized.

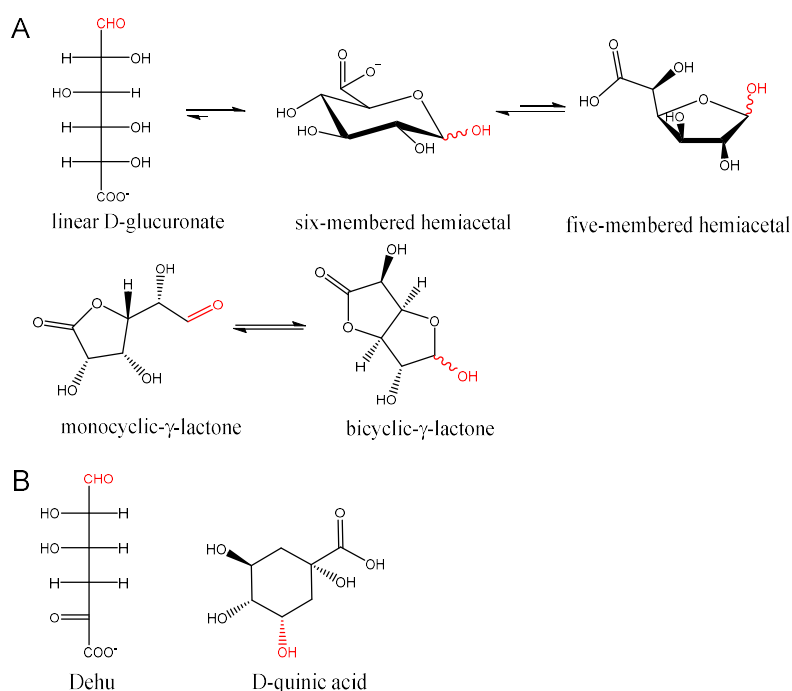


Figure 19: Different conformations of D-glucuronate and analogs thereof

(A) D-glucuronate can be present in the linear form, the six-membered hemiacetal, or the hemiacetal. Furthermore, lactones of D-glucuronate exist naturally, either as a monocyclic- γ -lactone or as a bicyclic- γ -lactone. However, lactones cannot be formed spontaneously from the linear or the hemiacetal conformations. Therefore, they are not believed to be the intermediate of the conversion of D-glucuronate to D-glucarate. To test, whether SpsADH oxidizes the aldehyde of the linear, open-chain conformation or the secondary alcohol of the hemiacetal conformations, one could test analogs as depicted in (B). 4-deoxy-L-erythro-5-hexulose uronate (Dehu) or D-quinic acid.

Furthermore, for a direct comparison with the inositol-route, the two-enzyme pathway should be conducted and analyzed. From the current point of view, it seems promising that the *in vitro* route could

compete with the *in vivo* inositol route considering that the reaction of SpsADH with glucarate dehydratase (GlucD), that is D-gluconate to 5-keto-4-deoxyglucarate (5-Kdg) resulted in ~70% conversion of gluconate (~7 g/L) without performing any optimization (Figure 12). Furthermore, SpsADH was used for the production of L-gulose from D-sorbitol. Despite the low catalytic efficiency of this reaction, 300 mM L-gulose could be produced in approximately 234 h.

In comparison to chemical catalysts for the oxidation of D-glucose to D-glucarate, SpsADH could be an alternative due to its specificity under ambient reaction conditions. Metal catalysts (e.g., Pd, Au, Pt) operate at temperatures around 40 to 60 °C and 5 to 10 bar O₂ pressure, resulting in considerable amounts of side products due to the oxidation of secondary alcohols yielding internal keto-products, which give rise to C-C fragmentation (Solmi et al., 2017). However, the activity of SpsADH needs to be optimized in order to become a competitive choice.

5.2 Synthesis of 5-hydroxy-2-oxovalerate

The enzymatic cascade reaction from D-glucuronate to 5-hydroxy-2-oxovalerate (Hov) was investigated for two reasons: Firstly, to collect first insights into the part of the reaction from D-glucose to 1,4-butanediol (BDO), for which enzymes were already available, that is uronate dehydrogenase (UDH) from *Agrobacterium tumefaciens*, glucarate dehydratase (GlucD) from *Actinobacillus succinogenes*, 5-keto-4-deoxyglucarate dehydratase (KdgD) from *Acinetobacter baylyi*, and ADHZ3 from *E. coli* with the amino acid substitutions S199L/S200N/N201D (ADHZ3 LND). Secondly, Hov should be produced for a screening of branched-chain ketoacid decarboxylase (KdcA) variants. However, these attempts were hampered by the chosen method of analysis, which was the derivatization of carboxylic acids with 4-APEBA and subsequent separation and detection by HPLC/MS (3.6.1.2). Using this method, it was not possible to detect 2-ketoglutaric semialdehyde (Kgsa) as the main product of the reaction using GlucD, KdgD, and ADHZ3 LND, which was found out later using anion exchange chromatography without derivatization (3.6.1.3). It remains to be shown, whether Kgsa cannot be derivatized or cannot be detected by MS. It is also possible that the reaction conditions of the derivatization lead to a reduction of Kgsa to Hov; thereby it would seem that Hov is the sole product of the cascade reaction.

With the knowledge gained from the analysis by anion exchange chromatography, ADHZ3 LND was identified as the bottleneck of the cascade reaction with Kgsa as the main product. This also explains the poor conversion of D-glucuronate by UDH, since ADHZ3 LND did not recycle NAD⁺ in sufficient amounts. In order to prepare Hov for the screening of KdcA variants, ADHZ3 LND activity and stability should be analyzed to ensure complete conversion of Kgsa to Hov. Meanwhile, KdcA variants were screened for enhanced activity with its native substrate ketoisovalerate (Weigl, 2014). Here, it was possible to identify the triple variant KdcA F381V/F382Q/G383L, which showed two-fold higher catalytic efficiency with ketoisovalerate as well as almost a three-fold higher catalytic efficiency towards valerate, a substrate analog of Hov. In order to analyze KdcA wildtype, the positive triple variant as well as other variants, for their activity with Hov, new attempts to prepare Hov have to be made. A first small-scale reaction of Kgsa with ADHZ3 LND showed that Hov can be separated and detected by the new analytical method (Table 11, line 9), paving the road for the optimization of the enzymatic cascade reaction from D-glucuronate to Hov or from D-glucose to Hov.

5.3 Enzymatic cascade reaction for the production of α -ketoglutarate

The second *in vitro* enzymatic cascade reaction analyzed was constituted of the enzymes UDH, GlucD, KdgD, and Kgsa dehydrogenase (KgsalDH) from *Pseudomonas putida*. The product of this reaction was α -ketoglutarate (aKG), an intermediate of the TCA cycle. For cofactor recycling the water-forming NADH oxidase (NOX) was applied. NOX was a crucial factor in this cascade reaction, since two enzymes, UDH and KgsalDH, depended on sufficient supply with NAD^+ . Therefore, NOX was characterized in detail, which led to the finding that it was not fully loaded with FAD, when overexpressed in *E. coli*. By loading the enzyme with FAD *in vitro*, a six-fold increase in specific activity was achieved. However, within the cascade reaction, NOX activity was not as high as calculated. Here, the diffusion of O_2 from the air into solution was the limiting factor. When operated in a bubble reactor, NOX activity could be increased 27-fold, however, at the expense of enzyme stability. Therefore, multiple additions of NOX over time were necessary to obtain full conversion of D-glucuronate and a yield of 92% aKG within 5 h. A more stable NOX, either by enzyme engineering, by substitution, or by immobilization, would make this process more economical. Also, a membrane assisted bubble reactor could be used to avoid direct contact with air (Rehn et al., 2016), or *in situ* generation of O_2 using hydrogen peroxide and catalase instead of supplying gaseous oxygen could lead to higher process stability of NOX.

UDH wildtype was used here, since the triple variant with improved thermostability was not available then. In contrast to the reaction cascade to Hov, full conversion of D-glucuronate could be observed, also over an extended period of time (50 h) without complete deactivation of UDH. Therefore, after engineering the stabilized variant, the influence of various additives and surfaces of reaction vessels on the stability of UDH was analyzed by Teresa Roth. As depicted in Figure 34 (section 6.4) the greatest influence was observed in presence of 0.1 mg/mL BSA. Here, the half-life of UDH was extended from 110 min to 161 h. 5% polyethylene glycol only extended the half-life to 5.3 h, and using glass instead of polypropylene resulted in a half-life of 15.1 h. Possibly, UDH instability is caused by a mixture of both, adsorption to the plastic surface of the reaction vessel and unfolding in diluted solution. Both can be avoided by adding BSA, which is able to saturate possible protein binding sites on plastic surfaces and leads to an effect termed “molecular crowding”. Here, the reduced available volume caused by the high amount of macromolecules decreases the configurational entropy for the unfolded state of a protein, therefore destabilizing the unfolded state and shifting the equilibrium toward the more compact native state (Minton 1981). This explains well why UDH instability was only seen when operated alone, but not in the cascade reaction, where a high enzyme load had the same effect as BSA. Addition of BSA even tops the stability gain of the engineered triple variant UDH A41P/H101Y/H236K. Therefore, using UDH wildtype in enzymatic cascade reaction is recommended, because of the higher stability and higher catalytic efficiency compared to the variant.

In the present state, GlucD is the bottleneck of the enzymatic cascade reaction. However, inhibition by the substrate, product, or intermediates was not observed. Instead, GlucD could be inactivated, for example, by oxygen, adsorption, or interaction with other proteins of the cascade reaction. The mode of inactivation needs to be elucidated in order to resolve this bottleneck.

5.4 Implications for BDO production

With the identification of SpsADH, the complete reaction pathway from D-glucose to BDO can now be described with six enzymes for eight reactions: D-glucose oxidase (GOX), SpsADH, GlucD, KdgD, KdcA, and ADHZ3 LND (Figure 20).

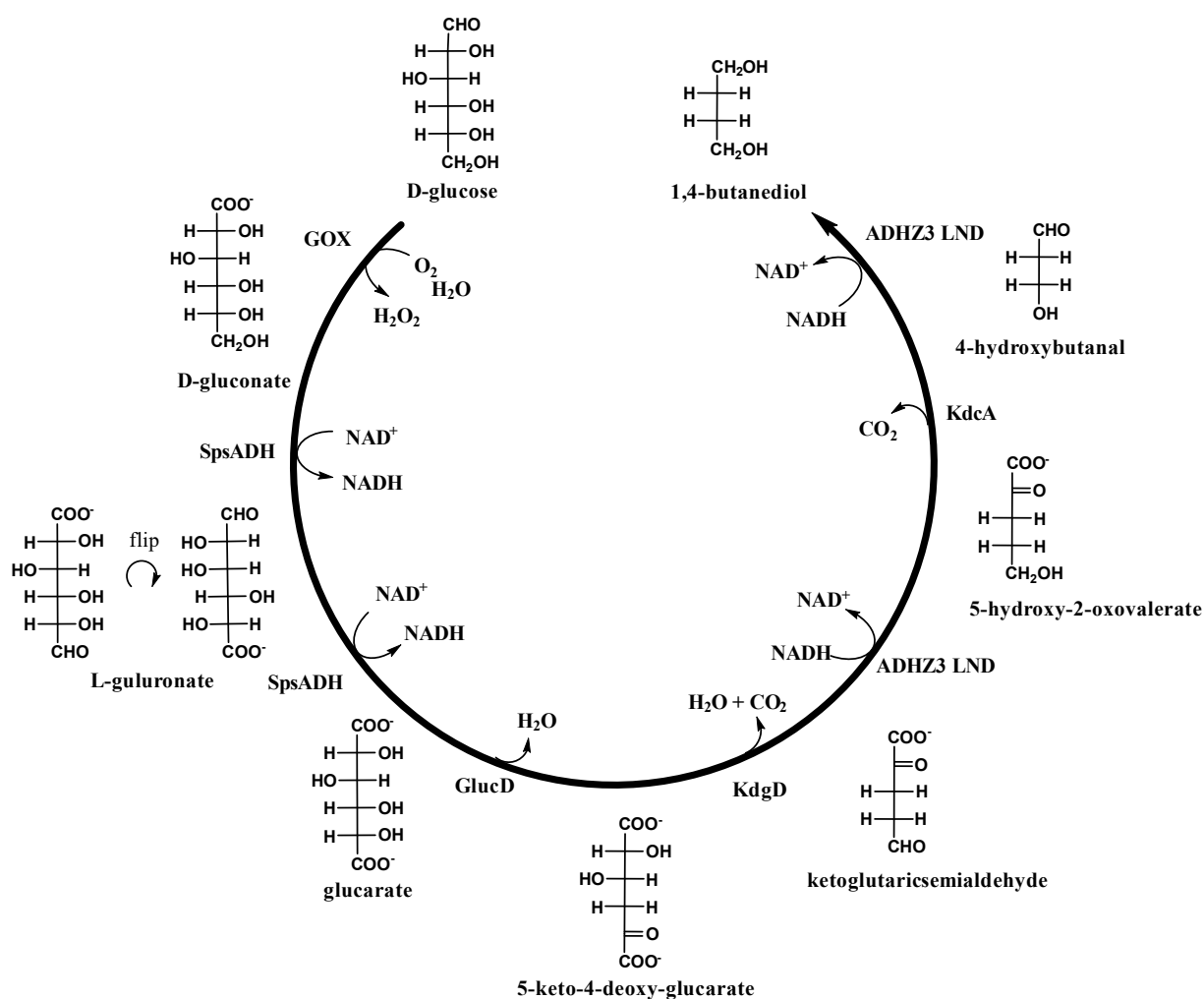


Figure 20: Synthesis route from D-glucose to BDO

D-glucose is converted to D-glucarate by glucose oxidase (GOX) and NAD⁺-dependent alcohol dehydrogenase from *Sphingomonas* species A1 (SpsADH). Two water molecules as well as one carbon dioxide are released to form ketoglutaric semialdehyde by the action of glucarate dehydratase (GlucD) and 5-keto-4-deoxy-glucarate dehydratase (KdgD). The alcohol dehydrogenase Z3 variant (ADHZ3 LND) reduces this intermediate as well as the intermediate 4-hydroxybutanal, which is formed after decarboxylation by the branched-chain ketoacid decarboxylase (KdcA). The final product is 1,4-butanediol (BDO).

The cofactor balance of NAD⁺/NADH is achieved within the cascade reaction. SpsADH generates two moles of NADH, which are recycled in the two reduction steps catalyzed by ADHZ3 LND. In order to ensure efficient cofactor recycling these two enzyme activities have to be adjusted carefully to each other. Therefore, ADHZ3 LND needs to be characterized in regard of its activity with Kgsa under various conditions, to find the one most suited for both the oxidation by SpsADH and the reduction by ADHZ3 LND. Furthermore, fast reduction of Kgsa is very critical, as Kgsa can form a Schiff base with amino acid side chains and is thereby removed from the reaction. Also, the formation of pyrrol-2-carboxylic acid from Kgsa and ammonium has to be avoided, as it decreases the overall yield and possibly inhibits KdcA, which could explain why activity was only observed with a substrate preparation

with short reaction time, whereas no activity was seen with the same preparation after it was further incubated overnight (Table 11).

For the first oxidation (D-glucose to D-gluconate), GOX can be used, which transfers two hydrides onto molecular oxygen instead of NAD^+ . The by-product of this reaction is hydrogen peroxide, which needs to be eliminated to avoid damage to the enzymes; this is generally achieved by adding catalase (Liese et al., 2008). GOX is already widely applied for *in vitro* diagnostics or in food and beverages, making it a readily available enzyme, with much information already at hand, facilitating its application in an *in vitro* enzymatic cascade reaction (Bankar et al., 2009). Naturally, data specific to this scope still needs to be gathered, for example, side reactivity toward or inhibition by reactants, or specific activity in various conditions to facilitate medium engineering of the cascade reaction. In addition, the enzymes ADHZ3 LND and KdcA have not been analyzed in this regard yet, and only little information is available from literature (Goetze et al., 2007; Pick et al., 2015). However, these detailed tests should be performed with variants that have before been engineered for higher activity toward their corresponding non-native substrates. For both enzymes a high throughput assay has already been developed (Pick et al., 2014; Schlüter, 2013). With the substrate Kgsa now being accessible, new variants of ADHZ3 LND can be screened, while for KdcA screening, the synthesis of Hov needs to be optimized and its stability must be tested as a ring closure can possibly occur. Concerning SpsADH, which also needs to be engineered to raise its specific activity towards D-gluconate, a 96 well expression system and a high throughput assay need to be evaluated for the screening of variants.

Apart from enzyme activity, stability is one of the major challenges when using enzymes *in vitro*. Within cells, enzymes are constantly degraded and reproduced, while *in vitro* no such cycle exists. Additionally, the stability can be higher within the cell than *in vitro*, as the macromolecular environment can contribute to stability (Bastos, 2016; Sarkar et al., 2014). In order to overcome this limitation, several strategies have been developed by researchers. Among these, immobilization is probably the most important one. Here, enzymes are fixed either to each other by cross-linking, fixed onto a carrier or encapsulated into a carrier (Sheldon and van Pelt, 2013). This allows recycling of the enzymes and can improve their stability (Y. Zhang et al., 2015). Other options to increase the stability are (1) using enzymes of thermophilic origin, (2) enzyme engineering, and (3) medium engineering (Bommarius and Paye, 2013).

Medium engineering is generally taken into account to increase both, enzyme activity and stability (Bommarius and Paye, 2013). Parameters include pH, buffer salt, ionic strength, reducing agents, metal ions, and co-solvents like glycerol. In the last decades, also non-natural conditions were found to assist in enzyme catalysis, e.g., non-aqueous solvents, ionic liquids, supercritical fluids, or high pressure (Eisenmenger and Reyes-De-Corcuera, 2009; S. M. Gupta et al., 2017; Lozano et al., 2017; Zhao, 2016). So far, medium engineering of the dehydration module of the cascade reaction (GlucD and KdgD) was performed including buffer salt, pH, temperature, and metals. For the oxidative part by SpsADH, the data proposes that the same conditions can be applied as it is active in ammonium bicarbonate at pH 8 and stable at 25 °C with a $t_{1/2}$ of 20 h. However, the reductive part will require different conditions, especially in regard of pH. Thermodynamically, oxidation is favored at higher pH, whereas reduction is favored at lower pH. This can also be observed in the catalytic rates of the corresponding enzymes. SpsADH is more active at pH 8 to 10 and ADHZ3 LND at pH 5 to 7 (Pick et al., 2014). However, both processes are linked by the NAD^+/NADH regeneration cycle making it uneconomical to separate them

using two reaction vessels. Enzyme engineering to shift the pH optimum of one of the enzymes is challenging and has only rarely been reported to be successful (Ma et al., 2016). A different possibility to enhance the activity was proposed by Zhang and Hess (2017). They state that the microenvironment upon immobilization on a DNA scaffold can mimic a lower pH for the tethered enzymes. Therefore, the scaffold for immobilization of enzymes is a critical decision and can vary for different proteins.

In the cascade reaction the supply of sufficient dissolved molecular oxygen has to be assured for the reaction of GOX. As it was already observed using NOX, this can state a bottleneck for the whole cascade reaction. For the NOX reaction, gaseous oxygen was provided successfully using a bubble reactor. However, enzymes can be inactivated by gas/liquid interfaces (Bommarius and Broering, 2005) and this was indeed observed with NOX and possibly GlucD. Other methods for oxygen supplementation avoiding excessive contact of the enzymes with air are (1) membrane-assisted aeration (Rehn et al., 2016), (2) bubble-free reactor design with silicon tubing, and (3) agitated cell reactor (Toftgaard Pedersen et al., 2017). In addition, the setup of the reaction could be changed to a two-pot system including one reactor with oxygen supplementation and one without. Thereby, the other enzymes could be spatially separated from GOX and catalase (CAT), avoiding their contact with molecular oxygen and hydrogen peroxide. Alternatively, the gold catalyst, which was used for the oxidation of sugars to aldonates, could be used instead of GOX. Such a chemo-enzymatic cascade reaction was already successfully applied by Sperl et al (2016); however, it requires CAT, since hydrogen peroxide is produced. Figure 21 illustrates the various reaction setups discussed.

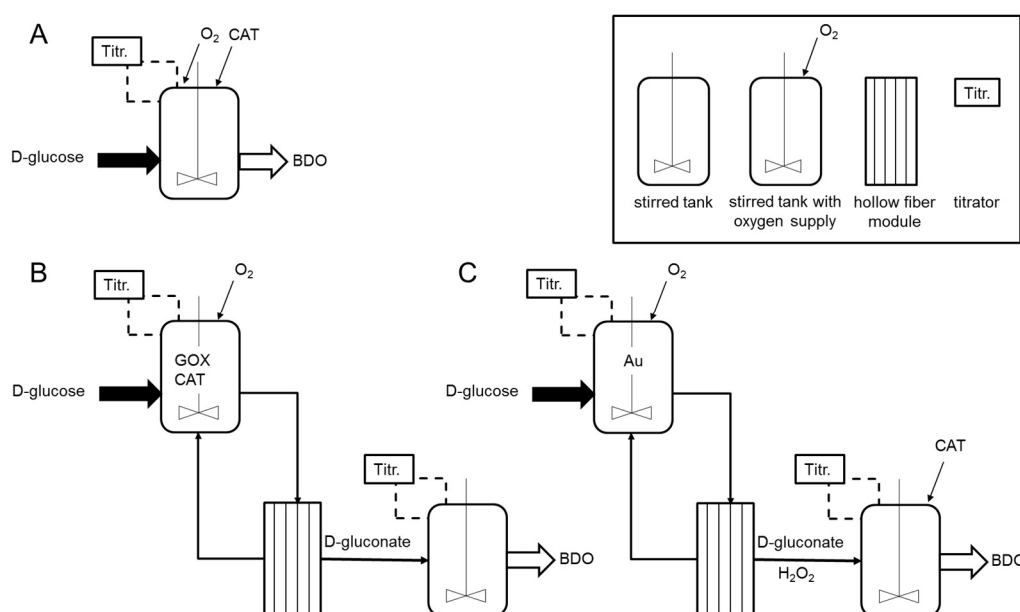


Figure 21: Possible reaction setups for the enzymatic production of BDO

A: One pot reaction of D-glucose to BDO in a stirred tank reactor in batch mode with pH control using a titrator (Titr.). Oxygen supply and addition of catalase (CAT) are necessary. B: Two-pot system with two separate stirred tank reactors in batch mode with pH control using titrators (Titr.). In the first tank, D-glucose is converted by glucose oxidase (GOX). Oxygen has to be supplied and hydrogen peroxide is removed by CAT. After conversion, the enzymes are removed using a hollow fiber module and D-gluconate is used as a substrate in the second reactor and converted to BDO. Thereby only the GOX is exposed to oxygen and hydrogen peroxide. C: Instead of GOX a gold catalyst can be used. Here, hydrogen peroxide is produced along with D-gluconate. Therefore, CAT has to be added in the second reaction step, or an intermediary module has to be included to remove hydrogen peroxide before entering the second enzyme reactor.

5.5 More enzymatic cascade reactions

Apart from the synthesis of BDO from D-glucose, a look at other possible substrates and products using the enzymes that were investigated in this thesis is provided. With this, the flexibility and opportunities of *in vitro* enzymatic cascade reactions is pointed out (Figure 22).

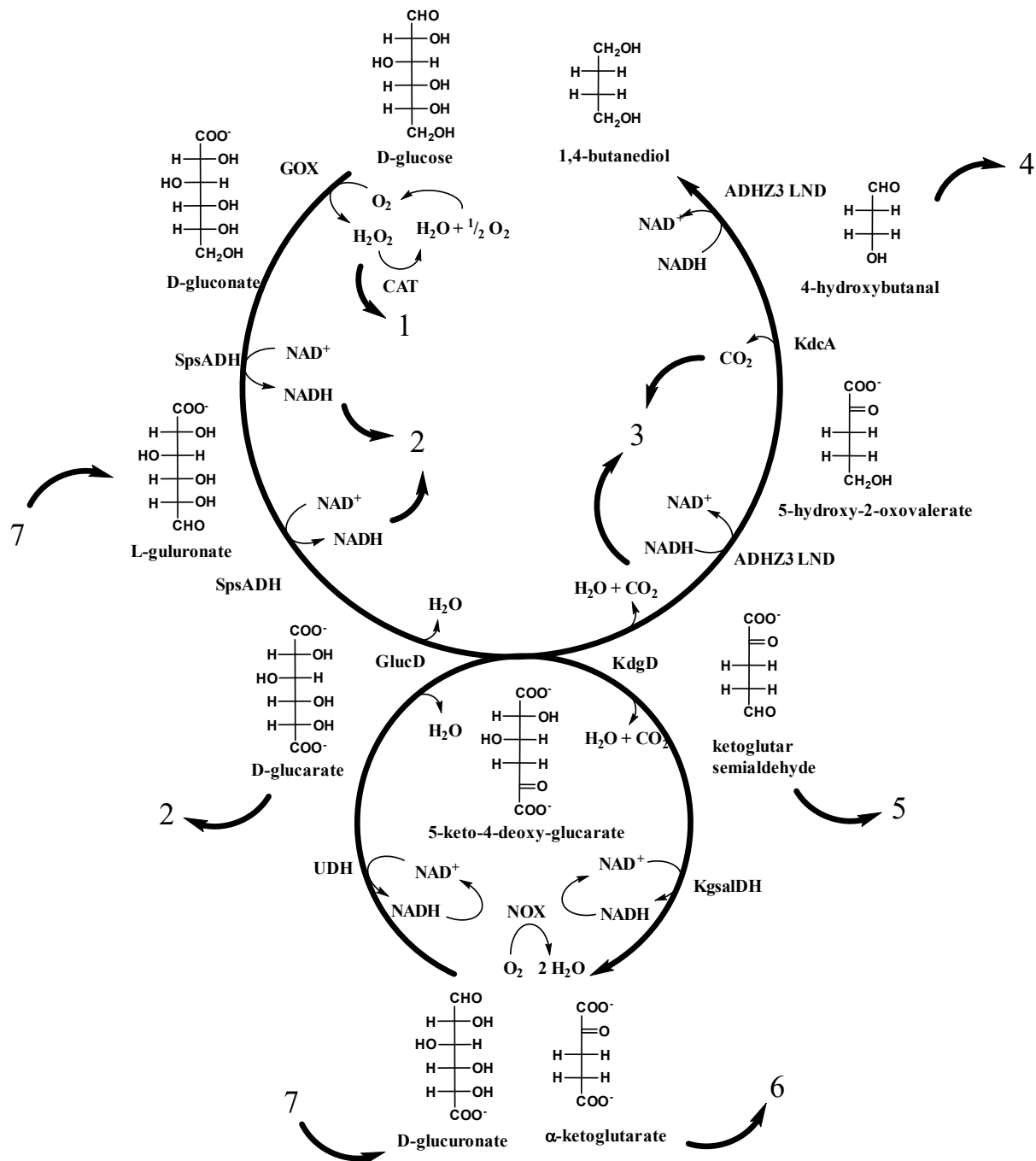


Figure 22: More enzymatic cascade reactions

0: Production of rare sugars using alcohol dehydrogenase from *Sphingomonas* species A1 (SpsADH). **1:** Use of H_2O_2 for oxidation reaction with OleT or P450 monooxygenases. **2:** Conversion of glucose to D-gluconate and three equivalents of NADH using glucose dehydrogenase (instead of glucose oxidase, GOX) and SpsADH. **3:** Enzymatic CO_2 utilization. **4:** Synthesis of succinic acid from 4-hydroxybutanal. **5:** Production of pyrrole-2-carboxylic acid. **6:** Synthesis of α -ketoglutaric acid. **7:** Instead of D-glucose, D-glucuronate or other uronic acids could be used as a substrate.

-
- 0 SpsADH can be applied for the production of rare sugars and aldaric acids.
- 1 Hydrogen peroxide generated by GOX can be used *in situ* for oxidation reactions catalyzed by P450 monooxygenases or OleT (Paul et al., 2014; Zachos et al., 2015).
- 2 D-glucose to D-glucarate coupled with reductase.
The US Department of Energy declared D-glucarate as one of the top value-added compounds that can be derived from biomass (Werpy, 2004). Among others, adipic acid can be derived from D-glucarate (Cavani et al., 2016), which is needed in nylon manufacturing.
Using D-glucose dehydrogenase and SpsADH, D-glucarate can be produced from D-glucose while generating three moles of NADH per mole of D-glucose. NADH is a precious reducing agent that can be used by reductases to produce chiral compounds from achiral starting materials. These are of great interest, especially in the pharmaceutical industry.
- 3 CO₂ can be used as a feedstock. Biocatalytic routes under investigation for the conversion of CO₂ include, for instance, the production of methanol by action of formate dehydrogenase, formaldehyde dehydrogenase, and an alcohol dehydrogenase (Yadav et al., 2014). CO can be synthesized by carbon monoxide dehydrogenase, which can be further converted by nitrogenases to longer chain carbons (Hu et al., 2011; Woolerton et al., 2011). Using ribulose-1,6-bisphosphate carboxylase oxygenase, CO₂ can enter the sugar biosynthesis pathways through the Calvin cycle, and with carbonic anhydrase, carboxylase, and oxidoreductases hydroxycarboxylic acids can be generated (Fosbøl et al., 2017; Lin et al., 2005).
- 4 4HB can be oxidized to succinic acid, which can also be used as a starting material for the synthesis of high performance chemicals like adipic acid, tetrahydrofuran, γ -butyrolactone, or N-methylpyrrolidone (Bozell and Petersen, 2010).
- 5 Kgsa can be used to produce pyrrol-2-carboxylic acid. Derivatives thereof are used in medical treatment of viral diseases, cancer, etc. (Bhardwaj et al., 2015; Khusnutdinov et al., 2010).
- 6 Kgsa can also be used to produce aKG, a compound of the central metabolism. It is used as a dietary supplement, component of infusion solutions or wound healing compounds, and as a building block for the chemical synthesis of heterocycles (Chernyavskaya et al., 2000; Huang et al., 2006; Stottmeister et al., 2005; Verseck et al., 2009).
- 7 L-gulonate derived from alginate and D-glucuronate from gum arabica or xanthan can be used as alternative substrates. In addition, D-galacturonate could be used, if GlucD could be engineered to dehydrate galactarate, as described by Gerlt et al. (2005). However, an attempt to construct such an enzyme variant was so far not successful (Schub, 2015).

6 Appendix

6.1 Gene sequences

>*ugd*h from *E. coli*:

```
ATGAAAATCACCATTTCGGTACTGGCTATGTAGGCTTGTCAAACGGGCTTCTAATCGCACAAAATCA
TGAGGTTGTGGCATTAGATATTTTACCAGTACAGCGTTGCTATGCTGAATGATCGGATATCTCCTATTG
TTGATAAGGAAATTCAGCAGTTTTTGAATCAGATAAAAATACACTTTAATGCCACATTAGATAAAAAT
GAAGCCTACCGGGATGCTGATTATGTCATCATCGCCACTCCAACCGACTATGATCCTAAAACATAATTA
TTTCAATACATCCAGTGTAGAATCAGTAATTAAGACGTAGTTGAGATAAAATCCTTATGCGGTTATGG
TCATCAAATCAACGGTTCCCGTTGGTTTTACCAGCAGCGATGCATAAGAAATATCGCACTGAAAATATT
ATATTCTCCCCGGAATTTCTCCGTGAGGGTAAAGCCCTTTACGATAATCTCCATCCTTACAGTATTGT
CATCGGTGAGCGTTTCCAGAACGCGCAGAACGTTTCGCTGCTCTGTTACAGGAAGGCGCGATTAAGCAA
ATATCCCGATGCTGTTTACCAGACTCCACTGAAGCAGAAGCGATTAACCTTTTGCAAACACCTACCTG
GCGATGCGCGTGGCGTACTTTAACGAAGTGGATAGCTATGCAGAAAGTTTAGGTCTGAATTTCCCGTCA
AATAATCGAAGGCGTTTGTCTCGACCCACGTATTGGCAACCATTAACAACATCCGTCGTTTGGTTATG
GTGGTTATTGTCTGCCGAAAGATACCAAGCAGTACTGGCGAACTACCAGTCTGTGCCGAAACCTG
ATCTCGGCAATTGTGATGCTAACCGCACGCGTAAAGATTTTATTGCCGATGCCATTTTGTCCAGCAA
GCCGCAAGTGGTGGGTATTTATCGTCTGATTATGAAGAGCGGTTTACGATAAACTTCCGTGCGTCTTCTA
TTCAGGGGATTATGAAACGTATCAAGGCGAAAGGTGTTGAAGTGATCATCTACGAGCCAGTGATGAAA
GAAGACTCATTCTTCAACTCTCGCCTGGAACGTGATCTCGCCACCTTCAAACAACAAGCCGACGTCAT
TATCTTAACCGAATGGCAGAAGAGCTTAAGGATGTGGCAGATAAGGTATACACCCGCGATCTCTTTG
GCAGCGACTAA
```

>*ugd*h from *Streptococcus pyogenes* codon-optimized for *E. coli*

```
CATATGAAAATTGCAGTTGCCGGTAGCGGTTATGTTGGTCTGAGCCTGGGTGTTCTGCTGAGCCTGCA
GAATGAAGTTACCATTGTTGATATTTCTGCCGAGCAAAGTGGACAAAATTAACAATGGTCTGAGTCCGA
TCCAGGATGAGTATATCGAATATTTCTGAAAAGCAAACAGCTGAGCATTAAAGCAACCTGGATAGC
AAAGCAGCATATAAGAAGCAGAGCTGGTTATTATTGCAACCCCGACCAATTATAACAGCCGCATCAA
CTATTTTGATACCCAGCATGTTGAAACCGTGATCAAAGAAGTCTGAGCGTTAATAGCCATGCAACCC
TGATTATCAAAGCACCATTCCGATTGGCTTTATTACCAGAAATGCGTCAGAAATTTAGACCCGATCGC
ATTATCTTTAGTCCGGAATTTCTGCGTGAAAGCAAAGCCCTGTATGATAATCTGTATCCGAGCCGAT
TATTGTGAGCTGCGAAGAAAATGATAGCCGAAAGTTAAAGCAGATGCCGAAAAATTTGCACTGCTGC
TGAAAAGCGCAGCCAAAAAAAACAATGTTCCGGTCTGATTATGGGTGCAAGCGAAGCAGAAGCAGTT
AAACTGTTTGCAAATACCTATCTGGCACTGCGTGTGCTATTTTAAACGAACTGGATACCTATGCAGA
AAGCCGTAAACTGAAATAGCCACATGATTATTCAGGGCATCAGCTATGATGATCGCATTGGTATGCATT
ACAATAATCCGAGCTTTGGCTATGGTGGTTATTGTCTGCCGAAAGATACAAAACAGCTGCTGGCAAAC
TATAACAATATTTCCGACAGCCCTGATTGAAGCAATTTGTGAGCAGCAATAATGTGCGCAAAAAGCTATAT
TGCCAAACAAATCATCAACGTGCTGAAAGAACAAGAAAGTCCGGTTAAAGTTGTTGGTGTGTATCGCC
TGATTATGAAATCCAACAGCGATAACTTTCTGTGAGAGCGCCATTAAAGATGTGATCGATATCCTGAAA
TCGAAAGACATCAAATCATCATCTATGAACCGATGCTGAACAAACTGGAAAGCGAAGATCAGAGCGT
TCTGGTTAATGATCTGGAAAACCTCAAACAAACAGGCCAACATTATCGTGACCAACCGCTATGATAATG
AACTGCAGGATGTGAAAACAAAGTGTATAGCCGTGATATCTTTGGTCCGATTAGCTCGAG
```

>Strings DNA fragment of *spsadh-NADP*, optimized for *E. coli*

```
GATCTACATATGTTCCCGGATCTGAAAGGTAAACGTGTTCTGATTACCGGTAGCAGCCAGGGTATTGG
TCTGGCAACCGCACGTCTGTTTGCACGTGCCGGTGCAAAGTTGGTCTGCATGGTCTGTAAGCACC GG
CAAATATTGATGAAACCATTGCAAGCATGCGTGCCGATGGTGGTATGATGATGATGATGATGATGATGAT
CTGGCGACCAGCGAAGCATGTCAGCAGCTGGTTGATGAATTTGTTGCAAAAATTTGGTGGCATCGATGT
GCTGATTAAACAATGCCGGTGGTCTGGTGGGTGTAACCGCTGCCGAAATTTGATGATACCTTTTATG
ATGCAGTGATGGATGCCAATATTCGTAGCGTTGTTATGACCACAAAATTTGCACTGCCGCATCTGGCA
GCAGCAGCAAAGCAAGCGGTGAGACCAGCGCAGTTATTAGCACCGGTAGTATTGCAGGTCATACCGG
TGGTGGTCCGGGTGCAAGTCTGTATGGTGCAGCCAAAGCATTTCTGCATAATGTGCATAAAAACCTGGG
TGGACTTTCATACCAAAGATGGTGTGCGTTTTTAACATTGTTAGTCCGGGTACAGTTGATACCGCATTT
CATGCAGATAAAAACCGAGGATGTTCTGATCGTATTAGCAATGGTATTCCGATGGGTGCTTTTGGCAC
CGCAGAAGAAATGGCTCCGGCATTTCTGTTTTTTGCAAGCCATCTGGCAAGCGGTTATATTACCGGTC
AGGTTCTGGATATTAATGGTGGCCAGTATAAACATTAACCTCGAGGATCTA
```

>Strings DNA fragment of *spsadh*, optimized for *E. coli*

GATCTACATATGTTTCAGCGACCTGAAAGGTAAACGTATTCTGATTACCGGTAGCACCGAAGGTATTGG
TATGGCAACCGCAATTGAACTGGCACGTTATGGTGCAGTTGTTGGTCTGAATAGCCATGTTGATCCGG
CAGATCCTGCACTGCTGCTGGGTAAACTGCGTGAAGCCGGTGGTGATGGTGCATTTTTTTCGTGCAGAT
ATCACCAAACCGCAGAATGTCAGCGTCTGGTTAGCGCATTGTTGAACGTTTTGATGGTATTGATGT
GCTGATTAACAATGCCGGTGGTCTGGCAGGTCGTAGCAATCTGGAAAATATTGATGATGCCTTTTTATG
ACCGTGTGATGGATCTGAATGGTCGTAGCGTTCTGATGATGACCAAATTTGCAATTCGGCATCTGCGT
GCAAGCGCAAAGCAAGCGGTACAACCAGCGCAGTTATTAGCACCGGTAGTATTGCAGCACGTGAAGG
TGGTGGTATTGGTGCCGGTGTATTATGCAGCAAGCAAAGCATGGCTGCATGATATTCATCGTAATTGGG
TGAAAGAGTTACCAAAGATAGCATCCGTTTTAACATTGTTGCACCGGGTACAGTTGATACCGCATTT
CATGCAGATAAAAGCGACGAAGTAAACCCGTTATTGCAAATAGCATTCCGATGGGTGCTTTTTGGCAC
CGTTCAAGAGCTGGCACCAGCCTATGTTTTTTTTGCAAGCCATGCCGCAAGCGGTTATATCACCGGTC
AGATTCTGGATGTTAATGGTGGTCAGATTTGTCCGTAACCTCGAGGATCTA

>*kgsaldh* from *Pseudomonas putida* KT2440

ATGCCTGAGATCCTCGGCCATAACTTCATCGCCGGTCAGCGCAGTGCCGCTGGCCCTCAGCGCCTGCA
GAGCCTGGACGCCAGCACTGGCGAAGCCCTGCCCTACAGCTTTGCCAGGCCACCGAAGCCGAAGTGG
ACAAAGCCGCCAAGGCCGCTGCCGCAGCCTTCGCCGATTTCCGCCAACTGGCCCCGGCGCGTCCGGCC
GAGTTCCTCGACGCCATCGCCGCTGAACTCGACGAACTGGATGACGCCTTCGTGCCCATCGTCTGCCG
CGAAACCGCCCTGCCCGCCGCCCGCATCCAGGGCGAGCGCGGCCGCACCAGCGGGCAGATGCGCCTGT
TCGCCCAAGTGTGTCGCCCGGGCGACTTTCTCGGCGCACGCATCGACCTGGCACTGCCCGAGCGCCAG
CCGCTGCCACGCGTAGACCTGCGCCAGATGCGCATCGGTGTAGGCCCGGTCCCGTGTTCGGGGCCAG
CAACTTCCCCTTGCCTTCTCCACCGCCGGGGTGATACCGCCGCCCTGGCCGCAGGCTGCCCGG
TGGTATTCAAGGCGCACAGCGGCCACATGGCCACGGCCGACCTGGTGCCTGCGCCATCGTGCAGGCC
GCTGAGCGGACCGGCATGCCCAAGGGCGTGTCAACATGGTATTTGGTGGCGGCGTGGGCGAGTGGCT
GGTCAAGCACCCGGCCATCCAGGCGGTTGGCTTCACCGGCTCGCTGAAAGGCGGTGATGCCCTTTGCC
GCATGGCCGCTGAGCGCCCGCAGCCAATCCCGGTGTTCCGCCGAGATGTCCAGCATCAACCCGGTCATC
ATCCTGCCAGGCGCCCTGGCCAAACGTGGCGAGGCCATTGCCCGCGAGTTGGCGGGGTCCGTGTGCAT
GGGTGCCGGGCAGTTCTGCACCAACCCTGGGCTGGTATTGGCTTGCAGTCGCCACAGTACAGCCAAC
TGCTCGCCGACCTTGGCCAGTACCTGGACCAGCAAGCCGGGCAAACCATGCTCAATGCTGGCGGCTTG
CACAGCTACGTCCGGCGCCTTGAACACTTGCATGCCCATGCCGGTATCGAGCATGTGGCCGGCCAGGT
GCAGGAAGGCAACCAGGCGCGCGCTCAGCTGTTCAAGGCCGATGCACGCCTGCTGGTCCGAGTCCGACC
CGCTGTTGCAGGAAGAAGTGTGTTGGGCCACCACCGTGGCCGTAGAGGTGCAGGACAACGACCAACTG
CGCGACGCGCTGCTCGGCCTGCGCGGCCAGCTGACC GCGACGCTGATCGGCGAAGCGGAGGACTTCGA
TGCCTTCGCCTGGCTGGTGCCGCTGCTGGAGGAGAAAGTCGGGCGAATCCTGGTCAATGGCTACCCGA
CCGGTGTGCAAGTCTGTGATGCCATGGTGCACGGCGGCCCGTACCCGGCGACCTCCGATGCGCGTGGC
ACCTCGGTCCGCACTTTGGCCATCGACCGCTTCTGCGCCCGGTGTGCTACCAGAACTACCCGCAGAC
GCTGCTGCCTGAGGCACTGCGCGACGGCAACCCGCTGGGGCTGCGGCGGTTGGTGAACGGTCAGTGG
GTGACGGGGCGATCTGA

6.2 Analysis of reaction products of SpsADH

Experimental procedure:

25 mM of aldionate or uronate were incubated in 50 mM AbC with 5 mM NAD⁺, 2.4 μg SpsADH and 0.15 μg NOX at 25 °C for 24 h. Fresh NOX (0.15 μg) was added two times. Controls contained neither NAD⁺ nor SpsADH.

The reactions were stopped by filtration using Spin columns (PES, 10K, VWR), the samples were then diluted 1:2 in water and analyzed by HPLC using the Metrosep column (Metrohm). The new method for dicarboxylic acids was applied with an isocratic elution with 30 mM AbC pH 10.4.

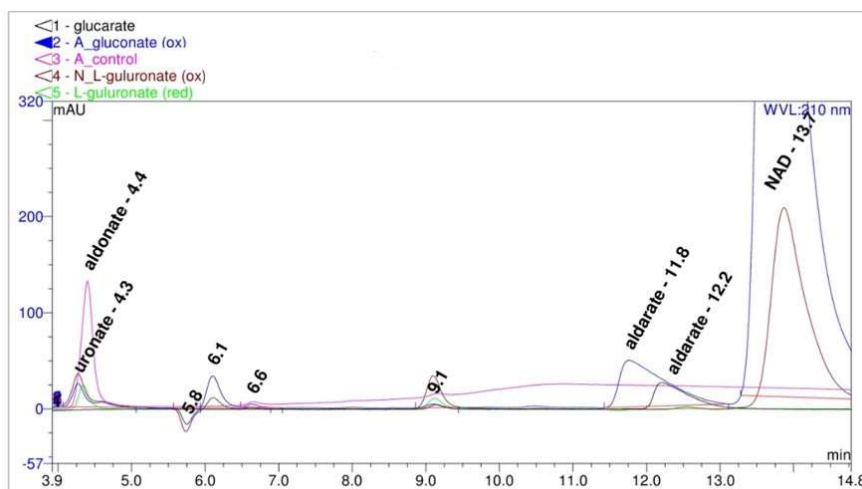


Figure 23: D-gluconate to D-glucarate

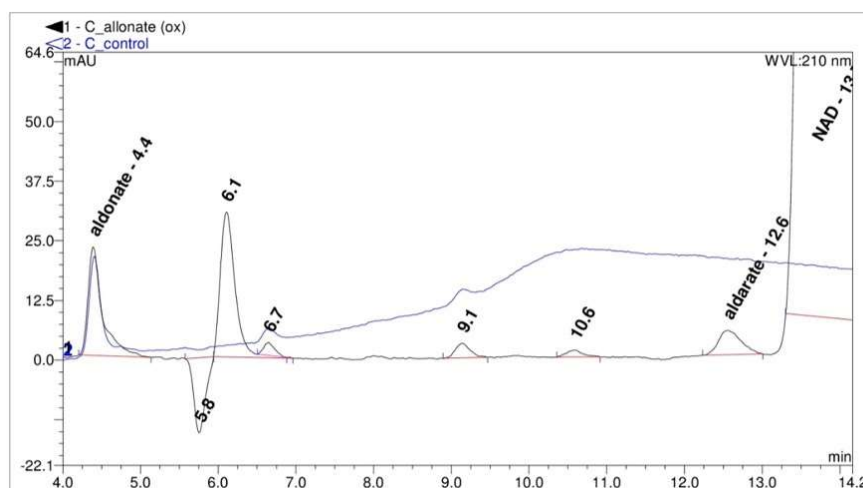


Figure 24: D-altronate to D-altrarate

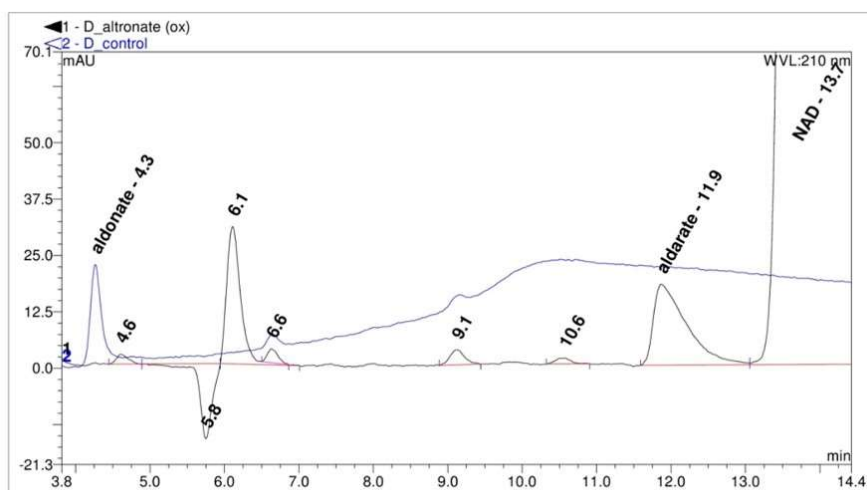


Figure 25: D-altronate to D-altrarate

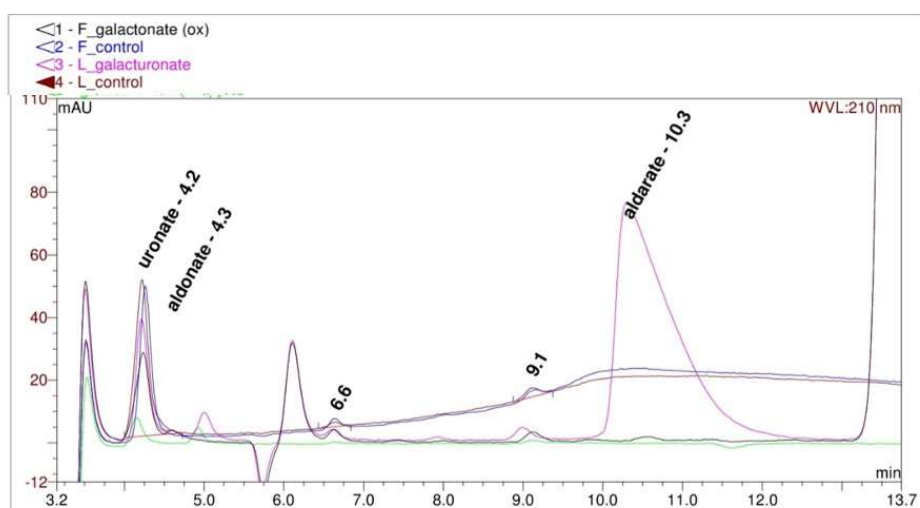


Figure 26: D-galactonate to D-galactarate

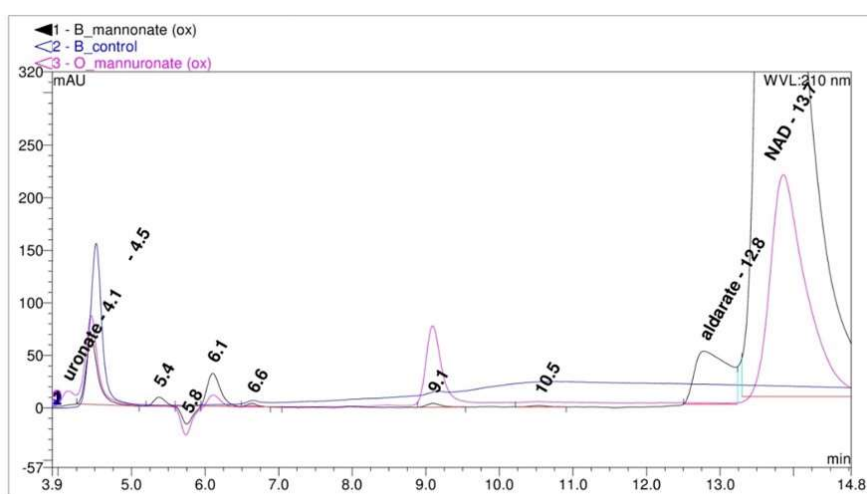


Figure 27: D-mannonate to D-mannarate

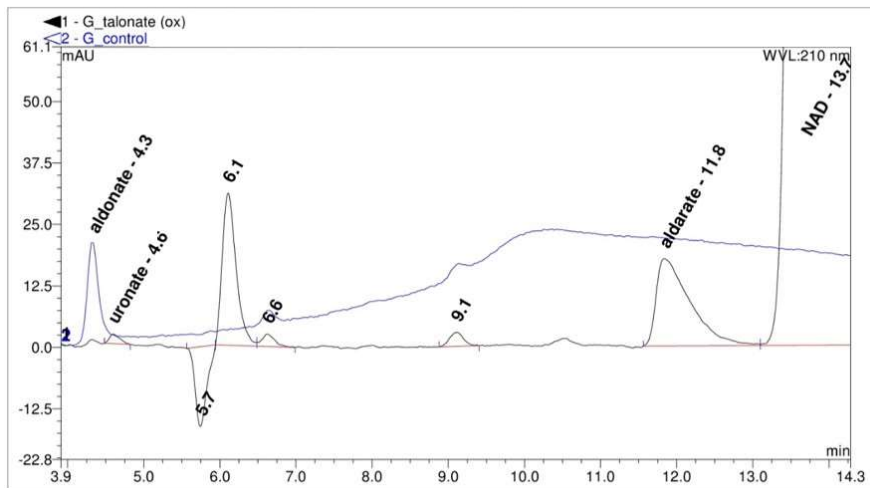


Figure 28: D-talonate to D-talarate

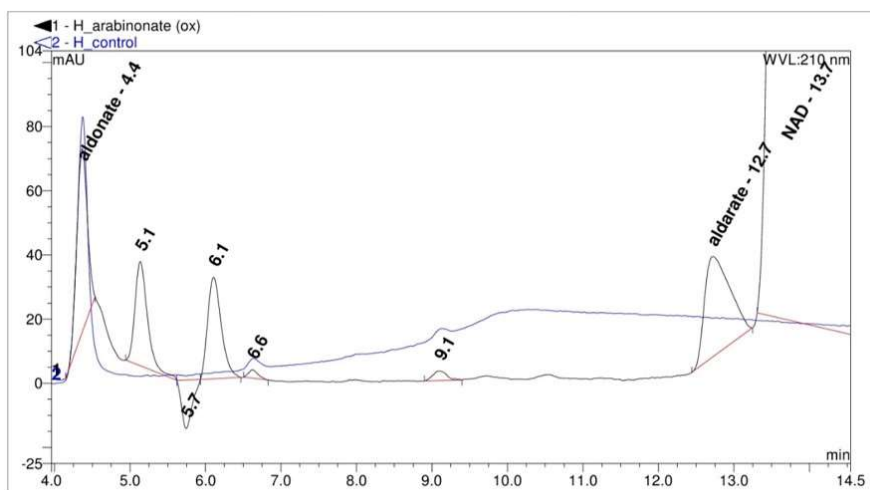


Figure 29: D-arabonate to D-arabinarate

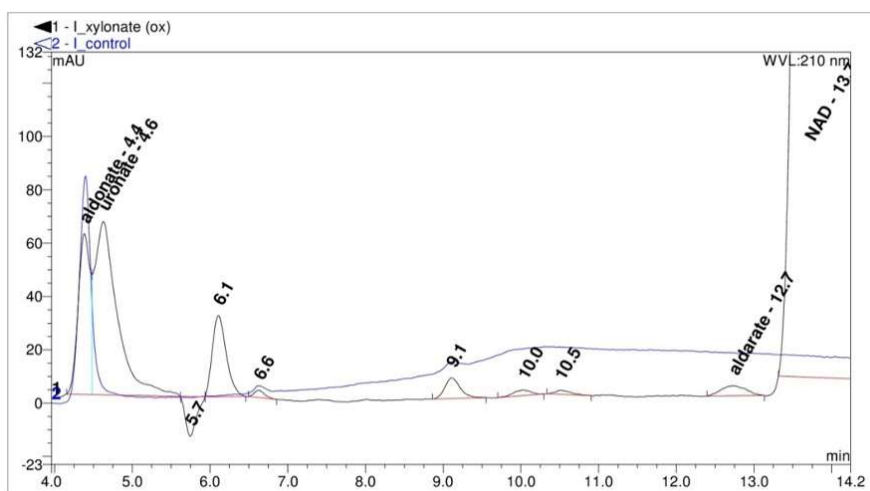


Figure 30: D-xylonate to D-xylarate

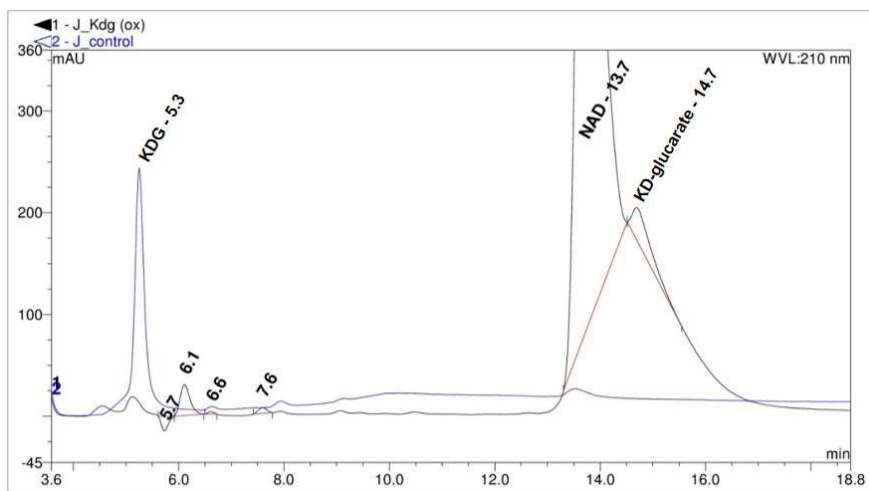


Figure 31: 2-Kdg to 2-ketodeoxyglucarate

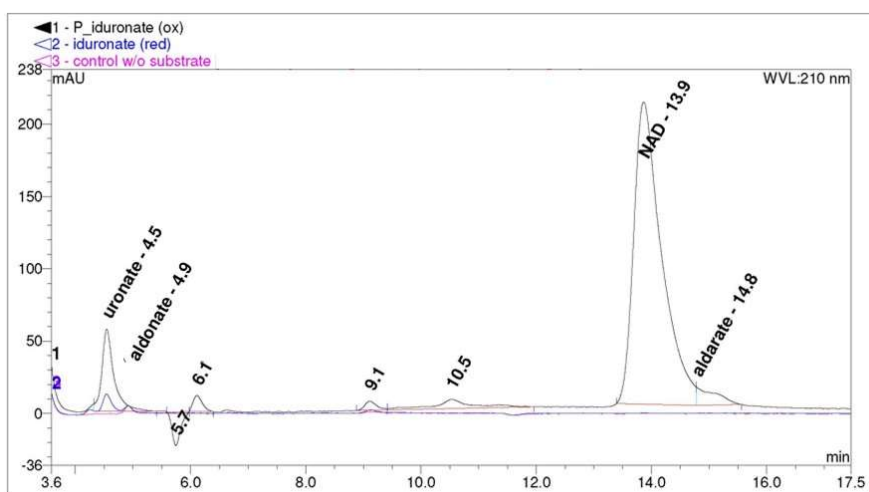


Figure 32: L-iduronate to idarate

6.3 Analysis of 4-APEBA derivatives by HPLC/MS

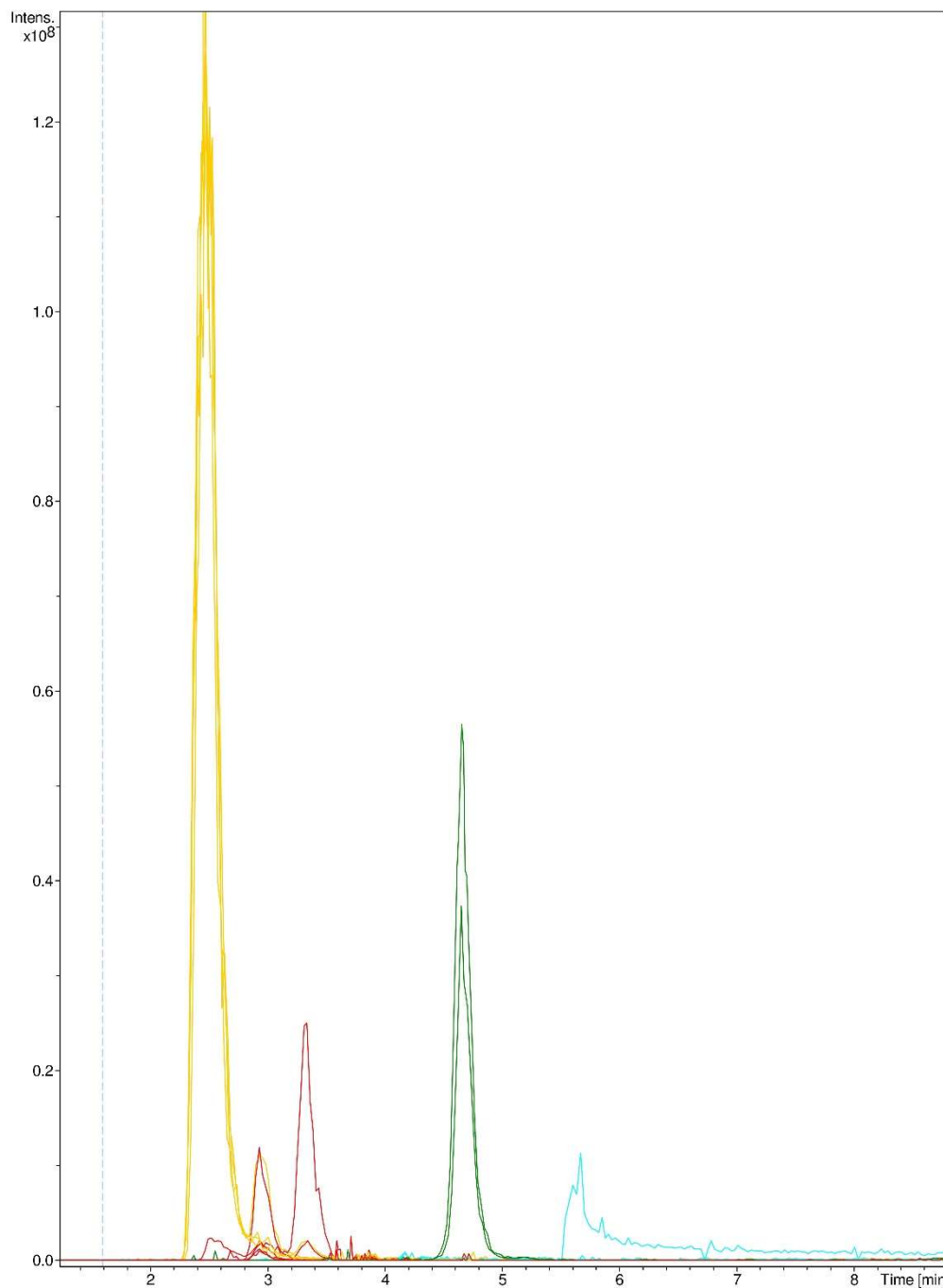


Figure 33: Detection of 4-APEBA derivatives by HPLC/MS

The method for derivatization and analysis is described in section 3.6.1.2. Yellow: m/z 539 (D-glucuronate), red: m/z 537 (D-glucarate 2.9 min, and 5-Kdg monoderivative 3.3 min), green: m/z 477 (Hov), blue: m/z 442 (5-Kdg diderivative)

6.4 Half-life of UDH under various conditions

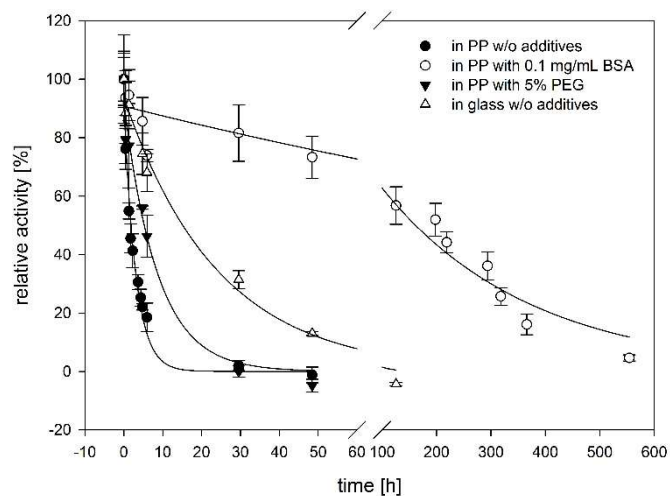


Figure 34: Half-life of UDH under various conditions

The half-life of UDH at 50 °C in polypropylene (PP) without additives was 110 min, with 5% polyethylene glycol (PEG) it was already 5.3 h, with 1 mg/mL BSA even 161 h. When incubated in glass without additives, the half-life was 15.1 h. The error bars indicate the standard deviation of three measurements.

6.5 Supplemental Information: Substrate scope of a dehydrogenase from *Shingomonas* species A1 and its potential application in the synthesis of rare sugars and sugar derivatives

Synthesis of aldonic acids

The following aldonic acids were synthesized by oxidation of the corresponding sugars using a gold catalyst: D-erythronate, D-threonate, D-arabonate, D-lyxonate, D-ribonate, D-xylonate, D-allonate, D-altronate, D-mannonate, D-galactonate, D-talonate, 2-deoxy-D-gluconate, and 3-deoxy-D-gluconate. The optimal ratios of sugar to catalyst (Table S) were found by stepwise addition of the catalyst to the reaction mixture with online monitoring of the reaction using a titrator.

Table S1: Synthesis of aldonic acids

Sugar	Au catalyst (mg)/ sugar (mmol)	conversion (%)	water content of product (%)
D-erythrose	180	92.5	11.38
D-threose	60	99.8	17.54
D-arabinose	10	99.7	2.22
D-lyxose	27	98.3	12.16
D-ribose	30	98.8	11.93
D-xylose	20	100	9.41
D-allose	60	99.3	15.37
D-altrose	40	97.1	12.60
D-mannose	30	92.0	1.94
D-galactose	8	100	11.94
D-talose	60.5	93.5	12.55
2-deoxy-D-glucose*	54.2	96.7	
3-deoxy-D-glucose*	75	95	

* not optimized

Verification of uronate formation by HPLC using the PMP method

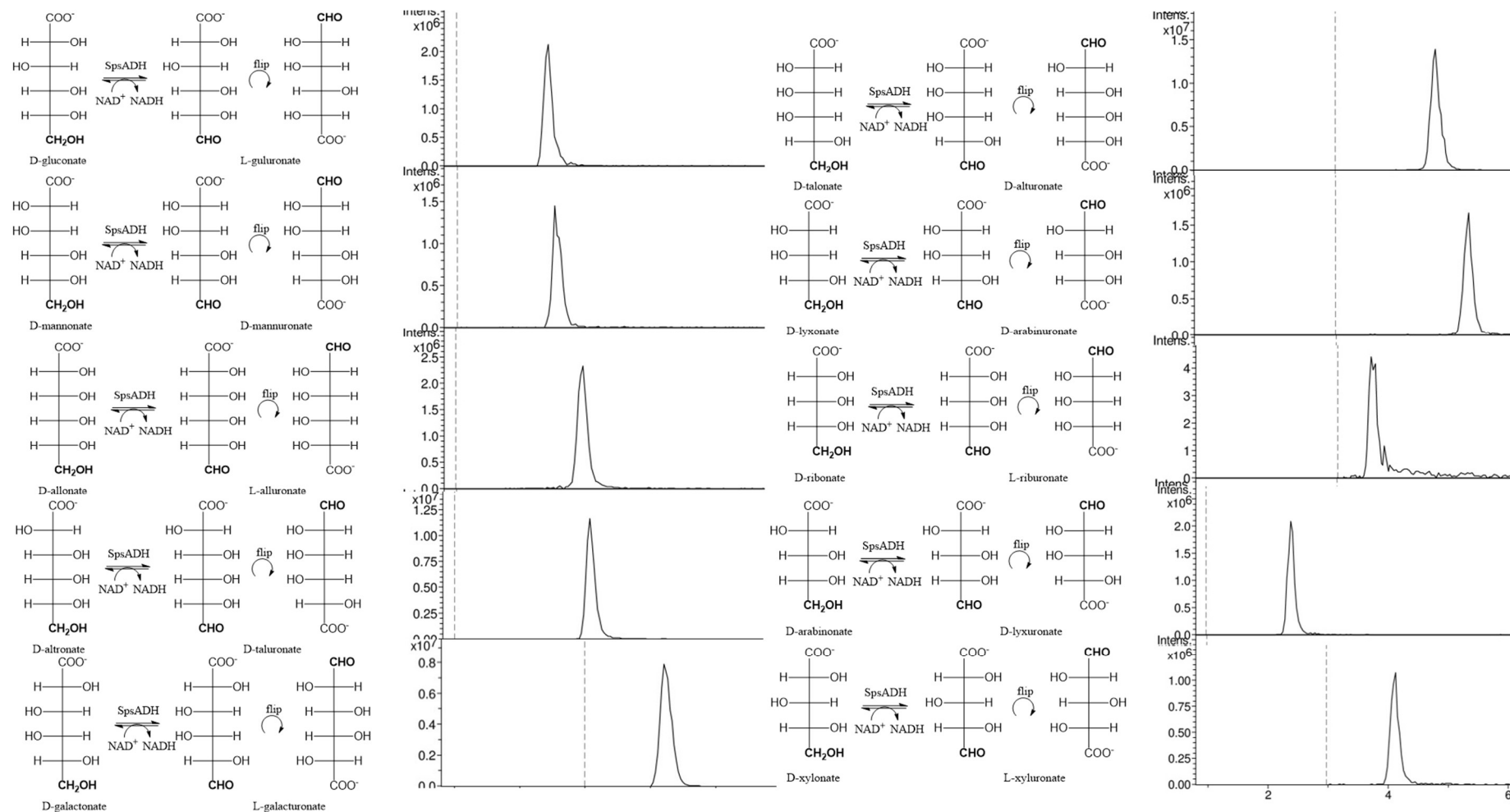


Figure S1: Product identification of aldonate oxidation

Aldonates are converted to uronic acids by SpsADH. These were derivatized with PMP (see experimental section of main paper) and analyzed by HPLC. The dotted line indicates the valve switch for MS measurement. A valve switch before 3 min was only performed with extracted samples, where access PMP was removed.

6.6 Supplemental Information: A water-forming NADH oxidase from *Lactobacillus pentosus* suitable for synthetic biomimetic cofactors



Figure S1 Multiple sequence alignment of NADH oxidases.

Amino acid sequences of *Lactobacillus pentosus* (Uniprot ID I8R785), *Lactobacillus sanfranciscensis* (Uniprot ID Q9F1X5), *Lactobacillus brevis* (Uniprot ID M5AB03), and *Lactococcus lactis* (Uniprot ID A2RIB7) were aligned using Clustal Omega (Sievers et al., 2011). The secondary structure assignment and the binding site for FAD/ADP of Nox from *L. sanfranciscensis* (PDB ID: 2CDU) is depicted above the alignment. The catalytically active Cys42 is marked in a red box.

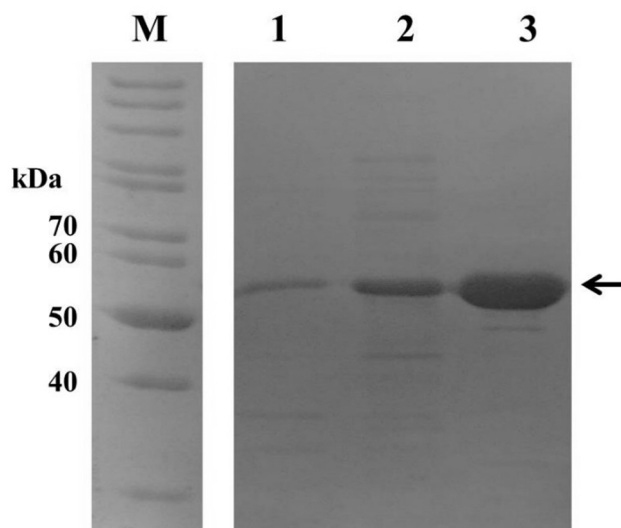


Figure S2: SDS-PAGE of LpNox purification.

Lane 1: insoluble fraction of the cell lysate, lane 2: soluble fraction of the cell lysate, lane 3: LpNox after purification. LpNox (arrow) is mainly found in the soluble fraction of the lysed cells. LpNox could be purified to >95 % homogeneity.

Reference

Sievers, F., Wilm, A., Dineen, D., Gibson, T.J., Karplus, K., Li, W., Lopez, R., McWilliam, H., Remmert, M., Söding, J., Thompson, J.D., and Higgins, D.G. (2011). Fast, scalable generation of high-quality protein multiple sequence alignments using Clustal Omega. *Molecular Systems Biology* 7, 539-539. doi: 10.1038/msb.2011.75.

6.7 Supplemental Information: *In vitro* metabolic engineering for the production of α -ketoglutarate

NADH stability

The chemical stability of dihydro nicotinamide adenine dinucleotide coenzyme (NADH) was investigated with respect to buffer [50 mM potassium phosphate pH 8.0 (KP) and 50 mM ammonium bicarbonate pH 7.9 (AbC)] and temperature (25 °C and 37 °C). For this, 2 mM NADH was incubated in safe-lock Eppendorf tubes at the indicated conditions. Every day, a sample of 30 μ L was diluted with 170 μ L of water in 96-well microtiter plates and analyzed at 340 nm using a Multiskan spectrum spectrophotometer (Thermo Fisher Scientific) at 25 °C. The decrease in absorbance is directly correlated to the inactivation of NADH (Rover Jr et al., 1998).

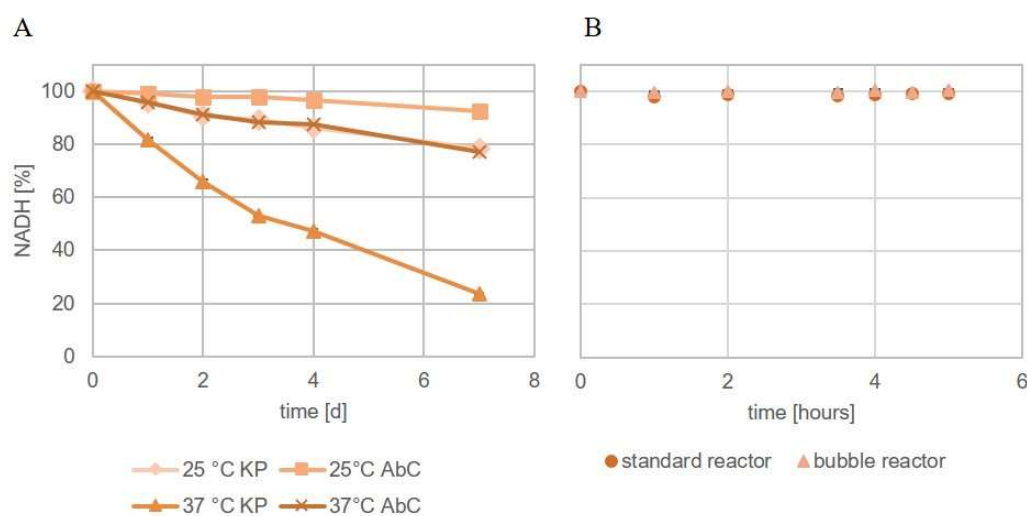


Figure S1: Stability of NADH

(A) After 7 days, 93% of NADH was still detectable in 50 mM AbC at 25 °C. At 37 °C, only about 80% NADH was left, which was the same as in KP at 25 °C. However, in KP at 37 °C, only 23% of NADH was still measurable. (B) NADH stability was not affected in the bubble reactor over a period of five hours.

Glucarate dehydratase from Actinobacillus succinogenes

The experimental descriptions can be found in the main publication.

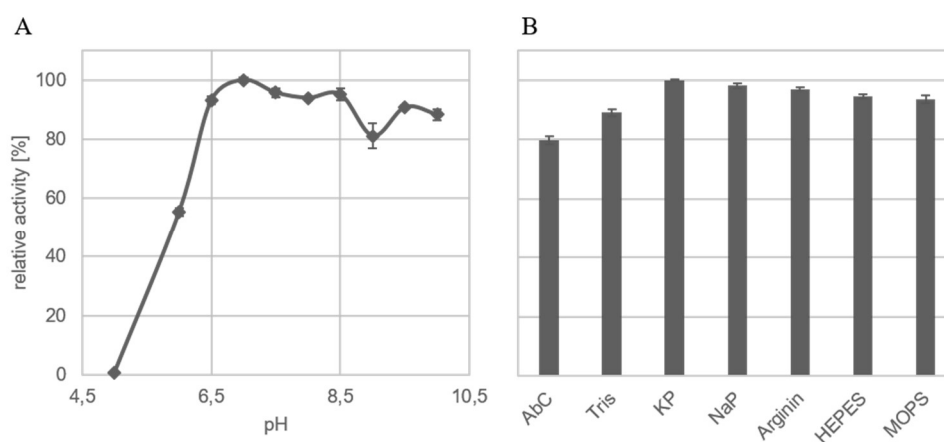


Figure S2: Dependence of GlucD activity on pH and buffers

(A) GlucD displays a rather unusual pH profile. After a sharp increase of activity between pH 5 and 6.5, the activity hardly drops at higher pH values. (B) GlucD activity is fairly comparable in various buffers at pH 8.0. Only in AbC does the activity drop as low as 80% compared with the highest activity in KP.

Table S1: Melting temperatures of GlucD in various buffers

The thermal stability of GlucD only varies within 1.5 °C in the different buffers tested. The lowest T_m of 57.0 °C is only seen in buffers with pH 8.0.

Buffer	T_m [°C]
HEPES pH 7.0	58.0
MOPS pH 7.0	58.5
Bis-Tris pH 7.0	57.5
KP pH 7.0	58.5
Tris pH 7.0	58.5
MOPS pH 7.5	58.0
Bis-Tris pH 7.5	58.5
KP pH 7.5	57.5
KP pH 8.0	57.0
AbC pH 8.0	57.0

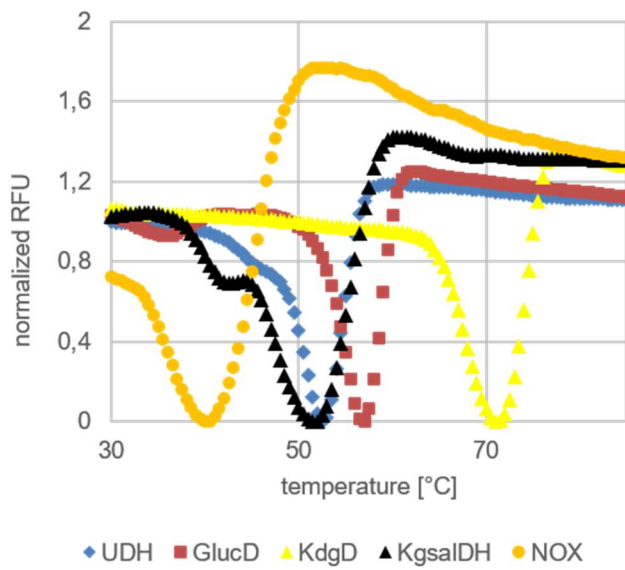
Thermal stability

Figure S3: Thermal unfolding of UDH, GlucD, KdgD, KgsalDH, and NOX in 50 mM AbC pH 7.9

The thermal unfolding of the enzymes was monitored with the thermofluor assay using SYPRO Orange. The melting temperature (T_M) of UDH was 52.2 °C, GlucD 57.0 °C, KdgD 71.0 °C, KgsalDH 51.5 °C, and NOX 40.0 °C in 50 mM AbC pH 7.9.

7 Abbreviations

2-Kdg	2-keto-3-deoxy-D-gluconate
4-APEBA	2-(4-aminophenoxy)ethyl(4-bromophenethyl)-dimethylammoniumbromide hydrobromide
5-Kdg	5-keto-4-deoxyglucarate
AbC	ammonium bicarbonate
ADH	alcohol dehydrogenase
ADHZ3 LND	triple variant of ADHZ3 from <i>E. coli</i> with the amino acid substitutions S199L/S200N/N201D
AIDH	aldehyde dehydrogenase
aKG	α -ketoglutarate
APS	ammonium persulfate
BDO	1,4-butanediol
<i>bt</i> UGDH	UGDH from <i>Bos taurus</i>
CAT	catalase
CFME	cell-free metabolic engineering
CO ₂	carbon dioxide
CO	carbon monoxide
CV	column volume
DBT cycle	design-build-test cycle
ddH ₂ O	double distilled water
Dehu	4-deoxy-L-erythro-5-hexulose uronate
DNA	deoxyribonucleic acid
dNTPs	deoxyribonucleotides
DMSO- <i>d</i> ₆	trideuterio(trideuteriomethylsulfinyl)methane
DSF	differential scanning fluorimetry
DTT	dithiothreitol
<i>E. coli</i>	<i>Escherichia coli</i>
<i>ec</i> UGDH	UGDH from <i>E. coli</i>
EDC	N-(3-dimethylaminopropyl)-N'-ethyl-carbodiimide-hydrochloride
EDTA	ethylenediaminetetraacetic acid
FAD	flavin adenine dinucleotide
FDH	formate dehydrogenase
GlucD	glucarate dehydratase
GOX	glucose oxidase
H ₂ O ₂	hydrogen peroxide
H ₂ O	water
Hov	5-hydroxy-2-oxovalerate
HEPES	2-(4-(2-hydroxyethyl)-1-piperazinyl)-ethansulfonic acid
HPLC	high performance liquid chromatography
IMAC	immobilized metal ion chelate affinity chromatography

IPTG	isopropyl- β -D-thiogalactopyranoside
k_{cat}	turnover number
$k_{\text{cat, app}}$	apparent turnover number
$k_{\text{cat}}/K_{\text{m}}$	catalytic efficiency
$k_{\text{d, app}}$	apparent deactivation rate
KdcA	branched-chain ketoacid decarboxylase
KdgD	5-keto-4-deoxyglucarate dehydratase
Kgsa	2-ketoglutaric semialdehyde
KgsalDH	Kgsa dehydrogenase
K_{m}	Michaelis-Menten constant
KP	potassium phosphate
LB medium	lysogeny broth medium
MS	mass spectrometry
MWCO	molecular weight cut off
m/z	ratio of mass to charge number
NAD ⁺ /H	nicotinamide adenosine dinucleotide, oxidized/reduced
NADP ⁺ /H	nicotinamide adenosine dinucleotide phosphate, oxidized/reduced
NaP	sodium phosphate
NMR	nuclear magnetic resonance
NOX	NADH oxidase
O ₂	molecular oxygen
OD	optical density at 600 nm
OX	oxidase
PCR	polymerase chain reaction
PDB	protein data bank
PES	polyether sulfone
PMP	1-phenyl-3-methyl-5-pyrazolone
PVDF	polyvinylidene fluoride
rpm	rounds per minute
SDS	sodium dodecyl sulfate
SDS-PAGE	sodium dodecyl sulfate polyacrylamide gel electrophoresis
SpsADH	NAD ⁺ -dependent alcohol dehydrogenase from <i>Sphingomonas</i> species A1
SpsADH-P	NADP ⁺ -dependent alcohol dehydrogenase from <i>Sphingomonas</i> species A1
SyPaB	synthetic pathway biotransformations
$t_{1/2}$	half-life
T _A	annealing temperature
TB medium	terrific broth medium
TCA cycle	tricarboxylic acid cycle
THF	tetrahydrofuran
T _M	melting temperature
TRIS	tris(hydroxymethyl)-aminomethane
TTN	total turnover number

UDH	uronate dehydrogenase
UDP-Glc	uridine diphosphate glucose
UGDH	UDP-glucose-6-dehydrogenase
v/v	volume/volume; 100 mL/100 mL correspond to 100% (v/v)
V_{\max}	maximum velocity of an enzyme
w/v	weight/volume; 100 g/100 mL correspond to 100% (w/v)

8 List of figures

Figure 1: Products made from BDO	1
Figure 2: Global consumption of BDO by region (2010)	2
Figure 3: Commercial BDO production processes.....	2
Figure 4: BDO production history and forecast	3
Figure 5: Fermentation processes for bio-BDO starting from D-glucose via the TCA cycle	4
Figure 6: Proposed in vitro enzymatic cascade reaction from D-glucose to BDO	12
Figure 7: Simple Cloning strategy after You and Zhang (2012).....	28
Figure 8: Enzymes to be identified for the oxidative module	41
Figure 9: Product identification of btUGDH.....	42
Figure 10: General properties of both SpsADH isozymes	44
Figure 11: Analysis of SpsADH product formation by anion exchange chromatography.....	58
Figure 12: Synthesis of 5-Kdg from D-gluconate by SpsADH and GlucD	58
Figure 13: Oxidation and reduction of uronates by SpsADH	59
Figure 14: Enzymes that were newly characterized or engineered	60
Figure 15: In vitro enzymatic cascade reaction for the synthesis of Hov.....	81
Figure 16: Influence of BSA and AbC buffer on Kgsa decline.....	95
Figure 17: Proposed Paal-Knorr reaction mechanism of Kgsa to pyrrole-2-carboxylate.....	95
Figure 18: Natural and artificial pathways from D-glucose to D-glucarate	97
Figure 19: Different conformations of D-glucuronate and analogs thereof.....	98
Figure 20: Synthesis route from D-glucose to BDO.....	101
Figure 21: Possible reaction setups for the enzymatic production of BDO	103
Figure 22: More enzymatic cascade reactions	104
Figure 23: D-gluconate to D-glucarate.....	108
Figure 24: D-altronate to D-altrarate.....	108
Figure 25: D-altronate to D-altrarate.....	109
Figure 26: D-galactonate to D-galactarate	109
Figure 27: D-mannonate to D-mannarate.....	109
Figure 28: D-talonate to D-talarate	110
Figure 29: D-arabinoate to D-arabinarate.....	110
Figure 30: D-xylonate to D-xylarate	110
Figure 31: 2-Kdg to 2-ketodeoxyglucarate	111
Figure 32: L-iduronate to idarate.....	111
Figure 33: Detection of 4-APEBA derivatives by HPLC/MS.....	112
Figure 34: Half-life of UDH under various conditions	113

9 List of tables

Table 1: Comparison of in vivo and in vitro enzymatic cascade reactions	7
Table 2: Bacterial strains.....	20
Table 3: Plasmids	20
Table 4: Oligodeoxyribonucleotides	22
Table 5: Standard PCR protocol	26
Table 6: Colony PCR protocol.....	26
Table 7: PCR protocol for the generation of complementary ends	29
Table 8: PCR protocol for the generation of the plasmid multimer	29
Table 9: Molecular weight and extinction coefficients determined with the ProtParam tool (ExPASy), and GenBank ID of all proteins used.	30
Table 10: Preparation of gels for SDS-PAGE.....	31
Table 11: Conditions and results of the enzymatic cascade reaction for the synthesis of Hov.	83

10 References

- 1,4-Butanediol (BDO) market by technology & application - 2019. (2015). Retrieved from <http://www.marketsandmarkets.com/Market-Reports/1-4-butanediol-market-685.html> on 18.10.17
- Aghaie, A., Lechaplais, C., Sirven, P., Tricot, S., Besnard-Gonnet, M., Muselet, D., . . . Perret, A. (2008). New insights into the alternative D-glucarate degradation pathway. *Journal of Biological Chemistry*, 283(23), 15638-15646. doi:10.1074/jbc.M800487200
- Amarnath, V., Amarnath, K., Valentine, W. M., Eng, M. A., & Graham, D. G. (1995). Intermediates in the Paal-Knorr synthesis of pyrroles. 4-Oxoaldehydes. *Chemical Research in Toxicology*, 8(2), 234-238.
- Arora, B., Mukherjee, J., & Gupta, M. N. (2014). Enzyme promiscuity: using the dark side of enzyme specificity in white biotechnology. *Sustainable Chemical Processes*, 2, 25-34. doi:10.1186/s40508-014-0025-y
- Axelrod, J., Kalckar, H. M., Maxwell, E. S., & Strominger, J. L. (1957). Enzymatic formation of uridine diphosphoglucuronic acid. *Journal of Biological Chemistry*, 224(1), 79-90.
- Baier, F., Chen, J., Solomonson, M., Strynadka, N. C., & Tokuriki, N. (2015). Distinct metal isoforms underlie promiscuous activity profiles of metalloenzymes. *ACS Chemical Biology*, 10. doi:10.1021/acscchembio.5b00068
- Bankar, S. B., Bule, M. V., Singhal, R. S., & Ananthanarayan, L. (2009). Glucose oxidase--an overview. *Biotechnology Advances*, 27(4), 489-501. doi:10.1016/j.biotechadv.2009.04.003
- Bastos, M. (2016). *Biocalorimetry: Foundations and contemporary approaches*: CRC Press
- Bendl, J., Stourac, J., Sebestova, E., Vavra, O., Musil, M., Brezovsky, J., & Damborsky, J. (2016). HotSpot Wizard 2.0: automated design of site-specific mutations and smart libraries in protein engineering. *Nucleic Acids Research*, 44(W1), W479-487. doi:10.1093/nar/gkw416
- Bertani, G. (1951). Studies on lysogenesis. I. The mode of phage liberation by lysogenic *Escherichia coli*. *Journal of Bacteriology*, 62(3), 293-300.
- Besenmatter, W., Kast, P., & Hilvert, D. (2007). Relative tolerance of mesostable and thermostable protein homologs to extensive mutation. *Proteins: Structure, Function, and Bioinformatics*, 66(2), 500-506. doi:10.1002/prot.21227
- Bhardwaj, V., Gumber, D., Abbot, V., Dhiman, S., & Sharma, P. (2015). Pyrrole: a resourceful small molecule in key medicinal hetero-aromatics. *RSC Advances*, 5(20), 15233-15266. doi:10.1039/C4RA15710A
- Bhattacharyya, A., & Manila, M. D. (2011).
- Bigley, A. N., Xu, C., Henderson, T. J., Harvey, S. P., & Raushel, F. M. (2013). Enzymatic neutralization of the chemical warfare agent VX: evolution of phosphotriesterase for phosphorothiolate hydrolysis. *Journal of the American Chemical Society*, 135. doi:10.1021/ja402832z
- Boer, H., Maaheimo, H., Koivula, A., Penttilä, M., & Richard, P. (2010). Identification in *Agrobacterium tumefaciens* of the D-galacturonic acid dehydrogenase gene. *Applied Microbiology and Biotechnology*, 86(3), 901-909. doi:10.1007/s00253-009-2333-9
- Bogorad, I. W., Lin, T.-S., & Liao, J. C. (2013). Synthetic non-oxidative glycolysis enables complete carbon conservation. *Nature*, 502(7473), 693-697. doi:10.1038/nature12575
<http://www.nature.com/nature/journal/v502/n7473/abs/nature12575.html#supplementary-information>
- Bommarius, A. S., & Broering, J. M. (2005). Established and novel tools to investigate biocatalyst stability. *Biocatalysis and Biotransformation*, 23(3-4), 125-139. doi:10.1080/10242420500218877
- Bommarius, A. S., & Paye, M. F. (2013). Stabilizing biocatalysts. *Chemical Society Reviews*, 42(15), 6534-6565. doi:10.1039/C3CS60137D
- Bozell, J. J., & Petersen, G. R. (2010). Technology development for the production of biobased products from biorefinery carbohydrates-the US Department of Energy's "Top 10" revisited. *Green Chemistry*, 12(4), 539-554. doi:10.1039/B922014C
- Bradford, M. M. (1976). A rapid and sensitive method for the quantitation of microgram quantities of protein utilizing the principle of protein-dye binding. *Analytical Biochemistry*, 72(1-2), 248-254. doi:http://dx.doi.org/10.1016/0003-2697(76)90527-3
- Burgard, A., Burk, M. J., Osterhout, R., Van Dien, S., & Yim, H. (2016). Development of a commercial scale process for production of 1,4-butanediol from sugar. *Current Opinion in Biotechnology*, 42, 118-125. doi:http://dx.doi.org/10.1016/j.copbio.2016.04.016
- Carbonell, P., Currin, A., Jervis, A. J., Rattray, N. J., Swainston, N., Yan, C., . . . Breitling, R. (2016). Bioinformatics for the synthetic biology of natural products: integrating across the Design-Build-Test cycle. *Natural Products Report*, 33(8), 925-932. doi:10.1039/c6np00018e
- Carlin, D. A., Hapig-Ward, S., Chan, B. W., Damrau, N., Riley, M., Caster, R. W., . . . Siegel, J. B. (2017). Thermal stability and kinetic constants for 129 variants of a family 1 glycoside hydrolase reveal that enzyme activity and stability can be separately designed. *PLOS ONE*, 12(5), e0176255. doi:10.1371/journal.pone.0176255
- Castillo, E., Casas-Godoy, L., & Sandoval, G. (2016). Medium-engineering: a useful tool for modulating lipase activity and selectivity *Biocatalysis* (Vol. 1, pp. 178).

- Cavani, F., Albonetti, S., Basile, F., Gandini, A., Wiley, J., & Sons. (2016). *Chemicals and fuels from bio-based building blocks*: Wiley-VCH Verlag GmbH & Company KGaA.
- Chen, G. S., Siao, S. W., & Shen, C. R. (2017). Saturated mutagenesis of ketoisovalerate decarboxylase V461 enabled specific synthesis of 1-pentanol via the ketoacid elongation cycle. *Scientific Reports*, 7, 11284. doi:10.1038/s41598-017-11624-z
- Chen, W.-p., & Kuo, T.-t. (1993). A simple and rapid method for the preparation of gram-negative bacterial genomic DNA. *Nucleic Acids Research*, 21(9), 1.
- Chernyavskaya, O. G., Shishkanova, N. V., Il'chenko, A. P., & Finogenova, T. V. (2000). Synthesis of alpha-ketoglutaric acid by *Yarrowia lipolytica* yeast grown on ethanol. *Applied Microbiology and Biotechnology*, 53(2), 152-158.
- Cho, H., Madden, R., Nisanci, B., & Torok, B. (2015). The Paal-Knorr reaction revisited. A catalyst and solvent-free synthesis of underivatized and N-substituted pyrroles. *Green Chemistry*, 17(2), 1088-1099. doi:10.1039/C4GC01523A
- Colin, P. Y., Kintses, B., Gielen, F., Miton, C. M., Fischer, G., Mohamed, M. F., . . . Hollfelder, F. (2015). Ultrahigh-throughput discovery of promiscuous enzymes by picodroplet functional metagenomics. *Nature Communications*, 6. doi:10.1038/ncomms10008
- Copley, S. D. (2014). An evolutionary perspective on protein moonlighting. *Biochemical Society Transactions*, 42. doi:10.1042/bst20140245
- Copley, S. D. (2015). An evolutionary biochemist's perspective on promiscuity. *Trends in Biochemical Sciences*, 40. doi:10.1016/j.tibs.2014.12.004
- Dairen Chemical Corp. Retrieved from http://www.dcc.com.tw/english/HomeStyle.aspx?urlFile=product/Products_10.htm on 31.01.2018
- Dauids, T., Schmidt, M., Bottcher, D., & Bornscheuer, U. T. (2013). Strategies for the discovery and engineering of enzymes for biocatalysis. *Current Opinion in Chemical Biology*, 17(2), 215-220. doi:10.1016/j.cbpa.2013.02.022
- The DAVY™ butanediol process. (2017). Retrieved from [http://www.jmprotech.com/images-uploaded/files/PD%20-%20Butanediol%20c2017\(3\).pdf](http://www.jmprotech.com/images-uploaded/files/PD%20-%20Butanediol%20c2017(3).pdf) on 31.01.2018
- Dror, A., Shemesh, E., Dayan, N., & Fishman, A. (2014). Protein engineering by random mutagenesis and structure-guided consensus of *Geobacillus stearothermophilus* lipase T6 for enhanced stability in methanol. *Applied and Environmental Microbiology*, 80(4), 1515-1527. doi:10.1128/aem.03371-13
- Dudley, Q. M., Karim, A. S., & Jewett, M. C. (2014). Cell-free metabolic engineering: Biomufacturing beyond the cell. *Biotechnology Journal*. doi:10.1002/biot.201400330
- Eggink, M., Wijtmans, M., Kretschmer, A., Kool, J., Lingeman, H., de Esch, I. J., . . . Irth, H. (2010). Targeted LC-MS derivatization for aldehydes and carboxylic acids with a new derivatization agent 4-APEBA. *Analytical and Bioanalytical Chemistry*, 397(2), 665-675. doi:10.1007/s00216-010-3575-1
- Eisenmenger, M. J., & Reyes-De-Corcuera, J. I. (2009). High pressure enhancement of enzymes: A review. *Enzyme and Microbial Technology*, 45(5), 331-347. doi:https://doi.org/10.1016/j.enzmictec.2009.08.001
- Fessner, W. D. (2015). Systems Biocatalysis: Development and engineering of cell-free "artificial metabolisms" for preparative multi-enzymatic synthesis. *Nature Biotechnology*, 32(6), 658-664. doi:10.1016/j.nbt.2014.11.007
- Fosbøl, P. L., Gaspar, J., Jacobsen, B., Glibstrup, J., Gladis, A., Diaz, K. M., . . . von Solms, N. (2017). Design and simulation of rate-based CO₂ capture processes using carbonic anhydrase (CA) applied to biogas. *Energy Procedia*, 114(Supplement C), 1434-1443. doi:https://doi.org/10.1016/j.egypro.2017.03.1268
- Gansbiller, M. (2014). *Identifizierung einer Alkoholdehydrogenase für die Reaktion von 2-Keto-3-desoxygluconsäure zu 2,6-dioxo-3-desoxygluconsäure, sowie der Folgereaktion zu 2-Keto-3-desoxyglucarsäure*. (Bachelor thesis), Technical University of Munich.
- Gerlt, J. A., Babbitt, P. C., & Rayment, I. (2005). Divergent evolution in the enolase superfamily: the interplay of mechanism and specificity. *Archives of Biochemistry and Biophysics*, 433(1), 59-70. doi:http://dx.doi.org/10.1016/j.abb.2004.07.034
- Gocke, D., Nguyen, C. L., Pohl, M., Stillger, T., Walter, L., & Mueller, M. (2007). Branched-chain keto acid decarboxylase from *Lactococcus lactis* (KdcA), a valuable thiamine diphosphate-dependent enzyme for asymmetric C-C bond formation. *Advanced Synthesis & Catalysis*, 349(8-9), 1425-1435. doi:10.1002/adsc.200700057
- Guo, W., Sheng, J., & Feng, X. (2017). Mini-review: *In vitro* metabolic engineering for biomufacturing of high-value products. *Computational and Structural Biotechnology Journal*, 15, 161-167. doi:https://doi.org/10.1016/j.csbj.2017.01.006
- Gupta, R. D. (2016). Recent advances in enzyme promiscuity. *Sustainable Chemical Processes*, 4(1), 2. doi:10.1186/s40508-016-0046-9
- Gupta, S. M., Kamble, M. P., & Yadav, G. D. (2017). Insight into microwave assisted enzyme catalysis in process intensification of reaction and selectivity: Kinetic resolution of (R,S)-flurbiprofen with alcohols. *Molecular Catalysis*, 440, 50-56. doi:https://doi.org/10.1016/j.mcat.2017.06.020

- Guterl, J. K., Garbe, D., Carsten, J., Steffler, F., Sommer, B., Reisse, S., . . . Sieber, V. (2012). Cell-free metabolic engineering: production of chemicals by minimized reaction cascades. *ChemSusChem*, 5(11), 2165-2172. doi:10.1002/cssc.201200365
- Hill, A. C. (1898). LXVI.-Reversible zymohydrolysis. *Journal of the Chemical Society, Transactions*, 73(0), 634-658. doi:10.1039/CT8987300634
- Hold, C., Billerbeck, S., & Panke, S. (2016). Forward design of a complex enzyme cascade reaction. *Nature Communications*, 7, 12971. doi:10.1038/ncomms12971
<http://www.nature.com/articles/ncomms12971#supplementary-information>
- Hu, Y., Lee, C. C., & Ribbe, M. W. (2011). Extending the carbon chain: hydrocarbon formation catalyzed by vanadium/molybdenum nitrogenases. *Science*, 333(6043), 753-755. doi:10.1126/science.1206883
- Huang, H. J., Liu, L. M., Li, Y., Du, G. C., & Chen, J. (2006). Redirecting carbon flux in *Torulopsis glabrata* from pyruvate to alpha-ketoglutaric acid by changing metabolic co-factors. *Biotechnology Letters*, 28(2), 95-98. doi:10.1007/s10529-005-4953-1
- Hult, K., & Berglund, P. (2007). Enzyme promiscuity: mechanism and applications. *Trends in Biotechnology*, 25(5), 231-238. doi:http://dx.doi.org/10.1016/j.tibtech.2007.03.002
- International Chemical Safety Cards (ICSC) 1104. (1999, 2017). Retrieved from http://www.ilo.org/dyn/icsc/showcard.display?p_lang=en&p_card_id=1104&p_version=2 on 30.01.2018
- Jeffryes, J. G., Colastani, R. L., Elbadawi-Sidhu, M., Kind, T., Niehaus, T. D., Broadbelt, L. J., . . . Henry, C. S. (2015). MINEs: open access databases of computationally predicted enzyme promiscuity products for untargeted metabolomics. *Journal of Cheminformatics*, 7(1), 44. doi:10.1186/s13321-015-0087-1
- Kashiyama, Y. (2012). EP2463374.
- Khersonsky, O., & Tawfik, D. S. (2010). Enzyme promiscuity: mechanistic and evolutionary perspective. *Annual Review of Biochemistry*, 79. doi:10.1146/annurev-biochem-030409-143718
- Khushboo, G., & Krishna, M. P. (2016). An overview of computational and experimental methods for designing novel proteins. *Recent Patents on Biotechnology*, 10(3), 235-263. doi:http://dx.doi.org/10.2174/1872208310666161013152249
- Khusnutdinov, R. I., Baiguzina, A. R., Mukminov, R. R., Akhmetov, I. V., Gubaidullin, I. M., Spivak, S. I., & Dzhemilev, U. M. (2010). New synthesis of pyrrole-2-carboxylic and pyrrole-2,5-dicarboxylic acid esters in the presence of iron-containing catalysts. *Russian Journal of Organic Chemistry*, 46(7), 1053-1059. doi:10.1134/s1070428010070158
- Koo, P. H., & Adams, E. (1974). Alpha-ketoglutaric semialdehyde dehydrogenase of *Pseudomonas*. Properties of the separately induced isoenzymes. *Journal of Biological Chemistry*, 249(6), 1704-1716.
- Korman, T. P., Sahachartsiri, B., Li, D., Vinokur, J. M., Eisenberg, D., & Bowie, J. U. (2014). A synthetic biochemistry system for the *in vitro* production of isoprene from glycolysis intermediates. *Protein Science*, 23(5), 576-585. doi:10.1002/pro.2436
- Kretschmer, A., Giera, M., Wijtmans, M., de Vries, L., Lingeman, H., Irth, H., & Niessen, W. M. (2011). Derivatization of carboxylic acids with 4-APEBA for detection by positive-ion LC-ESI-MS(/MS) applied for the analysis of prostanoids and NSAID in urine. *Journal of Chromatography. B, Analytical Technologies in the Biomedical and Life Sciences*, 879(17-18), 1393-1401. doi:10.1016/j.jchromb.2010.11.028
- Kroutil, W., & Rueping, M. (2014). Introduction to ACS Catalysis virtual special issue on cascade catalysis. *ACS Catalysis*, 4(6), 2086-2087. doi:10.1021/cs500622h
- Kuipers, R. K., Joosten, H. J., van Berkel, W. J., Leferink, N. G., Rooijen, E., Ittmann, E., . . . Schaap, P. J. (2010). 3DM: systematic analysis of heterogeneous superfamily data to discover protein functionalities. *Proteins*, 78(9), 2101-2113. doi:10.1002/prot.22725
- Laemmli, U. K. (1970). Cleavage of structural proteins during the assembly of the head of bacteriophage T4. *Nature*, 227(5259), 680-&. doi:10.1038/227680a0
- Lang, M. (2008). Tradition of ideas: Reppe Chemistry - BASF intermediates. Retrieved from <http://www.intermediates.basf.com/chemicals/topstory/reppe-chemie> on 18.10.17
- Lehmann, M., Pasamontes, L., Lassen, S. F., & Wyss, M. (2000). The consensus concept for thermostability engineering of proteins. *Biochimica et Biophysica Acta (BBA) - Protein Structure and Molecular Enzymology*, 1543(2), 408-415. doi:https://doi.org/10.1016/S0167-4838(00)00238-7
- Liese, A., Seelbach, K., & Wandrey, C. (2008). *Industrial biotransformations*: John Wiley & Sons.
- Lin, H., San, K. Y., & Bennett, G. N. (2005). Effect of *Sorghum vulgare* phosphoenolpyruvate carboxylase and *Lactococcus lactis* pyruvate carboxylase coexpression on succinate production in mutant strains of *Escherichia coli*. *Applied Microbiology and Biotechnology*, 67(4), 515-523. doi:10.1007/s00253-004-1789-x
- Linster, C. L., & Van Schaftingen, E. (2007). Vitamin C. *FEBS Journal*, 274(1), 1-22. doi:10.1111/j.1742-4658.2006.05607.x
- Lippow, S. M., Moon, T. S., Basu, S., Yoon, S.-H., Li, X., Chapman, B. A., . . . Prather, K. L. J. (2010). Engineering enzyme specificity using computational design of a defined-sequence library. *Chemistry & Biology*, 17(12), 1306-1315. doi:http://dx.doi.org/10.1016/j.chembiol.2010.10.012

- Lozano, P., Nieto, S., L. Serrano, J., Perez, J., Sanchez-Gomez, G., Garcia-Verdugo, E., & V. Luis, S. (2017). Flow biocatalytic processes in ionic liquids and supercritical fluids. *Mini-Reviews in Organic Chemistry*, 14(1), 65-74.
- Lutz, S. (2010). Beyond directed evolution - semi-rational protein engineering and design. *Current Opinion in Biotechnology*, 21(6), 734-743. doi:10.1016/j.copbio.2010.08.011
- Ma, F., Xie, Y., Luo, M., Wang, S., Hu, Y., Liu, Y., . . . Yang, G.-Y. (2016). Sequence homolog-based molecular engineering for shifting the enzymatic pH optimum. *Synthetic and Systems Biotechnology*, 1(3), 195-206. doi:https://doi.org/10.1016/j.synbio.2016.09.001
- Macgee, J., & Doudoroff, M. (1954). A new phosphorylated intermediate in glucose oxidation. *Journal of Biological Chemistry*, 210(2), 617-626.
- Medema, M. H., van Raaphorst, R., Takano, E., & Breitling, R. (2012). Computational tools for the synthetic design of biochemical pathways. *Nature Reviews Microbiology*, 10(3), 191-202.
- Mitsubishi Chemical: 1,4-Butandiol & tetrahydrofuran technology. (2017). Retrieved from http://www.mcc-license.com/technologies/pdf/Introduction_MCC_14BDO&THF_Process.pdf on 30.01.2018
- Moon, T. S., Dueber, J. E., Shiue, E., & Prather, K. L. (2010). Use of modular, synthetic scaffolds for improved production of glucaric acid in engineered *E. coli*. *Metabolic Engineering*, 12(3), 298-305. doi:10.1016/j.ymben.2010.01.003
- Moon, T. S., Yoon, S.-H., Lanza, A. M., Roy-Mayhew, J. D., & Prather, K. L. J. (2009). Production of glucaric acid from a synthetic pathway in recombinant *Escherichia coli*. *Applied and Environmental Microbiology*, 75(3), 589-595. doi:10.1128/AEM.00973-08
- Mülhardt, C. (2009). *Der Experimentator: Molekularbiologie, Genomics* (Vol. 6. Auflage): Akademischer Verlag Spektrum.
- Mullis, K. B., & Faloona, F. A. (1987). Specific synthesis of DNA in vitro via a polymerase-catalyzed chain reaction. *Methods in Enzymology*, 155, 335-350.
- Myung, S., Rollin, J., You, C., Sun, F., Chandrayan, S., Adams, M. W. W., & Zhang, Y. H. P. (2014). *In vitro* metabolic engineering of hydrogen production at theoretical yield from sucrose. *Metabolic Engineering*, 24, 70-77. doi:http://dx.doi.org/10.1016/j.ymben.2014.05.006
- Niesen, F. H., Berglund, H., & Vedadi, M. (2007). The use of differential scanning fluorimetry to detect ligand interactions that promote protein stability. *Nature Protocols*, 2(9), 2212-2221. doi:10.1038/nprot.2007.321
- Ninh, P. H., Honda, K., Sakai, T., Okano, K., & Ohtake, H. (2014). Assembly and multiple gene expression of thermophilic enzymes in *Escherichia coli* for *in vitro* metabolic engineering. *Biotechnology and Bioengineering*.
- Nobeli, I., Favia, A. D., & Thornton, J. M. (2009). Protein promiscuity and its implications for biotechnology. *Nature Biotechnology*, 27. doi:10.1038/nbt1519
- Nobili, A., Gall, M. G., Pavlidis, I. V., Thompson, M. L., Schmidt, M., & Bornscheuer, U. T. (2013). Use of 'small but smart' libraries to enhance the enantioselectivity of an esterase from *Bacillus stearothermophilus* towards tetrahydrofuran-3-yl acetate. *FEBS Journal*, 280(13), 3084-3093. doi:10.1111/febs.12137
- Norrgård, M. A., & Mannervik, B. (2011). Engineering GST M2-2 for high activity with indene 1,2-oxide and indication of an H-site residue sustaining catalytic promiscuity. *Journal of Molecular Biology*, 412. doi:10.1016/j.jmb.2011.07.039
- Nosrati, G. R., & Houk, K. N. (2012). SABER: a computational method for identifying active sites for new reactions. *Protein Science*, 21(5), 697-706. doi:10.1002/pro.2055
- Ostgard, D. (2015). BDO: "Catalyst Technologies and Raw Materials; which technology will prevail?". *Catalysts Insight*(8), 9-14.
- Pace, C. N., Vajdos, F., Fee, L., Grimsley, G., & Gray, T. (1995). How to measure and predict the molar absorption coefficient of a protein. *Protein Science*, 4(11), 2411-2423. doi:10.1002/pro.5560041120
- Packer, M. S., & Liu, D. R. (2015). Methods for the directed evolution of proteins. *Nature Reviews: Genetics*, 16(7), 379-394. doi:10.1038/nrg3927
- Pandya, C., Farelli, J. D., Dunaway-Mariano, D., & Allen, K. N. (2014). Enzyme promiscuity: Engine of evolutionary innovation. *Journal of Biological Chemistry*, 289(44), 30229-30236. doi:10.1074/jbc.R114.572990
- Parikka, K., & Tenkanen, M. (2009). Oxidation of methyl alpha-D-galactopyranoside by galactose oxidase: products formed and optimization of reaction conditions for production of aldehyde. *Carbohydrate Research*, 344(1), 14-20. doi:10.1016/j.carres.2008.08.020
- Paul, C. E., Churakova, E., Maurits, E., Girhard, M., Urlacher, V. B., & Hollmann, F. (2014). *In situ* formation of H₂O₂ for P450 peroxxygenases. *Bioorganic & medicinal chemistry*, 22(20), 5692-5696. doi:10.1016/j.bmc.2014.05.074
- Pavelka, A., Chovancova, E., & Damborsky, J. (2009). HotSpot Wizard: a web server for identification of hot spots in protein engineering. *Nucleic Acids Research*, 37(Web Server issue), W376-383. doi:10.1093/nar/gkp410
- Petzold, C., Chan, L. J., Nhan, M., & Adams, P. (2015). Analytics for metabolic engineering. *Frontiers in Bioengineering and Biotechnology*, 3, 135. doi:10.3389/fbioe.2015.00135
- Pick, A., Ott, W., Howe, T., Schmid, J., & Sieber, V. (2014). Improving the NADH-cofactor specificity of the highly active AdhZ3 and AdhZ2 from *Escherichia coli* K-12. *Journal of Biotechnology*, 189, 157-165. doi:10.1016/j.jbiotec.2014.06.015

- Pick, A., Schmid, J., & Sieber, V. (2015). Characterization of uronate dehydrogenases catalysing the initial step in an oxidative pathway. *Microbial Biotechnology*, 8(4), 633-643. doi:10.1111/1751-7915.12265
- Plotkin, J. S. (2016). The many lives of BDO. Retrieved from <https://www.acs.org/content/acs/en/pressroom/cutting-edge-chemistry/the-many-lives-of-bdo.html> on 01.02.2016
- Rahman, S. A., Cuesta, S. M., Furnham, N., Holliday, G. L., & Thornton, J. M. (2014). EC-BLAST: a tool to automatically search and compare enzyme reactions. *Nature Methods*, 11(2), 171-174. doi:10.1038/nmeth.2803
- Rehn, G., Pedersen, A. T., & Woodley, J. M. (2016). Application of NAD(P)H oxidase for cofactor regeneration in dehydrogenase catalyzed oxidations. *Journal of Molecular Catalysis B: Enzymatic*, 134, 331-339. doi:<https://doi.org/10.1016/j.molcatb.2016.09.016>
- Ringborg, R. H., & Woodley, J. M. (2016). The application of reaction engineering to biocatalysis. *Reaction Chemistry & Engineering*, 1(1), 10-22. doi:10.1039/C5RE00045A
- Rühmann, B., Schmid, J., & Sieber, V. (2014). Fast carbohydrate analysis via liquid chromatography coupled with ultra violet and electrospray ionization ion trap detection in 96-well format. *Journal of Chromatography A*, 1350, 44-50. doi:10.1016/j.chroma.2014.05.014
- Saiki, R. K., Gelfand, D. H., Stoffel, S., Scharf, S. J., Higuchi, R., Horn, G. T., . . . Erlich, H. A. (1988). Primer-directed enzymatic amplification of DNA with a thermostable DNA polymerase. *Science*, 239(4839), 487-491. doi:10.1126/science.2448875
- Sarkar, M., Lu, J., & Pielak, G. J. (2014). Protein crowder charge and protein stability. *Biochemistry*, 53(10), 1601-1606. doi:10.1021/bi4016346
- Schlüter, F. (2013). *Optimierung und Validierung von Testsystemen für den Nachweis der Decarboxylaseaktivität aus Lactococcus lactis*. (Master thesis), Technical University of Munich.
- Schub, J. (2015). *Veränderung der Substratspezifität der Glucarar-Dehydratase aus Actinobacillus succinogenes*. (Bachelor thesis), Technical University of Munich.
- Sevrioukova, I. F., & Poulos, T. L. (2013). Understanding the mechanism of cytochrome P450 3A4: recent advances and remaining problems. *Dalton Transactions*, 42. doi:10.1039/c2dt31833d
- Sharp, P. A., Sugden, B., & Sambrook, J. (1973). Detection of 2 Restriction Endonuclease Activities in *Haemophilus Parainfluenzae* Using Analytical Agarose-Ethidium Bromide Electrophoresis. *Biochemistry*, 12(16), 3055-3063. doi:10.1021/bi00740a018
- Sheldon, R. A., & van Pelt, S. (2013). Enzyme immobilisation in biocatalysis: why, what and how. *Chemical Society Reviews*, 42(15), 6223-6235. doi:10.1039/c3cs60075k
- Shiue, E., & Prather, K. L. (2014). Improving D-glucaric acid production from myo-inositol in *E. coli* by increasing MIOX stability and myo-inositol transport. *Metabolic Engineering*, 22, 22-31. doi:10.1016/j.ymben.2013.12.002
- Sieber, V., Pick, A., & Rühmann, B. (2012). Germany Patent No. WO 2012/127057 A1. W. I. P. Organization.
- Silva, C., Martins, M., Jing, S., Fu, J., & Cavaco-Paulo, A. (2017). Practical insights on enzyme stabilization. *Critical Reviews in Biotechnology*, 1-16. doi:10.1080/07388551.2017.1355294
- Solmi, S., Morreale, C., Ospitali, F., Agnoli, S., & Cavani, F. (2017). Oxidation of D-Glucose to Glucaric Acid Using Au/C Catalysts. *ChemCatChem*, 9(14), 2797-2806. doi:10.1002/cctc.201700089
- Sperl, J. M., Carsten, J. M., Guterl, J.-K., Lommès, P., & Sieber, V. (2016). Reaction design for the compartmented combination of heterogeneous and enzyme catalysis. *ACS Catalysis*, 6(10), 6329-6334. doi:10.1021/acscatal.6b01276
- Stemmer, W. P. (1994). Rapid evolution of a protein *in vitro* by DNA shuffling. *Nature*, 370(6488), 389-391. doi:10.1038/370389a0
- Stottmeister, U., Aurich, A., Wilde, H., Andersch, J., Schmidt, S., & Sicker, D. (2005). White biotechnology for green chemistry: fermentative 2-oxocarboxylic acids as novel building blocks for subsequent chemical syntheses. *Journal of Industrial Microbiology & Biotechnology*, 32(11-12), 651-664. doi:10.1007/s10295-005-0254-x
- Studier, F. W. (2005). Protein production by auto-induction in high-density shaking cultures. *Protein Expression and Purification*, 41(1). doi:10.1016/j.pep.2005.01.016
- Takase, R., Mikami, B., Kawai, S., Murata, K., & Hashimoto, W. (2014). Structure-based conversion of the coenzyme requirement of a short-chain dehydrogenase/reductase involved in bacterial alginate metabolism. *Journal of Biological Chemistry*, 289, 33198-33214. doi:10.1074/jbc.M114.585661
- Takase, R., Ochiai, A., Mikami, B., Hashimoto, W., & Murata, K. (2010). Molecular identification of unsaturated uronate reductase prerequisite for alginate metabolism in *Sphingomonas sp.* A1. *Biochimica et Biophysica Acta (BBA) - Proteins and Proteomics*, 1804(9), 1925-1936. doi:<http://dx.doi.org/10.1016/j.bbapap.2010.05.010>
- Taniguchi, H., Okano, K., & Honda, K. (2017). Modules for *in vitro* metabolic engineering: Pathway assembly for bio-based production of value-added chemicals. *Synthetic and Systems Biotechnology*. doi:<http://dx.doi.org/10.1016/j.synbio.2017.06.002>
- Toftgaard Pedersen, A., de Carvalho, T. M., Sutherland, E., Rehn, G., Ashe, R., & Woodley, J. M. (2017). Characterization of a continuous agitated cell reactor for oxygen dependent biocatalysis. *Biotechnology and Bioengineering*, 114(6), 1222-1230. doi:10.1002/bit.26267

- Tokuriki, N., & Tawfik, D. S. (2009). Stability effects of mutations and protein evolvability. *Current Opinion in Structural Biology*, 19(5), 596-604. doi:https://doi.org/10.1016/j.sbi.2009.08.003
- Turner, N. J. (2009). Directed evolution drives the next generation of biocatalysts. *Nature Chemical Biology*, 5(8), 567-573.
- Vaswani, S. (2012). *Process Economics Program: Bio-based 1,4-butanediol*. Retrieved from IHS:
- Verseck, S., Karau, A., & Weber, M. (2009). WO2009053489 A1.
- Wang, X., Huang, H., Xie, X., Ma, R., Bai, Y., Zheng, F., . . . Luo, H. (2016). Improvement of the catalytic performance of a hyperthermostable GH10 xylanase from *Talaromyces leycettanus* JCM12802. *Bioresource Technology*, 222(Supplement C), 277-284. doi:https://doi.org/10.1016/j.biortech.2016.10.003
- Weigl, J. (2014). *Veränderung der Substratspezifität einer Decarboxylase durch Enzym-Engineering*. Technical University of Munich.
- Weissermel, K., & Arpe, H.-J. (2008). *Industrial organic chemistry*. Weinheim: VHC Verlagsgesellschaft mbH.
- Werpy, T. P., G. ; Aden, A. ; Bozell, J. ; Holladay, J. ; White, J. ; Manheim, Amy ; Eliot, D. ; Lasure, L. ; Jones, S. (2004). Top value added chemicals from biomass. Volume 1 - Results of screening for potential candidates from sugars and synthesis gas.
- Woolerton, T. W., Sheard, S., Pierce, E., Ragsdale, S. W., & Armstrong, F. A. (2011). CO₂ photoreduction at enzyme-modified metal oxide nanoparticles. *Energy & Environmental Science*, 4(7), 2393-2399. doi:10.1039/C0EE00780C
- Yadav, R. K., Oh, G. H., Park, N. J., Kumar, A., Kong, K. J., & Baeg, J. O. (2014). Highly selective solar-driven methanol from CO₂ by a photocatalyst/biocatalyst integrated system. *Journal of the American Chemical Society*, 136(48), 16728-16731. doi:10.1021/ja509650r
- Ye, X., Honda, K., Sakai, T., Okano, K., Omasa, T., Hirota, R., . . . Ohtake, H. (2012). Synthetic metabolic engineering-a novel, simple technology for designing a chimeric metabolic pathway. *Microbial Cell Factories*, 11(1), 120. doi:10.1186/1475-2859-11-120
- You, C., & Percival Zhang, Y. H. (2012). Easy preparation of a large-size random gene mutagenesis library in *Escherichia coli*. *Analytical Biochemistry*, 428(1), 7-12. doi:https://doi.org/10.1016/j.ab.2012.05.022
- Zachos, I., Ga, Bauer, D., Sieber, V., Hollmann, F., & Kourist, R. (2015). Photobiocatalytic decarboxylation for olefin synthesis. *Chemical Communications*, 51(10), 1918-1921. doi:10.1039/C4CC07276F
- Zhang, Y.-H. P., Sun, J., & Ma, Y. (2016). Biomanufacturing: history and perspective. *Journal of Industrial Microbiology & Biotechnology*, 1-12. doi:10.1007/s10295-016-1863-2
- Zhang, Y.-H. P., Sun, J. B., & Zhong, J. J. (2010). Biofuel production by *in vitro* synthetic enzymatic pathway biotransformation. *Current Opinion in Biotechnology*, 21(5), 663-669. doi:10.1016/j.copbio.2010.05.005
- Zhang, Y., Ge, J., & Liu, Z. (2015). Enhanced activity of immobilized or chemically modified enzymes. *ACS Catalysis*, 5(8), 4503-4513. doi:10.1021/acscatal.5b00996
- Zhang, Y., & Hess, H. (2017). Toward rational design of high-efficiency enzyme cascades. *ACS Catalysis*, 6018-6027. doi:10.1021/acscatal.7b01766
- Zhao, H. (2016). Protein stabilization and enzyme activation in ionic liquids: Specific ion effects. *Journal of Chemical Technology and Biotechnology*, 91(1), 25-50. doi:10.1002/jctb.4837

11 Acknowledgments

Foremost, I would like to express my sincere gratitude to my advisor Prof. Volker Sieber. Thank you for your continuous support, your advice, and the many discussions and talks. It was great to have the opportunity to follow my own ideas led by your expertise and your encouragement.

Besides my advisor, I would like to thank the other professors of my thesis committee: Prof. Reinhard Sterner and Prof. Wolfgang Liebl.

My sincere thanks also goes to my mentor Prof. Katrin Gramman for her time, advice, and motivation.

Furthermore, I would like to thank Prof. Kenji Miyamoto and his group as well as the DAAD for the opportunity to conduct research at the Keio University in Japan.

Thanks to all colleagues at the Chair of Chemistry of Biogenic Resources as well as the Fraunhofer group BioCat and the KoNaRo. Especially, I would like to thank André Pick, Dr. Jörg Carsten, Dr. Fabian Steffler, Karola Wiesmüller and Anja Schmidt for the good atmosphere in our office, the fun, and the numerous discussions. André, without your motivation and your assistance this thesis would not be what it is, thank you. Petra Lommes and Manuel Döring I would like to thank for their immense help in the lab, as well as Dr. Broder Rühmann for his advice and help with the analytics. Special thanks goes to Dr. Jörg Carsten and Claudia Nowak for proofreading of the manuscript. Claudia Nowak, Nina Rimmel, Nadine and Dr. Josef Sperl I thank for their friendship and the good times during and after our time at the CBR.

I also want to thank Teresa Roth, Moritz Gansbiller, Julian Schub, Johannes Weigl and Franziska Schlüter for their effort during their Bachelor's and Master's theses.

Finally yet importantly, I would like to thank my family:

My parents Monika and Stephan, who supported me my whole life – Mama, du fehlst mir.

My siblings Regina with Matthias and Anton, and Christoph with Cathia, Mateo and Anahí Sophie, who are always there for me – I love you.

Marcel and my little Johanna, who motivate, encourage and support me in every way possible – I love you both with all my heart.

12 Curriculum Vitae

Barbara Beer

Date of Birth: 3. Nov 1986 in Hemau



Since Oct 2017	Research Associate Technical University of Munich Chair of Chemistry of Biogenic Resources
July – Sept 2014	Visiting Researcher Keio University, Yokohama, Japan Department of Biosciences and Informatics
May 2012 – Sept 2017	Doctoral Thesis Technical University of Munich Chair of Chemistry of Biogenic Resources
Oct 2011 – Apr 2012	Master Thesis University of Regensburg Institute of Biophysics and Physical Biochemistry
Oct 2009 – Apr 2012	Master studies in Biochemistry University of Regensburg
June – Aug 2009	Bachelor Thesis University of Regensburg Institute of Biophysics and Physical Biochemistry
Oct 2006 – Sep 2009	Bachelor studies in Biochemistry University of Regensburg
2006	Abitur Gymnasium Parsberg